Regulators of hypoxic filamentation in the human fungal pathogen *Candida albicans*

Inaugural dissertation

for the attainment of the title of doctor
in the Faculty of Mathematics and Natural Sciences

at the Heinrich Heine University Düsseldorf

by

Prashant Ramesh Desai

from Belgaum, India

Düsseldorf, July 2019

from the Institute of Molecular Mycology, Department Biology,

at the Heinrich Heine University Düsseldorf

Published by permission of the
Faculty of Mathematics and Natural Sciences at

Heinrich Heine University Düsseldorf

Supervisor: Prof. Dr. Joachim F. Ernst

Co-supervisor: Prof. Dr. Michael Feldbrügge

Date of the oral examination: 22.08.2019

Table of Contents

1. Introduction

1.1 Diversity of fungi: Environmental organisms to human fungal pathogens

Fungi are one of the most abundant, species-rich groups of organisms that mediate many critical processes of the world ecosystems (Dighton 2016). They can be found growing on almost any substrate on earth, from the deep ocean sediments to the human scalp and they can coexist with all other living organisms (bacteria, plants and animals) in diverse ecological niches (Peay *et al*., 2016). Fungi and animals diverged from a common ancestor about 760 million to 1.5 billion years ago (Barbee and Taylor 2010). During the span of a billion years of evolution, millions of fungal species have evolved on multiple occasions in the tree of life (James *et al*., 2006). Fossil history suggests that fungal activity has influenced plant and animal communities during the course of evolution (Mueller *et al*., 2008, Fisher *et al*., 2012). In the Palaeozoic era (250 to 500 million years ago), nutrient-acquiring mycorrhiza-like fungi facilitated the colonization of plants on diverse land surfaces; this plant-fungus symbiosis is not only considered as a pivotal step in the evolution of the terrestrial ecosystem, but is also attributed as a prominent factor for increase in levels of atmospheric oxygen, 500 million years ago (Ma) (Remy 1994, Heckman *et al*., 2001, Mills *et al*., 2018). Currently, the oldest fossil record of animal parasitism by a fungus is from the Cretaceous era (70 to 140 Ma) (Sung *et al*., 2008). One of the most astonishing alterations in host behaviour due to fungus interaction can be dated back to 48 million years: the parasitic fungus *Ophiocordyceps unilateralis-furcata* has a unique ecological strategy, which modifies the behaviour of an ant host. Infected ants climb into vegetation, bite vegetal materials and hang themselves upside down until death (''death grip'') for dispersal of fungal spores (*Anderson SB 2009,* Hughes *et al*., 2016).

History records for most of the fossilized unicellular fungi are incomplete, which generated problems to accurately map the phylogeny of fungal species (Lucking 2009, Blair 2009). Initially, fungi were characterized largely on morphological and physiological characteristics. However, within the last two decades, the use of whole genome sequencing and comparative genomic tools allowed an extensive analysis of the fungal kingdom. The phylogenetic tree of fungi is currently divided into seven phyla: the *Chytridiomycota*, *Blastocladiomycota*, *Neocallimastigomycota*, *Zygomycota*, *Glomeromucota*, *Ascomycota* and *Basidiomycota* (Ebersberger *et al*. 2011). Initially, it was estimated that about 1.5 million fungal species exist

on different habitats; however, a recent analysis of environmental DNA samples revealed about 3.5 to 5.1 million fungal species in the soil microbial community and in total, the currently known fungal species amount to around 100,000 (Blackwell 2011). Among these, several fungal species, in order to obtain nutrients, have evolved to diverse associations with individual or multiple host species of plants or animals (Tresender *et al.*, 2015, Zeilinger *et al*., 2016). Although most of fungal species are non-pathogenic and often benefit certain habitats (e.g. as mycorrhizal fungi that acquire nutrients and transfer them to plants), many fungal species can cause a serious threat to plants and animals (Sexton and Howlett 2006, Lutzoni *et al*., 2018). Fungal infections have detrimental effects on plant physiology and destroy at least 125 million tonnes of crops each year, amounting to about 60 billion dollars in damages. It has also been estimated that infection and disease of plants related to fungal pathogens leads to almost 64 % of host species extinction (Fisher *et al*., 2012).

In the recorded history of animal diseases until mid of the 20th century, mostly viral and bacterial infections were considered as major threats. However, due to various incidences such as global warming, intercontinental trade and excessive use of pesticides, the prevalence of animal and human fungal pathogens has drastically intensified (Fisher *et al*., 2012, Casadevall *et al*., 2018). In addition, global warming may have increased the occurrence of fungal diseases, because fungi can easily adapt to warmer temperatures (Garcia-Solache MA, & Casadevall 2010). For example, in last decade, the ascomycete fungus *Geomyces destructans* has caused white nose syndrome in bats, leading to decline of the bat population by 70% (Blehert *et al*., 2012). A recent survey has indicated a 40% loss in the diversity of amphibians in central America; this decline is mainly due to the fungal pathogen *Batrachichytrium dendrobatidis*, which has been shown to infect over 500 species of amphibians (Scheele *et al*., 2019). Independent studies have discovered several fungal species as the emerging pathogens against bees, coral reefs and sea turtles (Sarmiento-Ramírez *et al*., 2014, Foley *et al*., 2014, Soler-Hurtado *et al*., 2016). Overall, pathogenic fungi can cause existential stress or death to host species, and adversely affect the biodiversity of ecosystems.

Annually, more humans die due to invasive mycoses (~ 1.6 million) than to malaria or tuberculosis and around a billion of patients suffer each year either because of superficial or invasive fungal infections (Brown *et al*., 2012). Three major forms of superficial mycoses are represented by Dermatophytosis, superficial Candidiasis and infections by *Malassezia* (Tan

and Hsu 2018). It is estimated that 20-25% of the world population is affected by superficial fungal infections and that 10-15% of the population will be infected by a dermatophyte at some point in their lives (Havlickova *et al*., 2008). Dermatophytosis is an infection of skin, hair and nails caused by dermatophytes, mostly by *Trichophyton* and *Microsporum* species (Vermout *et al*., 2008). Dermatophytes are essentially not parts of normal skin microflora, but they are transmitted by direct or indirect contacts with infected individuals. Due to their keratinolytic ability, they infect keratinized tissues and cause inflammation (Achterman *et al*., 2012). The lipophilic yeast *Malaesszia* and *Candida* spp. are members of normal skin microflora of healthy individuals, but they can become pathogenic in case of major alteration in the skin flora or if the host immune system is compromised (Velegraki *et al*., 2015, Nett 2018). *Malassezia* spp. causes seborrhoea- a tenacious skin disorder, which presents symptoms of red, scaly, greasy, itchy, and inflamed skin (Ashbee 2006). *Candida* spp. can cause cutaneous, oropharyngeal and vaginal candidiasis. The common skin symptoms of *Candida* superficial infections are thickening of the skin, hyperkeratosis and white patches on erythematous background (Kashem and Kaplan 2016). Recurring superficial infections occur mainly in immunodeficient individuals or long-term hospitalized patients in intensive care units. Although the cases of superficial infections are high in numbers compared to invasive infections, the later form of fungal infections are of major concern, due to their high mortality rate (Webb *et al*., 2018).

Invasive fungal infections can cause life threatening diseases, as the responsible fungi can penetrate through deep body tissues and disseminate within internal organs (Kohlers *et al*., 2015). Recent global estimates for invasive fungal infections are ~700,000 cases of invasive candidiasis, ~500,000 cases of *Pneumocystis jirovecii* pneumonia, ~223,100 cases of cryptococcal meningitis, ~250,000 cases of invasive aspergillosis and ~100,000 cases of histoplasmosis, which occur annually (Brown *et al*., 2012, Bongomin *et al*., 2017). Mortality rates for invasive mycoses vary from 30 to 90% (Bongomin *et al*., 2017). Currently, around 600 fungal species are known to be pathogenic to humans, but the majority of the invasive fungal infections worldwide are caused by four fungal pathogens: *Candida spp.*, *Aspergillus fumigatus*, *Cryptococcus neoformans* (or *C. gatti*) and *Pneumocystis jirovecii* (Pfaller *et al*., 2006, Brown *et al*., 2012).

Invasive fungal infections are a globally emerging problem and a large majority of these cases is due to *Candida* species, especially *C. albicans*. Over the last couple of decades, patients with candidiasis have increased about 20 fold, because of the growing number of immunocompromised cases that includes individuals suffering from AIDS, undergoing organ transplantation or cancer chemotherapies and are treated by excessive amounts of antibacterial antibiotics (Pagano *et al*., 2011, Lortholary *et al*., 2013). An important factor for increment in patients of candidiasis, is significant increase in usage of invasive medical devices. *Candida* species have ability to form multicellular structures known as biofilms, on medical implants such as stents, shunts, pacemakers, endotracheal tubes, and various types of catheters (Ramage *et al*., 2006). Once a biofilm is formed, it becomes exceedingly difficult to get rid of fungal cells, because of their increased resistance to antifungal therapy and the ability of cells within biofilms to withstand host immune defences (Nobile & Johnson 2015). Studies have shown that catheter associated *C. albicans* biofilms can lead to bloodstream infection with prolonged fungemia, high antifungal therapy failure rates, increased risk of metastatic complications and death (Finkel and Mitchell 2011, Nobile and Johnson 2015). Despite an estimated cost of 7.2 billion dollars being spent annually for the treatment and usage of new antifungal drugs, the mortality rate of Candidiasis patients is still higher than 50% (Benedict *et al*., 2018).

Since several decades antifungal drugs used for the treatment of systemic candidiasis include amphotericin B (polyene-type) and azoles such as fluconazole (Perfect 2017). These two drugs belong to different class of antifungal agents and have different modes of action to restrict or to inhibit the growth of *Candida* species (Sanglard 2016). Because fungi are eukaryotes, they share high genome and proteome homologies with humans and therefore, most antifungal agents, in a dosage-dependent manner, inherently cause toxicity in humans (Hill *et al*., 2013). Amphotericin B is known to cause nephrotoxicity and renal failure, while repetitive use of fluconazole can lead to hepatotoxicity in patients suffering with Candidiasis (Mourad and Perfect 2018). In addition, clinical isolates of *Candida* species displaying strong resistance to most of the clinical antifungal agents have been documented repeatedly (Sanglard 2019). In the year 2000, a new class of antifungal agent was introduced in the clinic: echinocandin (caspofungin) inhibits the synthesis of a fungal cell wall component (1,3-β-D-glucan). Resistance against this drug has also been reported, which may be due to mutation in the

gene encoding target enzyme (β-glucan synthase) (Perlin 2015, Kordalewska *et al*., 2018). Moreover, the new species *Candida auris* has emerged in recent years in the clinic, which is highly resistant against all known antifungal agents (including caspofungin) and poses a major threat to all patients in intensive care units worldwide (Chowdhary *et al*., 2017). The unacceptably high mortality rate in candidiasis patients and emergence of drug resistance in *Candida* spp. is indicative of severe limitations and ineffectiveness of the current antifungal therapies used to combat candidiasis.

1.2 *Candida* species and candidiasis

The genus *Candida* is polyphyletic and contains approximately 200 different species, which are widely distributed in nature; many act as common constituents of normal microflora inhabiting skin, oral cavity and gastrointestinal tract of humans (Noble *et al*., 2017). Some of these fungal species can become opportunistic pathogens by undergoing a transition from a commensal to a pathogenic phase, induced by alterations in the host environment (Miranda *et al*., 2009). *Candida* species thereby rarely trigger infection in healthy people, but take advantage of an impaired immune system to proliferate within the host, which leads to candidiasis. Around 30 different *Candida* species are pathogenic to humans, but more frequently, *Candida albicans* and the non-albicans *Candida* species (*C. glabrata*, *C. parapsilosis, C. dubliniensis* and *C. tropicalis*) were isolated from clinical samples of patients suffering from candidiasis (Pfaller and Diekema 2007).

Between years 2004-2009, the whole-genome sequencing projects were initiated that established the genome of important fungal species of the Saccharomycotina subphylum, including *C. albicans* and non *C. albicans* species (Jones *et al*., 2004, Butler *et al*., 2009, Jackson *et al*., 2009). Comparative genomic tools enabled the evolutionary analysis of virulent traits across *Candida* species. *Candida* species belong to different phylogenetic clades and surprisingly, are related significantly to non-pathogenic yeast species (Gabaldón *et al*., 2016). For instance, *C. parapsilosis* belongs to a distant lineage compared to *C. albicans*, but is closely related to the non-pathogenic yeast *Lodderomyces elongisporus* (Fig.1). Also, *C. glabrata and C. tropicalis* have higher homology and phylogenetic relatedness to non-pathogenic yeasts *Saccharomyces cerevisiae* and *C. sojae* respectively, compared to all other pathogenic *Candida* species (Fig.1) (Munoz *et al*., 2018). The globally emerging pathogen *C. auris* is closely related to *C. lusitaniae* (Sharma *et al*., 2016). These results indicate that the emergence of

virulence has occurred several times in an independent manner within different clades of *Candida* species.

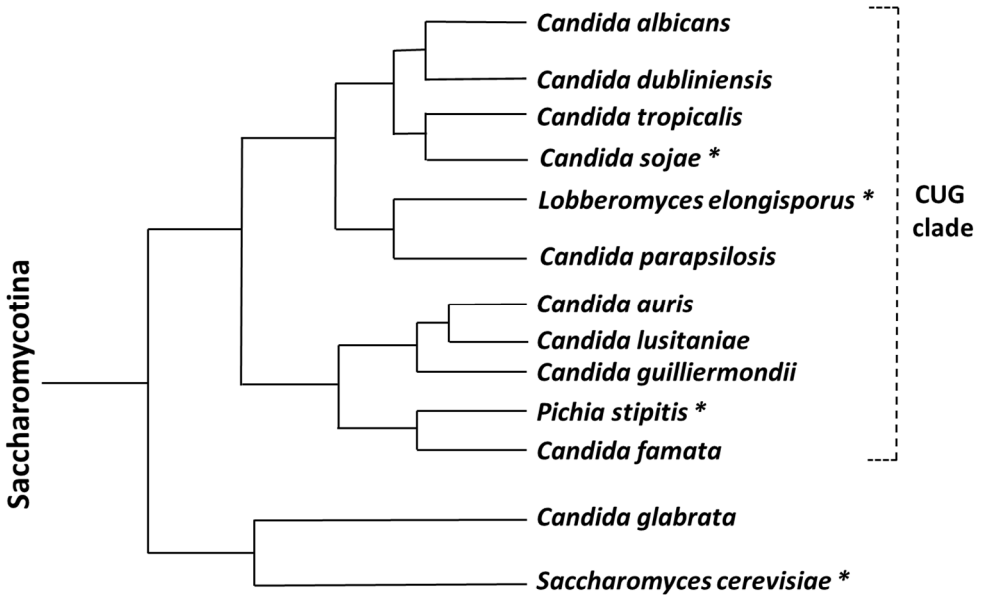

Fig. 1: Phylogeny between pathogenic and non-pathogenic species of Saccharomycotina. The organisms under CUG clade, translate CUG codons to serine instead of leucine. The non-pathogenic species are marked by asterisk. Figure modified from Fitzpatrick *et al*., 2006 and Munoz *et al*., 2018.

Whole genome comparisons across subphylum Saccharomycotina revealed that most of the pathogenic species share an evolutionary property as these organisms translate the CUG codon to serine instead of leucine (Massey *et al*., 2003). For *C. albicans* it has been shown that usage of an alternative genetic codon increases the diversity of its surface proteins, thus making it difficult to be recognized by the host immune system (Nather *et. al*., 2008, Miranda *et al*., 2011). The only exception for the CUG clade is *C. glabrata*, which is closely related to *S. cerevisiae*. Analysis of genomic variation in pathogenic *Candida* species has revealed that most of the pathogens from this group are diploid (*C*. *albicans*, *C*. *tropicalis*, *C*. *dubliniensis* and *C*. *parapsilosis*) with exception of two organisms being haploid (*C*. *glabrata* and *C. auris*) (Ruiz *et al*., 2019). Genomic comparison of *Candida* species revealed enrichment of 21 gene families in pathogenic species compared to non-pathogenic organisms, including genes encoding GPI anchored cell wall proteins, secreted lipases, secreted proteases, oligopeptide transporters and transcription factors (Butler *et al*., 2009). Expansion of gene families, for example by gene duplication followed by sequence divergence, were observed in certain pathogenic *Candida* species. This process can generate genetic and phenotypic novelty and

thereby influence the virulence of *Candida* species, such as in the case of *C. albicans* the adhesins gene family and the EPA gene family in *C. glabrata* (Hoyer *et al*., 2008, Kaur *et al*., 2007). Significant differences were observed within pathogenic Candida species for their ability to undergo hyphal morphogenesis. *C. albicans, C. dubliniensis* and *C. tropicalis* can undergo filamentous growth to form true hyphae, and are able to revert back to the unicellular yeast form (Sullivan *et al*., 2005, Lackey *et al*., 2013), while other species (*C. parapsilosis*, *C. glabrata and C. auris*) exists solely in yeast morphology but are not able to form true hyphae (Thompson *et al*., 2011, Wang *et al*., 2018). High degree of variability is also seen in the virulence traits of *Candida* species to evade the host immune system. For instance, to escape from immune cells, *C. albicans* if engulfed by macrophages undergoes morphogenesis and bursts out of macrophages by forming filaments (Lorenz *et al*., 2004). In contrast to this, *C. glabrata* can withstand the harsh condition within the phagosome and can proliferate in these conditions (Kasper *et al*., 2015). As different *Candida* species (*C. albicans*, *C. glabrata*, *C. tropicalis*, *C. dubliniensis* and *C. auris*) can infect humans and cause disease, yet maintain significant variability in virulent strategies, it appears that each virulent species might have evolved independently to survive within specific niches of host.

Candidiasis can be categorised into three groups: cutaneous (skin and its appendages), mucosal (oropharyngeal, esophageal, and vulvovaginal) and systemic (bloodstream infections, i.e., candidemia and other forms of invasive candidiasis).

1.2.1 Cutaneous candidiasis

Human skin is normally colonised by bacterial and fungal species. Although many of these species are commensal in nature, various fungal species such as *Candida*, *Rhodotorula* and *Malassezia* can become pathogenic (Findley *et al*., 2013, de Hoog *et al*., 2017). Generally, healthy skin microflora produces a dense population on cutaneous surfaces and protects the host from pathogens by generating nutritional competition. However, due to the predisposition of patients (e.g. immune deficiency) or external factors (e.g. antibiotic treatment), the skin microflora can become adversely altered to a less competitive environment and expose skin tissue to endogenous opportunistic pathogens, such as *Candida* species. *C. albicans* is known to modulate its cell surface proteins (adhesins) to adhere to the host cell and tissue surface. Also, it can produce lipases and hydrolases for penetration into deeper skin tissues to cause chronic infections (Mayer *et al*., 2013). Keratinocytes are the

predominant cell form in the epidermis, which can become infected by *C. albicans* and induce inflammatory responses from the host immune system (Schaller *et al*., 2002). In such cases, impaired immune response can lead to chronic mucocutaneous candidiasis (CMC). The risk of skin infection is higher in Psoriasis patients, as medication for Psoriasis can interfere with antifungal immune responses (Saunte *et al*., 2017). Innate immunity against *C. albicans* skin infections is driven by recognition of the pathogen by cutaneous stromal cells that alarm dendritic cells to activate tissue-resident secretion of interleukin-17 (IL-17) (Conti *et al*., 2015). IL-17 is a pro-inflammatory cytokine, which plays a pivotal role by recruiting neutrophils at the site of infection and establishes protection against *Candida* infection (Glocker *et al*., 2010, Huppler *et al*., 2012). Therefore, disturbances in IL-17 production or its signalling pathway can cause higher susceptibility to recurrent *Candida* infections (Mengesha and Conti 2017). Common types of *Candida* skin infection include intertrigo, diaper dermatitis, perianal dermatitis, and *Candida* balanitis (McGirt and Martins 2004, Klunk *et al*., 2014, Metin *et al*., 2018). In most of the cases, cutaneous candidiasis is nonlethal and can be treated with fluconazole (Eggimann *et al*., 2003). Nevertheless, the prevalence of cutaneous candidiasis is increasing worldwide, especially in neonates and in older patients, because of their contact with invasive monitoring devices in intensive care units (Arsenault *et al*., 2015). Neonatal candidiasis occurs during initial days after birth with oral thrust and diaper dermatitis; infections can occur during delivery (*Benjamin et al*., 2010). In older patients, superficial candidiasis occurs due to hyperalimentation, prolonged hospitalization and widespread use of broad-spectrum antibiotics (Weerasuriya and Snape 2008). Overall, multiple aspects such as age, hygiene, functioning of the immune system and nutrition can influence the susceptibility to candidiasis.

1.2.2 Mucosal candidiasis

Mucosal epithelia consist of ordered layers of epithelial cells on surfaces of respiratory, digestive and urogenital tracts. Mucosal lining covering the surface of internal organs provides an essential barrier between the host and outside environments. These epithelia play a central role in immune surveillance and secrete mucus, which forms an additional barrier against invading pathogens (Kim and Ho 2010). However, mucosal epithelia are also the major portal of entry for specialized pathogens. During inflammation the innermost linings of the organs are exposed to opportunistic pathogens, which are part of normal microflora

(Sansonetti and Medzhitov 2009). *Candida* species are members of normal microflora that reside on the oral, gastrointestinal and genital mucosa of healthy individuals. Therefore, several host factors such as poor hygiene, altered diet, dysbiosis, hormonal imbalance, uncontrolled diabetes, impaired immunity and use of antibiotics can lead to favourable conditions for *Candida* species to infect and proliferate on mucosal tissues (Williams and Lewis 2011). This is evident in case of AIDS, neutropenia, poorly controlled diabetes and xerostomia, as oral candidiasis occurs frequently in these patients (Challacombe and Naglik 2006, Rautemaa and Ramage 2011). The visual symptoms of oral candidiasis are large whitish plaques on erythematous mucosa, throat, tongue and gums, which is commonly known as oral thrush (Patil *et al*., 2015). 90% of the HIV infected patients suffer from oral thrush and undergo a prolonged phase of antifungal therapy. In such cases, clinical resistance is frequently observed due to prolonged exposure to antifungal agents (Kanafani and Perfect 2008). Denture stomatitis and angular cheilitis are other forms of oral candidiasis, in which erythematous lesions are observed in patients (Singh *et al*., 2014). The severity and extent of *Candida* infection is drastically increased in patients receiving corticosteroids (Sobel 2007). Also, in diabetes mellitus patients higher colonisation of *Candida* species is observed in the oral cavity (Rodrigues *et al*., 2019). Investigation of clinical samples from the scrapings of oral thrush has revealed the prevalence of *C. albicans*, which accounts for 70 % of all cases, while occurrence of *C. glabrata* and *C. troplicalis* is relatively low (Vazquez and Sobel 2002). In case of immuno-compromised patients, esophageal candidiasis is also frequently observed, which may arise as an extension of oral candidiasis. Vulvovaginal candidiasis (VVC) affects millions of women every year; 70-75% of women experience at least one episode of VVC and 50% of these women experience a second attack (Sobel 2007). Clinical manifestations are vaginal erythema, edema, vulvar pruritus and burning accompanied by vaginal soreness leading to dyspareunia (Jeanmonod and Jeanmonod 2019). If VVC is untreated, it may lead to complications such as pelvic inflammatory disease, menstrual disorder, pelvic abscess and infertility (Vijaya *et al*., 2014). In some cases, presence of *Candida* species in the vaginal region is not responsible for VVC; hence, to differentiate from asymptomatic women, diagnosis of clinical samples and laboratory confirmation is essential. *Candida* species associated with VVC are *C. albicans*, *C. glabrata*, *C. tropicalis*, *C. parapsilosis* and *C. krusei* (Jindal *et al*., 2007). Usually VVC can be treated with oral administration of azoles (ketoconazole, itraconazole or fluconazole), which are effective in the majority of cases;

however, in 8% of these cases, recurrent VVC (more than 4 episodes each year) is observed (Foxman *et al*., 2013). Although mortality is not observed in these cases, the high level of morbidity associated with VVC demands the discovery of effective antifungal drugs.

1.2.3 Systemic candidiasis

Each year around 700,000 people are affected by invasive candidiasis. Candidemia is a certain type of invasive candidiasis (blood infection) with highest mortality rate (40%) and is ranked as the fourth most common bloodstream infection in the intensive care units (Wisplinghoff *et al*., 2004). Medical devices such as catheters get infected by human contact and *Candida* species especially produce biofilms, which facilitate persistent colonisation of the fungus on synthetic devices (Ramage *et al*., 2006). Subsequently, dispersal of fungal cells from biofilms can lead to candidemia. In patients, who have undergone gastrointestinal surgery, the commensal population of *Candida* species from the GI tract can invade through translocation and enter the blood stream to cause systemic infection (Miranda *et al*., 2009). Once *Candida* species enters the bloodstream it disseminates into internal organs escalating to metastatic infections of kidney, liver, spleen, bones and the central nervous system (Clancy and Hong 2012). Individuals are at high risk for systemic candidiasis, if they suffer from neutropenia or immunocompromised conditions; also patients with gastrointestinal surgery, recipients of immunosuppressive drugs and critically ill patients with indwelling catheters can become infected (Delaloye and Calandra 2014). In these patients the symptoms of candidemia can range from no specific signs to septic shock. Moreover, in critically ill patients the symptoms of candidemia (fever, hypertension and multi-organ dysfunction) are indistinguishable from symptoms of sepsis, which can also occur due to bacterial infections (Filler and Kullberg 2002). Hence clinicians face difficulty in identifying high risk patients of candidemia, which impedes the prophylaxis and treatment of systemic candidiasis. Current diagnosis of candidemia using clinical samples (blood culture) is a time consuming process with limited accuracy, causes considerable delay in identification of patients (Kullberg *et al*., 2015). Untreated patients suffering from candidemia have mortality rates that are higher than 70% (Filler and Kullberg 2002). Over the years fluconazole and amphotericin B were mostly used for the treatment of systemic *Candida* infections. The incidence of resistance against fluconazole is higher in *C. albicans* and *C. glabrata*, while *C. krusei* is intrinsically resistant to fluconazole (Kett *et al*., 2011). Currently, echinocandin is becoming the preferred antifungal agent used for treatment

for systemic candidiasis (Ben-Ami *et al*., 2018). Despite the current prophylaxis and treatments, mortality rates are still unacceptably high in systemic candidiasis patients. Hence new approaches are needed to be infused to discover novel antifungal agents to treat systemic candidiasis.

1.3 C. albicans: An important model organism to study fungal pathogenesis

Based on the recent global survey of fungal diseases and distribution of *Candida* species in the cases of candidiasis, the prevalence of *C. albicans* is predominant (47% to 70%) compared to other *Candida* species (25% to 38%) (Tortorano *et al*., 2006, Horn *et al*., 2009, Berberi *et al*., 2015). Although several pathogenic species of *Candida* can cause candidiasis in humans, *C. albicans* remains as a major threat for immunocompromised patients and causes severe damage ranging from superficial infection to life threatening systemic candidiasis (Guinea 2014). Further studies on *in vivo* models for candidiasis have substantiated the formidable pathogenic potential of *C. albicans* compared to non *C. albicans* species (Arendrup *et al*., 2002, Koh 2013, Segal and Frenkel 2018). Also, several multidrug-resistant strains of *C. albicans* have been identified from patients suffering from candidiasis (Jensen *et al*., 2015). *C. albicans* displays a wide array of pathogenic abilities including colonisation in different host niches, morphological switching, flexibility to reassign CUG codon to serine (instead of leucine), acquired drug resistance, biofilm formation and evasion from host immune system (Santos *et al*., 1995, Sudbery 2011, MacCallum 2012, Erwig and Gow 2016 Ksiezopolska *et al*., 2018 and Lohse *et al*., 2018). These attributes make this organism an ideal model system to study fungal pathogenesis in detail, since methods to study *C. albicans* have been established (Magee *et. al*., 2003, Reuß *et al*., 2004, Vyas *et al*., 2015). Further investigation of specific molecular mechanisms leading to colonisation of experimental hosts will elucidate virulent attributes that contribute to the host adaptability, pathogenicity and fitness of *C. albicans*. Such studies can develop new avenues to generate effective antifungal therapy.

1.4 Morphological plasticity of *C. albicans*

C. albicans is a diploid polymorphic fungus, which has unique characteristics to switch from one morphological form to another (Fig. 1). It can exist in different vegetative forms, such as unicellular yeast, as pseudohypha or true hypha, depending on different environmental conditions (Sudbery *et al*., 2004). Yeast cells have oval-shaped morphology and divide by axial and bipolar budding. Pseudohyphal and hyphal cells typically grow in a polarised manner and

are attached end-to-end, such that subsequent rounds of cell division produce long multicellular filaments that may develop side branches. Pseudohyphal cells are ellipsoidal and have constrictions at the septal junctions, while hyphal cells have true septae that lack constrictions (Sudbery 2011). Apart from these growth forms, in nutrient starving conditions, *C. albicans* can also form chlamydospores, which are thick-walled cells that are typically formed at the ends of hyphal filaments (Staib and Morschhäuser 2007). Under zinc deprivation *C. albicans* forms gigantic cells namely goliath cells (Malavia *et al.*, 2017). Recently, a new phenotype was discovered for *C. albicans*, known as GUT (gastrointestinal induced transition), which are cells with large elongated morphology; this morphoform can be induced by consistent exposure to gastrointestinal (GI) tract by overexpression of the Wor1 regulatory protein (Pande *et al*., 2013). GUT cells suppress the propensity for tissue invasion and exhibit enhanced competitive fitness to colonise the GI tract of mice (Pande *et al*., 2013). Importantly, a detailed morphological observation of clinical isolates of *C. albicans* had revealed two distinct cellular morphologies of *C. albicans* named *white* and *opaque* cells (Slutsky *et al*., 1987). White yeast cells form creamy white colonies on solid media and microscopically are identical to *S. cerevisiae* in appearance. Comparatively, opaque cells form slightly dark and flattened colonies on agar surfaces but have a rod-like morphological appearance that carries protuberances (“pimples”) on the cell surface. In addition to the white and opaque cells, a *grey* cell phenotype was recently identified by in-vitro studies (Tao *et al*., 2014). Grey cells are smallest in size compared to all other cell types of *C. albicans*. Excluding the chlamydospore and goliath cell types, all the morphological forms mentioned above have significant roles either in host colonisation, infection and pathogenicity of *C. albicans* (Noble *et al*., 2017, Thompson *et al*., 2011). The different morphological forms of *C. albicans* are depicted in Fig.2.

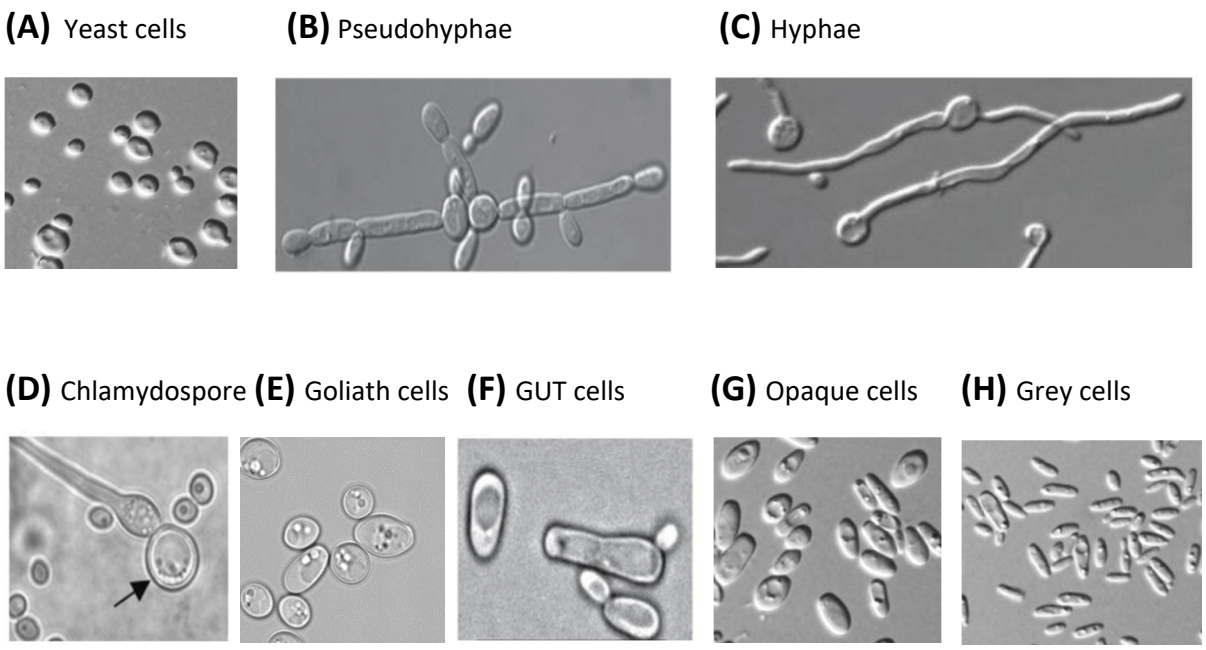

Fig. 2 : Different cell types of *C. albicans* : Yeast (A), pseudohyphae (B) and hyphae (C) morphology are observed in clinical samples from candidiasis patients; Chlamydospore and Goliath cell morphologies (D) and (E) were identified under nutrient starvation conditions. GUT cells (F) are highly efficient for GI tract colonisation. Opaque cell morphology (G) was observed on skin surfaces and *in vitro*; Grey cell morphology (H) was identified during *in vitro* studies. Images (A), (B), (C)were taken from Sudbery *et al*., 2011, (D) from Hickman *et al*., 2013 , (E) from Malavia *et al*., 2017, (F) from Pande *et al*., 2013, (G) and (H) from Tao *et al*., 2014.

1.5 Virulent attributes of *C. albicans*

During the course of infection *C. albicans* can colonize various host niches with drastically varying conditions with regard to nutrient availability, pH, oxygen and CO_2 levels (Silva Dantes *et al*., 2016). Such remarkable adaptability of *C. albicans* is incomparable with other non-pathogenic yeasts such as *S. cerevisiae,* which shares more than 50 % similarity in coding regions within its genome (Jones *et al*., 2004). Comparative genomic tools have shed light on enrichment of gene families: 10 secreted aspartyl proteases, 10 lipases, 8 oligo peptide transporters and 9 adhesins are unique to *C. albicans*. This high redundancy within gene families potentially empowers the organism to thrive in harsh *in vivo* conditions (Butler *et al*., 2009). More importantly, in recent years, several studies have identified multiple virulence traits of *C. albicans*, which enables the pathogen to survive in various host niches during infection (Mayer *et al*., 2013). Some of the important virulent attributes are described below.

1.5.1 Polygenic traits: Partners in crime

One of the essential aspects for commensalism and pathogenesis of *C. albicans* is to adhere to host tissue and abiotic surfaces. This is achieved by the adhesin gene (ALS) family which codes for glycosylphosphatidylinositol cell surface proteins (Als1-9). Adhesins facilitate attachment to biotic and abiotic surfaces (Phan *et al*., 2007, Wachtler *et al*., 2011, Murciano *et al*., 2012). *ALS3* a member of adhesin gene family that is highly upregulated during infection and is essential for virulence (Cheng *et al*., 2005, Naglik *et al*., 2011). Hwp1 is a GPI anchored adhesin that is another cell wall component of *C. albicans,* which facilitates adhesion to epithelial cells (Staab *et al*., 1999, Sundstrom *et al*., 2002). Following the adhesion to host cells, *C. albicans* can invade either by induced endocytosis or by active penetration. To initiate induced endocytosis, fungal cell surface invasin (Ssa1) binds to host receptors (E-cadherin or N-cadherin) and triggers engulfment of the fungal cell into host cells (Sun *et al*., 2010). However, for active penetration into host tissues, *C. albicans* undergoes yeast-to-hyphal morphogenesis. During this morphological transition, the *ECE1* gene is highly expressed, which codes a polyprotein that is processed by serine protease resulting into a potent toxin known as candidalysin, it permeabilizes the epithelial cell membranes causing cell lysis and damage of host tissue (Moyes *et al*., 2016). Under these conditions, *C. albicans* also can secrete proteases (Sap 1-10) and lipases (Lip1-10) to enhance the process of active penetration into the host cells (Wachtler *et al*., 2012 and Mayer *et al*., 2013). After active penetration into epithelial tissues, *C. albicans* can enter the bloodstream and switch its morphology back to the yeast from to facilitate dissemination into different organs. Blood can act as a rich source of glucose (4-7 mM) and other essential nutrients, although most host microenvironments contain heterogeneous carbon sources. Interestingly, *C. albicans* lacks catabolite repression resulting in remarkable metabolic flexibility by simultaneously utilizing simple carbon sources such as glucose, as well as complex carbohydrate sources to efficiently promote host colonisation and thereby of virulence of *C. albicans* (Childers *et al*., 2016, Miramon and Lorenz 2017). In specific niches, the human host induces nutritional immunity and starves colonising pathogens for essential micronutrients, such as iron, zinc and copper (Potrykus *et al*., 2014). To counter these activitities *C. albicans* expresses high affinity transporters (Rbt5/Als3 for Iron and Zrt1/Zrt2 for Zinc) to increase the assimilation of micro-nutrients (Crawford and Wilson 2015). During infection, *C. albicans* is often recognized by

phagocytes such as macrophages through Pathogen Recognition Receptors (PRRs) that interact with Pathogen Associated Molecular Patterns (PAMPs) on cell surface of *C. albicans*. Subsequently, the fungal cells are engulfed and directed to phagosome vesicles, which fuse with lysosomes to generate mature phago-lysosomes. These produce lethal oxidants such as reactive oxygen species, reactive nitrogen species and antimicrobial peptides to kill the engulfed fungal cells (Erwig and Gow 2016). To escape from such a fatal environment, *C. albicans* undergoes the yeast-to-hyphal transition and induces a lytic type of cell death by triggering inflammatory caspases, which rupture the host cell membrane and release intracellular contents (this type of host cell death is known as pyroptosis) (Uwamahoro *et al*., 2014, Wellington *et al*., 2014). Apart from these mechanisms, to escape from host immune recognition, *C. albicans* is also capable to mask its cell wall component β-glucan by a thick but permeable layer of mannans, β-glucan is immunogenic in nature and induces strong pro-inflammatory responses (Wheeler *et al*., 2008, Netea *et al*., 2006). Recent studies have shown that *C. albicans* tolerates translational ambiguity at CUG codon that generates structural variability in cell surface proteins, which influences recognition of fungal cells by immune cells (Miranda *et al*., 2013, Simoes *et al*., 2016). Furthermore, *C. albicans* can switch from white to opaque cell morphology; opaque cells are relatively resistant to phagocytosis (Lohse *et al*., 2009, Sasse *et al*., 2013). By using mouse models to study fungal infection, accumulating evidence has indicated that the white cell morphology might enable *C. albicans* to disseminate to host internal organs via the bloodstream, where it can undergo morphogenesis to grow invasively into deeper tissues (Si *et al*., 2013). In comparison, cells with opaque cell morphology are especially competent to adhere to the skin surface (Xie *et al*., 2014). Recent results using an *ex vivo* model for tongue infection have found a high level of fitness for fungal cells with a *grey* morphology (Tao *et al*., 2014). The currently known virulent attributes of *C. albicans* are depicted in Fig. 3.

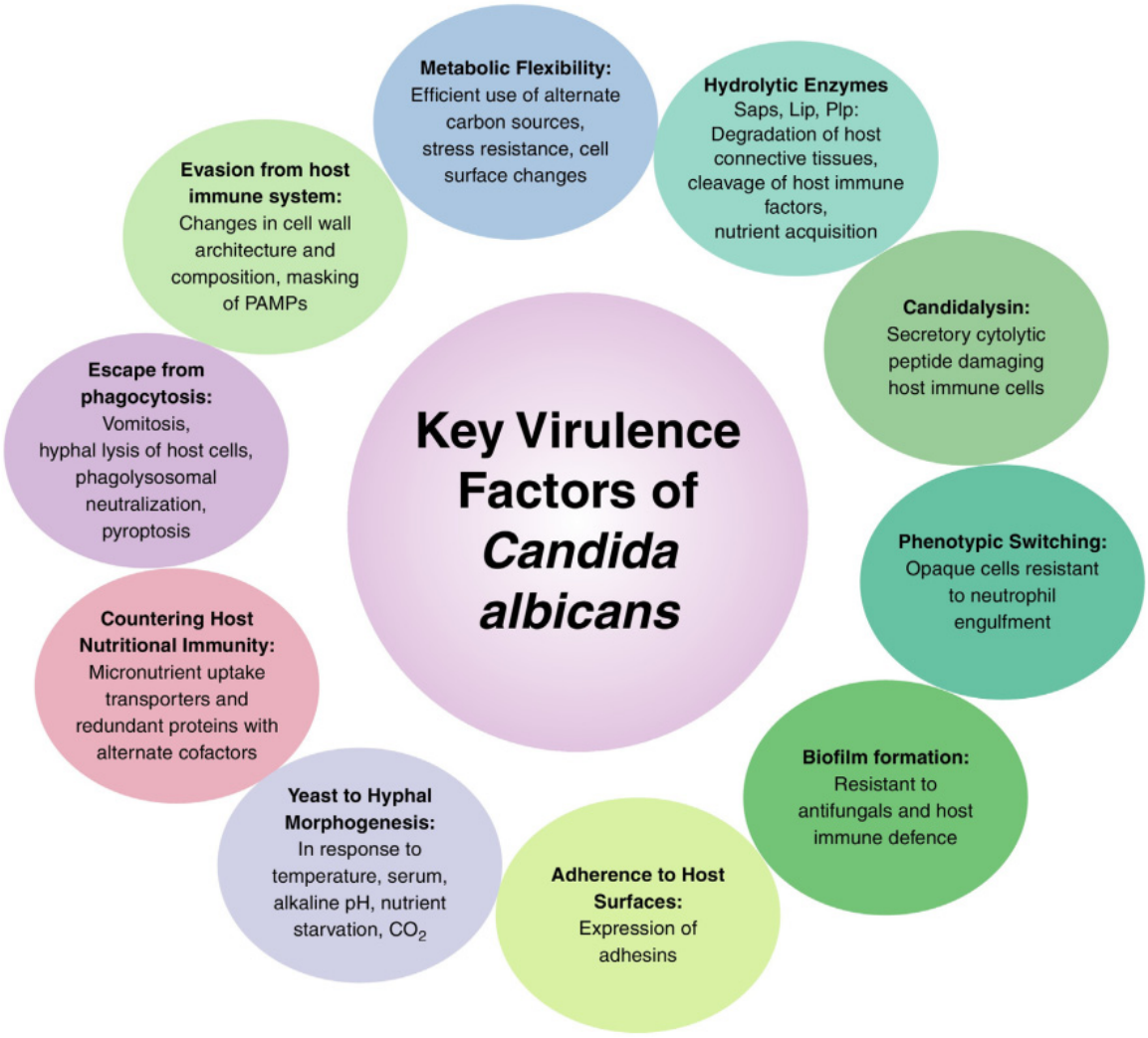

Fig. 3: The eminent attributes of *C. albicans* virulence and their implication in host colonisation and pathogenesis. (Picture taken from Dantes *et al*., 2016)

1.5.2 Dimorphism: A potent arsenal for virulence

The first experimental evidence to establish the correlation between morphology and virulence in *C. albicans*, was done by constructing transcription factors mutants (*efg1 cph1*), which are defective in filamentous growth and are unable to form hyphae in inducing conditions. These strains, which are locked in yeast morphology, were avirulent when tested in the mouse model of systemic candidiasis (Lo *et al*., 1997). These mutants were also susceptible to macrophages. Similarly, *C. albicans* mutants strains (*tup1*) locked in hyperfilamentous form, also displayed attenuated virulence (Braun *et al*., 2000). Moreover, when the expression of *NRG1* (a transcription factor), which represses the yeast-to-hyphal transition, was augmented using inducible promoters, the cells were locked in yeast morphoform, these strains were able to disseminate into various organs, but were completely

avirulent (Saville *et al*., 2003). Conversely, *C. albicans* strains overexpressing *UME6* that promotes yeast-to-hyphal transition, formed strong filaments under in vivo conditions and displayed enhanced virulence and damage of host tissue (Carlisle *et al*., 2009). These studies highlight the link between morphology and virulence. Another independent study (Zheng *et al*., 2004) showed that deletion of a G1 phase specific cyclin gene, *HGC1*, abolishes filamentation and reduced virulence. In 2010, a large scale homozygous mutant library was constructed by Noble group, targeting 674 coding genes, in the same study 115 infectivity attenuated mutants were identified, out of these around 40 mutants displayed defects in yeast to hyphal transition (Noble *et al*., 2010). Interestingly, the Kumamoto group (White *et al*., 2007) put forth first evidence that the yeast morphology of *C. albicans* is associated with commensalism. In this study, mice were orally fed with *C. albicans* strains, the fungal strains colonised the GI tract without causing infection and were tolerated by mice. The histopathological sections of gut regions of mice revealed that more than 90% of fungal cells were of yeast morphology. However, clinical samples of patients suffering from candidiasis have shown the presence of *C. albicans* cells in yeast, as well as hyphal morphology (Guarner and Brandt 2011). Hence it is plausible that the yeast morphoform is associated with virulence by facilitating rapid dissemination through the blood into different organs during systemic infection, while it also favours a commensal lifestyle in the gut (Thompson *et al*., 2011). On other hand, hyphal cells invade epithelial and endothelial cell layers and can also cause lysis of phagocytic cells (Gow and Hube 2012). Hence, existing in yeast or hyphal morphoform might benefit *C. albicans* to survive or to escape from specific host niches. (Fig. 4).

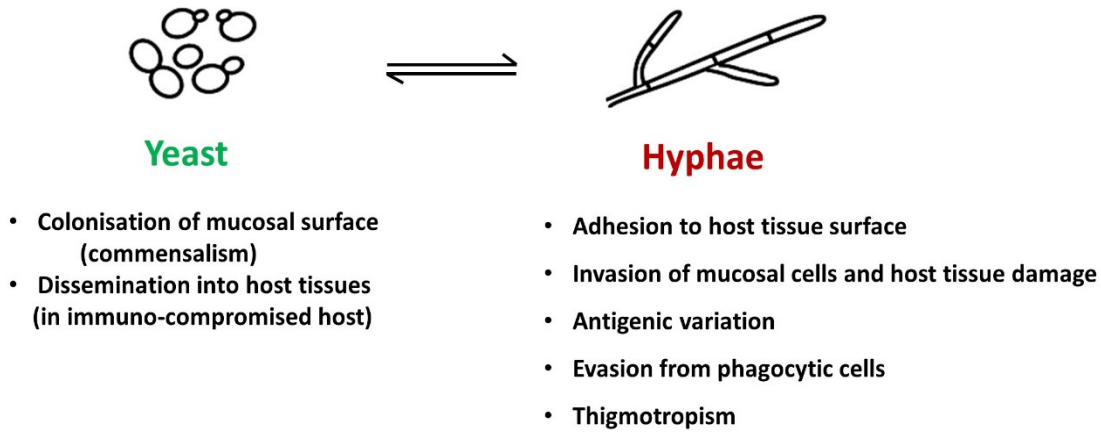

Fig. 4 : Relationship between morphology and virulence in *C. albicans.* Yeast and hyphal morphologies have important roles in commensal and virulent life styles of *C. albicans.* Scheme taken from Thompson *et al*., 2011.

1.6 Interaction with immune system: Recognition of yeast and hyphal morphology

In order to protect the human host from invading pathogens, the immune system functions by different mechanisms: innate and adaptive immune responses (Verma *et al*., 2015). The initial steps to generate innate immune responses against invading fungal cells are orchestrated by phagocytes. Phagocytes appear to act as a main line of defence against fungal pathogens, because clinical patients with impaired functioning of phagocytes are at major risk of fungal infections (Horn *et al*., 2009). Hence multiple studies have focused on cellular processes involved in phagocytosis of fungal cells. Firstly, the phagocytes (macrophages and neutrophils) migrate to the site of infection by chemotaxis. Secondly, through physical interaction with the fungal cell surface components (PAMPs), phagocytes recognise the fungal pathogens through PRRs. Lastly, the phagocytes engulf and kill the fungal pathogens by generating toxic environment in mature phagolysosomes (Dantes *et al*., 2016, Erwig and Gow 2016). Processes involved in recognition and engulfment of fungal cells by phagocytes are influenced by multiple factors. Fungal cell size, morphology and cell wall composition are the key elements that can hinder the recognition process of phagocytes. The average diameter of the yeast morphoform is 5-10 µm, which can be readily engulfed by macrophages, while hyphal cells are considerably bigger (average length from 20-50 µm) which hinders the uptake process of hyphal cells by macrophages (Lewis *et al*., 2012). The cellular morphology of *C. albicans* also acts as a crucial factor for recognition by phagocytes and immune cells, because cells with yeast and hyphal morphology vary significantly in the representation of PAMPs on the cell surface (Jacobsen and Hube 2012, Richardson and Naglik 2018). Also, it has been shown that the cellular response of phagocytes can vary depending on the immunogenic potential of PAMPs on yeast and hyphal cell surfaces (Moyes *et al*., 2010). Moreover, the composition and organisation of fungal cell wall components are also determining factors for immune recognition and response (Gow and Hube 2012, Erwig and Gow 2016). The main cell wall components of *C. albicans* comprise a layer containing *O*- linked and *N*-linked mannans and an inner layer consisting of β-1,3 and β-1,6 glucans, as well as chitin (Gow *et al*., 2011). β-glucans are extremely immunogenic in nature and constitute a potent fungal recognition signal by phagocytes, leading to augmented immune responses and recruitment of neutrophils (Netea *et al*., 2006, Hall *et al*., 2013). Hence masking of β-glucans by outer mannan layers impedes the process of immune recognition. However, immune recognition

of hyphal cells is considerably distinct from yeast recognition, as the cell wall composition differs in both morphoforms. Several cell wall proteins, such as Hwp1 (hyphal wall protein-1), Hyr1 (hyphally regulated protein-1), Als3 (agglutinin like sequence-3) and Ssa1 (a member of HSP70 chaperone family) are only observed on the surface of hyphal cells (Gow *et al*., 2011). In addition to this, hyphal mannans vary structurally from yeast mannans (Lowman *et al*., 2014). Hence there are major differences in PAMPs associated with yeast and hyphal cells of *C. albicans*. Matching these variations of the fungal cell surface, multiple host cell receptors known as pathogen recognition receptors (PRRs) exist, which can specifically recognise fungal PAMPs. Several PRRs, toll like receptors (TLRs), C type lectin receptors (dectin-1 and dectin-2) and recently identified ephrin type-A receptor (EphA2) can act independently upon interaction with fungal PAMPs to induce pro-inflammatory antifungal responses to eliminate yeast and hyphal cells (Gow *et al*., 2011, Swidergall *et al*., 2017, Richardson and Naglik 2018). In in vitro experiments, neutrophils migrated rapidly towards uptake of yeast cells, while slowly migrating macrophages were left with germinating hyphal cells and thus showed a delayed response and uptake (Rudkin *et al*., 2013). More interestingly, a study from the Naglik group (Moyes *et al*., 2010) has shown that the immune system can differentiate between a non-invading fungal colonisation (commensalism) from *Candida* invasion (pathogenesis). Once yeast and hyphal cells are in contact with epithelial cells, can induce activation of NF-kB in host cells and the initial MAPK response, which also results in the activation of the c-Jun transcription factor, but only the hyphal cells could stimulate a secondary MAPK response and activate the c-Fos transcription factor, generating a proinflammatory cytokine response (Moyes *et al*., 2010). The MAPK/MKP1/c-Fos response is strongly dose-dependent, indicating that a threshold level of activation needs to be reached before epithelial cells are fully activated (Moyes *et al*., 2010). The differential recognition of yeast and fungal cells by immune system are highlighted in Figure 5.

Upon exposure to fungal pathogens, the host immune system can also initiate adaptive immune responses. Dendritic cells, upon interaction with *C. albicans*, can lead to activation of $CD4^+$ T helper cells (T_H4 cell) cells and regulatory T cells (T_{reg} cell) (Erwig and Gow 2016). Th_4 cells can differentiate into T_H1 cells to orchestrate antifungal immune responses by releasing the proinflammatory cytokines IFN-ϒ, TNF-α and GM-CSF. Proinflammatory cytokines play critical roles in generating immune defence against *C. albicans* (Richardson and

Immune recognition and responses	Yeast morphology	Hyphal morphology
PAMPs	Ywp1, β-glucans and yeast cell specific mannans	Als3, Hwp1, Hyr1, Ssa1, Candidalysin and fungal cell specific-mannans
PRRs	Dectin-1 and EphA2	E-Caderin, EFGR, EphA2, Dectin-1, Dectin-2 and TLRs
Neutrophil (Phagocytosis/ killing)	High / Efficient	Strong/ Efficient
Macrophage (Phagocytosis/ killing)	High / Efficient	Low / Efficient
Dendritic cells (Phagocytosis/ killing)	High/ High	High/ Moderate
Epithelial cells (Activation of NF-κB and c-Jun)	Yes	Yes
Epithelial cells (Activation of Pro-inflammatory cytokines)	No	Yes, Dose dependent

Fig.5: Morphology-dependent interaction of host cells with *C. albicans*: Immune system differentially recognises yeast and hyphal cells of *C. albicans*. PAMPs: Pathogen associated molecular patterns, present on yeast or hyphal cell surfaces. PRRs: Pathogen recognition receptors are present on host cells which recognise PAMPs. Figure modified from Jacobsen *et al*., 2012.

Moyes 2015). The IFN-Ɣ cytokine induces activation of macrophages, enhances processing and presentation of antigens on dendritic cells and can also prompt antibody class switching in B cells, which is associated with antifungal properties (Lin *et al*., 2015). Activation of T_H17 cells (a subset of $CD4^+$ T helper cells) is considered to be pivotal for host defence against fungal pathogens (Ferwerda *et al*., 2009, Conti *et al*., 2009). T_H17 cells can recruit neutrophils at the site of infection by prompting the release of CXC chemokines (Hernandez-Santos and Gaffen 2012). T_H17 cells also generates the potent anti-fungal cytokines IL-17A, IL-17F and IL-22 (Naglik *et al*., 2017). IL-17 induces keratinocytes and epithelial cells to produce anti-microbial peptides and histatins with high antifungal activity (Liang *et al*., 2006, Conti *et al*., 2011).

1.7 Mammalian host environmental cues and influence on *C. albicans*

Mammalian hosts provide dynamic environments, which can be very hostile for colonising microorganisms. Availability of micronutrients, complex carbon sources, body temperature, immune cells, exposure to serum, competition with human microflora, as well as the presence or absence of O_2, CO_2, N-acetylglucosamine, peptidoglycan and other micronutrients can influence the growth of *C. albicans* (Noble *et al*., 2016). However, as *C. albicans* has evolved in close association with its human host, it is adapted to restraining *in vivo* conditions, which either induce stress or nutrient starvation. *C. albicans* has evolved with signalling pathways to sense stress-inducing conditions and generate signals necessary for stress-resistance and often induces expression of hypha-specific genes to undergo morphological switching (Sudbery *et al*., 2011). To clarify the underlying processes involved in morphological transitions occurring during host colonisation by *C. albicans*, it is important to identify the role of fungal morphogenetic regulators that are influenced by specific host niches or environmental cues.

1.7.1 Hypoxia: An underappreciated host associated factor

Molecular oxygen is important for cellular metabolism in eukaryotic organisms, as oxygen acts as an electron acceptor during mitochondrial respiration to generate chemical energy. Also, it is required for biosynthesis of sterols, unsaturated fatty acids and other metabolic processes (Summons *et al*., 2006, Raymond *et al*., 2006). The normal atmospheric level of O_2 is around 21 % (pO_2 of 159, Hg at sea level). However, the availability of free or dissolved oxygen in body fluids within the mammalian host is much lower compared to the atmospheric levels (Carreau *et al*., 2011). *C. albicans* thrives in host niches known to be oxygen-poor and oxygen depletion occurs often during colonization of mucosal surfaces, interaction with host cells, invasion of epithelia, engulfment by phagocytes and invasion into other internal organs (Fig.6) (Ernst and Tielker 2009, Grahl *et al*., 2012). The oxygenation profile in different organs of the human host is highlighted in Figure 6. The normal niche for commensal *C. albicans* is the human gastrointestinal tract, which has lower levels of O_2 (< 1%) (Karhausen *et al*., 2004). Also, within the site of infection and inflammation the oxygen levels are rapidly depleted, due to decreased tissue perfusion (Eltzchig and Carmeleit 2011). It is evident that *C. albicans* adapts to varying level of hypoxic conditions during host colonisation. However until today, the molecular mechanism that orchestrate the adaptation of *C. albicans* to hypoxic conditions

Host organs	pO2	
	mmHg	%
Air	160	21.1
Lungs	42.8	5.6
Alveoli	110	14.5
Arterial Blood	100	13.2
Venous Blood	40	5.3
Within host Cell	9.9	1.3
Brain	33.8	4.4
Skin (Superficial region)	8	1.1
Intestinal Tissue	57.6	7.6
Liver	40.6	5.4
Kidney	72	9.5

Fig. 6: Oxygen levels (pO_2 partial oxygen pressure) of various host organs and cells (modified from Ernst and Tielker 2009 and Carreau *et al*., 2011 **)**

are poorly understood. Hypoxia can also regulate host innate immune responses. Hypoxia inducible factor-1 (HIF-1), a transcription factor, which is hydroxylated in aerobic conditions and subsequently degraded; in the absence of oxygen, however, it is stable and induces hypoxic gene expression (Semenza *et al*.,2007, Simon and Keith 2008). HIF-1 functions downstream of dectin-1, which is a host cell receptor for fungal β-glucans (PAMP) (Cheng *et al*., 2014). Activation of dectin-1 leads to elevated levels of HIF-1, which facilitates immune responses by promoting cell activation and initiating pro-inflammatory responses. The concomitant release of cytokines leads to recruitment of further innate immune cells and effector cells for the cell-mediated immunity (Imtiyaz and Simon 2010). Therefore, hypoxia within a site of infection can influence the physiology of both *C. albicans* and immune cells and significantly affect the outcome of fungus-host interactions.

1.7.2 Exposure to carbon dioxide

The concentration of carbon dioxide in mammalian host can vary based on the anatomical sites. For e. g. during skin colonisation, *C. albicans* is exposed to lower levels of CO_2 (0.03%), but during host invasion CO_2 concentration can drastically increase up to 150 fold higher (5%) (Bahn and Muehlschlegel 2006). Also during colonisation *C. albicans* can metabolically generate CO_2, which can act as a signalling molecule to induce filamentous growth and virulence (Klengel *et al*., 2005, Hall *et al*., 2010). CO_2 in milieu can induce white-opaque switching and facilitate mating in *C. albicans* (Ramirez-Zavala *et al*., 2008 Huang *et al*., 2009). These studies indicate that, CO_2 can exert an influence on growth, metabolism and morphological switching in *C. albicans*. Therefore, sensing the alterations in the CO_2 levels in microenvironments is critical for *C. albicans* for host colonisation and pathogenesis. Abnormally elevated levels of CO_2 (also known as hypercapnia) can hamper the host innate immune response and dysregulate expression of cytokines and chemokines, this may indirectly benefit the colonising pathogen (O'Croinin *et al*., 2008, Gates *et al*., 2013).

1.8 Regulation of Morphogenesis

In *C. albicans*, three different signalling pathways are mainly involved in sensing different environmental cues and generating cellular responses to regulate hyphal morphogenesis. A schematic representation of major signalling pathway is depicted in Figure 7.

1.8.1 Signalling pathways

i) cAMP-PKA Pathway : The PKA pathway is one of the major signalling pathways conserved in eukaryotes, which plays a central role in growth, morphogenesis, *white-opaque* switching and virulence of *C. albicans* (Sonneborn *et al*., 2000, Bockmuhl *et al*., 2001, Biswas et al., 2007; Whiteway and Bachewich, 2007; Sudbery, 2011). The rapid changes in the environment are sensed by the Ras1 protein, which is localised at the plasma membrane of *C. albicans* (Piispanen *et al*., 2011); activation of Ras1 occurs by Cdc25 (guanine exchange factor), which stimulates the production of the secondary messenger cAMP (3'-5'-cyclic adenosine monophosphate) produced by adenylyl cyclase Cyr1 (Fang *et al*., 2006). Cyr1 contains highly conserved functional domains, which act as sensors for external signals such as peptidoglycan, CO_2, pH and temperature (Wang, 2013). Cyr1 is the only adenylyl cyclase

that synthesizes cAMPs in response to external signals. Homozygous mutants of *ras1* and *cyr1* in *C. albicans* are defective in filamentation and show highly attenuated virulence in the murine model of systemic infection (Feng Q *et al*., 1999, Rocha *et al*., 2001). Increased intracellular cAMP leads to dissociation of the regulatory subunit Bcy1 of protein kinase A and causes activation of catalytic subunits Tpk1 and Tpk2 (Sonneborn *et al*., 2000, Bockmuhl *et al*., 2001). Although kinases Tpk1 and Tpk2 have redundant roles in growth and phenotypic switching, Tpk1 mainly contributes to filamentation on solid medium, while Tpk2 is involved in hyphal growth in liquid medium (Sonneborn *et al*., 2000, Bockmuhl *et al*., 2001). Tpk2 phosphorylates a threonine residue (T206) in the APSES domain of the major transcriptional regulator Efg1 (Sonneborn *et al*., 2000, Bockmuhl *et al*., 2001). The activated form of Efg1 can initiate the induction of hypha-specific genes and other downstream transcriptional factors that play important roles in initiation and maintenance of filamentation (Stoldt *et al*., 1997, Biswas *et al*., 2007, Lassak *et al*., 2011).

ii) MAPK Pathway: Four different signalling pathways comprise MAP (mitogen-activated protein) kinase Mkc1, Cek1, Cek2 and Hog1, which are involved in sensing and transmitting responses of cells to different environmental cues (Monge *et al*., 2006). These pathways are mainly involved in generating cellular responses to changes in the growth medium, nutrient starvation, oxidative and osmotic stress, low temperature, pheromones and cell wall stress (Monge *et al*., 2006 Biswas *et al*., 2007). Mkc1 kinase is primarily involved in biogenesis of the cell wall and regulates filamentation, while Hog1 kinase mainly participates in generating responses to osmotic and oxidative stress. The Cek1-MAPK pathway has been shown to be involved in mating and filamentation. The Cek1- MAPK signal transduction pathway consists of a conserved set of kinases: Ste11 (a MAPKKK- mitogen-activated kinase kinase kinase), Hst7 (MAPKK- mitogen-activated kinase kinase) and Cek1 (MAPK- mitogen-activated kinase). The signalling of these kinases can be triggered by the three upstream transmembrane sensors Sho1, Msb2 and Opy2 (Herrero-de-Dios *et al*., 2014, Szafranski-Schneider *et al*., 2012). These sensors can integrate signals via GTPase Cdc42 and downstream protein kinase Cst20 (Ushinsky *et al*., 2002). Once Ste11 is activated via Cst20, it leads to three phosphotransfer steps, where the MAPKKK becomes phosphorylated and is followed by a cascade of phosphorylation, which eventually causes augmentation in the phosphorylated form of Cek1. These events are followed by activation of the downstream transcription factor Cph1.

Depending upon the upstream signal, Cph1 induces filamentation on solid medium (Liu *et al*., 1994), regulate genes involved in mating (Magee *et al*., 2002) or can generate transcriptional responses to quorum sensing molecules (Lin *et al*., 2013). Cph1 can also induce genes involved in galactose metabolism (Martchenko *et al*., 2007). Defects in the function of Cek1 kinase or in the regulation of its MAPK pathway leads to misregulation of filamentation and attenuated virulence (Csank *et al*., 1998). The MAPK-Cek1 pathway is also activated under nitrogen stress conditions using the ammonium permease Mep2 to activate filamentation (Biswas and Morschhauser 2005). Recently, Cph1-dependent MAPK signalling was also shown to be involved in white-opaque phenotypic switching in *C. albicans* (Ramírez-Zavala *et al*., 2013).

iii) RAM pathway: The "regulation of Ace2 and morphogenesis" (RAM Pathway) signalling pathway is involved in modulation of polarised growth, daughter cell separation and bud development of *C. albicans* (Saputo et al., 2012). Ace2 is a transcription factor that functions downstream of kinases Kic1 and Cbk1 in the RAM pathway (Song *et al*., 2008, Gutiérrez-Escribano *et al*. 2011). Kic1 phosphorylates Cbk1 kinase, which in association with its activator Mob2, regulates the Ace2 transcription factor (Gutiérrez-Escribano *et al*. 2011). During cell division, Ace2 localizes to daughter cells and drives expression of daughter cell-specific genes (Weiss 2012). Ace2 also regulates expression of chitinase and glucanase, which are involved in septum degradation and cell separation during the final steps of mitosis (Song *et al*., 2008). The cellular localisation and function of Ace2 is dependent on Cdc14, which is a cyclin-dependent phosphatase (Sanchez-Diaz *et al*., 2012). All the components of the RAM pathway contribute to regulation of genes involved in cell separation. The deletion of kinases *KIC1* and *CBK1*, or of *ACE2*, causes severe defects in cell separation, which generates a characteristic mutant phenotype consisting of a large lump of aggregated cells that are difficult to disintegrate (Saputo *et al*, 2012). Ace2 protein is found in two isoforms: a full-length form Ace2L, involved in septin ring formation during hyphal development that blocks cell separation, and the short form Ace2S that regulates the expression of cell separation genes (Calderon-Norena *et al*., 2015). In *C. albicans, ace2* mutants are sensitive to cell wall stress and display impaired virulence in the mouse model of systemic infection (Maccallum *et al*., 2006). The involvement of Ace2 in filamentation is dependent on specific growth conditions. *ace2* mutants form normal hyphae in the presence of serum, but show delayed hypha formation, when grown on Spider or Lee´s medium (Saputo *et al*., 2014). Interestingly, *ace2*

mutants display severe defects to induce filamentation under microaerophilic or hypoxic conditions (Mulhern *et al*., 2006, Saputo *et al*., 2014; van Wijlick *et al.*, 2016). Hence under hypoxic conditions, Ace2 is essential for filamentation. Furthermore, Ace2 increases expression of glycolytic genes and supresses expression of respiratory genes under hypoxia (Mulhern *et al*., 2006). Ace2 also regulates biofilm formation depending on oxygen levels. Under normoxic growth conditions, Ace2 is required for induction of biofilm-specific genes, while under hypoxia, Ace2 has no influence on biofilm formation (Kelly *et al*., 2004, Stichternoth *et al*., 2009). Functioning of the RAM pathway can also be influenced by components of the PKA pathway, as Tpk1 and Tpk2 kinases can suppress expression of Ace2 (Saputo *et al*., 2014). It was also shown that during the early stage of hyphal induction, cyclin-dependent kinase Cdc28, along with Hgc1 kinase, phosphorylates the transcriptional modulator Efg1 that represses the Ace2-mediated expression of cell separation genes (Wang *et al*., 2009). Taken together, these evidences suggest an antagonistic relationship of Efg1 and Ace2 during the initiation of the filamentation process, where Efg1 induces expression of hypha-specific genes, while repressing the Ace2-dependent expression of cell separation genes. In contrast, under hypoxic conditions, a reversal of roles is observed, as Efg1 functions as a repressor of filamentation under hypoxia (Setiadi *et al*., 2006), while Ace2 is required for induction of genes involved in filamentation. However it needs to be determined, how Ace2 influences the expression or activity of Efg1 to modulate filamentation under hypoxic conditions.

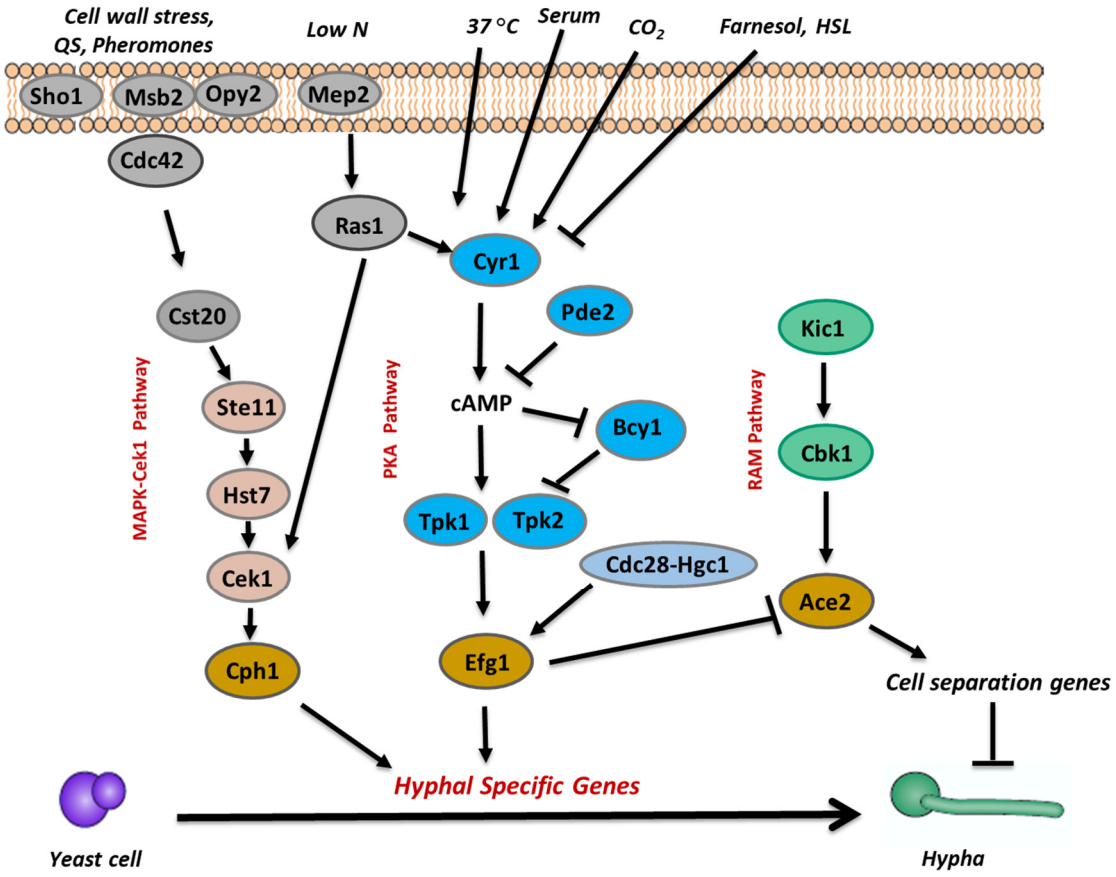

Fig. 7: Signal transduction pathway leading to expression of hypha-specific genes. The formation of hyphae in *C. albicans* is controlled by different signalling pathways that are activated by environmental cues. Shown are the 'mitogen activated protein kinase' (MAPK), the 'cAMP-dependent protein kinase A' (PKA) pathway and RAM (regulation of Ace2 and Morphogenesis) pathway which regulate filamentation. Protein colour coded as follows: MAPK pathway (pink), PKA pathway (blue), Ram pathway (green), transcription factors (yellow), other factors involved in signal transduction (grey). Modified from Herrero-de-Dios *et al*., 2014 and Sudbery, 2011.

1.8.2 Enhanced filamentous growth-1 (Efg1): A master regulator of multiple traits

Efg1 belongs to the ASPES family of transcription regulators, which have important roles in the regulation of morphogenesis in fungi. Under normoxia, Efg1 functions as a transcriptional activator of genes involved in filamentation, phenotypic switching, biofilm formation and chlamydospore formation in *C. albicans* (Stoldt *et al*., 1997, Braun and Johnson 1997, Sonneborn *et al*., 1999, Stichternoth *et al*., 2009). The cells lacking Efg1 show severe defects to form filaments upon exposure to serum under normoxia. It has been well established that

the function of Efg1 as an inducer of genes involved in filamentation is dependent on its phosphorylation status. Particularly, in response to environmental cues, Tpk2 and Cdc28-Hgc1 kinase (hypha specific G1 cyclin kinase) phosphorylates threonine residues at 206 and 179 of Efg1. Abolishment of phosphorylation at 206 and 179 residues of Efg1, hinders the filamentation process under normoxic conditions (Bockmühl and Ernst 2001, Wang *et al*., 2009). Efg1 directly regulates hypha-specific genes including *SAP4*, *SAP5*, *SAP6*, *ALS1*, *ALS3*, *HWP1*, *RBT1*, *RBT4*, *ECE1* and many other transcriptional regulator genes that are involved in maintenance of hyphal morphogenesis (Sharkey *et al*., 1999, Fu *et al*. 2002, Doedt T *et al*. 2004). Efg1 plays central role in maintaining cell wall architecture of *C. albicans* (Sohn *et al.,* 2003). Interestingly, cells lacking a single allele of *EFG1* showed changes in cell wall carbohydrate and protein composition of *C. albicans*. The heterozygous strains of *EFG1* also induced an altered the cytokine responses upon interaction with innate immune cells (Zavrel *et al*., 2012).

Genome-wide ChIP chip analysis of strains grown either in yeast- or filamentation-inducing medium revealed the DNA binding motif TATGCATA, which is specifically recognised by Efg1 (Lassak *et al*., 2011). Several promoter regions of genes involved in transcriptional regulation of morphogenesis (*TCC1*, *CZF1*, *NRG1*, *TEC1* and *EED1*) contain this Efg1 binding motif (Lassak *et al*., 2011). The Efg1-bound promoter regions in the genome of *C. albicans* were largely distinct during yeast and hyphal morphogenesis, highlighting the major shift in the transcriptional network of Efg1 in different growth conditions, which is mostly attained by differential phosphorylation of Efg1 (Bockmühl and Ernst 2001, Lassak *et al.,* 2011). The localization of Efg1 to the promoter of the encoding gene *EFG1* is observed in yeast growth and in hypha-inducing conditions. However, after inducing the transcriptional network necessary for hyphal initiation, Efg1 negatively regulates its own expression by downregulating the *EFG1* promoter activity (Lassak *et al*., 2011). Interestingly, the promoter region of *EFG1* is also occupied by Bcr1, Tec1, Ndt80, Brg1 and Rob1 transcriptional regulators during biofilm formation, indicating a complex rewiring of regulators requiring Efg1 for production of a dense biofilm architecture in *C. albicans* (Nobile *et al*., 2012). In addition to the involvement of Efg1 in the yeast-to-hypha transition and biofilm formation, Efg1 is also associated with phenotypic switching. The conversion of opaque to while cells is dependent on Efg1, as it is required for stable expression of white cell-specific genes and maintain

heritable white cell morphology. Deletion of *EFG1* blocks the cells in opaque cell morphology (Sonneborn *et al.,* 1999, Shrikantha *et al*., 2000, Noffz *et al*., 2008). Efg1 maintains white cell morphology by downregulating expression of *WOR1* (White-Opaque Regulator 1), a master regulator of opaque cell morphology. Once the expression *WOR1* is increased, Wor1 downregulates *EFG1* and induces white-opaque phenotypic switching. *WOR1* positively regulates its own promoter to maintain this high level of expression and allows stable inheritance of the opaque cells.

C. albicans strains lacking *EFG1* have defects in colonising the GI tract of mice (Pierce *et al*., 2012, Pierce *et al*., 2013). The availability of oxygen in the GI tract is poor; therefore, *C. albicans* is incessantly exposed to hypoxic conditions during gut colonisation. A transcriptomal analysis revealed that in *C. albicans* strains grown under hypoxia, the genes involved in respiratory metabolism are downregulated, whereas genes related to fermentative metabolism, especially glycolysis are upregulated (Setiadi *et al*., 2006). In addition, the expression of certain genes involved in fatty acid metabolism, ergosterol biosynthesis and stress response are upregulated under oxygen-poor conditions (Setiadi *et al*., 2006). Most of these metabolic adaptation were dependent on the hypoxic function of Efg1. Furthermore, Efg1 is required to prevent abnormal regulation of about 300 genes under hypoxia (Setiadi *et al*., 2006). In complete contrast to its normoxic function, Efg1 functions as a repressor of filamentation during hypoxic growth, as *efg1* homozygous mutants display hyperfilamentous growth under oxygen-poor environment at temperature ≤ 35°C (Setiadi *et al*., 2006; Noffz *et al*., 2008). These results indicate that Efg1 plays a crucial role in adaptation to hypoxic conditions, but molecular mechanisms and pathways related to Efg1 under hypoxic conditions are yet to be identified.

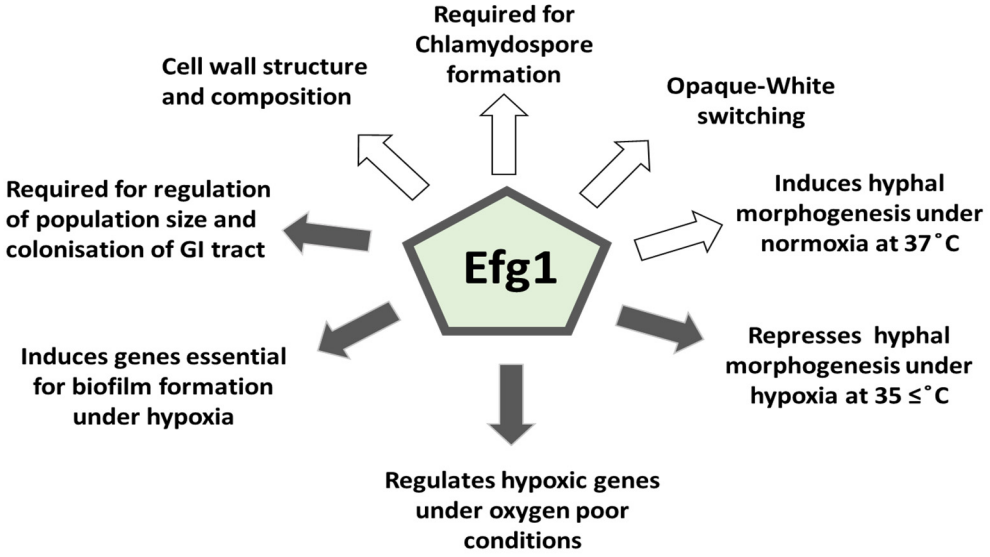

Fig. 8: Various cellular functions of Efg1 in *C. albicans* under normoxic and hypoxic conditions. Normoxic functions of Efg1 are highlighted with white arrows and hypoxic functions with grey arrows.

1.8.3 Transcriptional control of morphogenesis

In the yeast morphoform the expression of hypha-specific genes is negatively regulated by a protein complex consisting of transcriptional co-repressor Tup1 and the main transcriptional repressor Nrg1. The process of hyphal morphogenesis is achieved in two stages: hyphal initiation and hyphal maintenance (Lu *et al*., 2011, Lu *et al*., 2014). In response to environmental cues, the initial step is removal of filamentation repressor Nrg1 from the promoter region of hyphal-specific-genes. Following this process, the accessibility of promoter region of hypha-specific genes is increased for Brg1 (a GATA-transcription factor) that recruits histone deacetylase Hda1. Hda1 leads to chromatin remodelling and, in coordination with Brg1, promotes expression of hypha-specific genes. Subsequently, within the first 30 min of germ tube formation, the protein levels of Nrg1 are considerably decreased (Lu *et al*., 2011), but restored after 1 hour of hyphal induction to levels as in yeast cells (Lu *et al*., 2011, Lu *et al*., 2014). Hence to consistently maintain the filamentation process, once the expression of main hypha-specific genes is initiated, hypha-associated genes (HAGs), such as *UME6*, *EED1* and *HGC1*, are expressed ensuring the coherent expression of hypha-specific

genes (Basso et al., 2018). Ume6 a transcription factor induces expression of hypha-specific genes and downregulating *NRG1* (Banerjee *et al*., 2008, Carlisle and Kadosh 2010, Childers *et al*., 2015). Eed1 is required to form stable filaments, while its molecular function is largely unknown (Martin *et al*., 2011). Hgc1 is a cyclin dependent kinase, which is required for polarised growth by inhibiting the cell separation process in growing hyphae (Zheng *et al*., 2004). Consequently, strains lacking *UME6*, *EED1* or *HGC1* are able to initiate the filamentation process, but are unable to maintain polarised hyphal growth. Hence to maintain the expression of hypha-specific genes and to block the accessibility of repressor Nrg1 during maintenance of filamentation, expression of *UME6 and EED1* is essential. Also, a schematic representation of key events during hyphal initiation and maintenance is shown in figure 9.

In addition to Efg1 and Cph1, several transcription factors have been identified including Flo8, Czf1, Tec1 and Cph2, which can directly induce or positively affect the process of filamentation, (Brown *et al*., 1999, Lane *et al*., 2001, Schweizer *et al*., 2000, Cao *et al*., 2006). However, Ume6 appears to function downstream of all these transcriptional regulators, as overexpression of *UME6* induces filamentation process in all respective mutants, in inducing as well as non-inducing conditions (Banerjee *et al*., 2008, Clarlisle *et al*., 2009).

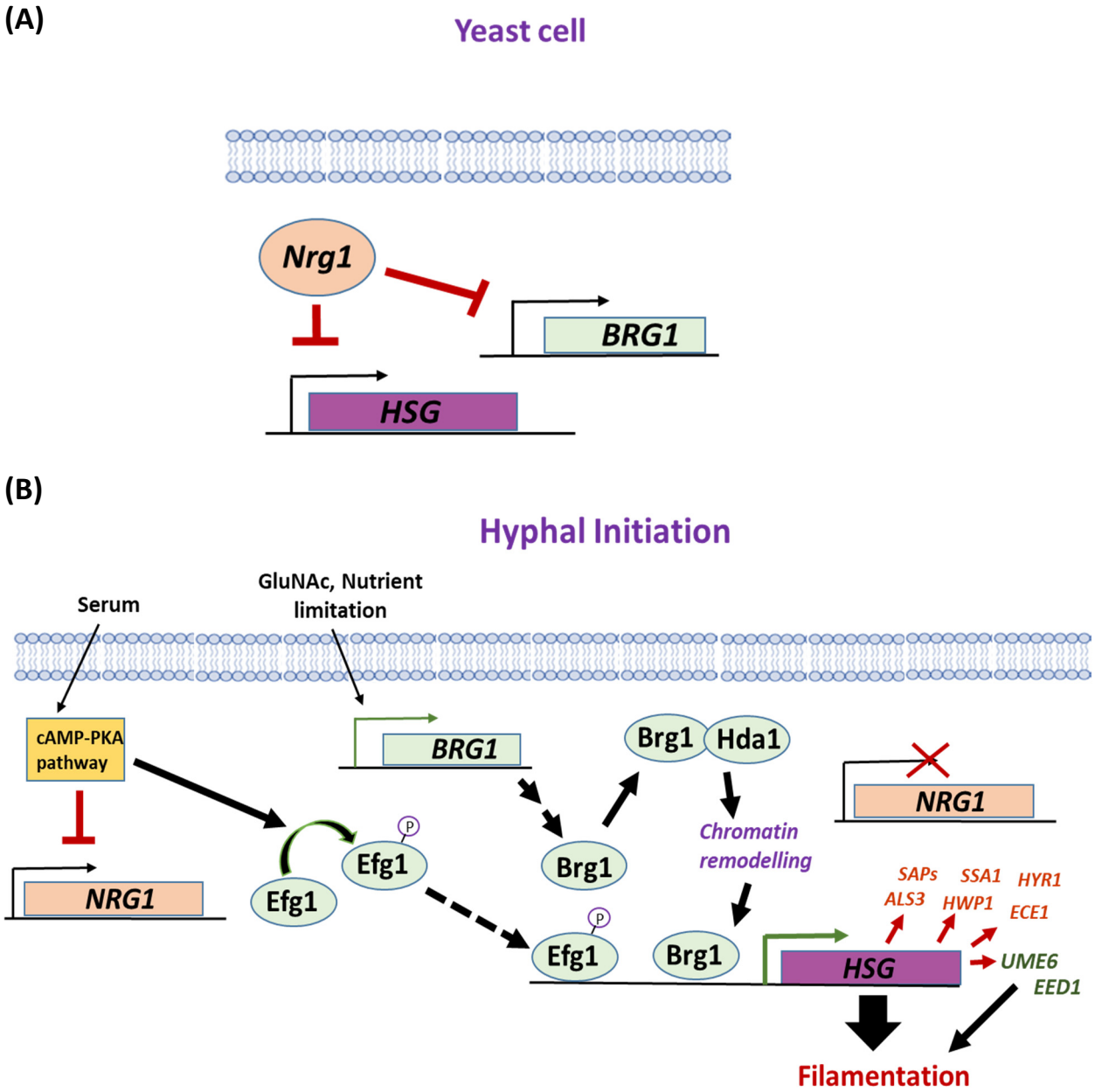
(A)
Yeast cell
Nrg1
BRG1
HSG
(B)
Hyphal Initiation
Serum
GluNAc, Nutrient limitation
cAMP-PKA pathway
BRG1
Brg1
Hda1
NRG1
Chromatin remodelling
Efg1
P
Efg1
Brg1
NRG1
SAPs
SSA1
HYR1
ALS3
HWP1
ECE1
Efg1
P
Brg1
HSG
UME6
EED1
Filamentation
(C)
Hyphal Maintenance
NRG1
Eed1
Ume6
Ume6
UME6
HSG

Fig. 9: Hyphal initiation and maintenance in *C. albicans*. (A) In non-inducing conditions, Nrg1 represses the expression of hypha-specific genes (HSGs) and Brg1. **(B)** Exposure to inducing conditions or environmental cues, such as presence of serum, GlcNAc or by nutrient starvation initiates hyphal morphogenesisHyphal initiation is characterized by a transient downregulation of Nrg1 via the cAMP-dependent PKA pathway and by activation of Efg1 by phosphorylation. The activated form of Efg1 can directly induce the expression of hypha- specific genes. Concurrently, environmental cues also induce expression of *BRG1*. Brg1 recruits Hda1 to promoter of HSGs, allowing chromatin remodelling that prevents Nrg1 binding to promotersof HSGs. Brg1 activates expression of HSGs (along with hypha-specific cell wall proteins). During expression of HSGs, genes essential for hyphal maintenance (*UME6*, *EED1*) are induced. **(C)** The hyphal maintenance is mainly governed by Ume6 and Eed1. Ume6 negatively regulates expression of *NRG1* and can induce its own expression along with consistent expression of HSGs under inducing conditions to form stable filaments. Although the molecular mechanism of Eed1 is yet to be identified, it is known to regulate *UME6* expression and is required for formation of stable filaments. Figure modified from Basso *et al*. 2018.

1.8.4 Growth and morphogenesis under host environmental cues

i) Metabolic adaptation to hypoxia: Hypoxic adaptation has been extensively studied in the yeast model organism *S. cerevisiae.* In *S. cerevisiae* under normoxic conditions (~21% O_2), Hap1 induces genes involved in respiration and promotes the biosynthesis of transcriptional repressors Rox1 and Mot3 that repress hypoxic genes by the action of the Tup1-Ssn6 complex (Mennella *et al*., 2003). Under hypoxic conditions, due limitation in haem biosynthesis, Rox1 and Mot3 expression is interrupted and expression of hypoxic genes are elevated (Becerra *et al*., 2002). Hypoxic conditions decreases production of ergosterols and studies in fission yeast *S. pombe* have revealed that upon depletion of sterols due to lack of oxygen, a precursor of Sre1 (a sterol regulatory elementary binding protein) migrates from the endoplasmic reticulum to the Golgi, where Sre1 is released by cleavage; Sre1 localizes to the nucleus and activates expression of several hypoxic genes (Hughes *et al*., 2005). In *S. cerevisiae*, homologues of the SREBP pathway are missing and transcription factor *UPC2* regulates genes involved in sterol biosynthesis under hypoxic conditions. Homologues of Sre1 have been identified in *Cryptococcus neoformans* and *Aspergillus fumigatus* and regulate hypoxic adaptation and virulence in these species (Willger *et al*., 2008, Chang *et al*., 2007 and Chun *et al*., 2007). *C. albicans* is capable to grow under hypoxic as well as anoxic conditions and modulates its metabolism according to the oxygen concentration in host niches. However, *C. albicans* lacks functional homologues of Rox1 and Sre1 proteins, which could contribute to hypoxic adaptation (Ernst and Teilker 2009). To delineate genes involved in hypoxic

adaptation, a transcriptome study revealed that transcription factor Upc2 upregulates genes involved in biosynthesis of ergosterol, while Efg1 is involved regulation of genes in unsaturated fatty acids, apparently to maximize incorporation of the scarce oxygen (Setiadi *et al*., 2006, Synnott *et al*., 2010). Glycolytic gene transcripts were upregulated by Ace2 and Tye7 to increase fermentative ATP production under oxygen-limiting conditions (Mulhern *et al*., 2006, Askew *et al*., 2009, Bonhomme *et al*., 2011). In an independent study, four different transcriptional regulators (Ahr1, Tye7, Sko1 and Ccr4) and their associated networks were identified, which are involved in early adaptive responses to hypoxia (Sellam *et al*., 2014). Interestingly, strains lacking *TYE7* showed defects in colonisation of the murine GI tract (murine model for commensalism) (Perez *et al*., 2013), and mutants lacking *ACE2* showed defects in filamentation under oxygen-limiting conditions, resulting in attenuated virulence in the mouse model of systemic candidiasis (Perez *et al*., 2013, MaCallum *et al*., 2006). These studies indicate that it is crucial for *C. albicans* to regulate fungal metabolism under host hypoxic conditions.

ii) Adaptation to varying levels of carbon dioxide: *C. albicans* senses CO_2 via two different pathways. In case of the first pathway, elevated levels of CO_2 (5%) are recognised by adenylyl cyclase Cyr1 which acts as a sensor and activates downstream cAMP/PKA pathway and Flo8 to induce filamentation in *C. albicans* (Klengel *et al*., 2005, Du *et al*., 2012). Alternate pathway comprises of Nce103 (a carbonic anhydrase), which is activated when the lower concentration of CO_2 are present in milieu. Nce103 converts CO_2 to HCO_3^-, which is utilised in cellular CO_2 fixation (Elleuche *et al*., 2010). Deletion of *NCE103* abolishes growth in low CO_2 growth conditions (Cottier *et al*., 2013). It was also identified that under low CO_2 conditions, Rca1 a transcriptional regulator upregulates *NCE103* expression. Recently, it was shown that in elevated CO_2 conditions, the alternative pathway consisting of *NCE103* and Rca1 is regulated by Sch9. Under high CO_2 environment, Pkh1/2 a serine threonine kinase related to the sphingolipid pathway, phosphorylates T570 of Sch9. Activated Sch9 phosphorylates Rca1, which abolishes the expression of *NCE103,* and low level of Nce103 do not enhance the CO_2 fixation (Pohlers *et al*., 2017). Conversely, in low CO_2 conditions, Sch9 is not activated which facilitates the *NCE103* expression and CO_2 fixation by Rca1 (Pohlers *et al*., 2017). These studies highlight that high and low level CO_2 environments are differentially recognised by distinct

pathways in *C. albicans.* And presence of CO_2 can influence metabolism, mating and morphogenesis in *C. albicans*.

iii) Influence of hypoxia and CO_2 on morphogenesis and pathogenesis of *C. albicans*: To investigate the influence of hypoxia on morphogenesis of *C. albicans*, embedded or microaerophilic conditions were used initially to mimic the growth in oxygen poor environment. Growth of single colony morphologies at temperature < 35°C were observed, in which condition *efg1* mutants that are locked in yeast morphology under most normoxic inducing conditions, displayed strikingly hyperfilamentous growth (Brown Jr. *et al*., 1999, Sonneborn *et al*., 1999; Setiadi *et al*., 2006). The hyperfilamenous phenotype of an *efg1* mutant was reasserted under defined growth conditions, where O_2 levels were restricted to < 1 % either in the presence or absence of CO_2 (Setiadi *et al*., 2006, Noffz *et al*., 2008). These studies indicate that in oxygen-poor growth conditions and at temperatures ≤ 35°C, Efg1 functions as a repressor of filamentation (Setiadi *et al*., 2006). Similarly, under hypoxia (0.2% O_2) but at high CO_2 levels, the Sch9 kinase was identified to repress filamentation, since *sch9* mutants showed hyperfilamentous growth under these conditions (Stichternoth *et al*., 2011). Sch9 functions downstream of Tor1 (target of rapamycin) kinase and the Tor1-Sch9 cascade is involved in sensing changes in nutrient conditions, maintenance of cell size, as well as regulation of adhesin genes and of ribosomal proteins (Bastidas *et al*., 2009, Liu *et al.*, 2010). In addition to its normoxic functions, Sch9 has important hypoxic functions, it senses hypoxia and CO_2 signals, and restricts filamentation by limiting the functioning of PKA (Tpk1 and Tpk2) and of Czf1, presumably by acting in coordination with the repressor role of Efg1, to favour growth in the yeast form under oxygen-poor conditions (Stichternoth *et al*., 2011). A representative model is depicted in figure 10. Rewiring in the functioning of Efg1 and Tor1-Sch9 pathway appears upon exposure to hypoxia with high CO_2 levels, which is distinct from the nomoxic role of Efg1 and Sch9 (Setiadi *et al*., 2006, Stichternoth *et al*., 2011). In addition to this under hypoxia, *C. albicans* is not dependent on the functions of Hda1 and Brg1 to initiate the hypoxic filamentation (Lu *et al*., 2013). These results indicate, presence of hypoxia and CO_2 in milieu, might influence the functioning of transcription factors and protein kinases that modulate the process of hyphal morphogenesis in *C. albicans*. Interestingly, the hypoxic regulators that are involved in modulating changes in metabolic processes (*TYE7*, *ACE2* and *EFG1*) or in regulation of morphogenesis (*ACE2, EFG1*, *SCH9 and UME6*) during hypoxic

growth, also play significant roles either in GI tract colonisation and/ or in virulence of *C. albicans* (Macallum *et al*., 2006, Banerjee *et al*., 2008, Liu *et al*., 2010, Pierce *et al*., 2012, Perez *et al*., 2013). Taken together, these studies suggest a correlation between genes involved in hypoxic adaptation and virulence of *C. albicans*. However several aspects related to hypoxic adaptation remain elusive. More importantly to study how *C. albicans* senses hypoxia and CO_2, and is able to regulate its morphological transitions under oxygen-limiting conditions to colonise host niches needs further investigation.

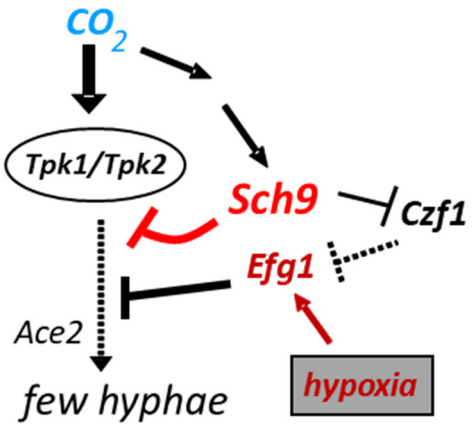

Fig. 10: Influence of hypoxia on morphogenesis in *C. albicans*: Under hypoxia (with elevated CO_2 conditions) Sch9 and Efg1 function as a repressors of filamentation at temperatures < 35 °C. Mutants of *SCH9* and *EFG1* show hyperfilamentous growth under hypoxia with CO_2. Sch9 limits the functions of PKA pathway and Czf1, and acts in coordination with Efg1 to repress filamentation under hypoxia (with CO_2) Representative models taken from Stichternoth *et al*., 2011

1.8.5 Translational control of morphogenesis

Transcriptional circuits and downstream target genes of transcriptional regulators operating under different growth conditions have been extensively studied. In contrast, there is a major deficit with regard to translational regulatory mechanisms in *C. albicans*. In *S. cerevisiae*, an important role of 5' untranslated regions (UTRs) in translational control has been established. 5' UTR of mRNA transcripts can control translational efficiency in yeast by cis regulatory elements, which include the 5' cap structures, the translation initiation motif, upstream open reading frame (uORF), internal ribosome entry sites and secondary structures of transcripts (Mignone *et al*., 2002). The 5' UTRs can form stable secondary structures, which interfere with translation by inhibiting ribosomal scanning (van der Velden and Thomas, 1999, Mignone *et al*., 2002). Another regulatory elements in the 5' UTRs of transcripts are upstream open

reading frames consisting of short coding sequences located upstream of the main ORF. Following translation of such uORFs, the ribosome disintegrates and reassembles at the main ORF leading to reinitation of translation (Leppeck *et al*., 2018). However, if upstream ORFs are longer than 30 codons, the ribosome disintegrates and aborts the translation process (Kozak 1987). Two uORFs have been found to down-regulate mRNA translation of two transcription factors (*GCN4* and *YAP1*) in *S. cerevisiae* (Vilela *et al.,* 1999, van der Velden and Thomas 1999*,* Mignone *et al.,* 2002*)*. In case of *C. albicans,* a recent study has identified around 80 different transcripts encoding proteins involved either in filamentation or white-opaque phenotypic switching or other processes important for *C. albicans* pathogenesis, contain unusually long (> 500 bp) 5' UTRs (Bruno *et al.*, 2010 and Sellam *et al.*,2010). Recently, a 3 kb-long 5' UTR of *UME6* was identified, which negatively regulates translation efficiency of the *UME6* transcript. (Childers *et al.,* 2014). Similarly, an extensive 5' UTR sequence in the *WOR1* regulator involved in white-opaque switching was found to negatively influence the translation of the *WOR1* transcript (Guan *et al.,* 2015). Thereby translational mechanisms provide important regulatory control that governs filamentation and phenotypic switching in *C. albicans.* However, considering the large set transcripts that carry long 5' UTR in *C. albicans*, the mechanisms involved in regulation of translation of these transcripts needs further investigation.

The 3.2 kb transcript of the *EFG1* in yeast-form (white cells) or hyphal cells is of particular interest in this context, as it contains a long 1100 bp of 5´ UTR. While in case of opaque cells, the *EFG1* transcript is 2 kb and has a relatively shorter (120 bp) 5´ UTR sequence. Hence it needs to be investigated, whether the 5´UTR of *EFG1* can influence metabolism, hyphal morphogenesis and phenotypic switching, by regulating the translational efficiency of *EFG1*.

1.9. Aim of this study

C. albicans colonizes the human host as a commensal, but it can also cause life-threating systemic infections in immunocompromised patients. During host colonisation, *C. albicans* is exposed to hostile microenvironments which can influence its commensal and virulent lifestyle; therefore, rapid adaptation to host niches is crucial for *in vivo* growth of *C. albicans*. Although oxygen-poor environments are frequently encountered by *C. albicans* during host colonisation, the underlying mechanisms that facilitate efficacious adaptation and proliferation of *C. albicans* within host hypoxic niches are poorly understood. Moreover, hypoxia-specific regulatory mechanisms, which govern the morphological transitions and modulate expression of virulence traits under poor oxygen conditions are largely unknown. The aim of this study was to identify hypoxic regulatory networks in *C. albicans* with a focus on mechanisms that govern the process of yeast-to-hyphal morphogenesis.

Specific objectives of this study are mentioned below:

1. Investigate the hypoxic functions of Efg1 and decipher its regulatory network associated with filamentation under oxygen-poor environments

2. Characterise the 5' UTR region of *EFG1* transcript and determine its significance in regulation of translation and filamentation

3. Determine the genomic binding sites of protein kinase A during yeast-to-hyphae transition

4. Identify novel transcriptional regulators involved in modulation of hypoxic filamentation

2. Results

2.1 Manuscripts

2.1.1 Summary Manuscript I

Hypoxia and temperature regulated morphogenesis in *Candida albicans*

Efg1 represses hypoxic filamentation at temperatures < 35°C. The structural requirements for the hypoxic functioning of Efg1 were investigated. Different strains producing variants of Efg1 were constructed. An Efg1 variant carrying a N-terminal deletion and single site mutated Efg1 variants for residues T179 and T206 were examined for their potential to repress hypoxic filamentation at different temperatures (25°C-37°C). Using these Efg1 variants, differential structural requirements for the normoxic and hypoxic functions of Efg1 were identified. Also, the genomic binding sites of Efg1 were identified for native Efg1, which revealed 300 hypoxia-specific target genes including the *STE11*, *CEK1* and *CPH1* genes of the Cek1-MAPK pathway. Based on experimental evidence, we established that Efg1 blocks hypoxic filamentation by downregulating the expression of *STE11*, *CEK1* and *CPH1* genes. The comparative analysis of Efg1 and Ace2 regulatory circuits revealed *BCR1* and *BRG1* as shared target genes under hypoxic conditions. Furthermore, to identify the hypoxic functions of Bcr1 and Brg1, a transcript analysis of *EFG1*, *ACE2*, *BCR1* and *BRG1* genes was done in *bcr1* and *brg1* mutants grown under hypoxic conditions. In addition, phenotypes of *efg1 bcr1* and *bcr1 brg1* double knockout mutants were tested under normoxia and hypoxia. These results elucidate a transcriptional regulatory circuit, where hypoxic repressors Efg1 and Bcr1 are intricately connected to hypoxic inducers Ace2 and Brg1 for regulation of hyphal morphogenesis of *C. albicans* growing under oxygen-limiting conditions. Therefore, under oxygen-poor environments, at temperature slightly below 37°C, *C. albicans* is dependent on the repressor functions of Efg1 and Bcr1 to restrict hypoxic filamentation and to proliferate in the yeast morphoform. However, exposure to hypoxia with combinatorial conditions like physiological temperature (37°C) and CO_2, can differentially activate the hypoxic regulatory circuit to initiate the process of hyphal morphogenesis.

2.1.2 Summary Manuscript II

The 5' untranslated region of the *EFG1* transcript promotes its translation to regulate hyphal morphogenesis in *Candida albicans*

5' untranslated regions (5' UTR) within transcripts can form three-dimensional structures affecting ribosome scanning and influence the translation efficiency of mRNAs. In the white-cell morphoform of *C. albicans*, the *EFG1* transcript carries a 5' UTR of 1170 nucleotides. To delineate the functional or regulatory regions of the 5' UTR of the *EFG1* transcript, the sequence of 5' UTR was replaced with six different truncated versions. In total, seven different strains, producing the *EFG1* transcript carrying either the full length 5' UTR or six different deletions in 5' UTR were grown under normoxia and hypoxia. Under normoxic conditions, in comparison to strains expressing full length 5' UTR, three strains expressing truncated versions of the 5' UTR displayed defects in forming filaments, similar to *efg1* null mutants. Similarly, under hypoxic conditions, these three strains showed defects in the suppression of hypoxic filamentation, again similar to *efg1* null mutant strains. Sequence analysis revealed that strains with defects in functioning of Efg1 were missing a 218 nt region in the 5' UTR of the *EFG1* transcript. Further analyses revealed that deletion of the 218 nt region does not restrict *EFG1* mRNA levels, but severely affects protein levels of Efg1. Ribosomal fractionation demonstrated that the full-length *EFG1* transcript was significantly enriched in the polysome fraction, while truncated transcripts lacking the 218 nt region were equally distributed in monosome and polysome fractions. The results indicate that a specific sequence within the 5' UTR of the *EFG1* transcript is required for its efficient translation. This positive regulatory function of the 5´UTR was confirmed by using a heterologous reporter gene activity assay. Hence an additional translational regulatory mechanism exists, which functions downstream of transcriptional regulatory circuits, perhaps to maintain stringency on the virulent attributes of *C. albicans.*

2.1.3 Summary Manuscript III

Morphogenesis regulated localization of protein kinase A to genomic sites in *Candida albicans*

In *C. albicans,* PKA isoforms (Tpk1 and Tpk2) have crucial roles as signalling kinases, as they mediate environmental cues and trigger hyphal morphogenesis. To examine a potential nuclear localization of Tpk1 and Tpk2, both isoforms were epitope-tagged and their genomic

localization was examined during yeast and hyphal growth of *C. albicans* strains. A significant number of Tpk genomic binding sites were identified in both yeast and hyphal cells, especially for the Tpk2 isoform. During yeast growth, Tpk1 and Tpk2 were bound mostly within ORFs of target genes, while during hyphal induction, binding regions were favoured in promoter regions of target genes. During yeast growth, Tpk2 bound preferentially to ORFs of genes encoding components of transcription factors that are involved in carbon source utilization. In contrast, during hyphal induction, Tpk2 binding sites were situated mostly in promoter regions of genes involved in filamentous growth (40 genes). Interestingly, several binding regions and downstream targets of Tpk2 targets during hyphal induction were overlapping with binding regions of Efg1. This indicates that Tpk2 resides on genomic locations close to Efg1 targets during morphogenesis, which might regulate Efg1 and downstream targets of PKA signalling pathway in the nucleus. Sequences representing the binding regions of Tpk2 during yeast growth frequently occurred within ORFs at ACCAC, CCACC or CAGC motifs, while during hyphal growth, the binding site preference was enriched for A_5GA_5 and A_2GA_5 motifs. These results suggest that genomic binding of Tpk2 might facilitate or prolong hyphal morphogenesis by acting on nearby transcription factors at their target genes.

2.1.4 Summary Manuscript IV

Genetic landscape of hypoxic filamentation in *Candida albicans*

Hypoxic niches are consistently present at the site of microbial infection within the human host, which can significantly influence the physiology of *C. albicans*. *In vitro* studies have shown that *C. albicans*, upon exposure to hypoxia, induces specific transcriptional responses, which facilitate metabolic adaptation to oxygen-limiting conditions. It was observed that hypoxia in combination with CO_2 can influence the functioning of a transcriptional regulator (Efg1) and a kinase (Sch9) to govern the process of hypoxic filamentation. To investigate the involvement of all currently known normoxic regulators of morphogenesis in hypoxic filamentation, 28 mutants defective in normoxic filamentation were subjected to phenotypic profiling under hypoxic conditions (also in combination with elevated CO_2 levels). This analysis revealed that some of the inducers of normoxic filamentation are also essential for induction of hypoxic filamentation. To identify novel hypoxia-specific regulators of morphogenesis, a set of 296 mutants lacking individual transcription factors or protein kinases was screened

under 8 different growth conditions. 21 mutants displayed defects to supress filamentation under hypoxia in the presence of 6 % CO_2, resembling the *sch9* mutant phenotype. Out of these 21 mutants, 12 mutants also showed defects to induce filamentation under normoxia, thereby resembling the *efg1* mutant phenotype. Out of the newly identified set of mutants, two representative mutants (*crf1* and *zcf14*) were subjected to transcript analyses and showed de-repression of the *UME6* transcript, which correlates with the hyperfilamentous growth of these mutants under hypoxia with elevated CO_2. Thus, Crf1 and Zcf14 are involved in effectively downregulating the hyphal inducer Ume6 to suppress hypoxic filamentation. The results indicate that *C. albicans* has evolved a surprisingly large number of transcriptional regulators to specifically suppress filamentation under hypoxia. Independent groups have established that during GI tract colonisation of *C. albicans*, *UME6*-mediated filamentous growth activates strong host immune responses, which is detrimental for the commensal lifestyle of *C. albicans*. Crf1 and Zcf14, along with other hypoxic regulators, may actively suppress unwanted filamentation of *C. albicans* in the gastrointestinal tract, which is able to activate immune responses and thereby favour the commensal yeast lifestyle of *C. albicans*.

2.2 Manuscript I: Hypoxia and temperature regulated morphogenesis in *Candida albicans*

Prashant R. Desai, Lasse van Wijlick, Dagmar Kurtz, Mateusz Juchimiuk, Joachim F. Ernst

Contribution to Manuscript: 40%

Prashant R. Desai was majorly involved in designing, performing and concluding the results. He was also involved in preparing final figures and writing the main part of the manuscript.

Individual contributor: for Figures 1 to 5 and supplemental figures S2, S3 and S6

Partial contribution: to Figures 8, 9, 10 and supplemental figure S8

Published in : PLoS Genetics, August 2015; 11(8):e1005447

Impact Factor: 7.528 (2014)

PLOS | GENETICS

RESEARCH ARTICLE

Hypoxia and Temperature Regulated Morphogenesis in *Candida albicans*

Prashant R. Desai[1☯], Lasse van Wijlick[1,2☯], Dagmar Kurtz[1], Mateusz Juchimiuk[1], Joachim F. Ernst[1,2]*

1 Department Biologie, Molekulare Mykologie, Heinrich-Heine-Universität, Düsseldorf, Germany, **2** Manchot Graduate School Molecules of Infection, Heinrich-Heine-Universität, Düsseldorf, Germany

☯ These authors contributed equally to this work.
* Joachim.ernst@uni-duesseldorf.de

OPEN ACCESS

Citation: Desai PR, van Wijlick L, Kurtz D, Juchimiuk M, Ernst JF (2015) Hypoxia and Temperature Regulated Morphogenesis in *Candida albicans*. PLoS Genet 11(8): e1005447. doi:10.1371/journal.pgen.1005447

Editor: Geraldine Butler, University College Dublin, IRELAND

Received: February 21, 2015

Accepted: July 15, 2015

Published: August 14, 2015

Data Availability Statement: All 16 files are available at the Candida Genome Database (http://www.candidagenome.org/download/systematic_results/Desai_2014/).

Funding: This work was supported by the Deutsche Forschungsgemeinschaft (Er47/11-1) to JFE, the Jürgen Manchot Stiftung Düsseldorf (http://www.moi.hhu.de/) to JFE and the ERA-NET PathoGenoMics project OXYstress (www.pathogenomics-era.net/FundedProjects3rdJoint) to JFE. The funders had no role in study design, data collection and analysis, decision to publish, or preparation of the manuscript.

Abstract

Candida albicans is a common commensal in the human gut but in predisposed patients it can become an important human fungal pathogen. As a commensal, *C. albicans* adapts to low-oxygen conditions and represses its hyphal development by the transcription factor Efg1, which under normoxia activates filamentation. The repressive hypoxic but not the normoxic function of Efg1 required its unmodified N-terminus, was prevented by phosphomimetic residues at normoxic phosphorylation sites T179 and T206 and occurred only at temperatures $\leq$35°C. Genome-wide binding sites for native Efg1 identified 300 hypoxia-specific target genes, which overlapped partially with hypoxic binding sites for Ace2, a known positive regulator of hypoxic filamentation. Transcriptional analyses revealed that *EFG1*, *ACE2* and their identified targets *BCR1* and *BRG1* encode an interconnected regulatory hub, in which Efg1/Bcr1 act as negative and Ace2/Brg1 act as positive regulators of gene expression under hypoxia. In this circuit, the hypoxic function of Ace2 was stimulated by elevated CO_2 levels. The hyperfilamentous phenotype of *efg1* and *bcr1* mutants depended on Ace2/Brg1 regulators and required increased expression of genes encoding Cek1 MAP kinase and its downstream target Cph1. The intricate temperature-dependent regulatory mechanisms under hypoxia suggest that *C. albicans* restricts hyphal morphogenesis in oxygen-poor body niches, possibly to persist as a commensal in the human host.

Author Summary

Candida albicans is an important cause of human disease that occurs if the fungus proliferates strongly on skin surfaces or in several internal organs causing superficial and systemic mycosis. Remarkably, at low cell numbers, *C. albicans* is also a normal inhabitant of mucosal surfaces and the gut and it is believed that its transition from the commensal to the virulent, highly proliferative state is a key event that initiates fungal disease. In the gut and other body niches, *C. albicans* adapts to an oxygen-poor environment, which downregulates its virulence traits including the ability to form hyphae. We report on a set of four transcription factors in *C. albicans* that form an interdependent regulatory circuit, which

Competing Interests: The authors have declared that no competing interests exist.

downregulates filamentation specifically under hypoxia at slightly lowered body temperatures (≤ 35°C). Disturbance of this circuit is expected to initiate the fungal virulence and proliferation in predisposed patients.

Introduction

Candida albicans is a regular fungal inhabitant of the human gastrointestinal tract and the skin [1–3] but in predisposed patients it can also cause life-threatening systemic disease [4]. Systemic candidiasis occurs if resident fungi translocate to the blood and proliferate massively in extraintestinal organs [5,6]. Currently, the requirements for *C. albicans* commensalism are being investigated using murine models of colonization, in which fungi are fed orally and monitored during transit and following exit of the gut [7–11]. In all studies, *C. albicans* cells growing in the gut lumen were found to propogate in the yeast form and not in the alternative hyphal form. Transciptomal analyses revealed that *C. albicans* adapts to conditions in the mouse gut or in internal organs by upregulation of genes related to growth, stress-resistance and cell surface components [12]. Several proteins required for gut colonization were identified by their defective mutant phenotypes [9,10,12]. In contrast, mutants lacking the transcription factor Efg1 or its homologue Efh1 were found to hyperproliferate in the murine gut [7–9], while overproduction of the Efg1-antagonist Wor1 stimulated excessive proliferation [9]. These results suggested that *C. albicans* limits its gastrointestinal growth by the repressive transcriptional activity of the Efg1 protein [8]. Gut mucosal damage, deficiencies in immune defenses and defects of the gut probiotic microbiome have been described as essential preconditions to allow translocation and systemic dissemination of *C. albicans* originating from the gut [11,13]. Despite this knowledge, the environmental cues and signaling pathways favouring commensal growth of *C. albicans* and its transition to the invasion and dissimination states are largely unclear.

Oxygen-poor locations are frequent in the human host and some niches including the gut may be anoxic [14,15], while other tissues including tissue of exposed skin are hypoxic [16,17]. Hypoxia has also been verified in the mouse gastrointestinal tract [18]. *C. albicans* adapts to hypoxia by increasing glycolytic and decreasing respiratory metabolism; furthermore, increased expression of genes required for the oxygen-dependent biosynthesis of compounds including ergosterol and unsaturated fatty acids procures maximal use of residual oxygen [19–21]. Under hypoxia, genes required for ergosterol biosynthesis are induced by the transcription factor Upc2 [20,22], while the transcription factors Efg1 and Ace2 both upregulate glycolysis and downregulate oxidative activities [19,23,24]. Efg1 is required for rapid transcriptomal adaptation to hypoxia [25], it controls the regulation of many hypoxic genes and prevents inappropriate hypoxic regulation of normoxic genes [14,19]. Besides their hypoxic metabolic functions, Efg1 and Ace2 also regulate the yeast-to-hypha transition, an important virulence trait of *C. albicans*, in an oxygen-dependent manner. Under normoxia, *efg1* mutants are unable to form hyphae indicating that Efg1 acts as an inducer of morphogenesis [26,27]. In contrast, Efg1 represses hyphal growth under hypoxia, which is apparent by hyperfilamentous growth of *efg1* mutants during hypoxic growth on an agar surface [19,23,28] or during embedment in agar [4,29] but not during growth in liquid media. The increased hyperfilamentous phenotype of an *efg1 efh1* double mutant demonstrated further that the Efg1 homolog Efh1 acts synergistically with Efg1 [23]. The function of Efg1 as a hypoxic repressor was strikingly temperature-dependent since *efg1* mutants were hyperfilamentous at temperatures ≤ 35°C, while at 37°C they were unable to form hyphae under both hypoxia and normoxia [19]. In contrast to Efg1,

the Ace2 protein was found to be largely dispensable for hyphal morphogenesis under normoxia [30–32] but it was required for filamentation under hypoxia [30,32]. Thus, Efg1 and Ace2 have opposing functions under hypoxia and recent results suggested that Efg1 represses *ACE2* expression [32], as well as expression of Ace2 target genes [32,33] under normoxia.

Both described hypoxic functions of Efg1, i. e. to regulate yeast proliferation of *C. albicans in vitro* and in the mouse gut *in vivo*, may be directed by similar if not identical regulatory circuits. In support of this notion, as compared to the wild-type strain, an *efg1* mutant not only was hyperproliferative in the mouse gut [7–9] but it also showed increased extraintestinal dissemination in animals exposed to hypoxia [34] and increased virulence in orally-inoculated mice [35]; in contrast, the virulence of the *efg1* mutant was strongly reduced in the systemic model of bloodstream-infection, i. e. under increased oxygen levels [27,35]. Hypoxia by decreased blood flow in individual gut villi had previously been shown to favor invasion and translocation of *C. albicans* across enterocytes [36]. Conceivably, the hypoxic repressor functions of Efg1 are relevant not only at temperatures <37°C, i.e. for fungal colonization of exposed skin tissue but also for translocation across gut epithelia. Here we identify a transcriptional regulatory hub describing the functions of Efg1 under hypoxia that controls the proliferation and morphogenesis of *C. albicans* in oxygen-limiting environments.

Results

Efg1 hypoxic function requires its unmodified N-terminus

Under hypoxia, Efg1 has been described as a temperature-dependent regulator of morphogenesis because it suppresses filamentation during surface growth at temperatures ≤35°C [19], while at 37°C it is required for hyphal growth [19] as under normoxia [26,27]. Properties of the *efg1* mutant were re-confirmed by growth on the surface of YPS agar, which under normoxia does not induce hypha formation in *C. albicans* [37]. Under hypoxia (0.2% O_2), the *efg1* mutant was unable to filament at 37°C, while it showed vigorous hyphal outgrowth at 34, 30 and 25°C; in contrast, under normoxia no filamentation was observed at 25°C (Fig 1A). At 37°C under hypoxia, the defective filamentation of an *efg1* homozygous mutant on YPS agar was fully restored not only by native Efg1 but also by an N-terminally HA-tagged Efg1 variant (Fig 1A) or by an Efg1 variant carrying a N-terminal deletion (Fig 1B), as under normoxia [38]. In contrast, at 25, 30 or 34°C the synthesis of HA-Efg1 did not prevent hyperfilamentation in an *efg1* genetic background, while native unmodified Efg1 had this activity (Fig 1A). The repressing function of authetic Efg1 was slightly reduced by deleting residues 9 to 74 (ΔN-Efg1) since colonies grown at 25°C (but not at 30 or 34°C) showed residual filamentation (Fig 1B). Thus, the morphogenetic repressor function of Efg1 requires its native N-terminus.

The structural requirements for hypoxic Efg1 functions were explored further by single-site mutated variants mutated for residues T206 and T179. T206 fits the consensus sequence for phosphorylation by PKA [39] and T179 is considered as the phosphorylation site of the Cdc28-Hgc1 kinase complex [33]; phosphorylation of both residues is needed for efficient hypha formation under normoxia [33,39]. *EFG1* versions encoding T206A, T206E, T179A and T179E variants were integrated into the genome of an *efg1* mutant and filamentation phenotypes of transformants were examined. All Efg1 variants were produced at similar levels during hypoxic growth (Fig 1C) as under normoxia [38], which was assayed by immunoblotting of cell extracts using a newly generated anti-Efg1 antiserum (S1 Fig). Interestingly, at 25, 30 and 34°C, both non-phosphorylatable variants T206A and T179A effectively repressed filamentation, while Efg1 variants mimicking phosphorylation (T206E and T179E) were unable to act as repressors (Fig 1B). This result suggests that opposite to its normoxic functions, the

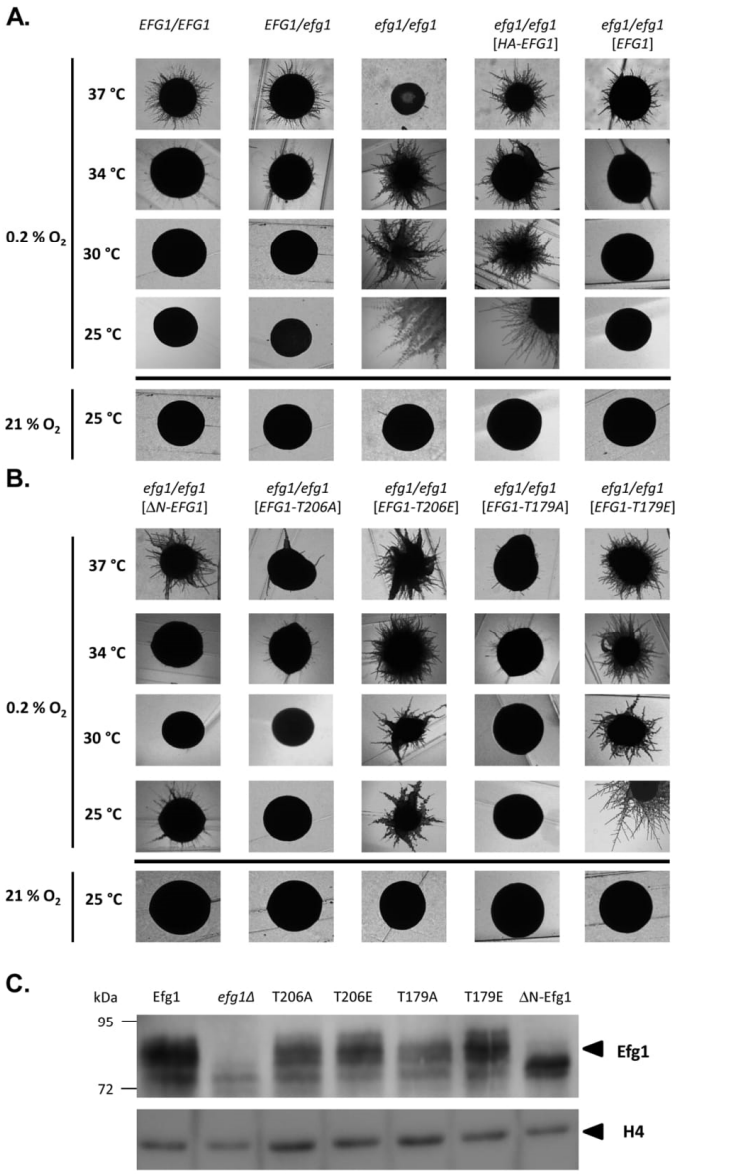

Fig 1. Hypoxia and temperature dependent filamentation regulated by Efg1 variants. (A, B) Colony phenotypes. Strains were grown under hypoxia (0.2% O_2) on the surface of YPS agar at 37°C (3 d), 34°C (3 d), 30°C (3 d) or 25°C (4 d) and under normoxia (21% O_2) at 25°C (4 d). (C) Efg1 immunoblot. Strains were

grown on YPS agar for 60 h at 25°C before cell harvesting by scraping off the colonies. 75 μg of protein in cell extracts were separated by SDS-PAGE (8% acrylamide) and immunoblots were developed using anti-Efg1 antiserum. Levels of histone H4 (loading control) were detected by anti-histone H4 antibodies. Strains tested were CAF2-1 (*EFG1/EFG1*), BCA0901 (*EFG1/efg1*), HLC52 (*efg1/efg1*), HLCEEFG1 (*efg1/efg1* [*HA-EFG1*]), HLCPEFG1 (*efg1/efg1* [*EFG1*]), HLCNEFG1 (*efg1/efg1* [*ΔN-EFG1*]), HLCEEFG1T206A (*efg1/efg1* [*EFG1-T206A*]), HLCEEFG1T206E (*efg1/efg1* [*EFG1-T206E*]), HLCEEFG1T179A (*efg1/efg1* [*EFG1-T179A*]) and HLCEEFG1T179E (*efg1/efg1* [*EFG1-T79E*]).

doi:10.1371/journal.pgen.1005447.g001

phosphorylated forms of Efg1 are inactive in hypoxic repression, while the non-phosphorylated forms are active.

Collectively, the results suggest that normoxic and hypoxic functions of Efg1 have different structural requirements. An unmodified native N-terminus of Efg1 and the lack of T206/T179 phosphorylation appear essential for its repressive functions under hypoxia at temperatures slightly below 37°C.

Genomic binding of native and HA-tagged Efg1 under hypoxia

The above experiments had shown that native but not HA-tagged Efg1 is active for morphogenetic repression under hypoxia at 25°C and 30°C. Next, we sought to identify genes that are hypoxically repressed by Efg1 but not HA-Efg1 under hypoxia. For this purpose genomic binding sites for both Efg1 versions were determined by ChIP chip analyses and compared. Binding of native Efg1 was determined in the Efg1$^+$ strain CAF2-1 using anti-Efg1 antibody for immunoprecipitation and the *efg1* mutant HLC52 [27] as the background control strain; binding of HA-Efg1 was established using anti-HA antibody and strain CAF2-1 as the reference control [40]. Cells were grown at 30°C (i. e. a temperature compatible with the hypoxic repressor function of Efg1) in liquid glucose-containing YPD medium. This experimental setup was chosen to focus on hypoxia-regulated targets under clearly defined conditions using uniformly exponentially-growing yeast cells and to exclude other targets, e. g. related to differential filamentation. Furthermore, normoxic targets for HA-Efg1 had been previously determined in identical conditions [40] and provided a useful dataset for comparisons.

Genomic binding sites for native Efg1 (221 sites corresponding to 300 ORFs) greatly outnumbered those for HA-tagged Efg1 (100 sites corresponding to 118 ORFs) and surprisingly little overlap was found for sites binding both proteins (23 sites); 198 sequences were exclusively bound by native Efg1 under hypoxia (Fig 2A). Little overlap was also detected between targets of HA-Efg1 under hypoxia and normoxia [40] (S2 Fig). Binding sites for both proteins are specified in S1 Table and are available at (http://www.candidagenome.org/download/systematic_results/Desai_2014/). Hypoxic binding occurred exclusively in promoter regions upstream of ORFs, marking these genes as potential regulatory targets (in case of divergently transcribed genes both ORFs were considered as regulatory targets). A significant subset of identified genes has a known or suspected role in hyphal growth of *C. albicans* (shaded area in Fig 2A). Genes binding both Efg1 and HA-Efg1 included *EFG1* itself [40], as well as seven genes encoding general morphogenetic regulators comprising *NRG1*, *TCC1* and *TYE7*. Forty-one genes were only bound by native Efg1 but not by HA-Efg1 under hypoxia including *BCR1*, *CEK1*, *CPH2*, *CYR1*, *STE11* and *TPK1*. Consensus sequences in promoters binding Efg1 proteins were calculated using the program RSAT dyad analysis [41] and revealed an enrichment for CA-containing motifs for both Efg1 and HA-Efg1 (Fig 2B) that may represent binding sites. This result suggests that although target promoters differ, untagged and tagged Efg1 proteins bind to identical sequences under hypoxia. Interestingly, the binding sequences resemble CA-containing sequences bound by HA-Efg1 during hyphal induction under normoxia but

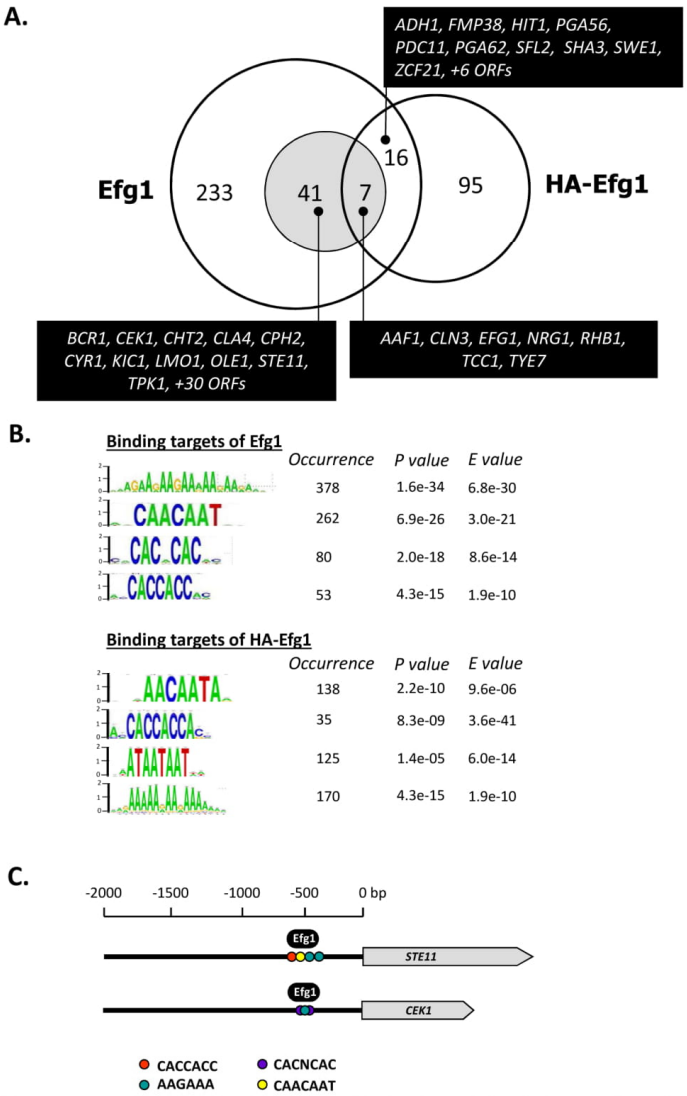

Fig 2. Genomic binding sites for Efg1. (A) Venn diagram listing numbers of genes bound by untagged Efg1 (Efg1) and HA-Efg1 under hypoxia. For Efg1, genomic binding sites were derived from ChIP chip experiments comparing strains CAF2-1 (*EFG1/EFG1*) and HLC52 (*efg1/efg1*); for HA-Efg1, strains HLCEEFG1 (*efg1/efg1* [*HA-EFG1*]) and DSC11 (*efg1/efg1* [*EFG1*]) were compared. The shaded circle encompasses genes in filamentous growth. (B) The program RSAT dyad analysis [43] was used to predict the DNA binding motif of Efg1 and HA-Efg1 from genomic binding regions. Predicted dyads for Efg1 and HA-Efg1 binding sites under hypoxic growth were ranked and the top-ranked sequences are shown with their P-/E-values. (C) Position of Efg1 binding sites in promoter regions. Arrows indicate ORFs of genes *STE11*,

CEK1 and *CPH1* and consensus sequences representing potential Efg1 binding sites in promoter regions are indicated by colored circles. The position of identified Efg1 binding (black oval) in *STE11* and *CEK1* promoters is indicated.

doi:10.1371/journal.pgen.1005447.g002

differ from the major binding site (EGR-box TATGCATA) in normoxically grown, yeast-form cells [40].

Gene ontology (GO) analysis of genes binding native Efg1 under hypoxia revealed an enrichment for genes involved in filamentation and transcription factor activity (Fig 3), as expected from the Venn diagram (Fig 2A). Several of these genes had previously been identified as targets of HA-tagged Efg1 grown under normoxia in liquid [40] or during biofilm formation [42]. Gene ontology assignments for HA-Efg1 are shown in S3 Fig.

Transcriptional regulation under hypoxia

The above results had indicated a subset of genes bound by native but not HA-tagged Efg1, which are known to be involved in the yeast-to-hypha transition. Efg1 binding in promoter regions of these genes suggested that they are transcriptionally regulated by Efg1, explaining the hypoxic repressor function of Efg1 on hyphal morphogenesis. To verify this notion, transcript levels of selected genes were monitored during the shift from normoxia to hypoxia in $Efg1^+$ cells (CAF2-1) and *efg1* mutant cells (HLC52). Genes *STE11*, *CEK1* and *CPH1* encode members of the Cek1 MAP kinase cascade, which is needed for hypha formation of *C. albicans* mainly during surface growth [43–45]; Efg1 binding occurs in the promoter region of *STE11* and *CEK1* genes at the CA-type consensus binding sequences (Fig 2C). Transcripts of genes *CYR1* and *TPK1* were also analyzed that encode adenylate cyclase and PKA isoform 1, respectively, which are members of the cAMP-dependent pathway of filamentation [46,47]. In addition, the *KIC1* transcript encoding a presumed regulator of the Ace2 transcription factor [48] was assayed since Ace2 stimulates hypoxic filamentation [30] (see below).

In the control strain, transcripts for the Cek1 MAP kinase, its downstream transcription factor Cph1 and for the Kic1 protein were present at low levels but increased temporarily at 10–20 min following the hypoxic shift (Fig 4). Remarkably, in *efg1* mutant cells, these transcripts were strongly upregulated suggesting hypoxic repression by Efg1. A completely different pattern of regulation was detected for the *STE11* gene encoding a kinase upstream of Cek1, as well as for the *CYR1* adenylate cyclase gene. Transcript levels for both of these genes decreased strongly during the hypoxic shift in the $Efg1^+$ strain and were significantly downregulated in the *efg1* mutant. Thus, the regulation of both *STE11* and *CYR1* did not fit the pattern of an Efg1-repressed but rather of an Efg1-induced gene; in addition, expression of both genes was down- and not upregulated during the course of hypoxic exposure. The *TPK1* transcript also was downregulated under hypoxia but the absence of Efg1 did not affect its levels. Collectively, these results suggest that under hypoxia Efg1 downregulates *CEK1*, *CPH1* and *KIC1* transcript levels to suppress filamentation, which becomes evident by the *efg1* mutant phenotype (Fig 1). Efg1 binding to *STE11*, *CYR1* and *TPK1* promoters may have other functions that are not directly related to repression of hypoxic filamentation.

Efg1 represses Cek1-dependent filamentation under hypoxia

To verify the transcriptional data we analyzed levels of the Cek1 MAPK protein and of its phosphorylated form by immunoblotting in wild-type and mutant strains grown under hypoxia and normoxia. Under hypoxia, the total amount of Cek1 and of its phosphorylated form (Cek1-P) was strongly increased in the *efg1* mutant as compared to the wild-type strain, while under normoxia Cek1 levels were unaltered in the mutant and Cek1-P was not detected

GO term (genome frequency)	Efg1 binding genes annotated to the term Name	Frequency	*P* value
A. Process			
Growth (8.8 %)	*AAF1*[ac] *ADA2** *BCR1*[bc] *BMH1 BNI4 CAS4 CCN1*[c] *CEK1 CHT2 CLA4*[c] *CLN3*[ac] *CPH2 CYR1 DBF2** *EFG1*[ac] *ENO1 ERG13 ERG3 FTR1 GLN3 GZF3 HGT1*[c] *IRO1 KIC1 LMO1 MP65 MSS4 MYO2 NDH51 NRG1*[ac] *OLE1*[c] *PCL5 PDX1*[c] *RAP1 RBD1 RFG1*[ac] *RHB1*[a] *RHO1 ROB1 STE11 STE4 STP2*[c] *TCC1*[ac] *TOP1 TPK1*[c]* *TYE7*[c] *ZCF17 ORF19.2397.3 ORF19.4459*[ac] *ORF19.6705*	17.4 %	0.001
Filamentous growth (8.5 %)	*AAF1*[ac] *ADA2** *BCR1*[bc] *BMH1 BNI4 CAS4 CCN1*[c] *CEK1 CHT2 CLA4*[c] *CLN3*[ac] *CPH2 CYR1 DBF2** *EFG1*[ac] *ENO1 ERG13 ERG3 GLN3 GZF3 HGT1*[c] *IRO1 KIC1 LMO1 MP65 MSS4 MYO2 NDH51 NRG1*[ac] *OLE1*[c] *PCL5 PDX1*[c] *RAP1 RBD1 RFG1*[ac] *RHB1*[a] *ROB1 STE11 STE4 STP2*[c] *TCC1*[ac] *TOP1 TPK1*[c]* *TYE7*[c] *ZCF17 ORF19.2397.3 ORF19.4459*[a] *ORF19.6705*	16.7 %	0.037
Symbiosis, encompassing mutualism through parasitism (2 %)	*AAF1*[ac] *ADA2** *ADH1 BCR1*[bc] *CAP1* CLA4 CPH2 CYR1 EFG1*[ac] *ENO1 FBA1 FTR1 HYR1 MET6 MP65 NRG1*[ac] *PGK1 SSA2 TDH3 XOG1*	7 %	0.001
B. Function			
Nucleic acid binding transcription factor activity (2.6 %)	*ADA2* BCR1*[bc] *CAP1* CAS4 CBF1*[a] *CPH2 EFG1*[ac] *GLN3 GZF3 NRG1*[ac] *RAP1 RFG1*[ac] *ROB1 RPN4 SFU1 STP2 TYE7*[c] *ZCF17 ZCF21 ORF19.173 ORF19.1757 ORF19.4972*	7.3 %	0.012
Sequence-specific DNA binding (6.5 %)	*ADA2* BCR1*[bc] *BMH1 CAP1* CBF1*[a] *EFG1*[ac] *GLN3 GZF3 NRG1*[ac] *RAP1 RFG1*[ac] *ROB1 RPN4 SFU1 STP2 TYE7*[c] *WOR3 ORF19.173 ORF19.1757*	13.8 %	0.028

Fig 3. GO categories of genes binding Efg1 under hypoxia. GO terms for Efg1 binding targets were identified in ChIP chip data using the CGD GO Term Finder tool (http://www.candidagenome.org/cgi-bin/GO/goTermFinder); the analysis was conducted in June 2013. Genome frequencies of genes corresponding to GO terms are expressed as percentages (gene number relative to 6,525 genes in the *C. albicans* genome; the frequency of genes binding Efg1 that correspond to a specific GO term are expressed relative to the total number of 287 genes binding Efg1). Superscripts of genes indicate known gene functions: a, Efg1 binding under yeast normoxia [40]; b, Efg1 binding in hypha-inducing conditions [40]; c, Efg1 binding in biofilm-inducing conditions [42]; *genes regulated by Efg1 during GI tract colonisation [8]. Blue Lettering indicates common target genes bound by Efg1 and HA-Efg1 under hypoxia. *P* values for overrepresented categories were calculated using a hyper geometric distribution with multiple hypothesis correction according to the GO Term Finder tool. The *P* value cutoff used was 0.05.

doi:10.1371/journal.pgen.1005447.g003

(Fig 5A). This result matches the observed increase in the *CEK1* transcript level in the *efg1* mutant (Fig 4B). Activation of MAP kinase activity was specific for Cek1 since the Mkc1 phosphorylation status was unaffected by the presence of Efg1 (Fig 5A).

To test if during hypoxic surface growth, excessive filamentation by the Cek1-Cph1 pathway is suppressed by the Efg1 protein we examined filamentation phenotypes under hypoxia in strains lacking or overproducing potential regulator proteins. We observed that a *cph1* mutant and colonies of an *efg1 cph1* double mutant did not form hyphae, unlike the hyperfilamentous *efg1* mutant (Fig 5B). In addition, overexpression of *STE11* and *CPH1* genes encoding members of the Cek1 signaling pathway by an anhydrotetracyclin-inducible promoter stimulated filamentation in the wild-type genetic background (Fig 5C). In this experiment, the failure of overexpressed *CEK1* to induce filamentation may reflect low activity of non-phosphorylated Cek1 in the absence of activation by an upstream kinase. Collectively, the results provide strong evidence that Efg1 represses hypha formation of *C. albicans* under hypoxia by repressing the biosynthesis and activity of the Cek1 MAP kinase pathway.

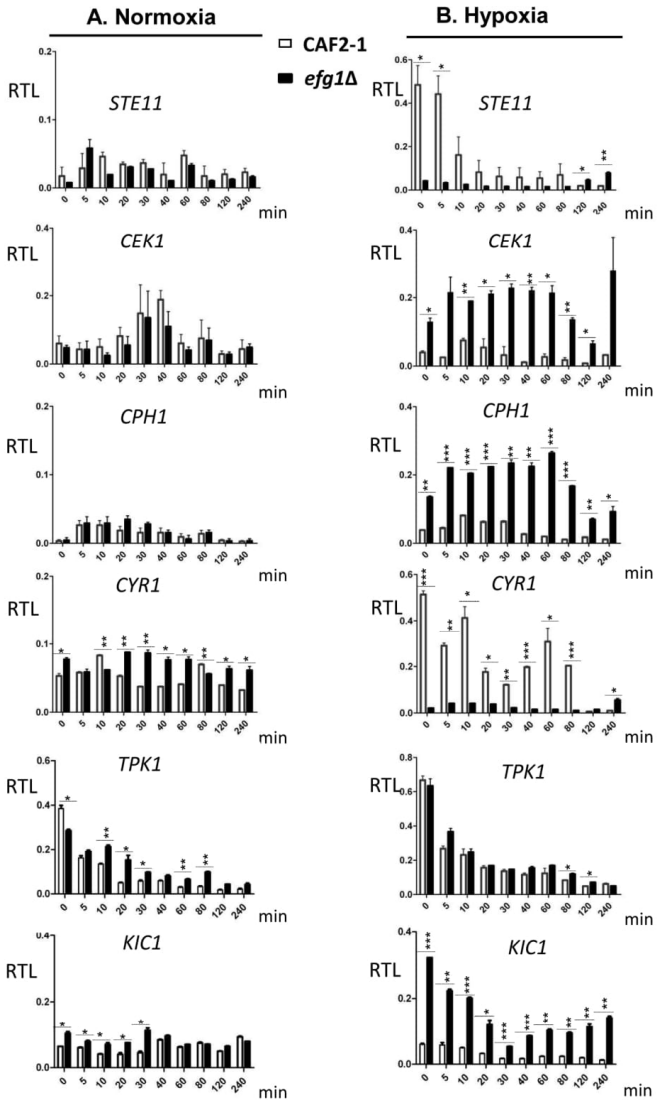

Fig 4. Transcriptional regulation of Efg1 target genes under normoxia and hypoxia. Strains were precultured under normoxia at 30°C in YPD medium and used for inoculation of 200 ml YPD cultures for normoxia, or under 0.2% O_2 for hypoxia. Cultures were incubated at 30°C under normoxia or hypoxia, and at the indicated times 20 ml of culture was withdrawn and used for preparation of total RNA. At each time point, two biological replicates and three technical replicates were assayed by qPCR using gene-specific primers. mRNA levels are expressed as means ± SEM of transcript levels relative to the *ACT1* transcript (RTL), for normoxia (A) and hypoxia (B) grown cultures. A two-tailed, unpaired *t* test comparing the RTL values of

control strain CAF2-1 and *efg1* mutant HLC52 was used to determine the statistical relevance. *, $P < 0.05$; **, $P < 0.01$; ***, $P < 0.001$.

doi:10.1371/journal.pgen.1005447.g004

Intersection of Ace2 and Efg1 regulatory circuits

Ace2 is a transcription factor that under hypoxia, unlike Efg1 at lower temperatures, is required for filamentation [30]. Efg1 represses the transcription of *ACE2* and of Ace2-dependent genes and binds to the *ACE2* promoter under normoxia [31, 32]. On the other hand, Ace2 and Efg1 have similar functions to stimulate glycolysis and to repress oxidative metabolism [23, 30]. These results suggested that Ace2 and Efg1 regulatory circuits overlap to jointly control filamentation of *C. albicans* under hypoxia. To verify this notion we compared genomic binding sites of Ace2 and Efg1 in cells grown under hypoxia. Strain CLvW004 (*ACE2-HA/ace2*) was constructed, which synthesizes the Ace2 protein with an added C-terminal triple HA-tag. This strain did not show any of the known *ace2* mutant phenotypes for antimycin A resistance, wrinkled colony growth [24,30] and sensitivity to the Pmt1 *O*-mannosylation inhibitor [49] indicating that the Ace2-HA fusion protein is functional (S4 Fig). For the identification of hypoxic Ace2 genomic binding sites, based on preliminary results, a broad ChIP chip screening strategy was chosen to identify all hypoxic targets including those targets requiring the presence of CO_2. For this purpose genomic binding sites for Ace2-HA in strain CLvW004 were determined following growth in 0.2% O_2/ 6% CO_2 and related to results of strain BWP17 synthesizing unmodified Ace2 for background correction; in parallel, normoxic binding sites were determined. Binding sites for Ace2 are listed in S2 and S3 Tables and deposited at http://www.candidagenome.org/download/systematic_results/Desai_2014/.

296 significant genomic Ace2 binding sites were identified in *C. albicans* promoter regions, while no binding occurred within ORFs (Fig 6A). The majority of binding sites (>80%) was identical in cells grown under hypoxia or normoxia (S5 Fig). Analysis with the RSAT program dyad analysis [41] revealed potential consensus binding sequences CAACAA, CACCAC, CAGCW and ATCAT for Ace2 (Fig 6B). The sequence CAGCW is similar to the CCAGC motif deduced from transcriptomal analyses of Ace2 [30] and matches the binding sequence of *S. cerevisiae* Ace2 [50]. Interestingly, the CAACAA and CACCAC motifs had also been observed as potential binding sites for native and tagged Efg1 (Fig 2B) suggesting that these sequences are targeted by both Ace2 and Efg1. Genomic positions for both proteins correspond to binding motifs, mostly to the CACCAC sequence, in a selected group of promoters (Fig 6C).

53 promoters bound both Ace2-HA and Efg1 and/or HA-Efg1 under hypoxia (Fig 7A). Gene ontology analysis of the corresponding genes revealed their preferential function as transcription factors to regulate processes of cell adhesion, biofilm formation and morphogenesis (Fig 7B). The transcription factors Brg1 [51] and Bcr1 [52] are known to regulate morphogenesis under normoxia but they also appear to function under hypoxia because they are under joint control of both Ace2 and (HA-) Efg1 in this environment (Fig 7B). Other common hypoxic Ace2/Efg1 target genes encode regulators with more specific functions including Aaf1 [53], Adh1 [54], Eed1 [55], Tye7 [56], Rfg1 [57], Wor2 [58], Wor3 [59] and Zcf21 [60]. In control experiments, binding targets were verified by qPCR following ChIP demonstrating strong enrichment of binding sites for Efg1, HA-Efg1 or Ace2-HA in a selected group of target promoters (S6 Fig). By this sensitive method, binding of HA-Efg1 (in addition to Efg1) was also detected at the *BCR1* promoter; furthermore, these data demonstrated the specificity of antibodies used for immunoprecipitation since anti-Efg1 antibody precipitated both Efg1 and HA-Efg1, while anti-HA antibody was specific for HA-Efg1 and Ace2-HA (S6 Fig).

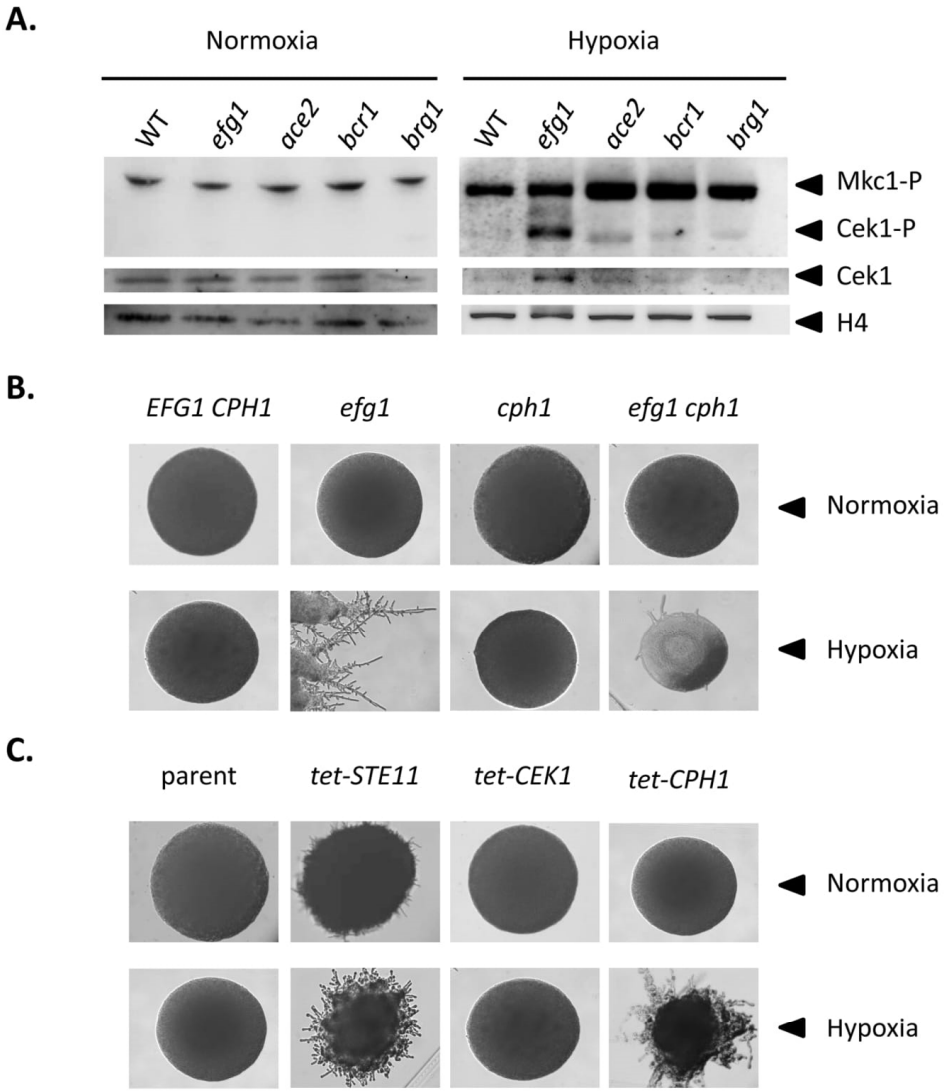

Fig 5. Hypoxic filamentation is activated by the Cek1 pathway. (A) Levels of MAP kinases in *C. albicans* mutants. *C. albicans* strains CAF2-1 (WT), HLC52 (*efg1*), MK106 (*ace2*), CJN702 (*bcr1*) and TF022 (*brg1*) were plated on YPS agar plates and incubated for 60 h at 25°C under normoxia or hypoxia (0.2% O_2). Colonies were scraped off the agar and cell extracts were used for immunoblotting. Anti-phospho-p44/42 antibody was used to detect the phosphorylated forms of MAP kinases Mkc1p and Cek1p. Total Cek1 (Cek1) and histone H4 levels (loading control) were detected by anti-Cek1 and anti histone H4 antibodies, respectively. (B, C) Phenotypes of *C. albicans* strains with altered expression of Efg1 target genes. Filamentation phenotypes were monitored following growth on YPS agar at 25°C under normoxia or hypoxia (0.2% O_2) for 3 d. (B) Mutant phenoypes. Comparisons of control strain CAF2-1 (*EFG1 CPH1*) and homozygous mutants HLC52 (*efg1*), JKC19 (*cph1*), HLC54 (*efg1 cph1*). (C) Overexpression phenotypes. Transformants expressing genes *STE11*, *CEK1* and *CPH1* under control of a tetracycline inducible promoter were grown on YPS medium containing 3 μg/ml anhydrotetracycline. Strains included CDC2907 (parent control), CECSTE11 (*tet-STE11*), CECCEK1 (*tet-CEK1*) and CDCCPH1 (*tet-CPH1*).

doi:10.1371/journal.pgen.1005447.g005

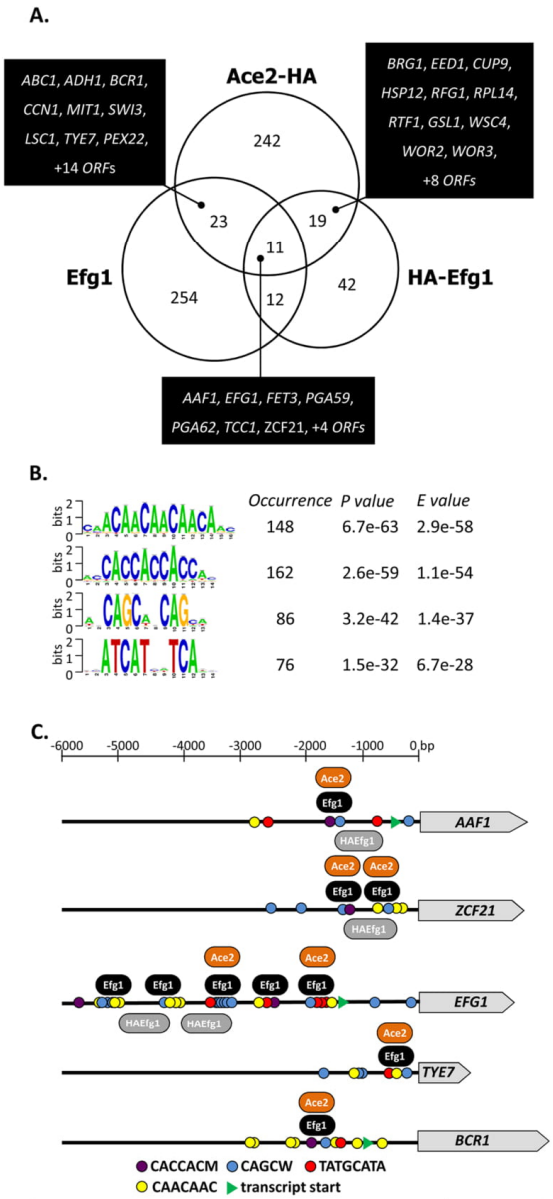

Fig 6. Genomic binding sites for Ace2. (A) Venn diagram showing numbers of genes bound by untagged Efg1 (Efg1), HA-Efg1 and Ace2-HA under hypoxia. For Efg1, genomic binding sites were derived from ChIP

chip experiments comparing strains CAF2-1 (*EFG1*/*EFG1*) and HLC52 (*efg1*/*efg1*), for Ace2-HA, strains CLvW004 (*ACE2-HA*/*ace2*) and BWP17 were compared. A set of 34 genes is common for Efg1 and Ace2-HA. (B) The program RSAT dyad-analysis [41] was used to predict the DNA binding motif of Ace2-HA from genomic binding regions. Predicted dyads for Ace2-HA binding sites under hypoxic growth were ranked and the top-ranked sequences are shown with their respective *P*- and *E*-values. (C) Position of Efg1 and Ace2-HA binding sites in promoter regions of target genes. Arrows indicate ORFs of genes *AAF1*, *TYE7*, *ZCF21*, *EFG1* and *BCR1*. Consensus sequences representing potential Efg1 and Ace2-HA binding sites in promoter regions are indicated by colored circles. The position of common identified sequences for Efg1 (black oval) and Ace2-HA (orange oval) binding in *AAF1*, *TYE7*, *ZCF21*, *EFG1* and *BCR1* promoters is indicated.

doi:10.1371/journal.pgen.1005447.g006

In addition, 242 genes were identified that only bound Ace2-HA but not (HA-)Efg1. This group was enriched for genes involved in glycolysis and oxidative metabolism (e. g. *PFK2*, *ACO1*, *LSC1*) confirming previous transcriptomal analyses [30]. Interestingly, genes involved in mitochondrial translation (*NAM2*, *ORF19.4929*, *ORF19.4705*, *EAF7*, *PIM1*) were also identified among Ace2 targets. The promoter of the *SCH9* gene encoding a kinase repressing hypha formation under hypoxia if CO_2 is present [37], was also identified as a hypoxic binding target of Ace2. Collectively, the group of "Ace2-only" genes appears to regulate metabolism and growth but also contains some genes for some relevant morphogenetic regulators including *FLO8* [61,62], *CAS5* [63], *SFL1* [64,65] and *WOR1* [58]. Conceivably, under hypoxia activation of *FLO8*, which is known to be required for CO_2 sensing [62], may be mediated by Ace2 (see below).

Efg1-Ace2 and its targets form an interdependent regulatory hub under hypoxia

Joint binding of Efg1 and Ace2 to target promoters under hypoxia suggested that both proteins regulate the respective genes on the transcriptional level. To clarify a specific role of hypoxia on gene regulation the transcript levels of selected Ace2-Efg1 target genes were determined under hypoxia and normoxia. Wild-type cells, as well as *ace2* and *efg1* mutant cells, were grown under normoxia and hypoxia (0.2% O_2) both in the absence or presence of CO_2 (6% CO_2); hypoxia in combination with elevated CO_2 levels was tested because previous results had suggested that this environment triggers specific patterns of gene expression [37]. Transcript levels were determined for Ace2-Efg1 target genes under hypoxia and normoxia (Fig 8).

First, mutual regulation of *EFG1* and *ACE2* was examined. In the wild-type strain, the *ACE2* transcript was strongly upregulated under hypoxia but only in the presence of CO_2; upregulation did not require CO_2 in the *efg1* mutant (Fig 8A) suggesting that Efg1 strongly represses *ACE2* under hypoxia also in the absence of CO_2. The *EFG1* transcript level was upregulated about twofold under hypoxia in the wild-type strain; this occurred even in the *ace2* mutant in the absence but not in the presence of CO_2. This mutual regulatory pattern of both genes indicated that under hypoxia, Efg1 acts as a transcriptional repressor independently of CO_2, while Ace2 requires CO_2 for its induction activity.

In a similar manner we analysed the hypoxic expression of two Ace2-Efg1 target genes encoding key morphogenetic regulators during biofilm formation under normoxia (*BCR1*, *BRG1*) (Fig 8B). Bcr1 is a positive regulator of biofilm formation, cell surface composition and filamentation [52,66,67], while Brg1 (Gat2) promotes hypha-specific gene expression during hyphal elongation [51,68,69] and promotes *ACE2* expression under normoxia [32]. The *BCR1* transcript was downregulated in the wild-type strain but upregulated in the *efg1* mutant under normoxia but more strongly under hypoxia revealing Efg1 as a strong hypoxic repressor of *BCR1*. In the *ace2* mutant the *BCR1* transcript was downregulated more strongly in the presence than in the absence of CO_2 suggesting that Ace2 upregulates *BCR1* in this environment,

A.

GO term (genome frequency)	Common Efg1, HA-Efg1 and Ace2-HA binding genes annotated to the term: Name	Frequency	*P* value
A. Process			
Cell adhesion (0.9 %)	*AAF1*, *BCR1*, *EED1*, *EFG1*, *orf19.4216*	9.4 %	0.036
Biofilm formation (2.2 %)	*ADH1*, *BCR1*, *BRG1*, *CSR1*, *EED1*, *EFG1*, *TYE7*	13.2 %	0.044
B. Function			
Nucleic acid binding transcription factor activity (3.4 %)	*BCR1*, *BRG1*, *CSR1*, *CUP9*, *EFG1*, *RFG1*, *TYE7*, *WOR2*, *ZCF21*, *orf19.173*	18.9 %	0.001
DNA binding (7 %)	*BCR1*, *BRG1*, *CSR1*, *CUP9*, *EFG1*, *RFG1*, *RTF1*, *TYE7*, *WOR3*, *ZCF21*, *orf19.173*, *orf19.4488*	22.6 %	0.014

B.

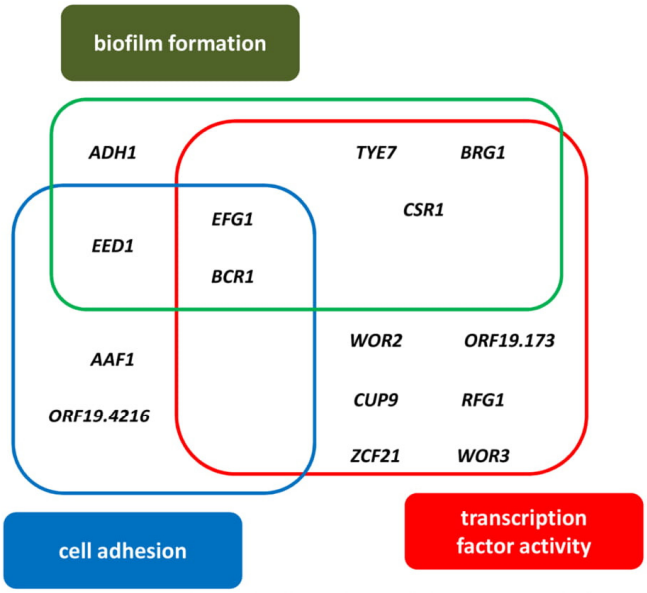

Fig 7. GO categories of common untagged Efg1 (Efg1), HA-Efg1 and Ace2-HA target genes under hypoxia. (A) GO terms for target genes identified by ChIP-chip analysis that are common for untagged Efg1, HA-Efg1 and Ace2-HA under hypoxia using the CGD GO Term Finder tool (http://www.candidagenome.org/cgi-bin/GO/goTermFinder); the analysis was conducted in May 2014. Genome frequencies of genes corresponding to GO terms are expressed as

percentages (gene number relative to 6,525 genes in the *C. albicans* genome; the frequency of genes that correspond to a specific GO term are expressed relative to the total number of 53 genes with either a binding region of untagged Efg1 or HA-Efg1 and Ace2-HA present in their 5'-UTR). *P* values for overrepresented categories were calculated using a hyper geometric distribution with multiple hypothesis correction according to the GO Term Finder tool. The *P* value cutoff used was 0.05. Colors indicate genes binding only untagged Efg1 (red), only HA-tagged Efg1 (blue) or both Efg1 versions (black). (B) Scheme depicting overlap between GO categories for common Efg1 and Ace2 target genes.

doi:10.1371/journal.pgen.1005447.g007

counteracting Efg1-mediated repression. In contrast to *BCR1* regulation, *BRG1* expression was upregulated in the wild-type strain under hypoxia and this upregulation was even enhanced in an *efg1* mutant but reduced in the *ace2* mutant. Thus, although *BCR1* and *BRG1* genes are regulated differently under hypoxia, Efg1 and Ace2 regulate these genes similarly, with Efg1 acting as repressor and Ace2 as an inducer of gene expression. Other genes encoding relevant transcription factors, including Tye7 [56], Aaf1 [53] and Zcf21 [60,70], were also controlled by Efg1/Ace2 (S7 Fig); these proteins regulate glycolysis, biofilm formation and/or commensalism of *C. albicans*.

In a previous report Bcr1 and Brg1 had been shown to bind to the *EFG1* promoter [42] suggesting feedback regulation between *EFG1-ACE2* and *BCR1/BRG1* genes under normoxia. To clarify the regulation under hypoxia *ACE2* and *EFG1* transcript levels were determined in *bcr1* or *brg1* mutants. The *ACE2* transcript was strongly downregulated in the *brg1* mutant in all conditions and largely increased in the *bcr1* mutant (not further increasing the already elevated level under hypoxia/CO_2) (Fig 8C). Thus, Brg1 activates and Bcr1 represses *ACE2* transcript levels. Brg1 also functions as an activator of the *EFG1* transcript under hypoxia, which did not increase in the *brg1* mutant in this condition.

On the other hand, gene products of *BCR1* and *BRG1* also mutually acted as negative regulators since the hypoxic downregulation of the *BCR1* transcript did not occur in a *brg1* mutant (showing even transcript upregulation) and the *BRG1* transcript was upregulated in the *bcr1* mutant under hypoxia (Fig 8D). Under normoxia, however, the *BRG1* transcript was strongly reduced in the *bcr1* mutant indicating that Bcr1 is a normoxic inducer but a hypoxic repressor for *BRG1*. Collectively, the results indicate that *EFG1*, *ACE2*, *BCR1* and *EFG1* genes form an interconnected regulatory hub, in which each participant regulates expression of the co-regulators. The transcriptional output of this unit is specific for hypoxia and is influenced significantly by CO_2 levels.

The Efg1-Ace2 regulatory hub regulates hyphal morphogenesis via the Cek1 pathway under hypoxia

The above transcript analyses had revealed that both *CEK1* and *CPH1* genes are repressed by Efg1 under hypoxia (Fig 4). Because Efg1 is part of an interconnected regulatory hub we re-examined the hypoxic/normoxic ratios of both transcripts in the respective mutant backgrounds (Fig 8E). In the wild-type strain, *CEK1* and *CPH1* transcripts were lowered in a hypoxic atmosphere without CO_2 but reached normoxic levels in the presence of CO_2 (Fig 8E). The repressive effect of Efg1 on both genes in this environment was clearly evident by strongly increased transcript levels in the *efg1* mutant. Under normoxia the Efg1 co-regulators Ace2, Bcr1 and Brg1 did not greatly influence *CEK1* or *CPH1* transcript levels. However, under hypoxia these regulators all repressed the *CEK1* transcript, while the *CPH1* transcript was downregulated only by Bcr1 (and Efg1). Consistently, protein levels of Cek1 and its phosphorylated form Cek1-P was upregulated under hypoxia (Fig 5A). Collectively, these results confirm the conclusion that Efg1 and its co-regulators control the Cek1 MAP kinase pathway.

To examine if and how members of the Efg1-Ace2 regulatory hub influence hyphal morphogenesis the colony phenotypes of control and mutant strains were recorded. Cells were

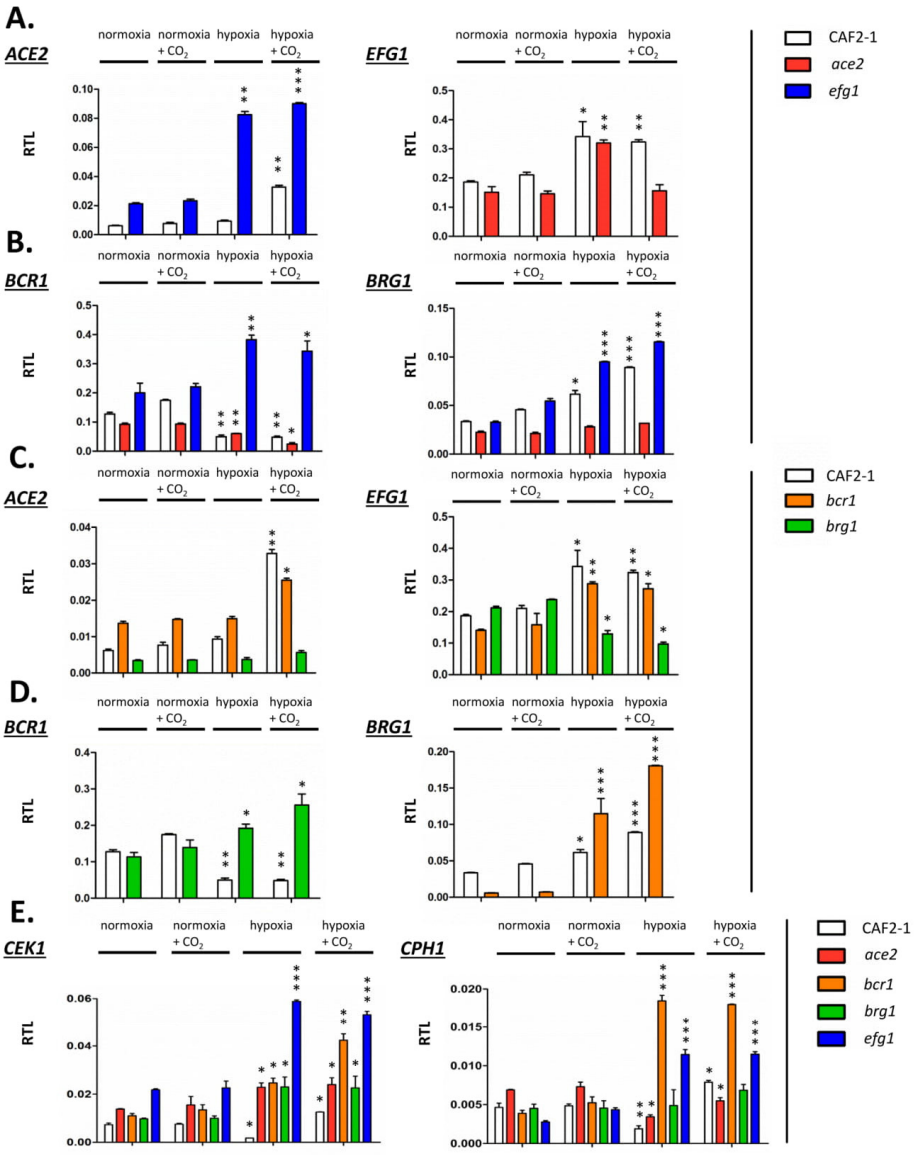

Fig 8. Transcriptional regulation of Efg1 and Ace2 target genes under hypoxia. Strains CAF2-1 (control), the *ace2* mutant MK106 and the *efg1* mutant HLC52 were precultured under normoxia at 30°C in YPD medium and used for inoculation of 100 ml YPD cultures. Cultures were incubated at 30°C under normoxia, under normoxia with addition of CO_2 (6%), under hypoxia (0.2% O_2) or under hypoxia with addition of CO_2 (0.2% O_2, 6% CO_2) until OD_{600} = 0.5 and total RNA was then isolated. Relative transcript levels were determined using *ACT1* transcript as the reference, as described in Fig 4. (A) Relative

transcript levels (RTL) for the *ACE2* transcript in strains CAF2-1 and HLC52 (*efg1*) and for the *EFG1* transcript in strains CAF2-1 and MK106 (*ace2*). (B to D) Relative transcript levels for the indicated transcripts in strains CAF2-1 (control), HLC52 (*efg1*), MK106 (*ace2*), CJN702 (*bcr1*) and strain TF022 (*brg1*). (E) Relative levels of *CEK1* and *CPH1* transcripts. Error bars represent standard deviation of the means. A two-tailed, unpaired t test comparing the cycle threshold values of samples grown in hypoxic and normoxic conditions for each mutant was used to determine the statistical relevance: *, $P < 0.05$; **, $P < 0.01$; ***, $P < 0.001$.

doi:10.1371/journal.pgen.1005447.g008

grown on YPS agar under hypoxia or normoxia, in the absence or presence of 6% CO_2 and at 25°C or 37°C. Under hypoxia, the control strain CAF2-1 showed no or sparse filamentation at 25°C but strong hypha formation at 37°C (Fig 9A). The *efg1* mutant was hyperfilamentous at 25°C but non-filamentous at 37°C verifying the previously reported dual repressor/activator role of Efg1 [19,23,29]. Strong hypha formation was also observed for the *bcr1* mutant at 25°C but unlike the *efg1* mutant, this mutant had a hyperfilamentous phenotype at 37°C. Both *ace2* and *brg1* mutant were defective in filamentation; this defect occurred for the *ace2* mutant in all conditions, whereas the *brg1* mutant was able to filament at 37°C in the presence of CO_2. Interestingly, under normoxia the wild-type strain presented vigorous filamentation at 37°C, while all single mutants showed complete or partial (*ace2* mutant) filamentation defects (S8 Fig). Thus, the Efg1, Ace2, Bcr1 and Brg1 regulators determine morphogenesis under both hypoxia and normoxia.

To establish if the hyperfilamentous phenotype of the *efg1* and *bcr1* mutants at 25°C requires Ace2 and/or Brg1 proteins double mutants were constructed and tested (Fig 9B). The construction of a homozygous *efg1 ace2* double mutant failed repeatedly suggesting that a *C. albicans* strain lacking both Efg1 and Ace2 is not viable; therefore, an *ace2/ace2 efg1/EFG1* heterozygous mutant (CLvW047) was constructed. Filamentation of the *efg1/EFG1* heterozygote was slightly but reproducibly increased at 25°C as compared to the control strain, while filamentation was reduced in strain CLvW047. The hyperfilamentous phenotype of the *bcr1* mutant (especially in the presence of CO_2) was also reduced in the *bcr1 ace2* double mutant. These results suggest that the increased hypha formation of *efg1* and *bcr1* mutants requires Ace2. The Brg1 protein is also needed for this phenotype because *efg1 brg1* and *bcr1 brg1* double mutants were completely defective for filamentation at 25°C; at 37°C, Brg1 was also needed for the *bcr1* phenotype in the absence of CO_2. In summary, the results indicate that hyphal morphogenesis of *C. albicans* under hypoxia is effectively repressed by Efg1 and Bcr1, counteracting the stimulatory effects of the Ace2 and Brg1 proteins.

Discussion

C. albicans is an opportunistic pathogen that inhabits the human host as a harmless commensal but that also can turn into a serious pathogen, which causes tenacious superficial and deadly systemic fungal disease. Candidiasis is typically caused by the strong proliferation of the same *C. albicans* strain that had inhabited the patient as a commensal before [6] raising questions about the molecular events that occur in the pathogen during the commensal-to-pathogen transition. As a commensal, *C. albicans* colonizes the gut and partly also mucosal surfaces [2,71–73]. Recent results have suggested that the fungus actively restrains its proliferation in the gut by transcriptional regulators Efg1 and Efh1 [7,8,74], while the Wor1 protein enhances gut colonization [9]. Events in the gut occur in oxygen-poor conditions (partly under anoxia) and mostly at elevated carbon dioxide concentrations [14,15]. Here we describe a transcriptional hub that downregulates filamentous growth of *C. albicans* and favors proliferation of its yeast form under hypoxic conditions. Surprisingly, this repressive activity involves regulators including Efg1, which positively regulate filamentation under normoxia.

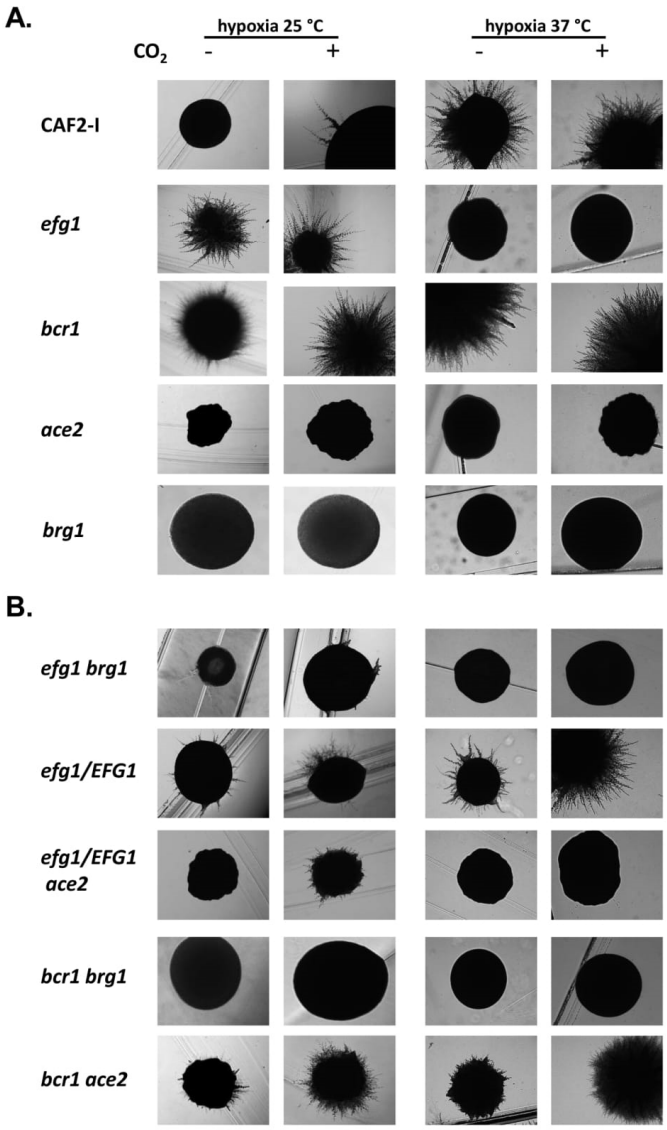

Fig 9. Hypoxic phenotypes of mutants lacking hypoxic regulators. The strains were grown under hypoxia (0.2% O_2) or hypoxia with 6% CO_2 on YPS agar for 4 d at 25°C or at 37°C for 3 d. (A) Strains included CAF2-1 (control), homozygous single mutants HLC52 (*efg1*), CJN702 (*bcr1*), MK106 (*ace2*) and TF022 (*brg1*). (B) Double knockout strains PDEB4 (*efg1 brg1*), PDBB4 (*bcr1 brg1*) and CLvW024 (*bcr1 ace2)* were tested. *ACE2* could not be disrupted in an *efg1* mutant background; therefore, the heterozygous mutant strain CLvW047 (*efg1/EFG1*, *ace2/ace2*) was constructed and its phenotype was compared to the *efg1/EFG1* strain DSC11.

doi:10.1371/journal.pgen.1005447.g009

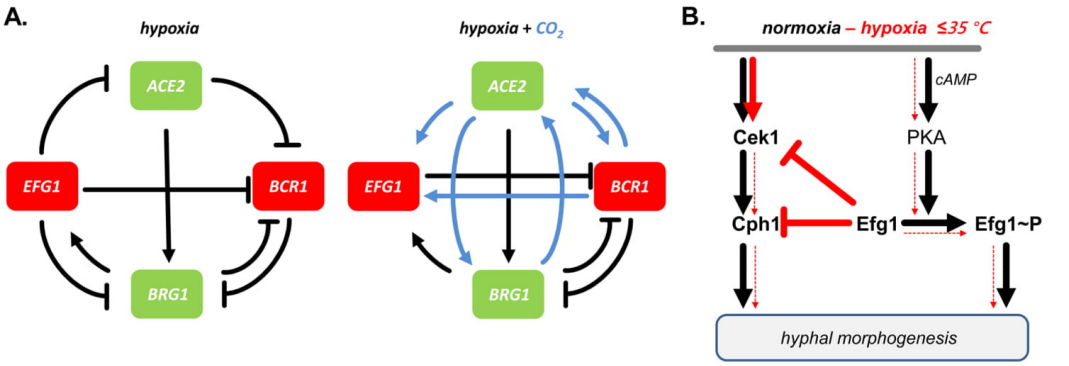

Fig 10. Models for transcriptional regulation and morphogenesis under hypoxia. (A) Transcriptional circuits. Hypoxic repressors Efg1 and Bcr1 (red) and hypoxic activators Ace2 and Brg1 (green) are mutually connected in regulatory circuits to regulate hypha formation of *C. albicans*. Note that regulatory circuits differ depending on the availability of CO_2 (blue arrows). (B) Morphogenetic signaling pathways. Under normoxia both Cek1 and PKA kinase pathways trigger hypha formation; Efg1 phosphorylation provides a major signalling input. Under hypoxia, at temperatures $\leq$ 35°C, low levels of Efg1 phosphorylation block the Cek1 pathway, thereby preventing hyphal induction by both pathways.

doi:10.1371/journal.pgen.1005447.g010

Efg1 directs several aspects of morphogenesis and metabolism in *C. albicans*. It has an important transcriptional role under hypoxia since it contributes to but also prevents hypoxic regulation of many genes [14,19]. The change to a hypoxia-specific pattern of gene expression requires Efg1 at an early time-point following a shift to hypoxia [25]. It is known that Efg1 has a dual role on hyphal morphogenesis: under hypoxia it acts as a hyphal repressor during growth on agar at temperatures $\leq$ 35°C [19,23,28], while under normoxia, Efg1 is a strong inducer of hypha formation [26,27]. The Efg1 signaling pathway under normoxia comprises adenylate cyclase Cyr1 activity that increases cAMP levels [46,47], which activates PKA isoforms Tpk1/Tpk2 and in turn Efg1 by phosphorylation of residue T206 [39]; an additional phosphorylation of T179 by the Cdc28-Hgc1 complex was also described to occur during hyphal morphogenesis [33]. Here we report that the hypoxic repressor function of Efg1 has specific structural requirements. Efg1 lost its repressor activity, when its N-terminal end was modified by extension and partially by deletion, while under normoxia such variants were active in hyphal induction [38]. Interestingly, chlamydospore formation, which is induced by oxygen limitation, also was found to require an undeleted N-terminus of Efg1 [28]. In addition, phosphomimetic residues at Efg1 phosphorylation sites (T179E, T206E) blocked the hypoxic repressor activity, while the corresponding alanine replacement variants were fully active in repression but inactive for the normoxic induction of hyphae [33,39]. This result corresponds to the lowered *CYR1* and *TPK1* transcript levels under hypoxia, which predicts lowered PKA activity and reduced T206 phosphorylation, thus resulting in enhanced hypoxic repressor activity of Efg1. With regard to Efg1 target sequences, the deduced CA-rich hypoxic binding sites did not match the major normoxic binding site TATGCATA for the yeast growth form, although Efg1 binds to CA- sequences shortly after hyphal induction [40]. Thus, the different functions of Efg1 as a hypoxic repressor involve different recognition and target sequences, as compared to normoxia.

Previously, synergistic and antagonistic functions of Efg1 and Ace2 transcription factors have been described. Both proteins enhance glycolytic and oxidative patterns of gene expression [23,30] and positively influence filamentation under normoxia [26,27,30–32]. In contrast,

under hypoxia Efg1 represses hypha formation [19,23,28], while Ace2 acts as an inducer [30,32]. Efg1 represses *ACE2* transcript levels, possibly by direct binding of Efg1 to the *ACE2* promoter [32]. To further characterize the functional intersection of both regulators we used ChIP chip analyses to compare their genomic binding patterns under hypoxia. A significant overlap of target genes was identified and the deduced Ace2 binding sequences in promoters included sequences resembling the ACCAGC motif for *S. cerevisiae* Ace2 [50] but also the above discussed CA-sequences representing hypoxic binding sites for Efg1. Interestingly, the group of genes targeted by both (HA-)Efg1 and Ace2 included important regulators of hyphal growth, biofilm formation and cell adhesion. Targets included the *EFG1* promoter, which thereby was confirmed not only as an autoregulatory target for Efg1 [40] but also identified as an Ace2 target. Confirming this result, Ace2 was required for upregulation of the *EFG1* transcript in a hypoxic CO_2-containing atmosphere, while Efg1 repressed the *ACE2* transcript as under normoxia [32]. We analyzed the mode of joint target gene regulation by the Efg1/Ace2 proteins by focusing on *BCR1* [52,66,67] and *BRG1 (GAT2)* [51,68,69], which regulate filamentation and were found to get hypoxically down- and, respectively, upregulated. Surprisingly, these genes were not only targets but also regulators of Efg1/Ace2 and they negatively regulated each other, thereby generating an interconnected regulatory loop (Fig 10A). Efg1 acted as hypoxic repressor of *BCR1/BRG1* and also of two other target genes (*TYE7*, *ZCF21*), while it was an inducer of *AAF1* expression (S3 Fig). In general, Ace2 activated hypoxic expression of all of these genes, especially in the presence of CO_2. Transcripts of hypoxia-upregulated genes including *EFG1*, *BRG1* and *TYE7* and of hypoxia-downregulated genes including *BCR1*, *AAF1* and *ZCF21* were all reduced if *ace2* mutant cells were grown hypoxically in the presence of CO_2. Interestingly, Ace2 bound strongly to the promoter of the *FLO8* gene, which encodes a CO_2 sensor interacting with Efg1 [38,62] that is required for white-to-opaque switching and for filamentous growth [61]. Thus, the lack of oxygen combined with an increased level of CO_2 generates an environment that elicits a specific regulatory response in *C. albicans*. These results are reminiscent of and confirm previous results for the hypoxia-specific, CO_2-dependent functions of Sch9 kinase [37] and the Ume6 regulator [75].

The morphogenetic output of the described hypoxic regulatory hub was tested by examining hypha formation on agar. The results confirmed that Ace2 is a positive factor for filamentation under hypoxia and partly also under normoxia [30,32], while Efg1 has a dual repressor/activator function under hypoxia/normoxia. Similar to Efg1, Bcr1 acted as a repressor of hypha formation at 25°C, especially in the presence of CO_2. Transcript data suggested that in this environment, Ace2 stimulates *BCR1* expression to ensure efficient blockage of hypha formation. Brg1 was needed for hypha formation at 37°C under hypoxia, but only in the absence of CO_2; in its presence, Brg1 was dispensable for filamentation. The *BRG1* transcript was repressed by Efg1 and activated by Ace2, largely independent of CO_2. As shown by the phenotypes of double mutants the increased filamentation of *efg1* and *bcr1* mutants depended on the activity of both Brg1 and Ace2. Thus, under hypoxia *C. albicans* restrains the stimulatory actions of both Brg1 and Ace2 on hyphal morphogenesis, using Efg1 and Bcr1 as repressors. While this study puts its focus on hypha formation, it is likely that other adaptation processes occurring under hypoxia, especially re-direction of metabolism to a fermentative mode, are regulated by transcription factors that link to the Efg1-Ace2 regulatory hub. Relevant transcription factors for this function could include Tye7 [56], Aaf1 [53] and Zcf21 [60], proteins that regulate glyolysis, biofilm formation and/or commensalism.

Which signaling pathway of morphogenesis is downregulated by Efg1 or Bcr1 proteins? Transcript analyses revealed that the genes encoding MAP kinase Cek1, its downstream target Cph1 and the kinase Kic1 are downregulated specifically under hypoxia by Efg1. The Cek1/Cph1 pathway is known to permit filamentation under normoxia during surface growth of

C. albicans [43–45], while in *S. cerevisiae*, Kic1 is part of the RAM pathway that activates Ace2 activity [48]. The repressive action of Efg1 and its co-regulators on the Cek1 pathway was verified by demonstrating that Efg1, Ace2, Bcr1 and Brg1 all act as repressors of *CEK1* transcript levels, while the *CPH1* transcript was especially repressed by Bcr1 and Efg1. Furthermore, Efg1- and Ace2-mediated repression of the Cek1 protein in its non-phosphorylated and phosphorylated form was also demonstrated. Confirming these results, an *efg1 cph1* double mutant was unable to filament, while overexpression of *CPH1* in a wild-type genetic background triggered hypha formation under hypoxia. These results clearly indicate that *C. albicans* actively suppresses filamentation mediated by the Cek1 pathway in certain oxygen-poor conditions to promote proliferation of the yeast form (Fig 10B). We have discovered this suppression *in vitro* slightly below the core body temperature (i. e. $< 37°C$) but this activity may also occur in the special molecular environment of the gastrointestinal tract or in hypoxic skin tissue [16,17]. Nevertheless, this scenario does not exclude that upregulation of hypoxic filamentation may occur under hypoxia, e. g. if the repressive action of Efg1 is blocked by the Czf1 protein [4]. In this situation, other regulators including Mss11 and Rac1, which were identified by their embedded growth phenotypes [76,77], may also promote hypoxic filamentation. A similar hyperfilamentous phenotype was also reported for mutants lacking the kinase Sch9, although elevated CO_2-levels were required in this case [37]. In the human gut, locally increased filamentation could favor anchoring of *C. albicans* to the epithelium and trigger strong fungal proliferation and systemic invasion mediated by invasion-specific regulators including Eed1 [8,55]. These events may initiate the pathogenic stage of fungal colonization, which will ultimately become apparent by the symptoms of disease. It appears that as a commensal *C. albicans* attempts to avoid immune responses and to maintain its residency by downregulation of filamentation and possibly other virulence traits. Strengthening of fungal commensalism, e. g. by novel therapeutic molecules or by probiotic microbes could become a promising strategy to combat serious fungal disease.

Materials and Methods

Strains and media

C. albicans strains are listed in S4 Table. Strains were grown in liquid YP medium (1% yeast extract, 2% peptone) containing 2% glucose (YPD) or 2% sucrose (YPS); solid media contained 2% agar. An Invivo200 hypoxia chamber (Ruskinn) was used for hypoxic growth under 0.2% O_2 [37]; liquid media were pre-equilibrated overnight under hypoxia before inoculation. Strains overexpressing genes using tetracyclin-inducible promoters were grown in/on YPS medium containing 3 μg/ml anhydrotetracycline.

C. albicans strains expressing *EFG1* variants

Oligonucleotides are listed in S5 Table. Plasmid pTD38-HA contains promoter and coding region for an N-terminally hemagglutinin (HA)-tagged Efg1 [38]. In this plasmid, HA-encoding sequences reside on a *Bgl*II and *Bam*HI fragment, which were removed in plasmid pPRDEFG1, in which the native *EFG1* ORF is preceded by a *Bam*HI site. Other plasmids carrying *EFG1* genes encoding Efg1 variants without HA tag were constructed in two steps, as in the case of pPRDNEFG1, in which nucleotides 25 and 222 of the *EFG1* ORF are deleted encoding a variant lacking residues Y9 to G74 of Efg1. Primers EFG1BamHIFor and EFG1BamHIRev were used for PCR amplification of the ORF of this variant, using plasmid pBI-HAHYD-D1 [38] as the template. The *Bam*HI-digested PCR fragment was inserted downstream of the *EFG1* promoter by ligation with the large *Bgl*II fragment of pTD38-HA to generate plasmid p2621NΔEFG1. The *Pac*I-*Spe*I fragment of this plasmid carrying the junction of the *EFG1*

promoter and its ORF was then used to replace the corresponding fragment in pTD38-HA. By this procedure, the mutated *EFG1* ORF was joined to its 3´-UTR. Similarly, the mutated *EFG1* alleles encoding the T206A and T206E mutations were transferred from plasmids pDB1 and pDB2 [39] into pTD38-HA to generate plasmids pPDEFG1T206A and pPDEFG1T206E. Analogous plasmids encoding T179A and T179E Efg1 variants were constructed by mutating the *EFG1* ORF by primer pairs EFG1179AFor/Rev and T179Efor/rev, respectively, using site-directed mutagenesis (QuikChange kit, Stratagene). The resultant plasmids pPDEFG1T179E and pPDEFG1T179A encode T179A and T79E variants of Efg1, respectively. All constructs were sequenced using primers EFG1seqFor, EFG1seqRev and Efg1SeqM to confirm the presence of the mutations within *EFG1*.

Plasmids were integrated into the chromosomal *EFG1* locus of *efg1* mutant HLC67 by transformation following digestion with *Pac*I in the *EFG1* promoter [38]. Their correct chromosomal integration was verified by PCR of gDNA using primers UTREfg1For and Efg1seqM.

C. albicans strains expressing HA-tagged Ace2

For localization studies of Ace2 a heterozygous mutant strain was constructed first. One *ACE2* ORF was replaced with a *lacZ-ACT1p-SAT1* cassette. The cassette was amplified from plasmid pStLacZ-SAT. All PCR products were separated on an agarose gel and purified using the QIAquick Gel Extraction Kit (Qiagen) before transformation. The oligonucleotides (lacZACE2for/lacZACE2rev) used for amplification, tagged the cassette with 90 bp of flanking sequence complementary to the *ACE2* ORF. The strain BWP17 was transformed and transformants were screened for nourseothricin resistance. Integration of the *lacZ-ACT1p-SAT1* cassette and replacement of the *ACE2* ORF was verified by Southern blot analysis using a probe for *SAT1*. The resulting heterozygous strain CLvW001 (*ace2-lacZ-ACT1p-SAT1/ACE2*) was used for C terminal tagging of Ace2. Oligonucleotides ACE2HAFor and ACE2HARev were used to amplify the triple HA-encoding sequence from plasmid p3HA-URA3 thereby adding homologous sequences of the 3‘- end of the *ACE2* ORF and 5‘-UTR of the *ACE2* allele to the amplicon. Strain CLvW001 was transformed for C terminal tagging of the remaining *ACE2* allele. Correct chromosomal integration at the *ACE2* locus was confirmed by colony-PCR using oligonucleotides ACE2For and HARev and by Southern blot analysis. The resulting strain CLvW004, expressing C-terminal HA-tagged Ace2 at the native locus was used to study chromosomal localization of Ace2-HA.

Construction of *ACE2* deletion strains

For the deletion of *ACE2* in the *bcr1* and *efg1* mutant background and in strain CAI4, plasmid pSFS5 was used, containing a modified *SAT1* flipper cassette [78]. The *ACE2* upstream and downstream regions were amplified with the oligonucleotide pairs CAF1ApaI/CAF2XhoI and CAR1SacII/CAR2SacI, for construction of the inner deletion cassette, and oligonucleotide pairs CAF3ApaI/CAF4XhoI and CAR3SacII/CAR4SacI for construction of the outer deletion cassette; the *ace2* mutant strain MK106 described by Kelly *et al.* [24] was used as the reference strain. gDNA of strain SC5314 was used to generate PCR products, which were digested with the indicated restriction enzymes and cloned on both sites of the *SAT1* flipper cassette in pSFS5 [78] resulting in plasmids pCLvW90 (inner cassette) and pCLvW91 (outer cassette). The deletion cassettes in plasmids pCLvW90 and pCLvW91 were released by digestion with *Sac*I and *Apa*I and used for transformation of strains using first the fragment containing the outer cassette and, after excision of the *SAT1* flipper cassette, with the second fragment containing the inner cassette. Integration of the deletion cassette was confirmed by colony PCR using oligonucleotides FLP1, which binds within the *FLP1* gene, and ACE2UTR5, which binds

upstream of the *ACE2* ORF. Transformants containing the *ACE2* deletion cassette were grown overnight in liquid YCB-BSA medium (20 g yeast carbon base, 4 g bovine serum albumin and 2 g yeast extract per liter) to induce excision of the cassette by FLP-mediated recombination; corresponding strains were identified by their small colony size on YPD plates containing 25 μg/ml nourseothricin. After excision of the second *SAT1* flipper cassette, deletion of both *ACE2* alleles was confirmed by Southern blot analysis. With this approach both *ACE2* alleles were deleted in the *bcr1* mutant strain CJN702 [52] resulting in strain CLvW024 and in CAI4 resulting in strain CLvW008. However, deletion of the second *ACE2* allele in the *efg1* mutant HLC52 [27] was not successful.

In an additional approach we tried to generate the *ace2 efg1* double knockout strain by deleting *EFG1* in the *ace2* mutant strain CLvW008 with the Ura-blaster disruption technique [79] but again we were not able to obtain a homozygous mutant strain suggesting that the double knockout is lethal. The *URA3* deletion cassette used for this approach was released from plasmid pBB503 [80] by digestion with *Hin*dIII and *Kpn*I. The fragment was purified and transformed into strain CLvW008 and transformants were selected for uridine prototrophy on SD agar. Integration of the cassette was confirmed by colony-PCR. In the resulting strain CLvW041 one chromosomal copy of *EFG1* was replaced by the sequence of *URA3* flanked by *hisG* sequences (*efg1*::*hisG-URA3-hisG*/*EFG; ace2*::*FRT*/*ace2*::*FRT*). Attempts to delete the second *EFG1* allele after removal of *URA3* [79] were not successful.

Construction of *BRG1* deletion strains

For deletion of *BRG1* gene in *efg1* (HLC52) and *bcr1* (CJN702) mutants the upstream region of the *BRG1* ORF was amplified by genomic PCR using primers BRG1 5UTRKpnIFor/KpnIRev and cloned into the *Kpn*I site of plasmid pSF5S to generate pSFS5-B5. The *BRG1* downstream region was amplified using primers BRG13UTRNot1For/SacIRev and cloned into *Not*I and *Sac*I sites of pSFS5-B5 to generate pSFS5-B5B3. The *Kpn*I-*SacI* fragment of this plasmid was used to transform *efg1* and *bcr1* mutant strains, selecting transformants on YPD agar containing nourseothricin (200 μg/ml). Correct genomic integration was confirmed by colony PCR using oligonucleotides FLP1, which binds within the *FLP1* gene, and BRG1UpFor, which binds upstream of the *BRG1* promoter region. Verified heterozygous transformants were grown in YCB-BSA medium to evict the disruption cassette and retransformed with the disruption fragment, as described [78]. Deletion of both *BRG1* alleles was confirmed by negative colony PCR using primer BRG1UpFor, which binds upstream to the *BRG1* ORF and BRG1midrev that is specific for the *BRG1* ORF. *BRG1* alleles were deleted in *efg1* (HLC52) and *bcr1* (CJN702) mutant strains resulting in strains PDEB4 (*efg1 brg1*) and PDBB4 (*bcr1 brg1*) respectively.

C. albicans strains overproducing signalling components

The plasmids pClp10TETSTE11, pClp10TETCEK1 and pClpTETCPH1 [81] encoding Ste11, Cek1 and Cph1 proteins were linearized with *Stu*I within the *RPS1* sequence and transformed into *C. albicans* CEC2907 [81] selecting for uridine prototrophy; the resultant strains were named CECSTE11, CECCEK1 and CECCPH1. Correct plasmid integration at the *RPS1* locus was confirmed by colony PCR using primers ClpUL and ClpUR.

Generation of an anti-Efg1 antiserum

A rabbit polyclonal anti-Efg1 antiserum was generated using His_{10}-tagged Efg1 produced in *E. coli*. The *EFG1* ORF (allele *ORF19.8243*) residing on a *Xho*I-*Bam*HI fragment was subcloned into pET19b (Novagen), downstream of the T7 RNA polymerase promoter. The resulting plasmid encoded a His_{10}-Efg1 fusion but contained a single CUG codon (residue 449) that encodes

serine in *C. albicans* but leucine in *E. coli*. This codon was changed to a UCG serine codon by site-directed mutagenesis using oligonucleotides pET19Serinhin/her, resulting in plasmid pET19-His-Efg1Kodon, which was transformed into *E. coli* Rosetta 2 (DE3)pLysS (Merck). Transformants were grown and the T7 promoter was induced according to instructions of the manufacturer. Cells were resuspended in buffer (20 mM CAPSO pH 9.5, 1 M NaCl, 1 mM EDTA, 20 mM imidazol, 0.1% Triton X100) and broken using 3 passages through a French press cell (Slaminco Spectronic Instruments). Crude extracts were cleared by centrifugation and applied to HisTrap columns connected to an ÄKTA prime plus fraction collector (GE Healthcare). The His_{10}-Efg1 fusion protein was eluted using CAPSO buffer containing 250 mM imidazol. Purified protein (100 μg) was injected on days 1, 14, 28 and 56 in 2 New Zealand White rabbits (performed by Eurogentec, Belgium). One rabbit generated high anti-Efg1 titers in ELISA tests and in immunoblottings (dilution 1:5000).

Immunodetection

YPD precultures were grown under normoxia overnight at 30°C in YPD medium and were used to inoculate 40 ml of YPD medium, which had been preincubated overnight under hypoxia (0.2% O_2). Starting with an initial density of OD_{600} = 0.1 cells were grown at 30°C under hypoxia to an OD_{600} = 1. Cells were harvested, frozen at -70°C for 1 h and then thawed by addition of 500 ml of CAPSO buffer (20 mM CAPSO pH 9,5, 1 M NaCl, 1 mM EDTA, 20 mM imidazole, 0,1% Triton X-100) containing protease inhibitor (Cocktail Complete, Mini, EDTA-free/Roche). Cells were broken at 4°C by shaking with one volume of glass beads (0.45 mm) in a FastPrep-24 shaker (MP Biomedicals) using 4–6 cycles for 40 s at 6.5 ms^{-1}; between cycles cells were placed on ice for 5 min. Debris was removed by centrifugation at 13,000 rpm for 5 min and protein in the supernatant was determined using the Bradford assay. 45 μg of the crude cell extract was separated by SDS-PAGE (8% polyacrylamide) and analysed by immunoblotting using anti-Efg1 antiserum (1:5,000) or anti-histone H4 (Abcam; 1:5,000) to detect histone H4 as loading control. Total Cek1 levels were detected by immunoblotting using anti-Cek1 antiserum [10], while phosphorylated Cek1 was detected using monoclonal rabbit anti-phospho-p44/42 antibody (Cell Signaling Technology). Anti-rabbit-IgG-HRP conjugate (1:10,000) was used as secondary antibody in all blottings. Signals generated by the chemiluminescent substrate (SuperSignal West Dura; Pierce) were detected by a LAS-4000 mini imager (Fujifilm) and evaluated by the Multi Gauge Software (Fujifilm).

Chromatin immunoprecipitation on microchips (ChIP chip)

The ChIP chip procedure was performed as described by Lassak *et al.* [40], except that the strains and antibodies used for immunoprecipitation were different. Two independent cultures were assayed for each combination of strains. Precultures were grown overnight under normoxia at 30°C in YPD medium and were shifted to YPD medium precalibrated under hypoxia (0.2% O_2, 30°C). The cells were allowed to grow from OD_{600} = 0.1 to 1. Two sets of strains were analysed: (1) wild-type strain CAF2-1 as test strain and *efg1* mutant HLC52 as control strain were compared to determine the genomic localization of untagged Efg1, using anti-Efg1 antibody for chromatin immunoprecipitation; (2) Strain HLCEEFG1 producing HA-tagged Efg1 as test strain and DSC11 (Efg1 producing) as control strain were compared to determine the genomic localization of HA-Efg1 using anti-HA antibody for chromatin immunoprecipitation. *C. albicans* genomic tiling microarrays were probed pairwise by immunoprecipitated chromatin as described previously [40]. For localization studies of Ace2, precultures were grown overnight under normoxia at 30°C in YPD medium and were used to inoculate medium preincubated under normoxia or hypoxia (0.2% O_2) with addition of 6% CO_2. Strain

CLvW004, producing HA-tagged Ace2 from its native locus and control strain BWP17 were used to determine the genomic localization of Ace2-HA using anti-HA antibody for immunoprecipitation. Significant binding peaks were defined as probes containing four or more signals above background in a 500 bp sliding window; the degree of significance depended on the FDR value. Results were visualized using the program SignalMap (version 1.9). The most significant binding peaks (FDR $\leq$ 0.05) for Efg1 (202 peak genomic binding sites), HA-Efg1 (106 peak genomic binding sites) and Ace2-HA (272 peak genomic binding sites), which coincided in both replicates, were analysed by the program RSAT dyad-analysis to predict DNA binding sequence [40].

Supporting Information

S1 Fig. Activity of rabbit anti-Efg1 antiserum. (A) Immunoblotting. Extracts of *efg1* mutant HLC67 (lane 2) and control strain CAF2-1 (lane 3) were separated by SDS-PAGE and blots were probed with anti-Efg1 antiserum (1: 5000). For comparison, 250 ng of *E. coli*-produced His_{10}-Efg1 protein was used (lane 1). (B) Immunoprecipitation. Efg1 was immunoprecipitated using anti-Efg1 antiserum and protein G-coated agarose beads. Immunoprecipitates from the control strain CAF2-1 (lane 1) and the *efg1* mutant HLC67 (lane 2) were analysed by immunoblotting using anti-Efg1 antiserum. The arrow indicates the migration of Efg1.
(PDF)

S2 Fig. Intersection of genomic binding sites for Efg1 and HA-Efg1 under hypoxia and normoxia. For Efg1, genomic binding sites were derived from ChIP chip experiments comparing strains CAF2-1 (*EFG1/EFG1*) and HLC52 (*efg1/efg1*); for HA-Efg1, strains HLCEEFG1 (*efg1/efg1* [*HA-EFG1*]) and CAF2-1 were compared. Normoxic binding sites for HA-Efg1 were obtained from Lassak *et al.* [40]. The shaded circle encompasses genes in filamentous growth.
(PDF)

S3 Fig. GO categories of genes binding HA-Efg1 under hypoxia. GO terms for Efg1 binding targets were identified in ChIP chip data using the CGD GO Term Finder tool (http://www.candidagenome.org/cgi-bin/GO/goTermFinder); the analysis was conducted in June 2013. Genome frequencies of genes corresponding to GO terms are expressed as percentages (gene number relative to 6,525 genes in the *C. albicans* genome; the frequency of genes binding Efg1 that correspond to a specific GO term are expressed relative to the total number of 106 genes binding HA-Efg1). Superscripts: a, Efg1 binding in yeast normoxia [40]; b, Efg1 binding in hyphae inducing conditions [40]; c, Efg1 binding in biofilm inducing conditions [42]. *P* values for overrepresented categories were calculated using a hyper geometric distribution with multiple hypothesis correction according to the GO Term Finder tool website (http://www.candidagenome.org/help/goTermFinder.shtml). The *P* value cutoff used was 0.05.
(PDF)

S4 Fig. Functionality of the HA tagged Ace2 protein. To verify the functionality of C-terminal HA-tagged Ace2 the phenotypes of three isolates of strain CLvW004 (*ACE2-HA/ace2*) was compared to mutant strain MK106 (*ace2/ace2*), wild-type strain BWP17 (*ACE2/ACE2*) and the heterozygous strain CLvW001 (*ACE2/ace2*). (A) Drop dilution assay for sensitivity to 4 μM Pmt1-inhibitor [49] and resistance to antimycin A (20 μg/ml). The agar plates were photographed after 2 d incubation at 30°C. The *ace2* mutant strain Mk106 shows enhanced sensitivity to the Pmt1-inhibitor and is less susceptible to the respiratory inhibitor antimycin A [30]. (B) Colonies of the indicated strains were photographed following growth for 2 d at 30°C on YPD agar. The *ace2* mutant strain Mk106 shows the wrinkled colony phenotype described previously [24]. Phenotypes of strains CLvW004.1–3 correspond to the heterozygous strain

CLvW001 indicating that the Ace2-HA protein in these strains is functional.
(PDF)

S5 Fig. Genomic binding sites for Ace2 under hypoxia and normoxia. Venn diagram showing numbers of genes bound by HA-tagged Ace2 under normoxic conditions (30°C, YPD) and hypoxic conditions (30°C, YPD 0.2% O_2 and 6% CO_2). Binding regions with the corresponding ORFs are listed in S2 and S3 Table. Genomic binding sites were derived from ChIP chip experiments comparing strains ClvW004 (*ACE2-HA/ace2*) and BWP17 (non tag control).
(PDF)

S6 Fig. Genomic localization of Ace2 and Efg1 on target promoters. (A) Binding positions identified by ChIP chip experiments. Binding positions of Efg1 (black ovals), Ace2-HA (orange ovals) and HA-Efg1 positions (grey ovals) identified by ChIP chip experiments are shown schematically. (B) Quantitation of Ace2, HA-Efg1 and Efg1 enrichment by ChIP on target promoters. Following ChIP the respective fold enrichment was determined by qPCR using oligonucleotide pairs shown by red arrows in A. Chromatin of strains CAF2–1 (Efg1) and HLCEEFG1 (HA-Efg1) was immunoprecipitated using anti-Efg1 and anti-HA antibody, respectively, as described in S1 Table. For Ace2 enrichment anti-HA antibody was used for immunoprecipitation of strain CLvW004 (Ace2-HA), as described in S2 Table. In a control experiment, ChIP followed by qPCR was also done using anti-Efg1 antibody on extracts of strain HLCEEFG1 (HA-Efg1). qPCR experiments were done using two biological replicates, which were assayed in triplicate. The mean fold enrichment (± standard deviation) for each protein was calculated relative to the respective no tag or mutant strain and normalized to the input sample. Statistical relevance is indicated by asterisks: *, $P < 0.05$; **, $P < 0.01$; ***, $P < 0.001$. The results verify the presence of proteins on target promoters; in addition, the presence of HA-Efg1 on the *BCR1* promoter, which was not found in the ChIP chip experiment, was revealed by the ChIP-qPCR experiment.
(PDF)

S7 Fig. Transcriptional regulation of selected Efg1 and Ace2 target genes under hypoxia. Strains CAF2-1 (control), the *ace2* mutant MK106 and the *efg1* mutant HLC52 were precultured under normoxia at 30°C in YPD medium and used for inoculation of 100 ml YPD cultures. Cultures were incubated at 30°C under normoxia, or normoxia with addition of CO_2 (6% CO_2), or under hypoxia (0.2% O_2), or under hypoxia with addition of CO_2 (0.2% O_2, 6% CO_2) until OD_{600} = 0.5 and total RNA was then isolated. Relative transcript levels were determined using *ACT1* transcript as the reference as described in Fig 4. Relative transcript levels (RTL) for the *AAF1*, *TYE7* and *ZCF21* transcripts in strains CAF2-1 (control), HLC52 (*efg1*) and MK106 (*ace2*). Error bars represent standard deviation of the means. A two-tailed, unpaired *t* test comparing the cycle threshold values of samples grown in hypoxic and normoxic conditions for each mutant respectively was used to determine the statistical relevance: *, $P < 0.05$; **, $P < 0.01$; ***, $P < 0.001$.
(PDF)

S8 Fig. Normoxic phenotypes of mutants lacking hypoxic regulators under hypoxia. The strains were grown under normoxia without or with 6% CO_2 on YPS agar for 4 d at 25°C or at 37°C for 3 d. Strains included CAF2-1 (control), homozygous single mutants HLC52 (*efg1*), CJN702 (*bcr1*), MK106 (*ace2*), TF022 (*brg1*) and double knockout strains PDEB4 (*efg1 brg1*), PDBB4 (*bcr1 brg1*) and CLvW024 (*bcr1 ace2*). *ACE2* could not be disrupted in an *efg1* mutant background; therefore, the heterozygous mutant strain CLvW047 (*efg1/EFG1*, *ace2*/*ace2*) was constructed and its phenotype was compared to the *efg1/EFG1* strain DSC11.
(PDF)

S1 Table. Binding of Efg1 to chromosomal sequences of *C. albicans* under hypoxia. Strain CAF2-1 producing wild-type Efg1 was grown in YPD medium at 30°C under hypoxic conditions (0.2% O_2), chromosomal cross-linking of proteins was done. Fragmented chromatin was immunoprecipitated using anti-Efg1 antibody and used as probe for tiling microarrays covering the *C. albicans* genome. Regions showing significantly increased binding of Efg1 compared to control strain HLC52 (*efg1/efg1*) are listed along with their nearest neigbouring ORFs designated left or right ORF if situated at descending and, respectively, ascending chromosomal coordinates. ORF orientations are indicated by the arrows. Other proteins binding to the same chromosomal region are also indicated. Binding regions within coding regions are marked in purple lettering and green shading indicates multiple binding regions. *, significant binding regions that do not overlap in both replicates.
(XLSX)

S2 Table. Binding of Ace2-HA to chromosomal sequences of *C. albicans* under hypoxia and CO_2. Strain CLvW004 producing Ace2-HA from its chromosomal ORF and reference strain BWP17 were grown in YPD medium at 30°C under hypoxic conditions and in presence of elevated CO_2 levels (0.2% O_2 and 6% CO_2). Chromosomal cross-linking of proteins was done and chromatin was fragmented before immunoprecipitation. For immunoprecipitation anti-HA antibody was used and the precipitated chromatin was spotted on a *C. albicans* whole-genome tiling microarray. Regions showing significant enrichment of Ace2-HA binding compared to control strain BWP17 are listet along with their nearest neighbouring ORFs. Other proteins binding to the same chromosomal region are indicated and are taken from Lassak *et al.* [40]. Binding targets of wild-type Efg1 or HA-Efg1 shared with Ace2-HA are indicated with red background color. Accordingly to transcriptomal data obtained by Mulhern *et al.* [30], up- and down-regulation of genes is indicated of identified Ace2-HA target genes.
(XLSX)

S3 Table. Binding of Ace2-HA to chromosomal sequences of *C. albicans* under normoxia. Strain CLvW004 producing Ace2-HA from its chromosomal ORF and reference strain BWP17 were grown in YPD medium at 30°C under normoxic conditions. Chromosomal cross-linking of proteins was done and chromatin was fragmented before immunoprecipitation. For immunoprecipitation anti-HA antibody was used and the precipitated chromatin was spotted on a *C. albicans* whole-genome tiling microarray. Regions showing significant enrichment of Ace2-HA binding compared to control strain BWP17 are listet along with their nearest neighbouring ORFs. Other proteins binding to the same chromosomal region are indicated and are taken from Lassak *et al.* [40]. Binding targets of wild-type Efg1 or HA-Efg1 shared with Ace2-HA are indicated with red background color, binding targets of Ace2-HA obtained uniquely under normoxic conditions are indicated with green background color. Accordingly to transcriptomal data obtained by Mulhern *et al.* [30], up- and down-regulation of genes is indicated of identified Ace2-HA target genes.
(XLSX)

S4 Table. *C. albicans* strains.
(PDF)

S5 Table. Oligonucleotides.
(PDF)

Acknowledgments

We thank C. D´Enfert, S. Noble and A. Mitchell for providing strains and/or plasmids. We are grateful to E. Román and J. Pla for supplying the anti-Cek1 antibody.

Author Contributions

Conceived and designed the experiments: JFE. Performed the experiments: PRD LvW DK MJ. Analyzed the data: PRD LvW JFE. Wrote the paper: PRD LvW JFE.

References

1. Scanlan PD, Marchesi JR. Micro-eukaryotic diversity of the human distal gut microbiota: qualitative assessment using culture-dependent and-independent analysis of faeces. ISME J. 2008; 2: 1183–1193. doi: 10.1038/ismej.2008.76 PMID: 18670396
2. Ghannoum MA, Jurevic RJ, Mukherjee PK, Cui F, Sikaroodi M, Naqvi A, et al. Characterization of the oral fungal microbiome (mycobiome) in healthy individuals. PLoS Pathog. 2010; 6: e1000713. doi: 10.1371/journal.ppat.1000713 PMID: 20072605
3. Iliev ID, Funari VA, Taylor KD, Nguyen Q, Reyes CN, Strom SP et al. Interactions between commensal fungi and the C-type lectin receptor Dectin-1 influence colitis. Science. 2012; 336: 1314–1317. doi: 10.1126/science.1221789 PMID: 22674328
4. Brown DH Jr, Giusani AD, Chen X, Kumamoto CAFilamentous growth of *Candida albicans* in response to physical environmental cues and its regulation by the unique *CZF1* gene. Mol Microbiol. 1999; 34: 651–662. PMID: 10564506
5. Odds FC, Davidson AD, Jacobsen MD, Tavanti A, Whyte JA, Kibbler CC, et al. *Candida albicans* strain maintenance, replacement, and microvariation demonstrated by multilocus sequence typing. J Clin Microbiol. 2006; 44: 3647–3658. PMID: 17021093
6. Miranda LN, van der Heijden IM, Costa SF, Sousa AP, Sienra RA, Gobara S, Santos CR, Lobo RD, Pessoa VP Jr, Levin AS. *Candida* colonisation as a source for candidaemia. J Hosp Infect. 2009; 72: 9–16. doi: 10.1016/j.jhin.2009.02.009 PMID: 19303662
7. White SJ, Rosenbach A, Lephart P, Nguyen D, Benjamin A, Tzipori S, et al. Self-regulation of *Candida albicans* population size during GI colonization. PLoS Pathog. 2007; 3: e184. PMID: 18069889
8. Pierce JV, Dignard D, Whiteway M, Kumamoto CA. Normal adaptation of *Candida albicans* to the murine gastrointestinal tract requires Efg1p-dependent regulation of metabolic and host defense genes. Eukaryot Cell. 2013; 12: 37–49. doi: 10.1128/EC.00236-12 PMID: 23125349
9. Pande K, Chen C, Noble SM. Passage through the mammalian gut triggers a phenotypic switch that promotes *Candida albicans* commensalism. Nat Genet. 2013; 45: 1088–1091. doi: 10.1038/ng.2710 PMID: 23892606
10. Prieto D, Román E, Correia I, Pla J. The HOG pathway is critical for the colonization of the mouse gastrointestinal tract by *Candida albicans*. PLoS One. 2014; 9: e87128. doi: 10.1371/journal.pone.0087128 PMID: 24475243
11. Koh AY. Murine models of *Candida* gastrointestinal colonization and dissemination. Eukaryot Cell. 2013; 12: 1416–1422. doi: 10.1128/EC.00196-13 PMID: 24036344
12. Rosenbach A, Dignard D, Pierce JV, Whiteway M, Kumamoto CA. Adaptations of Candida albicans for growth in the mammalian intestinal tract. Eukaryot Cell. 2010; 9: 1075–1086. doi: 10.1128/EC.00034-10 PMID: 20435697
13. Jawhara S, Thuru X, Standaert-Vitse A, Jouault T, Mordon S, Sendid B, Desreumaux P, Poulain D. Colonization of mice by *Candida albicans* is promoted by chemically induced colitis and augments inflammatory responses through galectin-3. J Infect Dis. 2008; 197: 972–980. doi: 10.1086/528990 PMID: 18419533
14. Ernst JF, Tielker D. Responses to hypoxia in fungal pathogens. Cell Microbiol. 2008; 11: 183–190. doi: 10.1111/j.1462-5822.2008.01259.x PMID: 19016786
15. Grahl N, Cramer RA Jr. Regulation of hypoxia adaptation: an overlooked virulence attribute of pathogenic fungi? Med Mycol. 2010; 48: 1–15. doi: 10.3109/13693780902947342 PMID: 19462332
16. Peyssonnaux C, Boutin AT, Zinkernagel AS, Datta V, Nizet V, Johnson RS. Critical role of HIF-1alpha in keratinocyte defense against bacterial infection. J Invest Dermatol. 2008; 128: 1964–1968. doi: 10.1038/jid.2008.27 PMID: 18323789
17. Evans SM, Schrlau AE, Chalian AA, Zhang P, Koch CJ. Oxygen levels in normal and previously irradiated human skin as assessed by EF5 binding. J Invest Dermatol. 2006; 126: 2596–2606. PMID: 16810299
18. He G, Shankar RA, Chzhan M, Samouilov A, Kuppusamy P, Zweier JL. Noninvasive measurement of anatomic structure and intraluminal oxygenation in the gastrointestinal tract of living mice with spatial and spectral EPR imaging. Proc Natl Acad Sci U S A. 1999; 96: 4586–45891. PMID: 10200306

19. Setiadi ER, Doedt T, Cottier F, Noffz C, Ernst JF. Transcriptional response of *Candida albicans* to hypoxia: linkage of oxygen sensing and Efg1p-regulatory networks. J Mol Biol. 2006; 361: 399–411. PMID: 16854431

20. Synnott JM, Guida A, Mulhern-Haughey S, Higgins DG, Butler G. Regulation of the hypoxic response in *Candida albicans*. Eukaryot Cell. 2010; 9: 1734–1746. doi: 10.1128/EC.00159-10 PMID: 20870877

21. Sellam A, van het Hoog M, Tebbji F, Beaurepaire C, Whiteway M, Nantel A. Modeling the transcriptional regulatory network that controls the early hypoxic response in *Candida albicans*. Eukaryot Cell. 2014; 13: 675–690. doi: 10.1128/EC.00292-13 PMID: 24681685

22. Silver PM, Oliver BG, White TC. Role of *Candida albicans* transcription factor Upc2p in drug resistance and sterol metabolism. Eukaryot Cell. 2004; 3: 1391–1397. PMID: 15590814

23. Doedt T, Krishnamurthy S, Bockmühl DP, Tebarth B, Stempel C, Russell CL, et al. APSES proteins regulate morphogenesis and metabolism in *Candida albicans*. Mol Biol Cell. 2004; 15: 3167–3180. PMID: 15218092

24. Kelly MT, MacCallum DM, Clancy SD, Odds FC, Brown AJ, Butler G. The *Candida albicans CaACE2* gene affects morphogenesis, adherence and virulence. Mol Microbiol. 2004; 53: 969–983. PMID: 15255906

25. Stichternoth C, Ernst JF. Hypoxic adaptation by Efg1 regulates biofilm formation by *Candida albicans*. Appl. Environ. Microbiol. 2009; 75: 3663–3672. doi: 10.1128/AEM.00098-09 PMID: 19346360

26. Stoldt VR, Sonneborn A, Leuker C, Ernst JF. Efg1, an essential regulator of morphogenesis of the human pathogen *Candida albicans*, is a member of a conserved class of bHLH proteins regulating morphogenetic processes in fungi. EMBO J. 1997; 16: 1982–1991. PMID: 9155024

27. Lo HJ, Köhler JR, DiDomenico B, Loebenberg D, Cacciapuoti A, Fink GR. Nonfilamentous *C. albicans* mutants are avirulent. Cell. 1997; 90: 939–949. PMID: 9298905

28. Sonneborn A, Bockmühl DP, Ernst JF. Chlamydospore formation in *Candida albicans* requires the Efg1p morphogenetic regulator. Infect Immun. 1999; 67: 5514–5517. PMID: 10496941

29. Giusani AD, Vinces M, Kumamoto CA. Invasive filamentous growth of *Candida albicans* is promoted by Czf1p-dependent relief of Efg1p-mediated repression. Genetics. 2002; 160: 1749–1753. PMID: 11973327

30. Mulhern SM, Logue ME, Butler G. *Candida albicans* transcription factor Ace2 regulates metabolism and is required for filamentation in hypoxic conditions. Eukaryot Cell. 2006; 5: 2001–2013. PMID: 16998073

31. Bharucha N, Chabrier-Rosello Y, Xu T, Johnson C, Sobczynski S, Song Q et al. A large-scale complex haploinsufficiency-based genetic interaction screen in *Candida albicans*: analysis of the RAM network during morphogenesis. PLoS Genet. 2011; 7: e1002058. doi: 10.1371/journal.pgen.1002058 PMID: 22103005

32. Saputo S, Kumar A, Krysan DJ. Efg1 directly regulates *ACE2* expression to mediate cross-talk between the cAMP/PKA and RAM pathways during *Candida albicans* morphogenesis. Eukaryot Cell. 2014; 13: 1169–1180. doi: 10.1128/EC.00148-14 PMID: 25001410

33. Wang A, Raniga PP, Lane S, Lu Y, Liu H. Hyphal chain formation in *Candida albicans*: Cdc28-Hgc1 phosphorylation of Efg1 represses cell separation genes. Mol Cell Biol. 2009; 29: 4406–4416. doi: 10.1128/MCB.01502-08 PMID: 19528234

34. Kim AS, Garni RM, Henry-Stanley MJ, Bendel CM, Erlandsen SL, Wells CL. Hypoxia and extraintestinal dissemination of *Candida albicans* yeast forms. Shock. 2003; 19: 257–262. PMID: 12630526

35. Bendel CM, Hess DJ, Garni RM, Henry-Stanley M, Wells CL. Comparative virulence of *Candida albicans* yeast and filamentous forms in orally and intravenously inoculated mice. Crit Care Med. 2003; 31: 501–507. PMID: 12576958

36. Gianotti L, Alexander JW, Fukushima R, Childress CP. Translocation of *Candida albicans* is related to the blood flow of individual intestinal villi. Circ Shock. 1993; 40: 250–257. PMID: 8375026

37. Stichternoth C, Fraund A, Setiadi E, Giasson L, Vecchiarelli A, Ernst JF. Sch9 kinase integrates hypoxia and CO_2 sensing to suppress hyphal morphogenesis in *Candida albicans*. Eukaryot Cell. 2011; 10: 502–511. doi: 10.1128/EC.00289-10 PMID: 21335533

38. Noffz CS, Liedschulte V, Lengeler K, Ernst JF. Functional mapping of the *Candida albicans* Efg1 regulator. Eukaryot Cell. 2008; 7: 881–893. doi: 10.1128/EC.00033-08 PMID: 18375615

39. Bockmühl DP, Ernst JF. A potential phosphorylation site for an A-type kinase in the Efg1 regulator protein contributes to hyphal morphogenesis of *Candida albicans*. Genetics. 2001; 157: 1523–30. PMID: 11290709

40. Lassak T, Schneider E, Bussmann M, Kurtz D, Manak JR, Srikantha T, et al. Target specificity of the *Candida albicans* Efg1 regulator. Mol Microbiol. 2011; 82: 602–618. doi: 10.1111/j.1365-2958.2011.07837.x PMID: 21923768

41. Van Helden J, Rios AF, Collado-Vides J. Discovering regulatory elements in non-coding sequences by analysis of spaced dyads. Nucleic Acids Res. 2000; 28: 1808–1818. PMID: 10734201

42. Nobile CJ, Fox EP, Nett JE, Sorrells TR, Mitrovich QM, Hernday AD, et al. A recently evolved transcriptional network controls biofilm development in *Candida albicans*. Cell.2012; 148: 126–138. doi: 10.1016/j.cell.2011.10.048 PMID: 22265407

43. Liu H, Köhler J, Fink GR. Suppression of hyphal formation *in Candida albicans* by mutation of a STE12 homolog. Science. 1994; 266: 1723–1726. Erratum in Science. 1995;267:217. PMID: 7992058

44. Csank C, Schröppel K, Leberer E, Harcus D, Mohamed O, Meloche S, et al. Roles of the *Candida albicans* mitogen-activated protein kinase homolog, Cek1p, in hyphal development and systemic candidiasis. Infect Immun. 1998; 66: 2713–2721. PMID: 9596738

45. Ernst JF. Transcription factors in *Candida albicans*—environmental control of morphogenesis. Microbiology. 2000; 146: 1763–1774. PMID: 10931884

46. Rocha CR, Schröppel K, Harcus D, Marcil A, Dignard D, Taylor BN, et al. Signaling through adenylyl cyclase is essential for hyphal growth and virulence in the pathogenic fungus *Candida albicans*. Mol Biol Cell. 2001; 12: 3631–3643. PMID: 11694594

47. Bockmühl DP, Krishnamurthy S, Gerads M, Sonneborn A, Ernst JF. Distinct and redundant roles of the two protein kinase A isoforms Tpk1p and Tpk2p in morphogenesis and growth of *Candida albicans*. Mol Microbiol. 2001; 42: 1243–1257. PMID: 11886556

48. Saputo S, Chabrier-Rosello Y, Luca FC, Kumar A, Krysan DJ. The RAM network in pathogenic fungi. Eukaryot Cell. 2012; 11: 708–717. doi: 10.1128/EC.00044-12 PMID: 22544903

49. Cantero PD, Ernst JF. Damage to the glycoshield activates *PMT*-directed *O*-mannosylation via the Msb2-Cek1 pathway in *Candida albicans*. Mol Microbiol. 2011; 80: 715–725. doi: 10.1111/j.1365-2958.2011.07604.x PMID: 21375589

50. Badis G, Chan ET, van Bakel H, Pena-Castillo L, Tillo D, Tsui K et al. A library of yeast transcription factor motifs reveals a widespread function for Rsc3 in targeting nucleosome exclusion at promoters. Mol Cell. 2008; 32: 878–887. doi: 10.1016/j.molcel.2008.11.020 PMID: 19111667

51. Du H, Guan G, Xie J, Sun Y, Tong Y, Zhang L, et al. Roles of *Candida albicans* Gat2, a GATA-type zinc finger transcription factor, in biofilm formation, filamentous growth and virulence. PLoS One. 2012; 7: e29707. doi: 10.1371/journal.pone.0029707 PMID: 22276126

52. Nobile CJ, Mitchell AP. Regulation of cell-surface genes and biofilm formation by the *C. albicans* transcription factor Bcr1p. Curr Biol. 2005; 15: 1150–1155. PMID: 15964282

53. Fu Y, Filler SG, Spellberg BJ, Fonzi W, Ibrahim AS, Kanbe T, et al. Cloning and characterization of CAD1/AAF1, a gene from *Candida albicans* that induces adherence to endothelial cells after expression in *Saccharomyces cerevisiae*. Infect Immun. 1998; 66: 2078–2084. PMID: 9573092

54. Bertram G, Swoboda RK, Gooday GW, Gow NA, Brown AJ. Structure and regulation of the *Candida albicans ADH1* gene encoding an immunogenic alcohol dehydrogenase. Yeast. 1996; 12: 115–127. PMID: 8686375

55. Martin R, Moran GP, Jacobsen ID, Heyken A, Domey J, Sullivan DJ, et al. The *Candida albicans*-specific gene *EED1* encodes a key regulator of hyphal extension. PLoS One. 6:e18394. Mol Microbiol. 2011;53: 969–983. doi: 10.1371/journal.pone.0018394 PMID: 21512583

56. Bonhomme J, Chauvel M, Goyard S, Roux P, Rossignol T, d'Enfert C. Contribution of the glycolytic flux and hypoxia adaptation to efficient biofilm formation by *Candida albicans*. Mol Microbiol. 2011; 80: 995–1013. doi: 10.1111/j.1365-2958.2011.07626.x PMID: 21414038

57. Kadosh D, Johnson AD. Rfg1, a protein related to the *Saccharomyces cerevisiae* hypoxic regulator Rox1, controls filamentous growth and virulence in *Candida albicans*. Mol Cell Biol. 2001; 21: 2496–2505. PMID: 11259598

58. Zordan RE, Miller MG, Galgoczy DJ, Tuch BB, Johnson AD. Interlocking transcriptional feedback loops control white-opaque switching in *Candida albicans*. PLoS Biol. 2007; 5: e256 PMID: 17880264

59. Lohse MB, Hernday AD, Fordyce PM, Noiman L, Sorrells TR, Hanson-Smith V, et al. Identification and characterization of a previously undescribed family of sequence-specific DNA-binding domains. Proc Natl Acad Sci U S A. 2013; 110: 7660–7665. doi: 10.1073/pnas.1221734110 PMID: 23610392

60. Pérez JC, Kumamoto CA, Johnson AD. *Candida albicans* commensalism and pathogenicity are intertwined traits directed by a tightly knit transcriptional regulatory circuit. PLoS Biol. 2013; 11: e1001510. doi: 10.1371/journal.pbio.1001510 PMID: 23526879

61. Cao F, Lane S, Raniga PP, Lu Y, Zhou Z, Ramon K, et al. The Flo8 transcription factor is essential for hyphal development and virulence in *Candida albicans*. Mol Biol Cell. 2006; 17:295–307. PMID: 16267276

62. Du H, Guan G, Xie J, Cottier F, Sun Y, Jia W, et al. The transcription factor Flo8 mediates CO_2 sensing in the human fungal pathogen *Candida albican*s. Mol Biol Cell. 2012; 23: 2692–2701. doi: 10.1091/mbc.E12-02-0094 PMID: 22621896

63. Bruno VM, Kalachikov S, Subaran R, Nobile CJ, Kyratsous C, Mitchell AP. Control of the *C. albicans* cell wall damage response by transcriptional regulator Cas5. PLoS Pathog. 2006; 2: e21. PMID: 16552442

64. Bauer J, Wendland J. *Candida albicans* Sfl1 suppresses flocculation and filamentation. Eukaryot Cell. 2007; 6:1736–1744. PMID: 17766464

65. Li Y, Su C, Mao X, Cao F, Chen J. Roles of *Candida albicans* Sfl1 in hyphal development. Eukaryot Cell. 2007; 6: 1736–1744.

66. Gutiérrez-Escribano P, Zeidler U, Suárez MB, Bachellier-Bassi S, Clemente-Blanco A, Bonhomme J, et al. The NDR/LATS kinase Cbk1 controls the activity of the transcriptional regulator Bcr1 during biofilm formation in *Candida albicans*. PLoS Pathog. 2012; 8: e1002683. doi: 10.1371/journal.ppat.1002683 PMID: 22589718

67. Guan G, Xie J, Tao L, Nobile CJ, Sun Y, Cao C, et al. Bcr1 plays a central role in the regulation of opaque cell filamentation in *Candida albicans*. Mol Microbiol. 2013; 89: 732–750. doi: 10.1111/mmi.12310 PMID: 23808664

68. Lu Y, Su C, Liu H. A GATA transcription factor recruits Hda1 in response to reduced Tor1 signaling to establish a hyphal chromatin state in *Candida albicans*. PLoS Pathog. 2012; 8: e1002663. doi: 10.1371/journal.ppat.1002663 PMID: 22536157

69. Su C, Lu Y, Liu H. Reduced TOR signaling sustains hyphal development in *Candida albicans* by lowering Hog1 basal activity. Mol Biol Cell. 2013; 24: 385–397. doi: 10.1091/mbc.E12-06-0477 PMID: 23171549

70. Vandeputte P, Ischer F, Sanglard D, Coste AT. In vivo systematic analysis of *Candida albicans* Zn2-Cys6 transcription factors mutants for mice organ colonization. PLoS ONE. 2011; 6: e26962. doi: 10.1371/journal.pone.0026962 PMID: 22073120

71. Mukherjee PK, Sendid B, Hoarau G2, Colombel JF, Poulain D, Ghannoum MA. Mycobiota in gastrointestinal diseases. Nat Rev Gastroenterol Hepatol. 2015; 12: 77–87. doi: 10.1038/nrgastro.2014.188 PMID: 25385227

72. Seed PC. The Human Mycobiome. Cold Spring Harb Perspect Med. 2014; 5(5).

73. Brown GD, Denning DW, Gow NA, Levitz SM, Netea MG, White TC. Hidden killers: human fungal infections. Sci Transl Med. 2012; 4: 165rv13.

74. Pierce JV, Kumamoto CA. Variation in *Candida albicans EFG1* expression enables host-dependent changes in colonizing fungal populations. MBio. 2012; 3: e00117–12. doi: 10.1128/mBio.00117-12 PMID: 22829676

75. Lu Y, Su C, Solis NV, Filler SG, Liu H. Synergistic regulation of hyphal elongation by hypoxia, CO(2), and nutrient conditions controls the virulence of *Candida albicans*. Cell Host Microbe. 2013; 14: 499–509 doi: 10.1016/j.chom.2013.10.008 PMID: 24237696

76. Su C, Li Y, Lu Y, Chen J. Mss11, a transcriptional activator, is required for hyphal development in *Candida albicans*. Eukaryot Cell. 2009; 8: 1780–1791. doi: 10.1128/EC.00190-09 PMID: 19734367

77. Hope H, Bogliolo S, Arkowitz RA, Bassilana M. Activation of Rac1 by the guanine nucleotide exchange factor Dck1 is required for invasive filamentous growth in the pathogen *Candida albicans*. Mol Biol Cell. 2008; 19: 3638–3651. doi: 10.1091/mbc.E07-12-1272 PMID: 18579689

78. Sasse C, Schillig R, Dierolf F, Weyler M, Schneider S, Mogavero S, et al. The transcription factor Ndt80 does not contribute to Mrr1-, Tac1-, and Upc2-mediated fluconazole resistance in *Candida albicans*. PLoS One. 2011; 6: e25623. doi: 10.1371/journal.pone.0025623 PMID: 21980509

79. Fonzi WA, Irwin MY. Isogenic strain construction and gene mapping in *Candida albicans*. Genetics. 1993; 134: 717–728. PMID: 8349105

80. Braun BR, Johnson AD. *TUP1*, *CPH1* and *EFG1* make independent contributions to filamentation in *Candida albicans*. Genetics. 2000; 155: 57–67. PMID: 10790384

81. Chauvel M, Nesseir A, Cabral V, Znaidi S, Goyard S, Bachellier-Bassi S, et al. A versatile overexpression strategy in the pathogenic yeast *Candida albicans*: identification of regulators of morphogenesis and fitness. PLoS One. 2012; 7: e45912. doi: 10.1371/journal.pone.0045912 PMID: 23049891

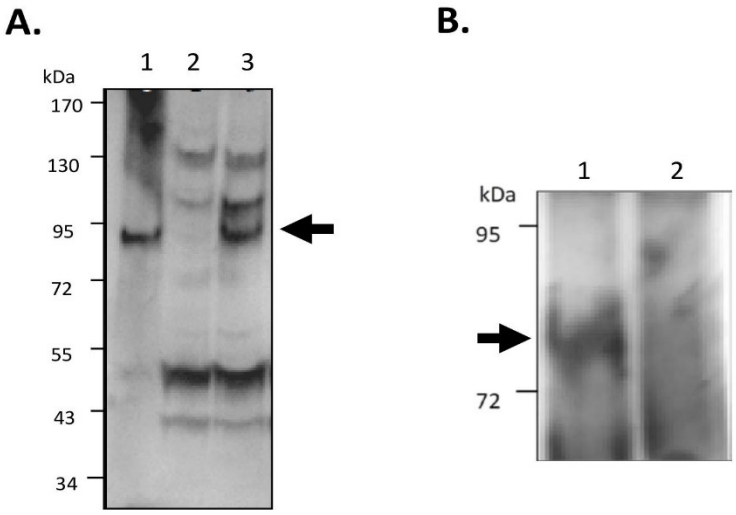

S1 Fig. Activity of rabbit anti-Efg1 antiserum. A. Immunoblotting. Extracts of *efg1* mutant HLC67 (lane 2) and control strain CAF2-1 (lane 3) were separated by SDS-PAGE and blots were probed with anti-Efg1 antiserum (1 : 5000). For comparison, 250 ng of *E. coli*-produced His_{10}-Efg1 protein was used (lane 1). **B.** Immunoprecipitation. Efg1 was immunoprecipitated using anti-Efg1 antiserum and protein G-coated agarose beads. Immunoprecipitates from the control strain CAF2-1 (lane 1) and the *efg1* mutant HLC67 (lane 2) were analysed by immunoblotting using anti-Efg1 antiserum. The arrow indicates the migration of Efg1.

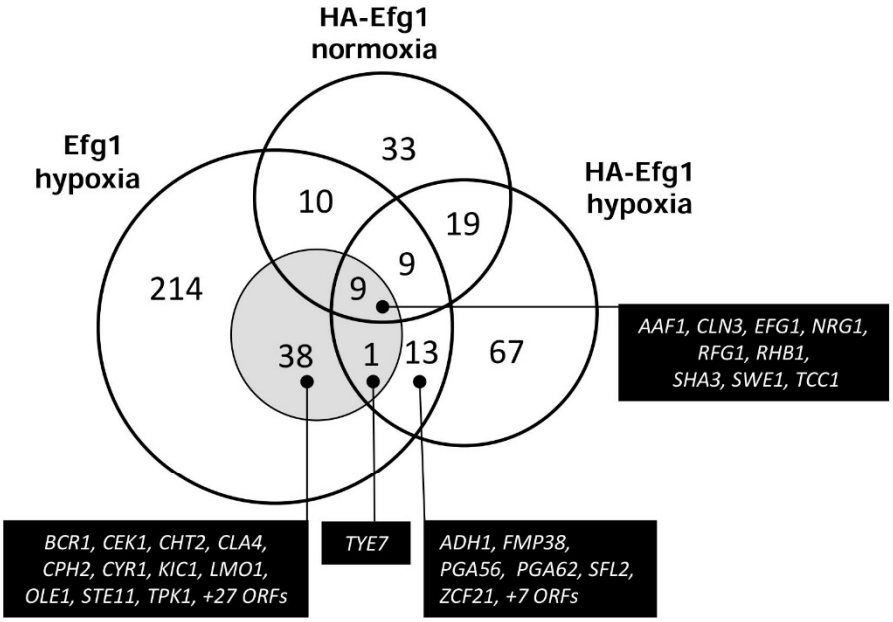

S2 Fig. Intersection of genomic binding sites for Efg1 and HA-Efg1 under hypoxia and normoxia. For Efg1, genomic binding sites were derived from ChIP chip experiments comparing strains CAF2-1 (*EFG1/EFG1*) and HLC52 (*efg1/efg1*); for HA-Efg1, strains HLCEEFG1 (*efg1/efg1* [*HA-EFG1*]) and CAF2-1 were compared. Normoxic binding sites for HA-Efg1 were obtained from Lassak *et al.* [40]. The shaded circle encompasses genes in filamentous growth.

GO term[1] (genome frequency)	HA-Efg1 binding genes annotated to the term[2] Name	Frequency[3]	*P* value[4]
A. Process			
Regulation of multi-organism process (1.6 %)	*AHR1 ALS1 BMH1 BRG1 CBK1 CRZ2[a] CSR1 CZF1[a] DEF1[a] EFG1[ac] SHA3[a] TEC1[a] TYE7*	11.4 %	1.39e-05
Regulation of filamentous growth (2.6 %)	*AHR1 BMH1 BRG1 CBK1 CLN3 CZF1 DEF1 EFG1[ac] NRG1[ac] RFG1[ac] RME1 TEC1[a] TYE7 WOR2[a]*	12.3 %	0.00066
Regulation of biosynthetic process (10.9 %)	*AAF1[ac] ADAEC AHR1 BMH1 BRG1 CBF1[a] CBK1 CLN3 CRZ2[a] CSR1 CUP9 CZF1 EFG1[ac] GZF3 HTB1 NRG1[ac] RFG1[ac] RME1 RPS23A RTF1 SBP1 SFU1 SHA3[a] TCC1[ac] TEC1[a] TYE7, WOR2[a] ZCF21 ORF19.4375*	25.4 %	0.00532
***B*. Function**			
Nucleic acid binding transcription factor activity (3.4 %)	*AHR1 BRG1 CBF1[a] CRZ2[a] CSR1 CUP9 CZF1 EFG1[ac] GZF3 NRG1[ac] RFG1[ac] RME1 SFU1 TEC1[a] TYE7 WOR2 ZCF21*	14 %	3.25e-05
Sequence-specific DNA binding (2.9 %)	*AHR1 BMH1 BRG1 CBF1[a] CSR1 CUP9 EFG1[ac] GZF3 NRG1[ac] RFG1[ac] RME1 SBP1 SFU1 TEC1[a] TYE7 WOR3*	14.9 %	1.83e-05

S3 Fig. GO categories of genes binding HA-Efg1 under hypoxia. GO terms for Efg1 binding targets were identified in ChIP chip data using the CGD GO Term Finder tool (http://www.candidagenome.org/cgi-bin/GO/goTermFinder); the analysis was conducted in June 2013. Genome frequencies of genes corresponding to GO terms are expressed as percentages (gene number relative to 6,525 genes in the *C. albicans* genome; the frequency of genes binding Efg1 that correspond to a specific GO term are expressed relative to the total number of 106 genes binding HA-Efg1). Superscripts: a, Efg1 binding in yeast normoxia [40]; b, Efg1 binding in hyphae inducing conditions [40]; c, Efg1 binding in biofilm inducing conditions [42]. *P* values for overrepresented categories were calculated using a hyper geometric distribution with multiple hypothesis correction according to the GO Term Finder tool website (http://www.candidagenome.org/help/goTermFinder.shtml). The *P* value cutoff used was 0.05.

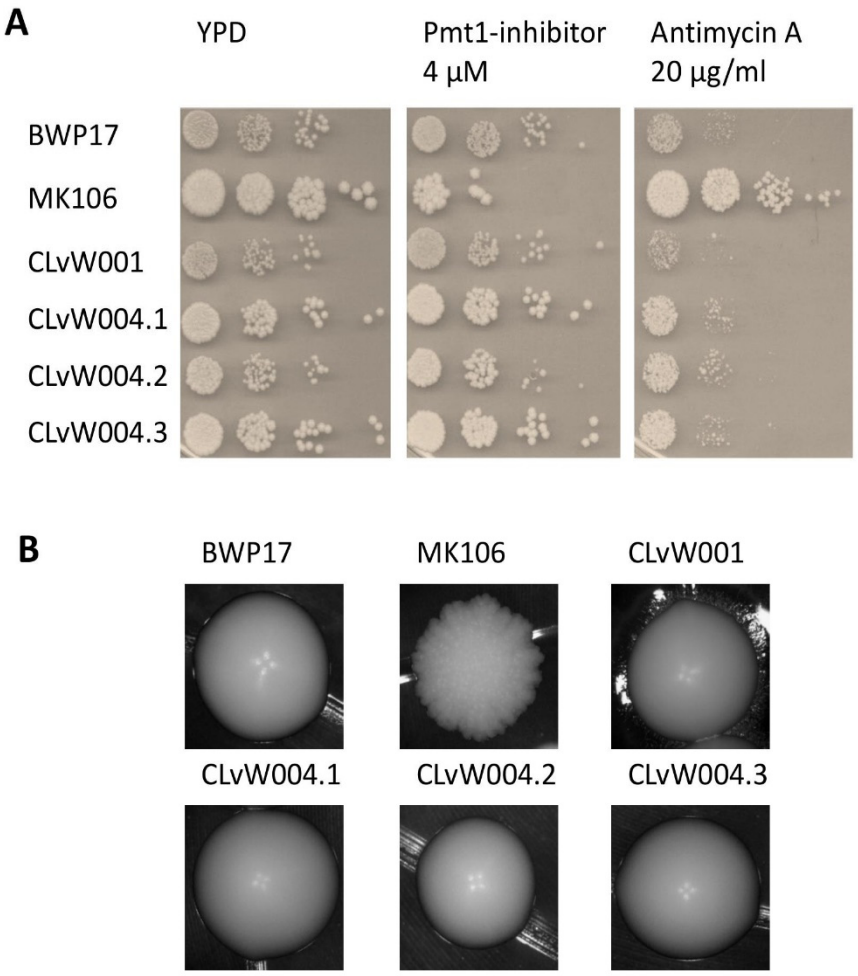

S4 Fig. Functionality of the HA tagged Ace2 protein. To verify the functionality of C-terminal HA-tagged Ace2 the phenotypes of three isolates of strain CLvW004 (*ACE2-HA/ace2*) was compared to mutant strain MK106 (*ace2/ace2*), wild-type strain BWP17 (*ACE2/ACE2*) and the heterozygous strain CLvW001 (*ACE2/ace2*). (A) Drop dilution assay for sensitivity to 4 µM Pmt1-inhibitor and resistance to antimycin A (20 µg/ml). The agar plates were photographed after 2 d incubation at 30 °C. The *ace2* mutant strain Mk106 shows enhanced sensitivity to the Pmt1-inhibitor [49] and is less susceptible to the respiratory inhibitor antimycin A [30]. (B) Colonies of the indicated strains were photographed following growth for 2 d at 30 °C on YPD agar. The *ace2* mutant strain Mk106 shows the wrinkled colony phenotype described previously [27]. Phenotypes of strains CLvW004.1-3 correspond to the heterozygous strain CLvW001 indicating that the Ace2-HA protein is functional.

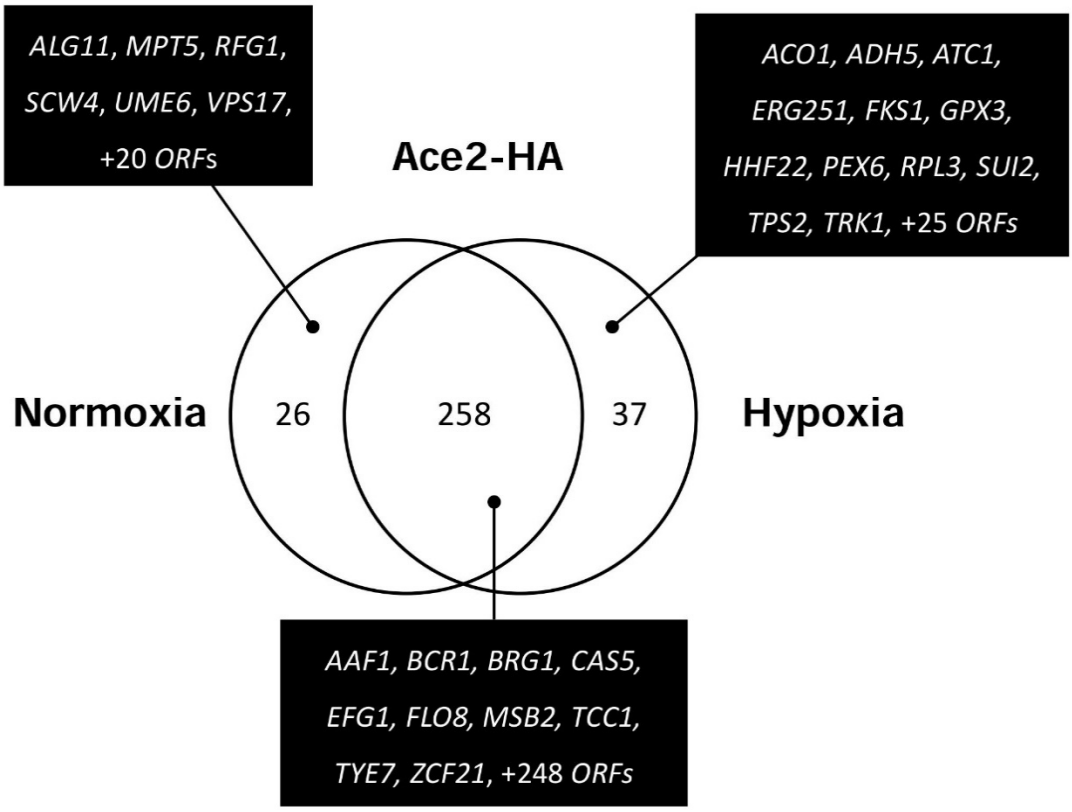

S5 Fig. **Genomic binding sites for Ace2**. Venn diagram showing numbers of genes bound by HA-tagged Ace2 under normoxic conditions (30 °C, YPD) and hypoxic conditions (30 °C, YPD 0.2 % O_2 and 6 % CO_2). Binding regions with the corresponding ORFs are listed in supplementary table S2 and S3. Genomic binding sites were derived from ChIP chip experiments comparing strains CLvW004 (*ACE2-HA/ace2*) and BWP17 (non tag control). For both conditions, 258 genes are common.

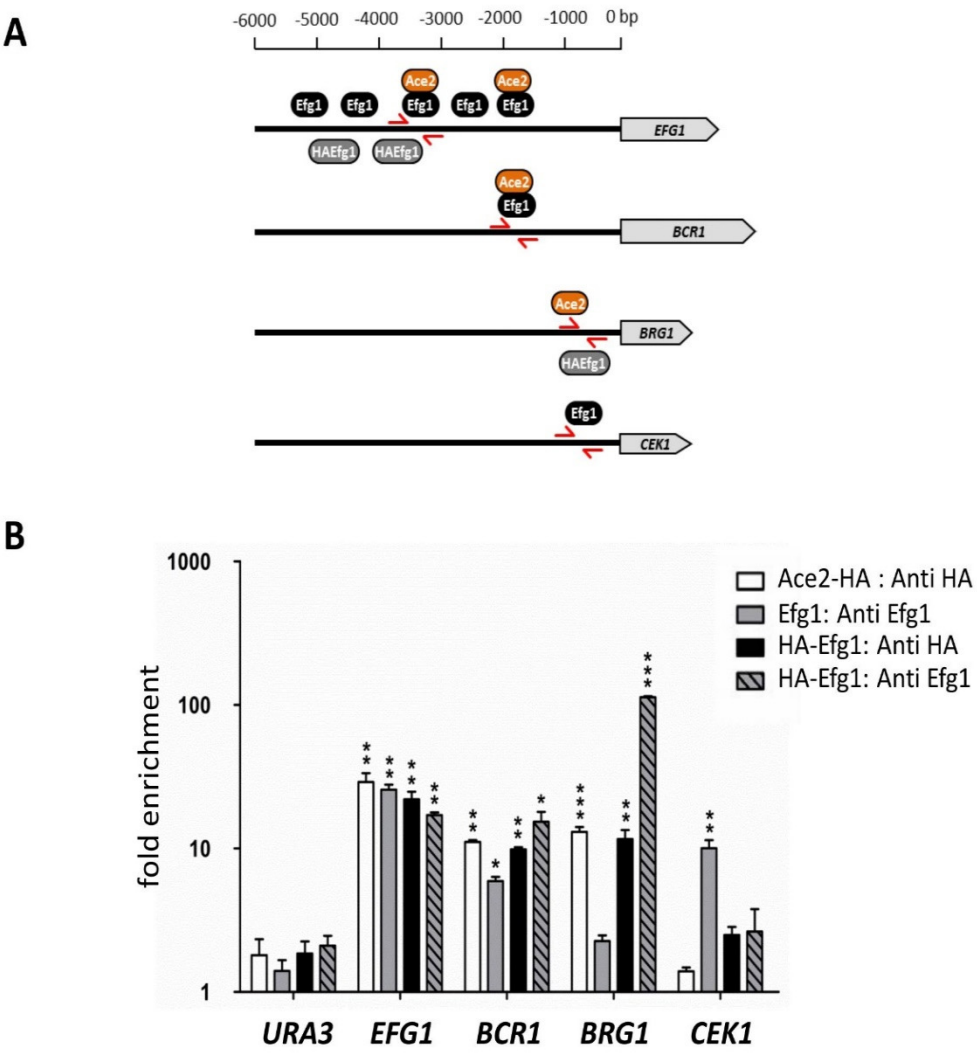

S6 Fig. Genomic localization of Ace2 and Efg1 on target promoters. (A) Binding positions identified by ChIP chip experiments. Binding positions of Efg1 (black ovals), Ace2-HA (orange ovals) and HA-Efg1 positions (grey ovals) identified by ChIP chip experiments are shown schematically. (B) Quantitation of Ace2, HA-Efg1 and Efg1 enrichment by ChIP on target promoters. Following ChIP the respective fold enrichment was determined by qPCR using oligonucleotide pairs shown by red arrows in A. Chromatin of strains CAF2 -1 (Efg1) and HLCEEFG1 (HA-Efg1) was immunoprecipitated using anti-Efg1 and anti-HA antibody, respectively, as described in S1 Table. For Ace2 enrichment anti-HA antibody was used for immunoprecipitation of strain CLvW004 (Ace2-HA), as described in S2 Table. In a control experiment, ChIP followed by qPCR was also done using anti-Efg1 antibody on extracts of strain HLCEEFG1 (HA-Efg1). qPCR experiments were done using two biological replicates, which were assayed in triplicate. The mean fold enrichment (± standard deviation) for each protein was calculated relative to the respective no tag or mutant strain and normalized to the input sample. Statistical relevance is indicated by asterisks: *, $P < 0.05$; **, $P < 0.01$; ***, $P < 0.001$. The results verify the presence of proteins on target promoters; in addition, the presence of HA-Efg1 on the *BCR1* promoter, which was not found in the ChIP chip experiment, was revealed by the ChIP-qPCR experiment.

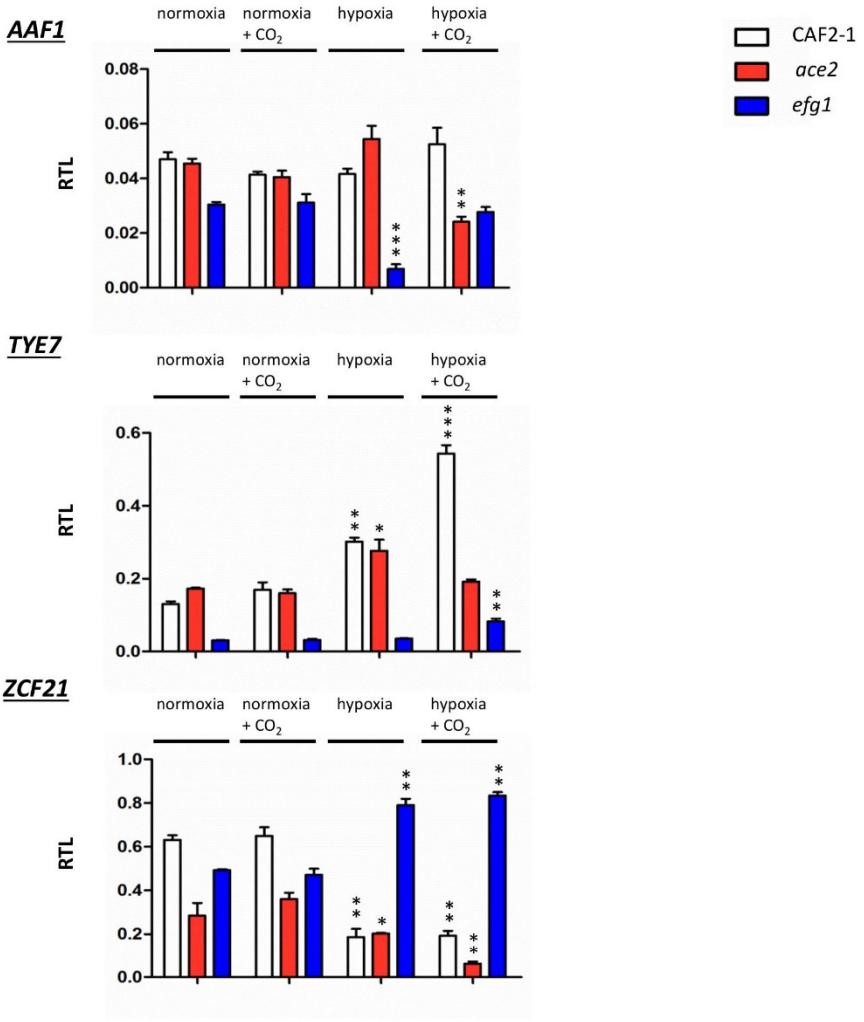

S7 Fig. Transcriptional regulation of selected Efg1 and Ace2 target genes under hypoxia. Strains CAF2-1 (control), the *ace2* mutant MK106 and the *efg1* mutant HLC52 were precultured under normoxia at 30 °C in YPD medium and used for inoculation of 100 ml YPD cultures under normoxia, or normoxia with addition of CO_2 (6 % CO_2), or under hypoxia (0.2 % O_2), or under hypoxia with addition of CO_2 (0.2 % O_2, 6 % CO_2). Cultures were incubated at 30 °C in the respective condition until OD_{600}= 0.5 and total RNA was then isolated. Relative transcript levels were determined using *ACT1* transcript as the reference as described in Fig. 4. Relative transcript levels (RTL) for the *AAF1*, *TYE7* and *ZCF21* transcripts in strains CAF2-1 (control), HLC52 (*efg1*) and MK106 (*ace2*). Error bars represent standard deviation of the means. A two-tailed, unpaired *t* test comparing the cycle threshold values of samples grown in hypoxic and normoxic conditions for each mutant respectively was used to determine the statistical relevance: *, $P < 0.05$; **, $P < 0.01$; ***, $P < 0.001$.

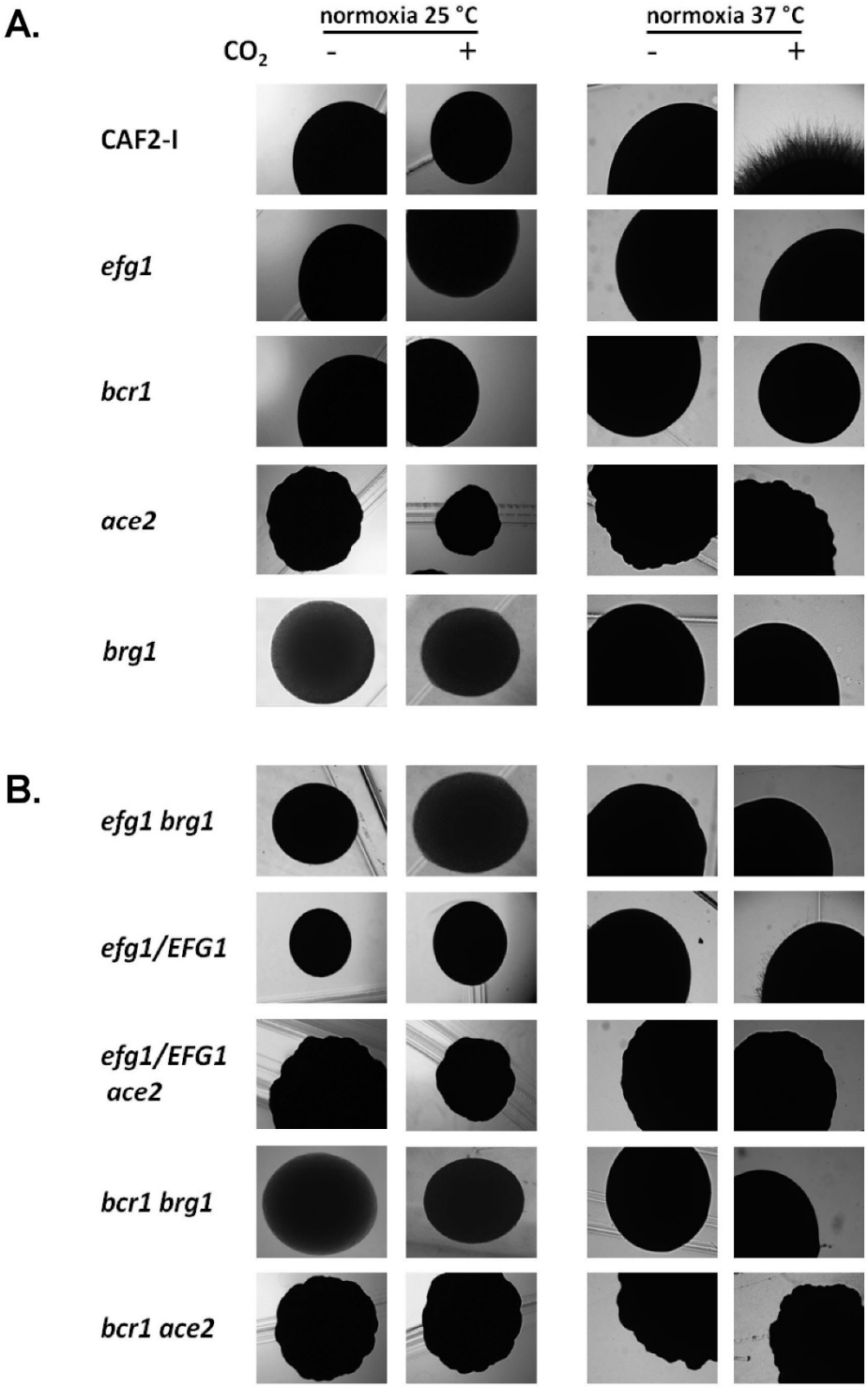

S8 Fig. Normoxic phenotypes of mutants lacking hypoxic regulators under hypoxia. The strains were grown under normoxia without or with 6 % CO_2 on YPS agar for 4 d at 25 °C or for 3d at 37 °C. Strains included CAF2-1 (control), homozygous single mutants HLC52 (*efg1*), CJN702 (*bcr1*), MK106 (*ace2*), TF022 (*brg1*) and double knockout strains PDEB4 (*efg1 brg1*), PDBB4 (*bcr1 brg1*) and CLvW024 (*bcr1 ace2).* *ACE2* could not be disrupted in an *efg1* mutant background; therefore, the heterozygous mutant strain CLvW047 (*efg1/EFG1, ace2/ace2*) was constructed and its phenotype was compared to the *efg1/EFG1* strain DSC11.

S4 Table. *C. albicans* strains

Strain	Genotype	reference/source
SC5314	wild-type	[1]
CAF2-1	*URA3/ura3::imm434*	[1]
CAI4	*ura3::imm434/ura3::imm434*	[1]
HLC52	Like CAI4 but *efg1::hisG/efg1::hisG-URA3-hisG*	[2]
HLC67	Like CAI4 but *efg1::hisG/efg1::hisG*	[2]
HLC46	Like CAI4 but *EFG1/efg1::hisG-URA3-hisG*	[2]
BCA0901	Like CAI4, but *EFG1/efg1::hisG-URA3-hisG*	[3]
JKC19	Like CAI4, but *cph1::hisG/cph1::hisG-URA3-hisG*	[4]
HLC54	Like CAI4 but *cph1::hisG/cph1::hisG efg1/efg1::hisG-URA3-hisG*	[2]
HLCE	Like HLC67 but *efg1::hisG/efg1::* [*EFG1p-URA3*]	[5]
HLCEEFG1	Like HLC67, but *efg1::hisG/efg1::*[*EFG1p-HA-EFG1-URA3*] (pTD38 HA/Pac1 integrated in *EFG1p*)	[5]
HLCPEFG1	Like HLC67, but *efg1::hisG/efg1::*[*EFG1p-EFG1-URA3*] (pPRDA208C/Pac1 integrated in *EFG1p*)	this study
HLCNEFG1	Like HLC67, but *efg1::hisG/efg1::*[*EFG1p-ΔN-EFG1-URA3*] (pPDNEFG1/Pac1 integrated in *EFG1p*)	this study
HLC67[pDB1]	Like HLC67, but *LEU2/leu2::PCK1p-EFG1*^{T206A}*-URA3*	[6]
HLC67[pDB2]	Like HLC67, but *LEU2/leu2::PCK1p-EFG1*^{T206E}*-URA3*	[6]
HLCEEFG1T206A	Like HLC67, but *efg1::hisG/efg1::*[*EFG1p-EFG1*^{T206A}*-URA3*] (pPDEFG1T206A/Pac1 integrated in *EFG1p*)	this study
HLCEEFG1T206E	Like HLC67, but *efg1::hisG/efg1::*[*EFG1p-EFG1*^{T206E}*-URA3*] (pPDEFG1T206E/Pac1 integrated in *EFG1p*)	this study
HLCEEFG1T179A	Like HLC67, but *efg1::hisG/efg1::*[*EFG1p-EFG1*^{T179A}*-URA3*] (pPDEFG1T179A/Pac1 integrated in *EFG1p*)	this study
HLCEEFG1T179E	Like HLC67, but *efg1::hisG/efg1::*[*EFG1p-EFG1*^{T179E}*-URA3*] (pPDEFG1T179E/Pac1 integrated in *EFG1p*)	this study
CEC2907	Like CAI4, but *his1::hisG/HIS1 arg4::hisG/ARG4 ADH1/adh1::TDH3p-carTA::SAT1*	[7]
CECSTE11	Like CEC2907, but *RPS1/RPS1::TETp-STE11-URA3* (pClp10TETSTE11/StuI integrated in *RPS1* locus)	this study
CECCEK1	Like CEC2907, but *RPS1/RPS1::TETp-CEK1-URA3* (pClp10TETCEK1/StuI integrated in *RPS1* locus)	this study
CECCPH1	Like CEC2907, but *RPS1/RPS1::TETp-CPH1-URA3* (pClp10TETCPH1/StuI integrated in *RPS1* locus)	this study
DSC11	*efg1::hisG/efg1::hisG::EFG1-dpl200 ura3::imm434/ura3::imm434::URA3*	[8]
BWP17	*ura3::imm434/ura3::imm434, his1::hisG/his1::hisG arg4::hisG/arg4::hisG*	[9]
MK106	Like SC5314, but *ace2::FRT/ace2::FRT*	[10]
CLvW001	Like BWP17, but *ace2::lacZ-SAT1/ACE2*	this study
CLvW004	Like CLvW001, but *ace2::SAT1/ACE2*^{HA}*::URA3*	this study
CLvW008	Like CAI4, but *ace2::FRT/ace2::FRT*	this study
SN250	*ura3Δ::imm434::URA3-IRO1/ura3Δ::imm434 arg4::hisG/arg4::hisG his1::hisG/his1::hisG leu2::hisG::CdHIS1/leu2::hisG::CmLEU2*	[11]
CLvW047	Like CLvW008, but *efg1::hisG-URA3-hisG/EFG1*	this study
CJN702	Like Bwp17, but *his1::hisG/his1::hisG::pHIS1 bcr1::URA3/bcr1::ARG4*	[12]
CLvW024	Like CJN702, but *ace2::FRT/ace2::FRT*	this study
TF022	*ura3Δ::imm434::URA3-IRO1/ura3Δ::imm434 arg4::hisG/arg4::hisG his1::hisG/his1::hisG leu2::hisG/leu2::hisG brg1Δ::CmLEU2/brg1Δ::CdHIS1*	[13]
PDEB4	Like HLC52, but *brg1::FRT/brg1::FRT*	this study
PDBB4	Like CJN702, but *brg1::FRT/brg1::FRT*	this study

References

1. Fonzi WA, Irwin MY. Isogenic strain construction and gene mapping in *Candida albicans*. Genetics. 1993;134: 717-728.

2. Lo HJ, Köhler JR, DiDomenico B, Loebenberg D, Cacciapuoti A, Fink GR. Nonfilamentous *C. albicans* mutants are avirulent. Cell. 1997;90: 939-949.

3. Braun BR, Johnson AD. *TUP1*, *CPH1* and *EFG1* make independent contributions to filamentation in *Candida albicans*. Genetics. 2000;155: 57-67.

4. Liu H, Köhler J, Fink GR. Suppression of hyphal formation *in Candida albicans* by mutation of a STE12 homolog. Science. 1994;266: 1723-1726. Erratum in Science. 1995;267:217.

5. Noffz CS, Liedschulte V, Lengeler K, Ernst JF. Functional mapping of the *Candida albicans* Efg1 regulator. Eukaryot Cell. 2008;7: 881-893.

6. Bockmühl DP, Ernst JF. A potential phosphorylation site for an A-type kinase in the Efg1 regulator protein contributes to hyphal morphogenesis of *Candida albicans*. Genetics. 2001;157: 1523-30.

7. Chauvel M, Nesseir A, Cabral V, Znaidi S, Goyard S, Bachellier-Bassi S, et al. A versatile overexpression strategy in the pathogenic yeast *Candida albicans*: identification of regulators of morphogenesis and fitness. PLoS One. 2012;7: e45912.

8. Park H, Myers CL, Sheppard DC, Phan QT, Sanchez AA, Edwards JE, Filler SG. Role of the fungal Ras-protein kinase A pathway in governing epithelial cell interactions during oropharyngeal candidiasis. Cell Microbiol 2005;7: 499–510.

9. Wilson RB, Davis D, Mitchell AP. Rapid hypothesis testing with *Candida albicans* through gene disruption with short homology regions. J Bacteriol. 1999;181: 1868-1874.

10. Kelly MT, MacCallum DM, Clancy SD, Odds FC, Brown AJ, Butler G. The *Candida albicans CaACE*2 gene affects morphogenesis, adherence and virulence. Mol Microbiol. 2004;53: 969-983.

11. Noble SM, French S, Kohn LA, Chen V, Johnson AD. Systematic screens of a *Candida albicans* homozygous deletion library decouple morphogenetic switching and pathogenicity. Nat Genet. 2010;42: 590-598.

12. Nobile CJ, Mitchell AP. Regulation of cell-surface genes and biofilm formation by the *C. albicans* transcription factor Bcr1p. Curr Biol. 2005;15: 1150-1155.

13. Homann OR, Dea J, Noble SM, Johnson AD. A phenotypic profile of the *Candida albicans* regulatory network. PLoS Genet. 2009;5: e1000783.

S1 Table. Binding of Efg1 to chromosomal sequences of *C. albicans* under hypoxia. Strain CAF2-1 producing wild-type Efg1 was grown in YPD medium at 30 °C under hypoxic conditions (0.2% O_2), followed by chromosomal cross-linking of proteins. Fragmented chromatin was immunoprecipitated using anti-Efg1 antibody and used as probe for tiling microarrays covering the *C. albicans* genome. Regions showing significantly increased binding of Efg1 compared to control strain Hlc52 (*efg1/efg1*) are listed along with their nearest neigbouring ORFs designated left or right ORF if situated at descending and, respectively, ascending chromosomal coordinates. ORF orientations are indicated by the arrows. Other proteins binding to the same chromosomal region are also indicated. Binding regions within coding regions are marked in purple lettering and green shading indicates multiple binding regions. *, significant binding regions did not overlap in both replicates.

Chr	binding region	size (bp)	left ORF	gene name	left ORF position	additional binding proteins	right ORF	gene name	right ORF Position	additional binding proteins
1	41740..42160	420	*ORF19.6080*	*BFA1*	40485<--41771		*ORF19.6079*		42606-->43505	
1	161400..164000	2600	*ORF19.6022*		160946<--162676		*ORF19.6021*	*IHD2*	167084-->167830	
1	238530..238840	310	*ORF19.3305*	*ZCF17*	236100<--238300					
1	281757..282429	672	*ORF19.3330.3*	*POX18*	280432<--280830		*ORF19.3331*	*ABC1*	282488-->284148	
1	293789..295440	1641	*ORF19.3336*		296059<--296517	Efg1 (Normoxia)				
1	343880..345560	1680	*ORF19.3358*	*LSC1*	342949<--343920		*ORF19.3359*	*ARP8*		
1	405320..406158	838	*ORF19.4528*		403100<--403700		*ORF19.4527*	*HGT1*	406700-->408300	
1	438840..442620	3780	*ORF19.3668*	*HGT2*	434400<--436100					
1	468060..469140	1080					*ORF19.3681*		469200-->471700	
1	496987..497743	756	*ORF19.3694*		496220<--496250					
1	513480..514940	1460	*ORF19.2929*	*GSC1*	506000<--511600					
1	624356..625250	894	*ORF19.2990*	*XOG1*	622280<--623598		*ORF19.2991*	*HOL1*	628104-->629850	
1	642960..643280	320	*ORF19.3001*	*TEM1*	642020<--642720		*ORF19.3002*	*RPS1*		
1	676300..677320	1020	*ORF19.3014*	*BMH1*	675150<--675950					
1	801402..801789	387	*ORF19.1028*	*ELA1*	798250<--799400		*ORF19.1027*	*PDR16*	801800-->802900	
1	811500..813800	2300	*ORF19.4457*	*BNI4*	806500<--811500					
1	817700..818450	750	*ORF19.4459*		813950<--815600	Efg1 (Normoxia)				
1	831858..832160	302					*ORF19.4468*		832180-->832700	
1	871387..871611	224	*ORF19.1051*	*HTA2*	870750<--871150		*ORF19.1052*		872000-->872400	
1	879390..879720	330	*ORF19.1057*		879400<--878800		*ORF19.1058*			
1	881900..882250	350	*ORF19.1060*		881450<--881950			*HHT21*	882240-->882660	
1	889200..892950	3750	*ORF19.1064*	*ASC2*	886000<--889200					
1	892300..892950	650	*ORF19.1065*	*SSA2*	890400<--892400					
1	896950..898000	1050					*ORF19.1069*	*RPN4*	898000-->899500	
1	913960..914230	270	*ORF19.5197*	*APE2*	911200<--914300					
1	945500..946100	600	*ORF19.6852*		943720<--944530		*ORF19.6852.1*		946320-->946508	
1	993420..993780	360	*ORF19.767*	*ERG3*	991690<--992840					
1	1032864..1033900	1036	*ORF19.48*		1028320<--1032500					
1	1035900..1036850	950	*ORF19.50*		1033920<--1035920		*ORF19.51*		1036980-->1040960	
1	1376850..1377800	950	*ORF19.6265.1*	*RPS14B*	1375920<--1376750		*ORF19.6265*	*RPS22A*	1377105-->1377500	
1	1833360..1833780	420	*ORF19.5114.1*		1832950<--1833140					
1	1835820..1836540	720	*ORF19.5117*	*OLE1*	1834360<--1835812					
1	1865684..1866220	536	*ORF19.395*	*ENO1*	1864240<--1865570		*ORF19.396*	*EAF6*	1866510-->1867150	
1	1913970..1914750	780	*ORF19.4737*	*TPO3*	1914900<--1916600					

1	1933440..1933890	450	*ORF19.4748*	*MSL1*	1933050<--1933450			*ORF19.4749*		1933890-->1935570
1	2052390..2053200	810	*ORF19.4792*		2050140<--2051810			*ORF19.4793*		2050000-->2051800
1	2098500..2099800	1300	*ORF19.4818*		2102700<--2104290					
1	2193660..2193990	330	*ORF19.4867*	*SWE1*	2189160<--2192700	Efg1 (Normoxia)		*ORF19.4869*	*SFU1*	2195410-->2196960
1	2252800..2254800	2000	*ORF19.4890*	*CLA4*	2249520<--2252470					
1	2256940..2257500	560	*ORF19.4892*	*TPK1*	2255640<--2256855					
1	2300880..2301120	240	*ORF19.4909.1*	*RPL42*	2300031<--2300730					
1	2307550..2307860	310	*ORF19.4912*		2305310<--2307240			*ORF19.984*	*PHO8*	2309140-->2310647
1	2401200..2402900	1700	*ORF19.2333*		2399740<--2401214			*ORF19.2332*		2403600-->2404380
1	2406060..2406510	450		*ADA2*	2404450<--2405790				*RPS17B*	2406591-->2407383
1	2437190..2437750	560						*ORF19.2309*	*RPL2*	2438200-->2440300
1	2441250..2441950	700	*ORF19.2308*		2442020<--2443140					
1	2491650..2492070	420	*ORF19.667.1*		2492140<--2492760					
1	2514000..2514450	450	*ORF19.657*	*SAM2*	2513620<--2514780					
1	2682800..2683800	1000	*ORF19.5234*	*RBD1*	2680634<--2682643			*ORF19.5233*		2683788-->2684135
1	2694600..2695800	1200	*ORF19.5228*	*RIB3*	2694013<--2694636			*ORF19.5227*		2695968-->2696465
1	2776700..2776800	100						*ORF19.6348*		2776744-->2779569
1	2852850..2853620	770	*ORF19.4936*		2853604<--2853999					
1	2869900..2871300	1400	*ORF19.4941*	*TYE7*	2869020<--2869829			*ORF19.4942*		2871337-->2871705
1	2890500..2891200	700	*ORF19.4952*		2891695<--2892633					
1	2910180..2910390	210	*ORF19.4960*		2907412<--2908446			*ORF19.4961*	*STP2*	2911732-->2913486
1	2943300..2943800	500	*ORF19.4972*		2935625<--2937571			*ORF19.4975*	*HYR1*	2944794-->2947553
1	2992290..2993110	820	*ORF19.4997*	*KIS2*	2987895<--2990032			*ORF19.4998*	*ROB1*	2993348-->2996389
1	3023800..3026000	2200	*ORF19.5014*		3022829<--3023536			*ORF19.5015*	*MYO2*	3026140-->3030825
1	3034100..3035260	1160	*ORF19.5017*	*DUR32*	3031584<--3033599			*ORF19.5019*		3035261-->3037345
1	3040660..3041150	490	*ORF19.5021*	*PDX1*	3039105<--3040358			*ORF19.5022*		3041593-->3043548
1	3051300..3051700	400	*ORF19.5024*	*GND1*	3045995<--3048182			*ORF19.5025*	*MET3*	3051624-->3053207
1	3071600..3072800	1200						*ORF19.5032*	*SIM1*	3074225-->3075343
1	3080420..3081050	630						*ORF19.5035*		3078708-->3080366
1	3112130..3112640	510	*ORF19.7218*	*RBE1*	3108246<--3109061			*ORF19.7219*	*FTR1*	3113806-->3114951
2	163500..164100	600								
2	465977..466288	311	*ORF19.1555*	*SAC3*	464538<--468209					
2	557960..558130	170	*ORF19.5826*		557079< 558713					
2	593190..594270	1080	*ORF19.5806*	*ALD5*	591488<--592987					
2	626356..626850	494	*ORF19.5785*		628280<--629158					
2	671450..671950	500	*ORF19.906*	*ROM2*	665520<--669665					
2	672552..672732	180						*ORF19.905*	*AVT7*	672821-->674143
2	774413..775099	686						*ORF19.852*	*SAP98*	775519-->776613
2	783780..784740	960						*ORF19.849*		785985-->788531
2	798300..798510	210	*ORF19.8464*	*STE11*	795730<--798201					
2	803500..803730	230	*ORF19.841*		802020<--804110					
2	815640..816150	510	*ORF19.835*		813549<--815909					
2	878200..878680	480	*ORF19.804*		877222<--878202					
2	883790..884532	742						*ORF19.799*	*STE4*	884534-->885907

2	901800..902400	600	*ORF19.1592*		901037<--901795		*ORF19.1591*	*ERG10*	902615-->903823	
2	954210..955076	866	*ORF19.4495*	*NDH51*	952547<--954019		*ORF19.4494*	*KTR2*	955166-->956605	
2	962090..962430	340	*ORF19.4490*	*RPL17B*	961440<--961997		*ORF19.4488*		965502-->968417	
2	974900..975120	220	*ORF19.144*	*SNU114*	971804<--974872					
2	997380..997680	300					*ORF19.191*	*KIC1*	997849-->1000524	
2	1024676..1024873	197	*ORF19.3521*	*ABH2*	1023164<--1023958		*ORF19.3522*		1026295-->1026600	
2	1105360..1106040	680	*ORF19.3568*	*RXT3*	1102641<--1104197		*ORF19.3569*		1106693-->1107811	
2	1301983..1302022	39	*ORF19.17*	*SCP1*	1301325<--1301909					
2	1345393..1345665	272	*ORF19.35.1*		1345203<--1345445					
2	1362880..1363240	360	*ORF19.1223*	*DBF2*	1357902<--1360034		*ORF19.1224*	*FRP3*	1365218-->1366075	
2	1367600..1368080		*ORF19.225*	*PEX22*	1367053<--1367676		*ORF19.3152*	*AMO2*	1317756-->1373771	
2	1377930..1379250	1320		*LSP1*	1379510<--1380463					
2	1482160..1482580	420	*ORF19.2284*		1481535<--1482554					
2	1661980..1662640	660					*ORF19.2165*		1662652-->1663488	
2	1723000..1723500	500					*ORF19.3627*		1722702-->1723421	
2	1825800..1827300	1500	*ORF19.207*	*PGA55*	1823947<--1828161					
2	1879160..1880200	1040		*MET10*	1872707<--1875991		*ORF19.4077*	*MIT1*	1880524-->1882158	
2	1991080..1991630	550	*ORF19.1375*	*LEU42*	1992242<--1993957					
2	2055040..2055440	400	*ORF19.1779*	*MP65*	2053567<--2054703		*ORF19.1778*		2056276-->2056590	
2	2066600..2066980	380					*ORF19.1773*	*RAP1*	2066997-->2068286	
2	2075585..2075817	232					*ORF19.1769*	*PLP2*	2075839-->2076636	
2	2088225..2088375	150					*ORF19.1765*		2088810-->2090066	
2	2100600..2101320	720	*ORF19.1759*	*PHO23*	2099138<--2100586		*ORF19.1757*		2102914-->2104665	
3	152960..153300	*340*					*ORF19.3071*	*MIH1*	155056-->157740	
3	162240..162640	*400*	*ORF19.1288*	*FOX2*	157976<--160696		*ORF19.1289*	*SCT1*	162857-->165169	
3	174030..174380	*350*					*ORF19.6164*		174381-->174707	
3	208320..208440	*120*					*ORF19.2506*		209733-->211526	
3	216009..216160	*151*					*ORF19.2509.1*		216500-->216709	
3	235900..236060	*160*	*ORF19.158*		232341<--233667		*ORF19.3153*	*MSS4*	236576-->238752	
3	245700..247800	*2100*	*ORF19.3156*		240982<--244245					
3	291720..292320	*600*	*ORF19.1715*	*IRO1*						
3	295400..296000	*600*	*ORF19.1714*	*PGA44*						
3	305450..305620	*170*	*ORF19.1709*		304792<--305175		*ORF19.1708*		306821--> 307480	
3	333720..335600	*1880*	*ORF19.1693*		324275<--332767		*ORF19.1691*		335872--> 336459	
3	338760..339040	*280*	*ORF19.1690*	*TOS1*	336918<-- 338324		*ORF19.1687*		342684--> 344987	
3	364700..364850	*150*	*ORF19.1676*		362744<--363850		*ORF19.1675*		365359--> 366561	
3	417640..418000	*360*	*ORF19.1658*		414753<--416640					
3	478200..478480	*280*	*ORF19.1624*		474903<-- 477388		*ORF19.1623*	*CAP1*	479014--> 480513	
3	500340..501430	*1090*	*ORF19.1616*	*FGR23*	499572<--502916					
3	510700..511380	*680*	*ORF19.1611*		509772<--510704		*ORF19.1610*		511399 -->512532	
3	517080..517280	*200*	*ORF19.1608*	*AYS1*	514997<--516763					
3	528720..528980	*260*	*ORF19.229*		527185<--528719					
3	550800..551065	*265*	*ORF19.242.2*	*SAP8*	548234<--549451		*ORF19.242.1*		551642--> 551830	
3	888466..888730	*264*	*ORF19.5870*	*CTP1*	887091<--888046					
3	1125000..1125400	*400*	*ORF19.5994*	*RHB1*	1126576<--1127130					

Efg1 (Normoxia)

3	1475328..1475640	312	*ORF19.7436*	*AAF1*	1477306<--1479144	Efg1 (Normoxia)				
3	1573640..1574000	360	*ORF19.6816*		1572570<--1573418		*ORF19.6814*	*TDH3*	1574973--> 1573418	
3	1721700..1722200	500	*ORF19.6736*		1719447<--1721336	Efg1 (Normoxia)				
3	1728270..1728540	270	*ORF19.6734*	*TCC1*	1730057<--1732303	Efg1 (Normoxia)				
4	39220..39840	620	*ORF19.5653*	*ATP2*	39465<--41389					
4	51040..51360	320	*ORF19.5660.1*		50930<--51211		ORF19.5661	*PTC1*	51522--> 52574	
4	128500..131800	3300	*ORF19.4167*		126574<--127113		ORF19.4166	*ZCF21*		
4	238480..240240	1760	*ORF19.4673*	*BMT9*	234413<--236764		ORF19.4672		240313--> 240615	
4	245400..246120	720	*ORF19.4669*	*AAT22*	244153<--245382					
4	255300..255540	240	*ORF19. 4660*	*RPS6A*	255674<--256809					
4	261750..262900	1150	*ORF19.4657*		263911<--265413					
4	316700..317200	500	*ORF19.4632*	*RPL20B*	315765<--316283					
4	347120..347520	400	*ORF19.4618*	*FBA1*	346020<--347099		ORF19.4617		348197--> 348733	
4	479840..480120	280	*ORF19.2765*	*PGA62*	480635<--481276		ORF19.2767	*PGA59*	471123--> 471464	
4	563934..569250	316	*ORF19.2726*		558959<--559897					Efg1 (Normoxia)
4	570720..570920	200	*ORF19.2725*		566926<--567228		ORF19.2724		571922--> 573418	
4	575480..575680	200	*ORF19.2723*	*HIT1*	577406<--577852	Efg1 (Normoxia)				
4	638800..639360	560	*ORF19.2686*		639378<--635720		ORF19.2685	*PGA54*	639770--> 640798	
4	1436070..1436220	150	*ORF19.2888*		1434188<--1434862		ORF19.2887		1436372--> 1436986	
4	1439500..1440400	900	*ORF19.2886*	*CEK1*	1437788<--1439056					
4	1470230..1470720	490	*ORF19.2877*	*PDC11*	1468241<--1469944	Efg1 (Normoxia)	ORF19.2876	*CBF1*	1471203--> 1472237	Efg1 (Normoxia)
4			*ORF19.3073*		1603087<--1603443					
5	33240..33780	540					*ORF19.978*	*BDF1*	30720--> 32849	
5	100700..101900	1200	*ORF19.938*		103156<--104601					
5	149940..151960	2020	*ORF19.922*	*ERG11*	148120<--149706					
5	161820..162000	180	*ORF19.568*	*SPE2*	159627<--160775		*ORF19.570*	*IFF8*	164521--> 16665	
5	208830..209040	210	*ORF19.1978*	*GIT2*	206349<--207953					
5	246700..247400	700	*ORF19.1960*	*CLN3*	244214<--245611					
5	254580..254730	150	*ORF19.1958*		253350<--255256					
5	342270..342900	630	*ORF19.4148*		340785<--342233		*ORF19.4149.1*		342916--> 351076	
5	351360..351720	360	*ORF19.4152*	*CEF3*	347719<--351076		*ORF19.4153*		353433--> 355034	
5	380340..380820	480	*ORF19.3207*	*CCN1*	377678<--379759					
5	854600..855500	900	*ORF19.1106*		848594<--850948					
5	871800..872160	360	*ORF19.3215*		872183<--872572					
5	921800..923800	2000	*ORF19.3895*	*CHT2*	919805<--921556		*ORF19.3897*			
5	947340..947820	480	*ORF19.3911*	*SAH1*	946010<--947362					
5	950100..952000	1900	*ORF19.3912*	*GLN3*	947849<--949897					
5	953460..954180	720	*ORF19.3914*		952095<--953387					
5	955800..956340	540	*ORF19.3915*		954174<--955478		*ORF19.3916*		956373--> 957956	
5	997800..998250	450	*ORF19.3942.1*	*RPL43A.3*	997147<--997796					
5	1040800..1041030	230	*ORF19.3967*	*PFK1*	1041235<--1044198					
5	1046000..1046320	320	*ORF19.11451*							
5	1047900..1050900	3000	*ORF19.11451*							
5	1085800..1087100	1300	*ORF19.3983*		1080849<--1083059		*ORF19.11467*			
5	1106700..1107550	850	*ORF19.3997*	*ADH1*	1107937<--1108986					

5	1138640..1139360	720	*ORF19.4012*	*PCL5*	1139318<--1140232						
6	31740..32580	840	*ORF19.1187*	*CPH2*	32572<--35133						
6	60500..60650	150	*ORF19.1195*		57658<--60009		*ORF19.1196*		60917-->63502		
6	90200..90850	650	*ORF19.4211*	*FET3*	87506<--89365	Efg1 (Normoxia)	*ORF19.4210*		92713-->94104	Efg1 (Normoxia)	
6	128632..129240	608	*ORF19.3653*	*FAT1*	129850<--131802						
6	133550..134300	750	*ORF19.3651*	*PGK1*	132037<--133290						
6	164070..165060	990	*ORF19.3649*	*CAN3*			*ORF19.85*	*GPX2*	165076-->165567		
6	173880..174320	440	*ORF19.90*			Efg1 (Normoxia)					
6	189000..191070	2070	*ORF19.96*	*TOP1*	186586<--188928		*ORF19.97*	*CAN1*	191821-->192821		
6	208530..209160	630	*ORF19.111*	*CAN2*	206049<--207755						
6	412860..413550	690	*ORF19.691*	*GPD2*	411560<--412675						
6	417460..417900	440	*ORF19.3508*		416316<--417449		*ORF19.3507*	*MCR1*	418020-->418925		
6	693120..693800	680	*ORF19.5618*		691040<--692998		*ORF19.5619*		693815--> 695932		
7	109500..109850	350	*ORF19.7055*		16320<--106646	Efg1 (Normoxia)	*ORF19.7054*		114110-->114475	Efg1 (Normoxia)	
7	128350..129050	700	*ORF19.7049*	*CYB5*	129228<--129608						
7	201940..202140	200	*ORF19.7018*	*RPS18*	202217<--203082						
7	378060..378480	420	*ORF19.6548*	*ISU1*	377224<--377787		*ORF19.6547*		379041-->379388		
7	669290..669420	130	*ORF19.5148*	*CDC35*	662738<--667810		*ORF19.5147*	*LMO1*	669600-->671519		
7	701550..702300	750	*ORF19.5132*		700597<--700977		*ORF19.5131*		703314-->705476		
7	730600..730800	200	*ORF19.1345*	*LIP8*	727502<--728884		*ORF19.1344*		731818-->732482		
7	768300..740500	2200	*ORF19.6705*		771047<--774184						
7	852520..852860	340	*ORF19.7196*		853153<--854634						
7	912200..913300	1100	*ORF19.7152*		907588<--908685	Efg1 (Normoxia)	*ORF19.7151*		915533-->915967	Efg1 (Normoxia)	
7	916400..917200	800	*ORF19.7150*	*NRG1*	918848<-- 919780	Efg1 (Normoxia)					
7	917800..918200	400	*ORF19.7150*	*NRG1*	918848<--919780	Efg1 (Normoxia)					
R	69500..70900	1400	*ORF19.7506*		67793<--76707		*ORF19.7504*		72120-->73049		
R	79260..79620	360	*ORF19.7502*		75931<--76707	Efg1 (Normoxia)					
R	114000..115000	1000	*ORF19.7489*		108226<--112632						
R	204530..204760	230	*ORF19.3264.1*		206338<--206502						
R	371460..371670	210	*ORF19.2551*	*MET6*	368753<--371056						
R	547770..548220	450	*ORF19.3719*		548260<--548730						
R	555500..556600	1100	*ORF19.173*		556961<--560263						
R	596200..596538	338	*ORF19.2823*	*RFG1*	600293<--602095	Efg1 (Normoxia)	*ORF19.2822*		585256-->586101	Efg1 (Normoxia)	
R	631700..631980	280	*ORF19.2833*	*PGA34*	630066<--630659						
R	649980..651120	1140	*ORF19.2842*	*GZF3*	647412<--649544		*ORF19.2843*	*RHO1*	653856-->654452		
R	688500..689300	800	*ORF19.2862*	*RIB1*	687001<--688029						
R	729900..730140	240	*ORF19.9934*								
R	730500..731060	560	*ORF19.2397.3*		731817<--732989						
R	777360..777610	250	*ORF19.4393*	*CIT1*	777837<--779333						
R	842820..843420	600	*ORF19.4376*		841223<--841970						
R	877050..877620	570	*ORF19.467*		878587<--880515						
R	894570..894760	190	*ORF19.475*		894751<--895851	Efg1 (Normoxia)	*ORF19.474*		892936-->894237	Efg1 (Normoxia)	
R	1047130..1047310	180	*ORF19.13687*		1044415<--1046835						
R	1146180..1146580	400	*ORF19.5289*		1146111< 1146425						
R	1372080..1372560	480	*ORF19.723*	*BCR1*	1368310<--1370352		*ORF19.721*		1378138-->1380198		

R	1660050..1660380	330	*ORF19.3665*		1658591<--1659187		*ORF19.6285*	*GLC7*	1660910-->1661902
R	1716800..1717600	800	***ORF19.610***	***EFG1***	**1723589<--1725166**	**Efg1 (Normoxia)**			
R	1718130..1718940	810	***ORF19.610***	***EFG1***	**1723589<--1725166**	**Efg1 (Normoxia)**			
R	1719360..1719780	420	***ORF19.610***	***EFG1***	**1723589<-- 1725166**	**Efg1 (Normoxia)**			
R	1721760..1721940	180	***ORF19.610***	***EFG1***	**1723589<--1725166**	**Efg1 (Normoxia)**			
R	1953120..1953680	560	*ORF19.7312*	*ERG13*	19514430< 1952785				
R	2157930..2158670	690	*ORF19.7585*	*INO1*	21556?4<--2157196		*ORF19.7586*	*CHT3*	2161835-->2163538
R	2168900..2169400	500	*ORF19.7592*	*FAA4*	2172618<--2174708	**Efg1 (Normoxia)**			
R	2204300..2204700	400	*ORF19.7610*	*PTP3*	2206947<--2209715				

Table 1. Binding of HA-Efg1 to chromosomal sequences of *C. albicans* under hypoxia. Strain HLCEEFG1 producing HA-Efg1 was grown in YPD medium at 30 °C under Hypoxic conditions (0.2% O_2) linking of proteins was done. Fragmented chromatin was immunoprecipitated using anti-Efg1 antibody and used as probe for tiling microarrays covering the *C. albicans* genome. Regions showing s binding of Efg1 compared to control strain CAF2-1 (WT) are listed along with their nearest neigbouring ORFs designated left or right ORF if situated at descending and, respectively, ascending chro ORF orientations are indicated by the arrows. Other proteins binding to the same chromosomal region are also indicated. Binding regions within coding regions are marked in purple lettering and g multiple binding regions. *, significant binding regions did not overlap in both replicates.

Chr	binding region	size (bp)	left ORF	gene name	left ORF position	additional binding proteins	right ORF	gene name	right ORF Position
1	267520..269120	1600	*ORF19.3325*		265492<--267474				
1	447360..447760	2480	*ORF19.3669*	*SHA3*	442472<--444259	Efg1 (Normoxia)			
1	534560..537040	2480	*ORF19.2942*	*DIP5*	532457<--534217				
1	536080..536960	1040					*ORF19.2943.5*		536985-->537284
1	674080..675120	1040	*ORF19.3013*	*CDC12*	672554<--673909				
1	675200..676640	1440	*ORF19.3014*	*BMH1*	675145<--675939				
1	719080..719640	560					*ORF19.3043*		719686-->720741
1	817680..818320	640	*ORF19.4459*		813949<--815640	Efg1 (Normoxia)			
1	1081920..1082320	400					*ORF19.4056*	*BRG1*	1082678-->1083949
1	1088040..1088920	880	*ORF19.450*		1085006<--1085239	Efg1 (Normoxia)			
1	1165207..1165400	193	*ORF19.411*		1163651<--1164670		*ORF19.410.3*		1166924-->1167627
1	1167680..1169040	1360	*ORF19.2495*	*GSL1*	1169252<--1173967				
1	1195340..1195660	320	*ORF19.2478.1*		1195221<--1196758				
1	1409085..1409335	250	*ORF19.6253*	*RPS23A*	1409046<--1409483				
1	1565580..1566240	660	*ORF19.4438*	*RME1*	1578967<--1580490			*CEN1*	1563083-->1565967
1	2106070..2106540	470	*ORF19.4820*		2107090<--2108712				
1	2193920..2194750	830	*ORF19.4867*	*SWE1*	2189160<--2192696	Efg1 (Normoxia)	*ORF19.4869*	*SFU1*	2195405-->2196958
1	2299520..2300000	480	*ORF19.4909*	*CBK1*					
1	2401600..2403400	1800	*ORF19.2333*		2399724<--2401214		*ORF19.2332*		2403598-->2404392
1	2300000..2300720	720	*ORF19.4909.1*	*RPL42*	2300032<--2300710				
1	2433560..2433750	190					*ORF19.2310.1*	*RPL29*	2434130-->2434321
1	2434320..2434560	240					*ORF19.2310*		2434657-->2435635
1	2588300..2590400	2100					*ORF19.5282*		2593345-->2594787
1	2698160..2698360	200	*ORF19.5226*	*WRS1*	2696598<--2697872				
1	2698360..2698720	360	*ORF19.5225.2*		2698355<--2699181				
1	2839320..2839860	540	*ORF19.4931*		2836544<--2838889		*ORF19.4931.1*	*RPL14*	2839943-->2840692
1	2869020..2869180	160	*ORF19.4941*	*TYE7*	2869020<--2869829				
1	2870360..2871320	960	*ORF19.4942*						

1	3164200..3164360	160	*ORF19.7251*	*WSC4*							
2	28680..28770	90	*ORF19.2111.2*	*RPL38*	28566<--28802						
2	28920..29170	250	*ORF19.2111*		28906<--28802						
2	162460..162850	390	*ORF19.2024*		163117<--163476	Efg1 (Normoxia)					
2	164030..164235	205	*ORF19.2023*	*HGT7*	164467<--166107	Efg1 (Normoxia)					
2	744840..745940	1100	*ORF19.868*	*ADAEC*	740829<--742466	Efg1 (Normoxia)	*ORF19.867*		747283-->748896		
2	1333020..1333500	480	*ORF19.33*		1332647<--1332957						
2	1394900..1395150	250	*ORF19.2231*		1392837<--1393616						
2	1887340..1887550	210					*ORF19.4081*		1889255-->1889755		
2	1927620..1929200	1580						*CEN2*	1927255-->1930214		
2	2190200..2190430	230	*ORF19.5341*		2189961<--2190749						
3	127980..128450	470	*ORF19.5383*	*PMA1*	133120<--135807						
3	153360..153680	320	*ORF19.3071*	*MIH1*	155056<--157740						
3	538240..538600	610	*ORF19.234*	*PHA2*	537221<--538228						
3	539100..539380	360	*ORF19.236*	*RPL9B*	538929<--539504						
3	818360..818680	280	*ORF19.6925*	*HTB1*	817960<--818352		*ORF19.6924*	*HTA1*	818897-->819295		
3	825760..826560							*CEN3*	823333-->826481		
3	826740..827380	320	*ORF19.2812*		826589<--828100						
3	855640..856520	800					*ORF19.5854*	*SBP1*	856949-->857797		
3	941400..941960	880	*ORF19.5904*	*RPL19A*	941386<--942394						
3	955800..956340	540	*ORF19.5908*	*TEC1*	949870<--952101	Efg1 (Normoxia)					
3	1117920..1118050	130	*orf19.5991*			Efg1 (Normoxia)	*ORF19.5992*	*WOR2*	1118833-->1120173		
3	1125110..1125270	160	*ORF19.5994*	*RHB1*	1126576<--1127130	Efg1 (Normoxia)					
3	1356690..1357440	750	*ORF19.7380*			Efg1 (Normoxia)	*ORF19.7381*	*AHR1*	1362620-->1364494		
3	1475390..1475880	490	*ORF19.7436*	*AAF1*	1477306<--1479144	Efg1 (Normoxia)					
3	1721900..1723700	1800	*ORF19.6736*			Efg1 (Normoxia)					
3	1727110..1728860	1750	*ORF19.6734*	*TCC1*	1730057<--1732303	Efg1 (Normoxia)					
3	1759380..1759730	350	*ORF19.6715*		1757968<--1758276	Efg1 (Normoxia)	*ORF19.6713*		1761919-->1763124		
4	128200..131300	3100	*ORF19.4166*	*ZCF21*	131943<--133832						
4	479920..480720	800	*ORF19.2765*	*PGA62*	480635<--481276						
4	569300..571200	1900	*ORF19.2725*		566926<--567228		*ORF19.2724*		571922-->573418		
4	574900..577300	2400	*ORf19.2723*	*HIT1*	577406<--577852	Efg1 (Normoxia)					
4	780000..780850	850	*ORF19.1313*		773035<--774255		*ORF19.1311*	*SPO75*	782925-->785510		
4	992100..992900	800					*ORF19.3821*		992579-->996216		
4	993300..994300							*CEN4*	992579-->9996216		
4	1048400..1048520	120	*ORF19.3794*	*CSR1*	1042268<--1044124						
4	1099800..1100460	660	*ORF19.740*	*HAP41*	1097336<--1099281	Efg1 (Normoxia)					
4	1425000..1425960	960					*ORF19.2842*		1426618-->1429254		

4	1470300..1471000	700	*ORF19.2877*	*PDC11*	1468241<--1469944	Efg1 (Normoxia)			
4	1504610..1504748	138	*ORF19.3134*		100282<--100722		*ORF19.3133*	*GUT2*	1507275-->1509227
4	1522500..1523000	500	*ORF19.2876*	*CZF1*	1471203<--1472237	Efg1 (Normoxia)			
5	250650..251292	642	*ORF19.1960*	*CLN3*	244214<--245611		ORF19.1959		253350-->254321
5	469320..469800	480					ORF19.4216		473411-->473917
5	855300..855950	650	*ORF19.1105.3*		855473<--855730				
5	896460..896700	240	*ORF19.1286*		896484<--896840				
5	997800..998460	660	*ORF19.3942.1*	*RPL43A*	997147<--997746				
5	998280..998460	180	*ORF19.3944*	*GRR1*	998281<--1000623				
5	1046310..1046610	300	*ORF19.3968*		1051721<--1052032			*CEN5*	468716-->471745
6	90040..91350	1310	*ORF19.4211*	*FET3*	87506<--89365	Efg1 (Normoxia)	*ORF19.4210*		92713-->94104
6	173880..174244	364		*orf19.20*					
6	217480..217640	160						*FAD2*	218253-->219563
6	403520..403660	140	*ORF19.687.1*	*RPL25*	402823<--403696				
6	788340..788835	495					*ORF19.5741*	*AIS1*	791472-->795254
6	980890..982000	1110		*CEN6*	980040<--983792				
7	109660..110040	380	*ORF19.7055*		106320<--106646	Efg1 (Normoxia)	*ORF19.7054*		114110-->114475
7	132100..132560	460					*ORF19.7047*	*RTF1*	132567-->134273
7	426420..427230	810		*CEN7*	425812<--428712				
7	451320..451680	360	*ORF19.6514*	*CUP9*	449876<--450910	Efg1 (Normoxia)			
7	917000..917900	900					*ORF19.7150*	*NRG1*	918848-->919780
R	338600..339100	500	*ORF19.2529.1*		338130<--338318	Efg1 (Normoxia)			
R	515580..516720	1140	*ORF19.3737*		512535<--514916				
R	589800..590000	200	*ORF19.2822*		585256<--586101	Efg1 (Normoxia)	*ORF19.2823*	*RFG1*	600293-->602095
R	839300..839900	600	*ORF19.4375*		839137<--839925				
R	840300..840650	300	*ORF19.4375.1*	*RPS30*	840283<--840810				
R	874600..876000	1400	*ORF19.467*		878587<--880515				
R	1315980..1316160	180	*ORF19.3868*		1315882<--1316235	Efg1 (Normoxia)			
R	1529050..1529250	200	*ORF19.2360*	*CRZ2*	1514505<--1521155				
R	1607700..1609200	1500	*ORF19.6127*	*LPD1*	1606104<--1607579		*ORF19.6126*	*KGD2*	1609238-->1610563
R	1714600..1717600	3000	*ORF19.610*	*EFG1*	1723589<--1725166	Efg1 (Normoxia)			
R	1772000..1772650	650	*ORF19.6375*	*RPS20*	1772309<--1772668				
R	2103400..2106000	2600	*ORF19.7561*	*DEF1*	2106215<--2108878	Efg1 (Normoxia)			
R	2168900..2169600	700	*ORF19.7592*	*FAA4*	2172618<--2174708	Efg1 (Normoxia)			

S3 Table. Binding of Ace2-HA to chromosomal sequences of *C. albicans* under normoxia. Strain CLvW004 producing Ace2-HA from its chromosomal ORF and reference strain BWP17 were grown in YPD medium at 30 °C under normoxic conditions. Chromosomal cross-linking of proteins was done and chromatin was fragmented before immunoprecipitation. For immunoprecipitation anti-HA antibody was used and the precipitated chromatin was spotted on a *C. albicans* whole-genome tiling microarray. Regions showing significant enrichment of Ace2-HA binding compared to control strain BWP17 are listet along with their nearest neighbouring ORFs. Other proteins binding to the same chromosomal region are indicated and are taken from Lassak *et al* . [40]. Binding targets of wild-type Efg1 or HA-Efg1 shared with Ace2-HA are indicated with red background color, binding targets of Ace2-HA obtained uniquely

Chr	binding region	size (bp)	left ORF	gene name	left ORF position	additional binding proteins	right ORF	gene name	right ORF Position
1	7841..8275	434	*ORF19.13531*	*CTA2*	10718<--11485				
1	87268..87643	375	*ORF19.6054*	*BUL2*	87249<--85081		*ORF19.6053*	*ECM38*	87901-->89811
1	91736..93009	1273					*ORF19.6048*		93971-->94900
1	310988..311305	317					*ORF19.3344*	*VPS17*	311194-->312753
1	386515..386762	247	*ORF19.4536*		386295<--384805				
1	443876..445132	1256	*ORF19.3669*	*SHA3*	444229<--442442				
1	481694..482321	627	*ORF19.3689*		486470<--484839				
1	529487..531017	1530					*ORF19.2941*	*SCW4*	530180-->531916
1	771329..772704	1375	*ORF19.1133*		771008<--767144				
1	859362..860358	996	*ORF19.1041*		859401<--857914				
1	1065969..1066247	278	*ORF19.4062*	*TRY2*	1066194<--1067309				
1	1081669..1082323	654					*ORF19.4056*	*BRG1*	1082699-->1083970
1	111654..111936	282	*ORF19.6041*	*RPO41*	111026<--107124				
1	1174050..1174323	273	*ORF19.2494*		1174293<--1175759				
1	1291466..1293116	1650					*ORF19.2662*	*ATC218*	1293702-->1293097
1	1317798..1320016	2218	*ORF19.1822*	*UME6*	1316979<--1314448	HA-Efg1 (normoxia)			
1	1390429..1390775	346	*ORF19.6261*		1389741<--1382920				
1	1497356..1497593	237	*ORF19.6203*		1497166<--1494230				
1	1552870..1554106	1236					*ORF19.4443*		1553615-->1554169
1	1867832..1868037	205	*ORF19.397*		1867699<--1867256		*ORF19.398*		1867970-->1868443
1	2229588..2229837	249					*ORF19.4884*	*WOR1*	2230568-->2232925
1	2282001..2282196	195					*ORF19.4903*	*GPI12*	2282393-->2283454
1	2553541..2553862	321	*ORF19.1155*	*DPP1*	2553615<--2552761		*ORF19.1154*		2554349-->2554822
1	2577684..2577955	271	*ORF19.1140*		2577623<--2576997				
1	2749592..2749753	161	*ORF19.3756*	*CHR1*	2749710<--2747789		*ORF19.3755*		2749829-->2750491
1	2752108..2752359	251					*ORF19.6362*		2752616-->2757016
1	2759309..2759592	283	*ORF19.6358*	*MMS2*	2759325<--2758829		*ORF19.6357*	*MAD1*	2759790-->2761880
1	2764327..2764726	399	*ORF19.6356*	*PRP6*	2764649<--2761914		*ORF19.6355*	*RRB1*	2764846-->2766399

1	2774136..2774509	373	*ORF19.6350*		2773130<--2772588		*ORF19.6349*	*RVS99*	2774849-->2775856
1	2788755..2788926	171	*ORF19.6343*	*FEN1*	2788244<--2787231		*ORF19.6342*		2789607-->2790092
1	2803025..2803506	481	*ORF19.4917*		2803179<--2802532				
1	2805639..2805969	330	*ORF19.4918*	*TRA98*	2805372<--2803813		*ORF19.4919*	*CTN4*	2805700-->2807010
1	2807712..2808181	469					*ORF19.4921*	*YFW1*	2808006-->2810177
1	2854713..2854982	269					*ORF19.4936.1*		2854984-->2855199
1	2871462..2871716	809	***ORF19.4941***	***TYE7***	2869848<--2868839	Efg1 (hypoxia)			
1	2934342..2934758	416	*ORF19.4970*		2933952<--2932225				
1	2971929..2972206	277					***ORF19.4991***	***MPT5***	2976172-->2978988
1	3011053..3011437	384	*ORF19.5006.1*	*SNC2*	3010047<--3009640		*ORF19.5007*	*ACT1*	3011501-->3013289
1	163192..163956	764	*ORF19.6022*		162676<--160946				
1	290470..291182	712	*ORF19.3334*	*RPS2*	290460<--289711		*ORF19.3335*		291859-->292461
1	308710..309143	433	*ORF19.3341*		308500<--306632		*ORF19.3342*		309136-->310986
1	344379..344729	350	***ORF19.3358***	***LSC1***	343919<--342948	Efg1 (hypoxia)	*ORF19.3359*		345578-->348778
1	473351..475375	2024					*ORF19.3682*	*CAX4*	474953-->475678
1	619987..620177	190					*ORF19.2989*		620167-->621195
1	718672..719605	933					***ORF19.3043***	***TGL2***	719688-->720743
1	893816..894200	384	*ORF19.1066*		893769<--893005		*ORF19.1067*		895187-->895972
1	1122505..1122672	167	*ORF19.431*		1122320<--1119993				
1	1250416..1250835	419	*ORF19.2452*		1249532<--1248285		*ORF19.2451*	*PGA45*	1251622-->1253010
1	1512469..1513395	926					*ORF19.6196*		1513369-->1513935
1	1610668..1610890	222					*ORF19.4423*		1611113-->1614334
1	2595231..2595559	328					*ORF19.5281*		2595412-->2599074
1	2620707..2620948	241	*ORF19.5269*		2620599<--2619208		*ORF19.5268*	*NUT2*	2621047-->2621559
1	2767288..2767489	201	*ORF19.6354*		2767135<--2766485		*ORF19.6353*	*LPF40*	2767870-->2769948
1	2790207..2790434	227					*ORF19.6341*	*RIB7*	2790384-->2791298
1	2831400..2831561	161	*ORF19.4928*		2829632<--2827377		*ORF19.4929*		2832124-->2835648
1	2839170..2839331	161	***ORF19.4931***		2838924<--2836579	HA-Efg1 (hypoxia)	***ORF19.4931.1***		2839978-->2840727
1	2890707..2891612	905					***ORF19.4952***		2891732-->2892670
1	2896486..2896938	452	*ORF19.4954*	*PPA1*	2896192<--2895602		*ORF19.4955*	*SPS2*	2896843-->2898429
1	2931444..2931724	280	*ORF19.4969*	*XRN1*	2930822<--2926240				
1	3017160..3017444	284	*ORF19.5010*	*DIM1*	3017120<--3016140		*ORF19.5011*		3017953-->3020229
1	3076372..3076521	149	*ORF19.5033*	*ATG12*	3076363<--3075869		*ORF19.5034*	*YBP1*	3076776-->3078707
1	3163835..3164032	197	***ORF19.7251***	***WSC4***	3164394<--3162919	HA-Efg1 (hypoxia)			
1	32744..32988	244	*ORF19.2107.1*	*STF2*	33351<--33620		*ORF19.2108*	*PGA9*	32587-->31637
1	62620..62860	240	*ORF19.2090*	*ECM16*	62936<--59145		*ORF19.2089*	*NYV1*	63257-->64177
2	234732..234914	182	*ORF19.1990*		234444<--232552				

2	305109..305421	312	*ORF19.1479*		304225<--301883		*ORF19.1480*		305495-->306025
2	535888..536244	356	*ORF19.5842*		535695<--534910		*ORF19.5841*		536330-->537088
2	585599..586161	562	*ORF19.5812*		585586<--584321		*ORF19.5811*	*MET1*	586286-->587971
2	587969..588273	304					*ORF19.5809*		588296-->589657
2	828388..828888	500	*ORF19.829*	*SCH9*	827878<--825515				
2	963789..963998	209	***ORF19.4490***	*RPL17*	961980<--961423	Efg1 (hypoxia)	***ORF19.4488***	***SWI3***	965485-->968400
2	1316490..1317142	652					*ORF19.24*	*RSB11*	1317217-->1318578
2	1340887..1341353	466					*ORF19.35*	*SKY2*	1341138-->1344068
2	1770659..1770967	308	*ORF19.3606*		1770360<--1769839		*ORF19.3605*		1771101-->1771826
2	1797354..1797663	309	***ORF19.225***		1796447<--1795362	Efg1 (hypoxia)	*ORF19.223*		1797689-->1800073
2	1842607..1842881	274	*ORF19.204*		1840229<--1839615		*ORF19.203*		1842959-->1844470
2	1857917..1858111	194	*ORF19.4066*		1856790<--1854379				
2	1883592..1883939	347					*ORF19.4079*		1883767-->1884558
2	1896579..1897081	502					*ORF19.4090*		1898301-->1896796
2	1959173..1959431	258	*ORF19.1397*		1958642<--1957932		*ORF19.1396*	*AGE2*	1960782-->1961945
2	116183..116795	612					*ORF19.2057*	*YTA12*	117048-->119588
2	155250..155786	536	*ORF19.2031*		155268<--154526		*ORF19.2030*		155823-->156296
2	327015..327177	162					*ORF19.1490*	*MSB2*	327702-->331931
2	336007..336287	280	*ORF19.1491*	*SNU71*	335997<--334153		***ORF19.1492***	***PRP39***	336552-->338519
2	429195..429403	208	***ORF19.1534***	*ZRT3*	427370<--429145				
2	549769..550317	548	***ORF19.5831***		549458<--548142		***ORF19.5830***	*LHS1*	550341-->553139
2	572071..572863	792					*ORF19.5818*	*SUR2*	573066-->574094
2	660174..660417	243	*ORF19.909*	*STP4*	660179<--659049				
2	789975..790975	1000					*ORF19.847*		791066-->792154
2	822632..823052	420	*ORF19.832*		822404<--819356				
2	919877..920124	247					*ORF19.4513*		920879-->922069
2	956685..956995	310					*ORF19.4492*	*EBP2*	956922-->958202
2	1009610..1009989	379					*ORF19.4128*		1010681-->1011985
2	1104636..1105023	387	*ORF19.3568*	*RXT3*	1104183<--1102627				
2	1164935..1165312	377	*ORF19.6881*		1164794<--1164147		*ORF19.6882*	*OSM1*	1165487-->1166998
2	1187147..1187465	318	*ORF19.6893*		1187201<--1185839				
2	1403997..1404286	289					*ORF19.2237.1*		1404254-->1404933
2	1554538..1554886	348	*ORF19.1864*		1554405<--1552246		*ORF19.1863*		1554715-->1556503
2	1632520..1632667	147					*ORF19.2181*		1632178-->1632708
2	1680188..1680349	161	*ORF19.1351*		1679933<--1679193				
2	1685026..1685304	278	*ORF19.1348*		1685131<--1684568				
2	1802346..1802508	162	*ORF19.220*	*PIR1*	1801740<--1800700				

2	1876679..1876854	175	*ORF19.4076*	*MET10*	1875988<--1872704				
2	1879647..1879982	335						**ORF19.4077**	***MIT1***
2	1893206..1893376	170	*ORF19.4085*		1893261<--1892620			*ORF19.4086*	
2	2139486..2139660	174	*ORF19.1742*		2138454<--2137432				
2	13097..13527	430	*ORF19.5468*		12501<--12190			*ORF19.5467*	
2	877355..877585	230	*ORF19.5864*		877338<--875701			*ORF19.5865*	
3	776603..777066	463						*ORF19.6951*	*DPL1*
3	807277..807523	246	*ORF19.6930*	*SIC1*	807031<--806315			*ORF19.6929*	
3	1038620..1039215	595	*ORF19.5952*		1038697<--1037381			*ORF19.5953*	*SFP1*
3	1072160..1072466	306	*ORF19.5965*		1072248<--1069021			*ORF19.5966*	
3	1093084..1093262	178						*ORF19.5978*	
3	1305553..1305863	310	*ORF19.7362*		1302603<--1300389			*ORF19.7363*	
3	1445006..1445426	420						*ORF19.7400*	
3	1496185..1496554	369	*ORF19.7444*		1494922<--1493897			*ORF19.7445*	
3	1727020..1727262	242						**ORF19.6734**	***TCC1***
3	892929..893238	309	*ORF19.5871*		893071<--890979				
3	1118625..1118860	235						**ORF19.5992**	***WOR2***
3	1233227..1233512	285						*ORF19.6986*	
3	1475513..1475883	370						**ORF19.7436**	***AAF1***
3	1491955..1492166	211	*ORF19.7441*		1491938<--1491012			*ORF19.7442*	
3	1510669..1511153	484						*ORF19.7451*	
3	48034..48219	185	*ORF19.5657*	*SWC1*	48100<-45137				
3	131436..131638	202	*ORF19.4167*		127111<--126572			**ORF19.4166**	***ZCF21***
4	248259..248536	277	*ORF19.4668*		248276<--246123				
4	282782..283309	527						*ORF19.4649*	
4	420730..420888	158						*ORF19.4579*	
4	480605..481016	411						**ORF19.2765**	***PGA62***
4	538595..538903	308	*ORF19.2739*		538696<--536978				
4	543774..546002	2228	*ORF19.2737*		545945<--543717				
4	551457..551678	221						*ORF19.2733*	
4	555823..556043	220	*ORF19.2731*		553564<--553226			*ORF19.2730*	
4	569822..570064	242	**ORF19.2725**		567226<--566924	HA-Efg1 (normoxia a		**ORF19.2724**	
4	665440..665998	558	*ORF19.2674*		665137<--664109			*ORF19.2673*	
4	901830..902078	248	*ORF19.1429*		901816<--901376			*ORF19.1428*	
4	958836..959072	236	*ORF19.3840*		959031<--954805			*ORF19.3839*	
4	982132..982341	209						*ORF19.3823*	
4	990641..990855	214	**ORF19.3821**		990526<--989339	HA-Efg1 (hypoxia)			

2	1880521-->1882155								
2	1893505-->1894155								
2	13756-->14265								
2	877626-->880223								
3	777441-->779210								
3	807898-->808425								
3	1041453-->1042790								
3	1072444-->1072785								
3	1093310-->1094524								
3	1306218-->1308440								
3	1446629-->1451336								
3	1496429-->1497916								
3	1730074-->1732320								
3	1118847-->1120187								
3	1234039-->1236246								
3	1477326-->1479164								
3	1492186-->1493082								
3	1511052-->1515023								
3	131941-->133830								
4	283241-->286831								
4	421115-->422041								
4	480632-->481273								
4	551575-->553128								
4	553936-->555756								
4	571920-->573416								
4	665706-->666725								
4	902225-->902740								
4	961031-->962392								
4	982321-->987258								

4	1020888..1021863	975	*ORF19.3803*	*MNN24*	1020679<--1018910		*ORF19.3802*	*PMT6*	1022709-->1025207
4	1048206..1048473	267	***ORF19.3794***	***CSR1***	1044143<--1042287	HA-Efg1 (hypoxia)	*ORF19.3793*		1048418-->1049593
4	119205..119456	251	*ORF19.4173*		119171<--117582				
4	125737..125901	164	*ORF19.4169*		125651<--125256		*ORF19.4168*		126013-->126516
4	149067..149317	250					*ORF19.4711*		150355-->152169
4	167790..168189	399	*ORF19.4702*		167605<--166703		*ORF19.4701*		168466-->169392
4	241195..241666	471					*ORF19.4670*	*CAS5*	241403-->243868
4	263241..263484	243					***ORF19.4657***		263907-->265409
4	277969..278128	159					*ORF19.4651*		278269-->278688
4	294547..294757	210					*ORF19.4643*		294803-->301954
4	336726..336904	178	*ORF19.4624*		336394<--335036				
4	342226..342418	192	*ORF19.4622*		342120<--340963				
4	449574..449864	290	*ORF19.4560*	*BFR1*	449237<--447849		*ORF19.2775*	*IDI1*	450181-->451035
4	681943..682094	151					*ORF19.2665*		682598-->686252
4	806517..806676	159	*ORF19.1298*		806323<--803789		*ORF19.1297*		807459-->809654
4	972793..973252	459	*ORF19.3829*		972279<--970633				
4	1263263..1263475	212					*ORF19.1258*		1264022-->1264735
4	1269196..1269522	326	*ORF19.1259*		1269246<--1264915				
4	1301093..1301343	250	*ORF19.1274*		1298570<--1296879		*ORF19.1275*		1302092-->1304095
4	30117..30380	263	*ORF19.979*	*FAS1*	29661<--23548				
4	94280..94512	232	*ORF19.940*		93594<--89881		*ORF19.939*		95043-->98102
5	102915..103182	267					***ORF19.938***		103156-->104601
5	217717..218023	306	*ORF19.1972*		217288<--215867		*ORF19.1971*		218221-->219705
5	380339..380796	457	***ORF19.3207***	***CCN1***	379761<--377680	Efg1 (hypoxia)			
5	406103..406467	364	*ORF19.3195*	*HIP1*	404636<--402837		*ORF19.3193*	*FCR3*	407979-->409178
5	443455..443624	169	*ORF19.3174*		443369<--440835				
5	453619..453945	326	*ORF19.3170*		453571<--451385				
5	155228..155460	232	*ORF19.921*		153233<--151176		*ORF19.920*		156807-->158162
5	175021..175219	198					*ORF19.576*		175559-->176047
5	347903..348110	207	*ORF19.4151*		347572<--345242				
5	529019..529265	246	*ORF19.4245*		527060<--525714		*ORF19.4246*		529711-->531504
5	568004..568222	218	*ORF19.4266*		568051<--566677				
5	851168..851516	348	***ORF19.1106***		850957<--848603	Efg1 (hypoxia)			
5	861451..861765	314	*ORF19.3219*		861340<--859535				
5	513893..514105	212	*ORF19.4239*		513647<--511632				
5	522151..522532	381	*ORF19.4242*	*CST20*	521590<--517904				
5	599825..600166	341	*ORF19.4282*		598167<--597259				

5	1107056..1107300	244						***ORF19.3997***	***ADH1***	1107881-->1108930
5	4563..5065	502						*ORF19.6337*		5545-->6489
5	60497..60663	166	***ORF19.1195***		60013<--57662	Efg1 (hypoxia)		***ORF19.1196***		60921-->63506
6	97579..97753	174	*ORF19.4208*	*RAD52*	97417<--95723					
6	107748..107995	247						*ORF19.4199*		107932-->109503
6	173917..174207	290						***ORF19.90***		174680-->176944
6	304142..304599	457	*ORF19.3434*		301246<--298277			*ORF19.3433*	*OYE23*	304843-->306063
6	319400..319632	232	*ORF19.3431*		317782<--314096			*ORF19.3430*	*BUD21*	319776-->320810
6	339382..339625	243						*ORF19.3421.1*		339664-->340248
6	349369..349608	239	*ORF19.3420*		348886<--348503			*ORF19.3419*	*MAE1*	350713-->352605
6	421895..422171	276						*ORF19.3505*		422337-->424733
6	430038..430268	230	*ORF19.3501*		429691<--426551			*ORF19.3499*		434464-->434967
6	444405..444602	197	*ORF19.3494*		444313<--443213			*ORF19.3453*		444683-->447643
6	474206..474375	169	*ORF19.3468*	*ALG11*	472898<--471069			*ORF19.3469*		474238<--475425
6	549988..550214	226	*ORF19.5537*		548965<--547667			*ORF19.5539*		552727-->553569
6	603094..603382	288	*ORF19.5568*		603308<--602358			*ORF19.5569*		603848-->606529
6	630120..630398	278						*ORF19.5584*		630618-->633050
6	640292..640524	232	*ORF19.5586*		640372<--637424					
6	730739..730929	190	*ORF19.5705*	*NAM2*	730549<--727964			*ORF19.5710*		731035-->734520
6	821237..821408	171	*ORF19.5753*	*HGT10*	819180<--817540					
6	837437..837820	383	*ORF19.5759*		836974<--832487					
6	867771..868136	365	*ORF19.5775*		864791<--863253			*ORF19.1221*		876496-->877833
6	875889..876332	443						*ORF19.1221*		876496-->877833
6	898101..898410	309	*ORF19.4557*		897780<--894497					
6	90037..90595	558	***ORF19.4211***	*FET3*	89370<--87511	HA-Efg1 (normoxia a		***ORF19.4210***		92718-->94109
6	711941..712284	343						*ORF19.5627*		712343-->713449
6	954958..955148	190	*ORF19.1090*		954989<--954642			*ORF19.1091*		955216-->957288
6	962825..962993	168	*ORF19.1093*	*FLO8*	962206<--959828					
6	969214..969419	205						*ORF19.1097*	*ALS2*	971475-->976745
6	1028365..1028747	382	*ORF19.2160*		1027136<--1025391			*ORF19.2163*		1028841-->1031354
6	132431..132677	246						*ORF19.7047*	*RTF1*	132567-->134273
6	147491..147734	243						*ORF19.7041*		148191-->150485
7	179372..179581	209	*ORF19.7027*		179318<--176562					
7	197995..198262	267						*ORF19.7020*	*KEX1*	198461-->200569
7	226954..227152	198	*ORF19.7006*		226654<--223297					
7	235013..235204	191	*ORF19.6896*		232413<--230875					
7	312089..312282	193						*ORF19.6580*		312573-->313265

7	329445..329682	237							ORF19.6573		329718-->336476
7	350127..350842	715	ORF19.6563		349795<--347816				ORF19.6562		350992-->352287
7	375318..375638	320	ORF19.6551		375267<--374593				ORF19.6550		375747-->376631
7	389345..389658	313	ORF19.6540	PFK2	388801<--385961				ORF19.6539		390350-->391846
7	392764..392967	203	ORF19.6538		392514<--392023				ORF19.6537		393006-->393698
7	419339..419895	556							ORF19.6525		419663-->421988
7	410407..410669	262	ORF19.6530		409253<--408390				ORF19.6529	CDC34	411057-->411791
7	413027..413320	293	ORF19.6528		412926<--412315						
7	437730..438044	314	ORF19.6518		437290<--435305				ORF19.6517		438040-->439230
7	451625..451894	269	**ORF19.6514**	**CUP9**	450912<--449878	HA-Efg1 (normoxia and hypoxia)					
7	465046..465507	461							ORF19.6506		465072-->467138
7	476843..477195	352	ORF19.6498		476933<--475905						
7	493528..493763	235							ORF19.6486		493963-->494421
7	519989..520286	297	ORF19.6472		519627<--519139				ORF19.6470		520558-->521115
7	632455..633164	709							ORF19.5169		633454-->635175
7	8643..8842	199	ORF19.7545		7566<--4884				ORF19.7544		9111-->9863
7	864303..864578	275							ORF19.7186	CLB4	864775<--863315
7	172196..172884	688	ORF19.3283		172342<--171653						
R	201809..202075	266	ORF19.3265.1		201735<--201475				ORF19.3265		202225-->203895
R	334667..334909	242	ORF19.2527		334491<--333205				ORF19.2528		334922-->336910
R	509931..510278	347	ORF19.3742		509369<--508644				ORF19.3740	PGA23	510511-->511359
R	556779..557328	549							**ORF19.173**		556964-->560266
R	598390..599287	897							ORF19.2823	RFG1	600293<--602095
R	874612..874814	202							**ORF19.467**	**WOR3**	878593-->880521
R	926791..927553	762	ORF19.496		926380<--923609				ORF19.498	EAF7	928331-->929716
R	963503..963739	236							ORF19.522	PIM1	963564-->966800
R	1125308..1125600	292	ORF19.556		1124656<--1124237				ORF19.557		1125739-->1126764
R	1157158..1157584	426	ORF19.5286		1156504<--1155638				ORF19.5285		1158030-->1158629
R	1259394..1260341	947	ORF19.454	SFL1	1258170<--1255753						
R	1271946..1272327	381							ORF19.451		1274207-->1276684
R	1285179..1285413	234	**ORF19.3852**		1285014<--1282627						
R	1372318..1372553	235	**ORF19.723**	**BCR1**	1370542<--1368320	Efg1 (hypoxia)					
R	1469903..1470143	240	ORF19.1847		1469576<--1467687						
R	1659779..1660018	239	ORF19.6286		1659219<--1658623				ORF19.6285	GLC7	1660942-->1661934
R	1718524..1718725	201							**ORF19.610**	**EFG1**	1723620-->1725197
R	1723278..1723663	385							**ORF19.610**	**EFG1**	1723620-->1725197
R	1759755..1759942	187	ORF19.589	VPS21	1759114<--1758464				ORF19.6365	PTP1	1760210-->1761328

S2 Table. Binding of Ace2-HA to chromosomal sequences of *C. albicans* under hypoxia and addition of CO_2. Strain CLvW004 producing Ace2-HA from its chromosomal ORF and reference strain BWP17 were grown in YPD medium at 30 °C under hypoxic conditions and in presence of elevated CO_2 levels (0.2 % O_2 and 6 % CO_2). Chromosomal cross-linking of proteins was done and chromatin was fragmented before immunoprecipitation. For immunoprecipitation anti-HA antibody was used and the precipitated chromatin was spotted on a *C. albicans* whole-genome tiling microarray. Regions showing significant enrichment of Ace2-HA binding compared to control strain BWP17 are listet along with their nearest neighbouring ORFs. Other proteins binding to the same chromosomal region are indicated and are taken from Lassak *et al*. [40]. Binding targets of wild-type Efg1 or HA-Efg1 shared with Ace2-HA are indicated with red background color.

Chr	binding region	size (bp)	left ORF	gene name	left ORF position	additional binding proteins	right ORF	gene name	right ORF Position
1	7841..8275	434	*ORF19.13531*	*CTA2*	10718<--11485				
1	87268..87643	375	*ORF19.6054*	*BUL2*	87249<--85081		*ORF19.6053*	*ECM38*	87901-->89811
1	91736..93009	1273					*ORF19.6048*		93971-->94900
1	386515..386762	247	*ORF19.4536*		386295<--384805				
1	443876..445132	1256	*ORF19.3669*	*SHA3*	444229<--442442				
1	771329..772704	1375	*ORF19.1133*		771008<--767144				
1	1065969..1066247	278	*ORF19.4062*	*TRY2*	1066194<--1067309				
1	1081669..1082323	654					***ORF19.4056***	***BRG1***	1082699-->1083970
1	1174050..1174323	273	*ORF19.2494*		1174293<--1175759				
1	1291466..1293116	1650					*ORF19.2662*	*ATC218*	1293702-->1293097
1	1390429..1390775	346	*ORF19.6261*		1389741<--1382920				
1	1497356..1497593	237	*ORF19.6203*		1497166<--1494230				
1	1552870..1554106	1236					*ORF19.4443*		1553615-->1554169
1	1867832..1868037	205	*ORF19.397*		1867699<--1867256		*ORF19.398*		1867970-->1868443
1	2229588..2229837	249					***ORF19.4884***	***WOR1***	2230568-->2232925
1	2282001..2282196	195					*ORF19.4903*	*GPI12*	2282393-->2283454
1	2553541..2553862	321	*ORF19.1155*	*DPP1*	2553615<--2552761		*ORF19.1154*		2554349-->2554822
1	2577684..2577955	271	*ORF19.1140*		2577623<--2576997				
1	2749592..2749753	161	*ORF19.3756*	*CHR1*	2749710<--2747789		*ORF19.3755*		2749829-->2750491
1	2752108..2752359	251					*ORF19.6362*		2752616-->2757016
1	2759309..2759592	283	*ORF19.6358*	*MMS2*	2759325<--2758829		*ORF19.6357*	*MAD1*	2759790-->2761880
1	2764327..2764726	399	*ORF19.6356*	*PRP6*	2764649<--2761914		*ORF19.6355*	*RRB1*	2764846-->2766399
1	2774136..2774509	373	*ORF19.6350*		2773130<--2772588		*ORF19.6349*	*RVS99*	2774849-->2775856
1	2788755..2788926	171	*ORF19.6343*	*FEN1*	2788244<--2787231		*ORF19.6342*		2789607-->2790092
1	2803025..2803506	481	*ORF19.4917*		2803179<--2802532				
1	2805639..2805969	330	*ORF19.4918*	*TRA98*	2805372<--2803813		*ORF19.4919*	*CTN4*	2805700-->2807010
1	2807712..2808181	469					*ORF19.4921*	*YFW1*	2808006-->2810177
1	2854713..2854982	269					*ORF19.4936.1*		2854984-->2855199
1	2871462..2871716	809	***ORF19.4941***	*TYE7*	2869648<--2868839	Efg1 (hypoxia)			
1	2934342..2934758	416	*ORF19.4970*		2933952<--2932225				
1	3011053..3011437	384	*ORF19.5006.1*	*SNC2*	3010047<--3009640		*ORF19.5007*	*ACT1*	3011501-->3013289
1	231980..232506	526	***ORF19.3302***		229786<--227684	HA-Efg1 (normoxia)			

1	267962..269100	1138	**ORF19.3325**	**GLG21**	267472<--265490	HA-Efg1 (hypoxia)					
1	534538..537448	2910	*ORF19.2942*	*DIP52*	534219<--532460				*ORF19.3038*	*TPS2*	709534-->712200
1	709163..709459	296									
1	944334..947063	2729	**ORF19.6852**		944553<--943726	Efg1 (hypoxia)			**ORF19.2495**	**GSL1**	1169273-->1173989
1	1168052..1169064	1012							*ORF19.6213*		1484856-->1485758
1	1483827..1484221	394	*ORF19.6214*	*ATH1*	1483075<--1479839				*ORF19.4449*	*LYS7*	1540781-->1541527
1	1539849..1540065	216	*ORF19.4450*	*ZCF23*	1538490<--1536790				*ORF19.4440*		1558228-->1560747
1	1557823..1558176	353	*ORF19.4441*	*DNA43*	1557992<--1556196						
1	1585052..1585329	277	*ORF19.4436*	*GPX2*	1584961<--1584446				*ORF19.675*		2475630-->2476268
1	2474390..2475561	1171	*ORF19.675.1*		2473989<-2473852						
1	163192..163956	764	*ORF19.6022*		162676<--160946				*ORF19.3335*		291859-->292461
1	290470..291182	712	*ORF19.3334*	*RPS2*	290460<--289711				*ORF19.3342*		309136-->310986
1	308710..309143	433	*ORF19.3341*		308500<--306632				*ORF19.3359*		345578-->348778
1	344379..344729	350	**ORF19.3358**	***LSC1***	343919<--342948	Efg1 (hypoxia)			*ORF19.3682*	*CAX4*	474953-->475678
1	473351..475375	2024							*ORF19.2989*		620167-->621195
1	619987..620177	190							**ORF19.3331**	***ABC1***	282447-->284147
1	281746..283031	1285							**ORF19.3043**	***TGL2***	719688-->720743
1	718672..719605	933							*ORF19.1067*		895187-->895972
1	893816..894200	384	*ORF19.1066*		893769<--893005						
1	1122505..1122672	167	*ORF19.431*		1122320<--1119993				*ORF19.2451*	*PGA45*	1251622-->1253010
1	1250416..1250835	419	*ORF19.2452*		1249532<--1248285				*ORF19.6196*		1513369-->1513935
1	1512469..1513395	926							*ORF19.4423*		1611113-->1614334
1	1610668..1610890	222							*ORF19.5281*		2595412-->2599074
1	2595231..2595559	328							*ORF19.5268*	*NUT2*	2621047-->2621559
1	2620707..2620948	241	*ORF19.5269*		2620599<--2619208				*ORF19.6353*	*LPF40*	2767870-->2769948
1	2767288..2767489	201	*ORF19.6354*		2767135<--2766485				*ORF19.6341*	*RIB7*	2790384-->2791298
1	2790207..2790434	227							*ORF19.4929*		2832124-->2835648
1	2831400..2831561	161	*ORF19.4928*		2829632<--2827377				**ORF19.4931.1**		2839978-->2840727
1	2839170..2839331	161	**ORF19.4931**		2838924<--2836579	HA-Efg1 (hypoxia)			**ORF19.4952**		2891732-->2892670
1	2890707..2891612	905							*ORF19.4955*	*SPS2*	2896843-->2898429
1	2896486..2896938	452	*ORF19.4954*	*PPA1*	2896192<--2895602						
1	2931444..2931724	280	*ORF19.4969*	*XRN1*	2930822<--2926240				*ORF19.5011*		3017953-->3020229
1	3017160..3017444	284	*ORF19.5010*	*DIM1*	3017120<--3016140				*ORF19.5034*	*YBP1*	3076776-->3078707
1	3076372..3076521	149	*ORF19.5033*	*ATG12*	3076363<--3075869						
1	3163835..3164032	197	**ORF19.7251**	***WSC4***	3164394<-3162919	HA-Efg1 (hypoxia)			*ORF19.2108*	*PGA9*	32587-->31637
2	32744..32988	244	*ORF19.2107.1*	*STF2*	33351<--33620				*ORF19.2089*	*NYV1*	63257-->64177
2	62620..62860	240	*ORF19.2090*	*ECM16*	62936<--59145						
2	234732..234914	182	*ORF19.1990*		234444<--232552				*ORF19.1480*		305495-->306025
2	305109..305421	312	*ORF19.1479*		304225<--301883				*ORF19.5841*		536330-->537088
2	535888..536244	356	*ORF19.5842*		535695<--534910						

2	585599..586161	562	*ORF19.5812*		585586<--584321		*ORF19.5811*	*MET1*	586286-->587971
2	587969..588273	304					*ORF19.5809*		588296-->589657
2	828388..828888	500	*ORF19.829*	*SCH9*	827878<--825515				
2	963789..963998	209	***ORF19.4490***	*RPL17*	961980<--961423	Efg1 (hypoxia)	***ORF19.4488***	***SWI3***	965485-->968400
2	1316490..1317142	652					*ORF19.24*	*RSB11*	1317217-->1318578
2	1340887..1341353	466					*ORF19.35*	*SKY2*	1341138-->1344068
2	1770659..1770967	308	*ORF19.3606*		1770360<--1769839		*ORF19.3605*		1771101-->1771826
2	1797354..1797663	309	***ORF19.225***		1796447<--1795362	Efg1 (hypoxia)	*ORF19.223*		1797689-->1800073
2	1842607..1842881	274	*ORF19.204*		1840229<--1839615		*ORF19.203*		1842959-->1844470
2	1857917..1858111	194	*ORF19.4066*		1856790<--1854379				
2	1883592..1883939	347					*ORF19.4079*		1883767-->1884558
2	1896579..1897081	502					*ORF19.4090*		1898301-->1896796
2	1959173..1959431	258	*ORF19.1397*		1958642<--1957932		*ORF19.1396*	*AGE2*	1960782-->1961945
2	116183..116795	612					*ORF19.2057*	*YTA12*	117048-->119588
2	155250..155786	536	*ORF19.2031*		155268<--154526		*ORF19.2030*		155823-->156296
2	327015..327177	162					*ORF19.1490*	*MSB2*	327702-->331931
2	572071..572863	792					*ORF19.5818*	*SUR2*	573066-->574094
2	660174..660417	243	*ORF19.909*	*STP4*	660179<--659049				
2	789975..790975	1000					*ORF19.847*		791066-->792154
2	822632..823052	420	*ORF19.832*		822404<--819356				
2	919877..920124	247					*ORF19.4513*		920879-->922069
2	956685..956995	310					*ORF19.4492*	*EBP2*	956922-->958202
2	1104636..1105023	387	*ORF19.3568*	*RXT3*	1104183<--1102627				
2	1164935..1165312	377	*ORF19.6881*		1164794<--1164147		*ORF19.6882*	*OSM1*	1165487-->1166998
2	1187147..1187465	318	*ORF19.6893*		1187201<--1185839				
2	1554538..1554886	348	*ORF19.1864*		1554405<--1552246		*ORF19.1863*		1554715-->1556503
2	1680188..1680349	161	*ORF19.1351*		1679933<--1679193				
2	1685026..1685304	278	*ORF19.1348*		1685131<--1684568				
2	1802346..1802508	162	*ORF19.220*	*PIR1*	1801740<--1800700				
2	1876679..1876854	175	*ORF19.4076*	*MET10*	1875988<--1872704				
2	1879647..1879982	335					***ORF19.4077***	***MIT1***	1880521-->1882155
2	1893206..1893376	170	*ORF19.4085*		1893261<--1892620		*ORF19.4086*		1893505-->1894155
2	2139486..2139660	174	*ORF19.1742*		2138454<--2137432				
2	623114..623431	317	*ORF19.5789*		622945<--622277		*ORF19.5788*		623651-->626379
2	749035..749443	408					*ORF19.866*	*RAD30*	749865-->751787
2	1077383..1077657	274	*ORF19.3553*		1077153<--1076170				
2	1111969..1113009	1040					*ORF19.3573*		1112912-->1116385
2	1888295..1888470	175					***ORF19.4081***		1889252-->1889752
2	1921625..1921782	157					*ORF19.1601*		1921931-->1923100
3	13097..13527	430	*ORF19.5468*		12501<--12190		*ORF19.5467*		13756-->14265

3	877355..877585	230	*ORF19.5864*		877338<--875701		*ORF19.5865*		877626-->880223
3	776603..777066	463					*ORF19.6951*	*DPL1*	777441-->779210
3	807277..807523	246	*ORF19.6930*	*SIC1*	807031<--806315		*ORF19.6929*		807898-->808425
3	1038620..1039215	595	*ORF19.5952*		1038697<--1037381		*ORF19.5953*	*SFP1*	1041453-->1042790
3	1072160..1072466	306	*ORF19.5965*		1072248<--1069021		*ORF19.5966*		1072444-->1072785
3	1093084..1093262	178					*ORF19.5978*		1093310-->1094524
3	1305553..1305863	310	*ORF19.7362*		1302603<--1300389		*ORF19.7363*		1306218-->1308440
3	1445006..1445426	420					*ORF19.7400*		1446629-->1451336
3	1496185..1496554	369	*ORF19.7444*		1494922<--1493897		*ORF19.7445*		1496429-->1497916
3	1727020..1727262	242					***ORF19.6734***	***TCC1***	1730074-->1732320
3	892929..893238	309	*ORF19.5871*		893071<--890979		***ORF19.5992***	***WOR2***	1118847-->1120187
3	1118625..1118860	235					*ORF19.6986*		1234039-->1236246
3	1233227..1233512	285					***ORF19.7436***	***AAF1***	1477326-->1479164
3	1475513..1475883	370					*ORF19.7442*		1492186-->1493082
3	1491955..1492166	211	*ORF19.7441*		1491938<--1491012		*ORF19.7451*		1511052-->1515023
3	1510669..1511153	484							
4	48034..48219	185	*ORF19.5657*	*SWC1*	48100<--45137		***ORF19.4166***	***ZCF21***	131941-->133830
4	131436..131638	202	*ORF19.4167*		127111<--126572				
4	248259..248536	277	*ORF19.4668*		248276<--246123		*ORF19.4649*		283241-->286831
4	282782..283309	527					*ORF19.4579*		421115-->422041
4	420730..420888	158					***ORF19.2765***	***PGA62***	480632-->481273
4	480605..481016	411							
4	538595..538903	308	*ORF19.2739*		538696<--536978		*ORF19.2730*		553936-->555756
4	555823..556043	220	*ORF19.2731*		553564<--553226				
4	569822..570064	242	***ORF19.2725***		567226<--566924	HA-Efg1 (nor and hypoxia), I	***ORF19.2724***		571920-->573416
4	665440..665998	558	*ORF19.2674*		665137<--664109		*ORF19.2673*		665706-->666725
4	901830..902078	248	*ORF19.1429*		901816<--901376		*ORF19.1428*		902225-->902740
4	958836..959072	236	*ORF19.3840*		959031<--954805		*ORF19.3839*		961031-->962392
4	982132..982341	209					*ORF19.3823*		982321-->987258
4	990641..990855	214	***ORF19.3821***		990526<--989339	HA-Efg1 (hypoxia)			
4	1020888..1021863	975	*ORF19.3803*	*MNN24*	1020679<--1018910		*ORF19.3802*	*PMT6*	1022709-->1025207
4	1048206..1048473	267	***ORF19.3794***	*CSR1*	1044143<--1042287	HA-Efg1 (hypoxia)	*ORF19.3793*		1048418-->1049593
4	156748..157165	417	*ORF19.4706*		156361<--155864		*ORF19.4705*		157320-->158915
4	318539..318875	336	*ORF19.4631*	*ERG251*	318193<--317228				
4	673775..674045	270	*ORF19.2670*		673767<--672892				
4	772472..772673	201	*ORF19.1314*		772094<--770685				
4	119205..119456	251	*ORF19.4173*		119171<--117582				
4	125737..125901	164	*ORF19.4169*		125651<--125256		*ORF19.4168*		126013-->126516
4	149067..149317	250					*ORF19.4711*		150355-->152169
4	167790..168189	399	*ORF19.4702*		167605<--166703		*ORF19.4701*		168466-->169392

4	241195..241666	471							ORF19.4670	CAS5	241403-->243868
4	263241..263484	243							**ORF19.4657**		263907-->265409
4	277969..278128	159							ORF19.4651		278269-->278688
4	294547..294757	210							ORF19.4643		294803-->301954
4	336726..336904	178	ORF19.4624		336394<--335036						
4	342226..342418	192	ORF19.4622		342120<--340963						
4	449574..449864	290	ORF19.4560	BFR1	449237<--447849				ORF19.2775	IDI1	450181-->451035
4	681943..682094	151							ORF19.2665		682598-->686252
4	806517..806676	159	ORF19.1298		806323<--803789				ORF19.1297		807459-->809654
4	972793..973252	459	ORF19.3829		972279<--970633						
4	1263263..1263475	212							ORF19.1258		1264022-->1264735
4	1269196..1269522	326	ORF19.1259		1269246<--1264915						
4	1301093..1301343	250	ORF19.1274		1298570<--1296879				ORF19.1275		1302092-->1304095
5	30117..30380	263	ORF19.979	FAS1	29661<--23548						
5	94280..94512	232	ORF19.940		93594<--89881				ORF19.939		95043-->98102
5	217717..218023	306	ORF19.1972		217288<--215867				ORF19.1971		218221-->219705
5	380339..380796	457	**ORF19.3207**	**CCN1**	379761<--377680	Efg1 (hypoxia)					
5	406103..406467	364	ORF19.3195	HIP1	404636<--402837				ORF19.3193	FCR3	407979-->409178
5	443455..443624	169	ORF19.3174		443369<--440835						
5	453619..453945	326	ORF19.3170		453571<--451385						
5	465380..466233	853	ORF19.3161		465405<--464443						
5	472765..473253	488							**ORF19.4216**	**HSP12**	473414-->473920
5	155228..155460	232	ORF19.921		153233<--151176				ORF19.920		156807-->158162
5	175021..175219	198							ORF19.576		175559-->176047
5	347903..348110	207	ORF19.4151		347572<--345242						
5	529019..529265	246	ORF19.4245		527060<--525714				ORF19.4246		529711-->531504
5	568004..568222	218	ORF19.4266		568051<--566677						
5	851168..851516	348	**ORF19.1106**		850957<--848603	Efg1 (hypoxia)					
5	513893..514105	212	ORF19.4239		513647<--511632						
5	522151..522532	381	ORF19.4242	CST20	521590<--517904						
5	599825..600166	341	ORF19.4282		598167<--597259						
5	1107056..1107300	244							**ORF19.3997**	**ADH1**	1107881-->1108930
6	4563..5065	502							ORF19.6337		5545-->6489
6	60497..60663	166	**ORF19.1195**		60013<--57662	Efg1 (hypoxia)			**ORF19.1196**		60921-->63506
6	107748..107995	247							ORF19.4199		107932-->109503
6	173917..174207	290							**ORF19.90**		174680-->176944
6	304142..304599	457	ORF19.3434		301246<--298277				ORF19.3433	OYE23	304843-->306063
6	319400..319632	232	ORF19.3431		317782<--314096				ORF19.3430	BUD21	319776-->320810
6	339382..339625	243							ORF19.3421.1		339664-->340248
6	349369..349608	239	ORF19.3420		348886<--348503				ORF19.3419	MAE1	350713-->352605

6	378815..379061	246	*ORF19.3405*		378232<--376640			*ORF19.3404*			379021-->380502
6	421895..422171	276						*ORF19.3505*			422337-->424733
6	430038..430268	230	*ORF19.3501*		429691<--426551			*ORF19.3499*			434464-->434967
6	444405..444602	197	*ORF19.3494*		444313<--443213			*ORF19.3453*			444683-->447643
6	549988..550214	226	*ORF19.5537*		548965<--547667			*ORF19.5539*			552727-->553569
6	603094..603382	288	*ORF19.5568*		603308<--602358			*ORF19.5569*			603848-->606529
6	630120..630398	278						*ORF19.5584*			630618-->633050
6	640292..640524	232	*ORF19.5586*		640372<--637424						
6	730739..730929	190	*ORF19.5705*	*NAM2*	730549<--727964			*ORF19.5710*			731035-->734520
6	821237..821408	171	*ORF19.5753*	*HGT10*	819180<--817540						
6	837437..837820	383	*ORF19.5759*		836974<--832487						
6	867771..868136	365	*ORF19.5775*		864791<--863253			*ORF19.1221*			876496-->877833
6	875889..876332	443						*ORF19.1221*			876496-->877833
6	898101..898410	309	*ORF19.4557*		897780<--894497						
6	90037..90595	558	***ORF19.4211***	***FET3***	89370<--87511	HA-Efg1 (nor and hypoxia), I		***ORF19.4210***			92718-->94109
6	711941..712284	343						*ORF19.5627*			712343-->713449
6	954958..955148	190	*ORF19.1090*		954989<--954642			*ORF19.1091*			955216-->957288
6	962825..962993	168	*ORF19.1093*	*FLO8*	962206<--959828						
6	969214..969419	205						*ORF19.1097*	*ALS2*		971475-->976745
6	1028365..1028747	382	*ORF19.2160*		1027136<--1025391			*ORF19.2163*			1028841-->1031354
7	132431..132677	246						*ORF19.7047*	*RTF1*		132567-->134273
7	147491..147734	243						*ORF19.7041*			148191-->150485
7	197995..198262	267						*ORF19.7020*	*KEX1*		198461-->200569
7	226954..227152	198	*ORF19.7006*		226654<--223297						
7	235013..235204	191	*ORF19.6896*		232413<--230875						
7	312089..312282	193						*ORF19.6580*			312573-->313265
7	329445..329682	237						*ORF19.6573*			329718-->336476
7	350127..350842	715	*ORF19.6563*		349795<--347816			*ORF19.6562*			350992-->352287
7	375318..375638	320	*ORF19.6551*		375267<--374593			*ORF19.6550*			375747-->376631
7	389345..389658	313	*ORF19.6540*	*PFK2*	388801<--385961			*ORF19.6539*			390350-->391846
7	392764..392967	203	*ORF19.6538*		392514<--392023			*ORF19.6537*			393006-->393698
7	419339..419895	556						*ORF19.6525*			419663-->421988
7	410407..410669	262	*ORF19.6530*		409253<--408390			*ORF19.6529*	*CDC34*		411057-->411791
7	413027..413320	293	*ORF19.6528*		412926<--412315						
7	437730..438044	314	*ORF19.6518*		437290<--435305			*ORF19.6517*			438040-->439230
7	451625..451894	269	***ORF19.6514***	***CUP9***	450912<--449878	HA-Efg1 (nor and hypoxia)					
7	465046..465507	461						*ORF19.6506*			465072-->467138
7	476843..477195	352	*ORF19.6498*		476933<--475905						
7	493528..493763	235						*ORF19.6486*			493963-->494421
7	519989..520286	297	*ORF19.6472*		519627<--519139			*ORF19.6470*			520558-->521115

7	632455..633164	709			7566<--4884				ORF19.5169		633454-->635175
R	8643..8842	199	ORF19.7545		172342<--171653				ORF19.7544		9111-->9863
R	172196..172884	688	ORF19.3283		201735<--201475				ORF19.3265		202225-->203895
R	201809..202075	266	ORF19.3265.1		334491<--333205				ORF19.2528		334922-->336910
R	334667..334909	242	ORF19.2527		509369<--508644				ORF19.3740	PGA23	510511-->511359
R	509931..510278	347	ORF19.3742						**ORF19.173**		556964-->560266
R	556779..557328	549							**ORF19.467**	**WOR3**	878593-->880521
R	874612..874814	202							ORF19.498	EAF7	928331-->929716
R	926791..927553	762	ORF19.496		926380<--923609				ORF19.522	PIM1	963564-->966800
R	963503..963739	236							ORF19.557		1125739-->1126764
R	1125308..1125600	292	ORF19.556		1124656<--1124237				ORF19.5285		1158030-->1158629
R	1157158..1157584	426	ORF19.5286		1156504<--1155638						
R	1259394..1260341	947	ORF19.454	SFL1	1258170<--1255753				ORF19.451		1274207-->1276684
R	1271946..1272327	381									
R	1372318..1372553	235	**ORF19.723**	**BCR1**	1370542<--1368320	Efg1 (hypoxia)					
R	1469903..1470143	240	ORF19.1847		1469576<--1467687						
R	1659779..1660018	239	ORF19.6286		1659219<--1658623				ORF19.6285	GLC7	1660942-->1661934
R	1718524..1718725	201							**ORF19.610**	**EFG1**	1723620-->1725197
R	1723278..1723663	385							**ORF19.610**	**EFG1**	1723620-->1725197
R	1759755..1759942	187	ORF19.589	VPS21	1759114<--1758464				ORF19.6365	PTP1	1760210-->1761328
R	1885618..1886042	424							RDN18		
R	1888916..1889176	260	RDN5						RDN18		
R	1892603..1893207	604	RDN5						RDN58		
R	1919596..1919753	157	ORF19.7293		1919006<--1916934						
R	2106048..2106312	264							**ORF19.7561**	**EED1**	2106249-->2108912
R	456371..456650	279	ORF19.2608		455035<--454025						
R	1229936..1230397	461	ORF19.6630		1229108<--1228704						
R	1234621..1234953	332							ORF19.6626		1235075-->1235701
R	1461771..1461933	162	ORF19.1854	HHF22	1461360<--1461043				ORF19.1853	HHT2	1462318-->1462728
R	1741688..1741957	269	ORF19.600		1741164<--1737995						
R	1787351..1787780	429	ORF19.6385	ACO1	1785923<--1783590						
R	1832192..1832373	181	ORF19.6415.1		1831395<--1831225				ORF19.6417		1832500-->1835028
R	78276..78466	190	**ORF19.7502**		76707<--75931	Efg1 (hypoxia), HA-Efg1 (normoxia)					
R	590631..590875	244	**ORF19.2822**		586104<--585259	HA-Efg1 (nor and hypoxia)			**ORF19.2823**	**RFG1**	600296-->602099
R	1093988..1094309	321							ORF19.646	GLN1	1095535-->1096656
R	1196472..1196912	440	ORF19.5843		1194914<--1194066						
R	1200478..1200718	240	ORF19.6653		1200545<--1198899				ORF19.6652		1201138-->1202460
R	1445167..1445556	389							ORF19.707		1445481-->1447400
R	1477563..1477801	238	ORF19.1843		1477285<--1475594				ORF19.1842		1479665-->1484341
R	1955700..1956129	429	ORF19.7313		1955547<--1954102				ORF19.7314		1957926-->1958723

2.3 Manuscript II: The 5´ untranslated region of *EFG1* transcript promotes its translation to regulate hyphal morphogenesis in *Candida albicans*

Prashant R. Desai, Klaus Lengeler, Mario Kapitan, Silas Matthias Janßen, Paula Alepuz, Ilse Jacobsen and Joachim F. Ernst

Contribution to Manuscript: 80 %

Prashant R. Desai was majorly involved in designing, performing and concluding the results. He prepared all the figures. He wrote the initial draft and was also involved in the editing of the final draft of the manuscript.

Individual contributor: for Figures 1 to 6

Published in : mSphere, August 2018; 3(4): e00280-18

Impact Factor : 3.5 (2018)

AMERICAN SOCIETY FOR MICROBIOLOGY | mSphere®

RESEARCH ARTICLE
Molecular Biology and Physiology

The 5′ Untranslated Region of the *EFG1* Transcript Promotes Its Translation To Regulate Hyphal Morphogenesis in *Candida albicans*

Prashant R. Desai,[a] Klaus Lengeler,[a]* Mario Kapitan,[b,c] Silas Matthias Janßen,[a] Paula Alepuz,[d,e] Ilse D. Jacobsen,[b,c] Joachim F. Ernst[a]*

[a]Department Biologie, Molekulare Mykologie, Heinrich-Heine-Universität, Düsseldorf, Germany
[b]Microbial Immunology, Leibniz Institute for Natural Product Research and Infection Biology (Hans Knöll Institute), Jena, Germany
[c]Institute for Microbiology, Friedrich-Schiller-University, Jena, Germany
[d]Departamento de Bioquímica y Biología Molecular, Universitat de València, Burjassot, Valencia, Spain
[e]ERI Biotecmed, Universitat de València, Burjassot, Valencia, Spain

ABSTRACT Extensive 5′ untranslated regions (UTR) are a hallmark of transcripts determining hyphal morphogenesis in *Candida albicans*. The major transcripts of the *EFG1* gene, which are responsible for cellular morphogenesis and metabolism, contain a 5′ UTR of up to 1,170 nucleotides (nt). Deletion analyses of the 5′ UTR revealed a 218-nt sequence that is required for production of the Efg1 protein and its functions in filamentation, without lowering the level and integrity of the *EFG1* transcript. Polysomal analyses revealed that the 218-nt 5′ UTR sequence is required for efficient translation of the Efg1 protein. Replacement of the *EFG1* open reading frame (ORF) by the heterologous reporter gene *CaCBGluc* confirmed the positive regulatory importance of the identified 5′ UTR sequence. In contrast to other reported transcripts containing extensive 5′ UTR sequences, these results indicate the positive translational function of the 5′ UTR sequence in the *EFG1* transcript, which is observed in the context of the native *EFG1* promoter. It is proposed that the 5′ UTR recruits regulatory factors, possibly during emergence of the native transcript, which aid in translation of the *EFG1* transcript.

IMPORTANCE Many of the virulence traits that make *Candida albicans* an important human fungal pathogen are regulated on a transcriptional level. Here, we report an important regulatory contribution of translation, which is exerted by the extensive 5′ untranslated regulatory sequence (5′ UTR) of the transcript for the protein Efg1, which determines growth, metabolism, and filamentation in the fungus. The presence of the 5′ UTR is required for efficient translation of Efg1, to promote filamentation. Because transcripts for many relevant regulators contain extensive 5′ UTR sequences, it appears that the virulence of *C. albicans* depends on the combination of transcriptional and translational regulatory mechanisms.

KEYWORDS 5′ UTR, *Candida albicans*, *EFG1*, filamentation, hyphal morphogenesis, posttranscriptional regulation, translation

Transcriptional networks are known to govern growth and virulence of the human fungal pathogen *Candida albicans*. Transcription factors have been identified that regulate the interconversion between its yeast cell form and a filamentous hyphal form, or the rod-like opaque form. Efg1 is a key basic-helix-loop-helix (bHLH)-type regulatory protein that controls hyphal morphogenesis in a dual manner, promoting filamentation under normoxia in the presence of environmental cues (1, 2) but repressing it under hypoxia (3, 4). Its promoting function depends on increased histone acetylation and

Received 19 May 2018 **Accepted** 8 June 2018 **Published** 5 July 2018

Citation Desai PR, Lengeler K, Kapitan M, Janßen SM, Alepuz P, Jacobsen ID, Ernst JF. 2018. The 5′ untranslated region of the *EFG1* transcript promotes its translation to regulate hyphal morphogenesis in *Candida albicans*. mSphere 3:e00280-18. https://doi.org/10.1128/mSphere.00280-18.

Editor Aaron P. Mitchell, Carnegie Mellon University

Address correspondence to Joachim F. Ernst, Joachim.ernst@uni-duesseldorf.de.

* Present address: Klaus Lengeler, Yeast & Fermentation, Carlsberg Research Laboratory, Copenhagen, Denmark; Joachim F. Ernst, Department Biologie, c/o Institut für Mikrobiologie, Düsseldorf, Germany.

This paper is dedicated to the memory of André Goffeau.

chromatin remodeling at promoters of target genes (5), which facilitate hyphal initiation; shortly thereafter, however, *EFG1* expression is strongly downregulated to prevent its interference with subsequent processes required for hyphal formation (6, 7). Under hypoxia, Efg1 represses the expression of genes encoding hyphal inducers Ace2 and Brg1, thereby downregulating filamentation (8), and it regulates the hypoxia-specific expression of numerous genes. Furthermore, by counteracting expression of *WOR1*, Efg1 prevents switching to the opaque form and favors the yeast morphology (9). The activity of the Efg1 protein is regulated by posttranslational modifications, including phosphorylation by cAMP-dependent protein kinase A (PKA) in response to environmental cues (10, 11). The overall activity of Efg1 is required for biofilm formation (12–14) and virulence (2) of *C. albicans*.

In eukaryotes, the level, processing, localization, and/or structure of the primary transcript determines the initial amount of the encoded protein, which is subsequently lowered by different rates of proteolytic degradation. Some such posttranscriptional processes and their underlying mechanisms have been described in *C. albicans* to regulate levels of proteins, including transcription factors (15, 16). Transcript degradation involves poly(A) tail removal by deadenylase subunits Ccr4/Pop2 (17), hydrolysis of the 5′ cap by decapping activators Dhh1/Edc3 (18) and decapping enzyme Dcp1 (18), and mRNA digestion by exonuclease Xrn1/Kem1 (19, 20). RNA binding proteins Puf3 (21) and Zfs1 (22) also appear to be involved in decay of transcripts. Mutants lacking these degradative activities show defects in filamentation and/or biofilm formation, although specific targets have not yet been defined. The specific degradation of the transcript encoding Nrg1, a strong repressor of filamentation, was described to depend on an antisense transcript that originates from the locus encoding the Brg1 hyphal activator (23). The localization of transcripts also regulates filamentation of *C. albicans*, as was shown for the She3 protein that binds several transcripts involved in filamentation and transports them to the bud site of yeast cells or to the tips of hyphae (24); the Sec2 protein operating at the hyphal tip appears to specifically localize its own transcript to this location (25). It is assumed that localized translation procures directed delivery of such proteins to their sites of action. In recent years, the localization, degradation, and/or translation of certain transcripts was found also to depend on promoter sequences, suggesting that already during transcription, regulatory factors for these functions may become loaded onto the emerging transcript (26–28).

The structure of the 5′ untranslated region (UTR) of transcripts controls translation in eukaryotes. Strong evidence supports the importance of AUG context sequence on translational initiation (29, 30). Upstream open reading frames (uORFs) within the 5′ UTR can control translation of the downstream main ORF (31, 32), as has been described for the *C. albicans GCN4* gene that regulates the amino acid starvation response, as well as filamentation and biofilm formation (33). Cap-independent translation that is initiated at internal ribosome entry sites (IRESs) has been described for gene transcripts responsible for invasive growth in the yeast *Saccharomyces cerevisiae* (34). In addition, 5′ UTR sequences may contain binding sites for binding proteins that facilitate localization (35) and potentially translation of transcripts. In *C. albicans*, the Dom34 protein, known for its general role in no-go decay of mRNAs, was also shown to bind the 5′ UTR of specific transcripts encoding Pmt-type mannosyl transferases and favor their translation (36). Similarly, the Ssd1 RNA binding protein may positively affect translation of specific sets of transcripts involved in cell wall integrity and polarized growth (37, 38). Remarkably, many transcripts encoding essential regulators of cell morphology contain extensive 5′ UTRs, including *UME6* (3,041 nucleotides [nt]), *CZF1* (2,071 nt), *WOR1* (2,978 nt), and *EFG1* (1,139 nt of long transcript) (39). The long 5′ UTRs of *UME6* and *WOR1* genes were recently shown to downregulate translation of their transcripts (40, 41), possibly by forming a tight three-dimensional structure that blocks scanning by ribosomal 40S subunits. In both cases, regulated release of translational blockage may be mediated by host environmental cues that alter the 5′ UTR structure (42), e.g., in the presence of specific RNA binding proteins. Nonnative, functional expression of *EFG1* has been achieved by placing the *EFG1* ORF (without the 5′ UTR

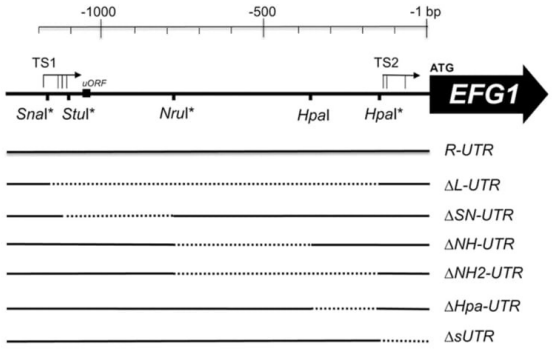

FIG 1 Upstream region of the *EFG1* gene. Schematic representation of the *EFG1* upstream region in strain ATCC 10231 indicating start positions of the large transcript (TS1) around position −1100 and of the small transcript (TS2) around position −100. The large and small transcripts are the major transcripts observed in white (yeast) and opaque growth forms, respectively (Fig. S1). A small upstream open reading frame (uORF) encoding 4 amino acids is shown as a black box; it is missing in strain SC5314. Positions of restriction sites used to construct deletions in the 5′ UTR sequence are as indicated; sites marked by asterisks were introduced by site-specific mutagenesis. While *R-UTR* denotes the full-length 5′ UTR-*EFG1* region, the Δ series shows deleted *EFG1* alleles lacking sequences between restriction sites in the 5′ UTR (dotted lines), affecting mostly the large transcript but also the small transcript (Δ*sUTR*). Plasmids harboring native and deleted forms of *EFG1* were integrated into the *EFG1* upstream region of *efg1*/*efg1* mutant HLC67.

sequence) downstream of the heterologous *C. albicans PCK1* and *ACT1* promoters (1, 3, 43, 44). Here, we report that the extensive 5′ UTR of the major *EFG1* transcript nevertheless has a significant positive role for the functional expression of the *EFG1* ORF. A specific sequence within the 5′ UTR is required to stimulate translation of the *EFG1* transcript, to permit efficient hyphal morphogenesis.

RESULTS

Deletions in the 5′ UTR of *EFG1*. In the yeast growth form (white), the transcript start sites for the main *EFG1* transcript are known to cluster around position −1100 relative to the ATG of the *EFG1* ORF, generating a transcript of 3.3 kb (6, 43, 45). Referring to the sequence of ATCC 10231 (used here for deletion analysis), start sites lie at positions −1170, −1143, and −1112 (amended from the work of Tebarth et al. [6]) or at −1125 (−1117 in strain SC5314 [39]); in agreement, the start site in strain WO-1 was mapped at position −1173 (45) (Fig. 1). In the rod-like opaque growth form, however, low levels of a shortened *EFG1* transcript of 2.2 kb occur (43), for which start sites at positions −145 and −162 were identified (45), and a start position of −74 was also observed for a minor fraction of the *EFG1* transcript in yeast-form cells (6).

To construct deletions in the 5′ UTR sequence, restriction enzyme sites were inserted, singly or in combination, into a plasmid-resident *EFG1* gene, including 3.2 kb of its upstream sequence (allele *R-UTR*). Sequences between restriction sites were deleted, resulting in six deleted *EFG1* alleles lacking 5′ UTR sequences of the large transcript (Δ*L-*, Δ*SN-*, Δ*NH-*, Δ*NH2-*, and Δ*Hpa-UTR*) or the small transcript (Δ*sUTR*) (Fig. 1; see also Fig. S1 in the supplemental material). The resulting plasmids were chromosomally integrated into the upstream region of the *EFG1* locus in strain HLC67 (2), which lacks the *EFG1* ORF (but retains its upstream sequences) on both homologous chromosomes.

5′ UTR sequence enhances filamentation. *C. albicans* mutants lacking the Efg1 protein are unable to form hyphae at 37°C under all conditions, while at temperatures of <35°C, if cells are grown under hypoxia on agar surfaces, their filamentation is derepressed (4). This dual function of Efg1 as activator and as repressor of morphogenesis becomes apparent during surface growth of cells under hypoxia (0.2% O_2) at

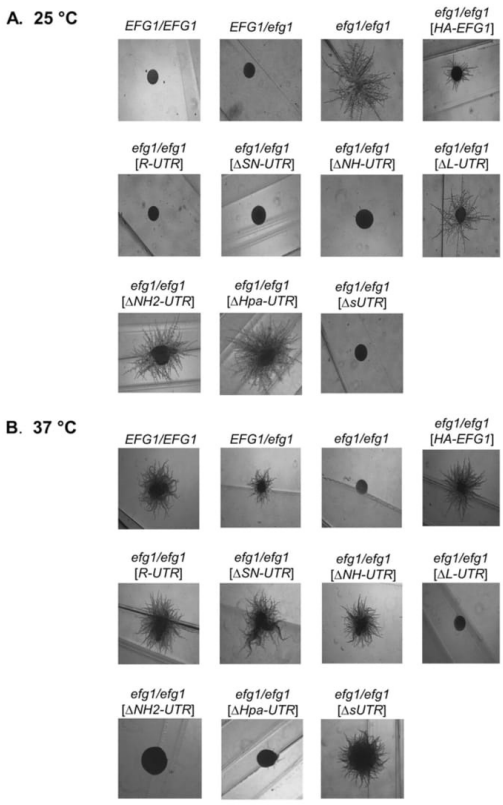

FIG 2 Colony phenotypes of strains expressing deletions in the 5′ UTR of *EFG1*. Strains CAF2-1 (*EFG1/EFG1*), BCA09 (*EFG1/efg1*), HLC67 (*efg1/efg1*), HLCEEFG1 (*HA-EFG1/efg1*), PDUWT (*efg1/R-UTR-EFG1*), PDUSN (*efg1/ΔSN-UTR-EFG1*), PDUNH (*efg1/ΔNH-UTR-EFG1*), PDULG (*efg1/ΔL-UTR-EFG1*), PDUSH (*efg1/ΔNH2-UTR-EFG1*), PDUHH (*efg1/ΔHpa-UTR-EFG1*), and PDUsU (*efg1/ΔsUTR-EFG1*) were grown on Spider medium either at 25°C for 3 days (A) or at 37°C for 2 days (B), under hypoxic conditions (0.2% O_2). The data show representative colony morphologies, which were imaged by light microscopy.

either 25°C or 37°C (Fig. 2). Cells carrying at least one functional *EFG1* allele are able to filament at 37°C but not at 25°C, while nonfunctional alleles are hyperfilamentous at 25°C but not at 37°C. The only exception to this pattern, as described previously (8), is mediated by the *HA-EFG1* allele, which promotes hypha formation at 37°C but lacks repressor function at 25°C, thus leading to filamentation at both temperatures.

EFG1 alleles containing either the full-length 5′ UTR (*R-UTR*) or deleted alleles Δ*SN-UTR*, Δ*NH-UTR*, and Δ*sUTR* were fully active in promoting filamentation at 37°C and repressing it at 25°C (Fig. 2). Because deletions in these alleles encompassed a small uORF sequence, it appears that its presence is not required for hypha formation. In contrast, alleles containing Δ*L-UTR*, Δ*NH2-UTR*, and Δ*Hpa-UTR* performed as nonfunctional *EFG1* alleles that did not stimulate filamentation at 37°C but allowed strong filamentation at 25°C. The latter alleles were all lacking the 218-bp HpaI fragment that was solely deleted in the Δ*Hpa-UTR* allele. To confirm these results, the function of the various alleles was also tested under normoxia using liquid induction medium containing 10% serum at 37°C, which demonstrated similar filamentation phenotypes as those that were observed during surface growth (Fig. 3). Thus, these results indicate that the

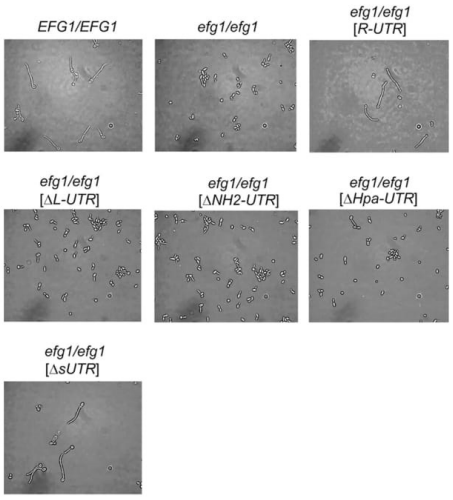

FIG 3 Cell morphologies of strains expressing deletions in the 5′ UTR of *EFG1* after serum induction. Strains were grown in YPD at 30°C and diluted into prewarmed YP medium containing 10% horse serum at 37°C. Cells were incubated for 30 min at 37°C and imaged by phase-contrast microscopy. Strain designations are as in Fig. 2.

218-nt HpaI fragment in the 5′ UTR of *EFG1* is required for production and/or activity of Efg1, promoting filamentation at 37°C and repressing it at 25°C. Filamentation phenotypes obtained for all tested *EFG1* alleles are summarized in Fig. 4.

Deleted 5′ UTR alleles do not lower *EFG1* transcript levels. To clarify the reasons for the inactivity of *EFG1* alleles in cells lacking the 5′ UTR completely (Δ*L-UTR*) or partially (Δ*Hpa-UTR*), *EFG1* transcript levels were determined by quantitative PCR (qPCR). Both shortened alleles resulted in significantly elevated transcript levels compared to wild-type cells (*EFG1/EFG1*) or to cells expressing the *R-UTR* allele containing the full-length 5′ UTR (Fig. 5A). The observed increase was highest in cells pregrown for 12 h in yeast extract-peptone-dextrose (YPD) ($t = 0$) but clearly apparent also after

Medium / Strains	Spider Hypoxia 25 °C	Spider Hypoxia 37 °C	YP+10 % Serum 37 °C
EFG1/EFG1	Yeast	Hyphae	Hyphae
EFG1/efg1	Yeast	Hyphae	Hyphae
efg1/HA-EFG1	Yeast	Hyphae	Hyphae
efg1/R-UTR-EFG1	Yeast	Hyphae	Hyphae
efg1/ΔL-UTR-EFG1	Hyphae	Yeast	Yeast
efg1/ΔSN-UTR-EFG1	Yeast	Hyphae	Hyphae
efg1/ΔNH-UTR-EFG1	Yeast	Hyphae	Hyphae
efg1/ΔHpaI-UTR-EFG1	Hyphae	Yeast	Yeast
efg1/ΔNH2-UTR-EFG1	Hyphae	Yeast	Yeast
efg1/ΔsUTR-EFG1	Yeast	Hyphae	Hyphae

FIG 4 Summary of filamentation phenotypes of *C. albicans* strains carrying deletions in the 5′ UTR of *EFG1*.

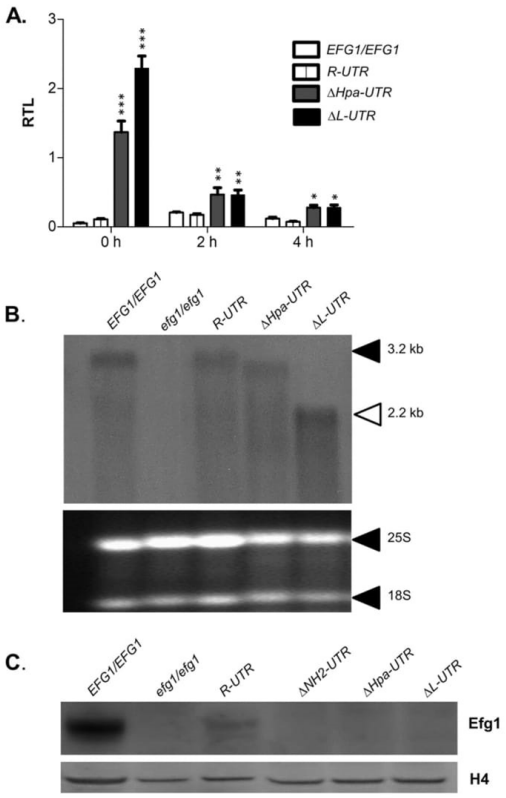

FIG 5 A 5′ UTR deletion increases *EFG1* transcript and decreases Efg1 protein levels. Strains CAF2-1 (*EFG1/EFG1*), PDUWT (*R-UTR*), PDUHH (Δ*Hpa-UTR*), and PDULG (Δ*L-UTR*) were examined for *EFG1* transcript and Efg1 protein levels. (A) Strains were pregrown for 12 h in YPD ($t = 0$ h), diluted into YPD, and grown for 2 and 4 h at 30°C; levels of the *EFG1* transcript were determined by qPCR, using the *ACT1* transcript as an internal reference to calculate relative transcription levels (RTL). Error bars display standard errors of the means derived from biological triplicates. A two-tailed, unpaired *t* test comparing the RTL values of control CAF2-1 and other strains was used to determine the statistical relevance. *, $P < 0.05$; **, $P < 0.01$; ***, $P < 0.001$. (B) In addition, the *EFG1* transcript in the RNA of strains grown for 6 h in YPD was examined by Northern analysis (top), using 8 μg RNA for loading. Note that the *EFG1* transcript size (3.2 kb) is reduced greatly only for the Δ*L-UTR* variant, which lacks most of the 5′ UTR. 25S (3.4-kb) and 18S (1.8-kb) rRNAs (61) stained by ethidium bromide were used as a loading control (bottom). (C) To determine Efg1 protein levels, strains were grown in YPD medium at 30°C to the logarithmic phase and cell extracts derived from 1 OD_{600} equivalent of cells were separated by SDS-PAGE and analyzed by immunoblotting, using either anti-Efg1 antibody or anti-histone H4 antibody for probing. Levels of histone H4 served as loading controls.

short-term growth for 2 and 4 h. It can be concluded that the low Efg1 activity of the Δ*L-UTR* or Δ*Hpa-UTR* alleles cannot be explained by lowered *EFG1* transcript levels. To verify that the respective transcripts were intact, cellular RNA was also examined by Northern blotting. As expected, wild-type cells and cells containing the *R-UTR* allele contained an *EFG1* transcript of about 3.2 kb (6, 42, 44), while the *efg1* mutant was lacking this transcript (Fig. 5B). Remarkably, the mutated alleles encoded *EFG1* transcripts with sizes reflecting the extent of 5′ UTR deletions, i.e., the size of the transcript encoded by the Δ*Hpa-UTR* allele was only slightly reduced, while the Δ*L-UTR* transcript was shortened to about 2 kb, approximating the size that occurs in opaque-type cells

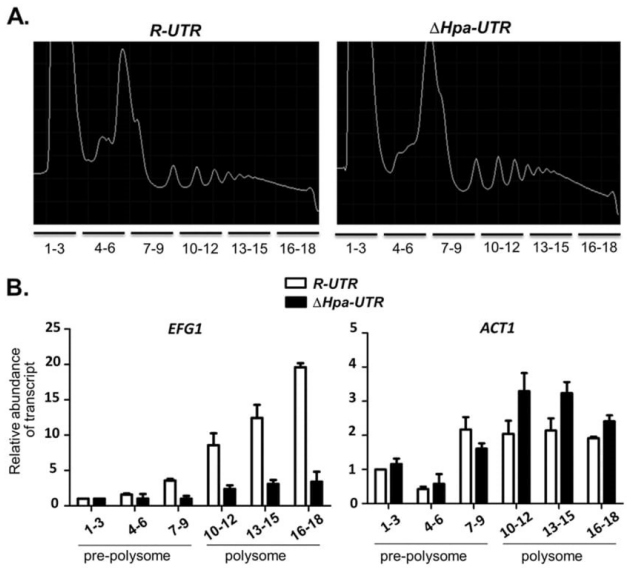

FIG 6 Transcript fractionation on polysome gradients. (A) Strains PDUWT (*R-UTR*) and PDUHH (Δ*Hpa-UTR*), pregrown in YPD medium at 30°C, were transferred to YP medium containing 10% horse serum at 37°C and incubated for 15 min. Cellular extracts of strains were centrifuged in a 10 to 50% sucrose gradient, which was subsequently fractionated. Nucleic acids in gradient fractions were detected by absorbance (A_{260}). Note that prepolysome fractions 1 to 9 contain 40S, 60S, and 80S rRNA. (B) *EFG1* and *ACT1* transcripts in gradient fractions were detected by qPCR after adding a known amount of an *in vitro*-generated transcript of the *CaCBGluc* gene as a calibrator. Data shown represent values that are normalized to *EFG1* or *ACT1* mRNA abundance in fraction 1. Each bar represents the normalized mean *EFG1* or *ACT1* transcript level of two independent experiments with three technical replicates and includes the standard error of the mean.

(42, 44). These results indicate that the *EFG1* transcript encoded by the inactive, deleted 5′ *EFG1* alleles is not differentially processed or degraded.

Efg1 protein produced by deleted 5′ UTR alleles. To verify Efg1 protein levels produced by the deleted 5′ UTR alleles, cell extracts were analyzed by immunoblotting, using an anti-Efg1 antiserum described previously (7, 46). The Efg1 protein was detected strongly in wild-type cells (carrying two *EFG1* alleles) and also, with reduced intensity, in cells carrying a single *R-UTR* allele containing the full-length 5′ UTR (Fig. 5C). In contrast, no Efg1 protein was observed in cells expressing the truncated 5′ UTR versions Δ*L-UTR*, Δ*Hpa-UTR*, and Δ*NH2-UTR*, which are functionally inactive. It can be concluded that the latter alleles do not produce significant amounts of Efg1 protein, in spite of expressing high *EFG1* transcript levels.

Truncation of the 5′ UTR deletion reduces translation of *EFG1*. The above results had suggested that the 5′ UTR of the *EFG1* transcript contains a 218-nt sequence corresponding to the small HpaI fragment of the *EFG1* upstream region, which is required for efficient translation of Efg1. To test this hypothesis, polysome analyses were carried out using cellular lysates of strains expressing *EFG1* alleles containing the full-length 5′ UTR (*R-UTR*) or the partially deleted variant (Δ*Hpa-UTR*). As expected, profiles obtained by sucrose gradient centrifugation were similar in the two strains, showing a prepolysomal fraction (containing 40S, 60S, and 80S rRNA) and several polysomal peaks (Fig. 6A). Transcript levels of *EFG1* and the *ACT1* housekeeping gene in the prepolysomal and polysomal fractions were examined by qPCR, using a spiked-in control RNA as a reference. The results demonstrate that the *EFG1* transcript containing the full-length 5′ UTR is significantly enriched in the polysomal fraction compared to

the prepolysomal fraction (Fig. 6B), while in cells expressing the Δ*Hpa-UTR* allele, the *EFG1* transcript occurred in similar amounts in pre- and polysomal fractions. In contrast, the *ACT1* transcript used as a control was increased in the polysomal fraction and occurred in similar amounts in the two types of cells (slightly increased in cells with the Δ*Hpa-UTR* allele). The results indicate that a specific deletion within the 5′ UTR of the *EFG1* transcript impairs its translation.

ORF-independent function of the 5′ UTR sequence. The observed positive effect of the 5′ UTR of the *EFG1* transcript on its translation could operate either independently or dependently on its native context upstream of the *EFG1* ORF. This possibility was examined by replacing the *EFG1* ORF in control strain PDUWT (*efg1/R-UTR-EFG1*) by the heterologous *CaCBGluc* sequence that encodes click beetle luciferase (47); thereafter, the resulting strain EFG1GN contained the allele *EFG1p-R-UTR-CaCBGluc*. Likewise, the *EFG1* ORF was replaced in strain PDUHH (*efg1/*Δ*Hpa-UTR-EFG1*), resulting in strain DUTRinEFG1GN containing allele *EFG1p-*Δ*Hpa-UTR-CaCBGluc*. As controls, the *CaCBGluc* gene was also used to replace one allele of the *ACT1* ORF in both PDUWT and PDUHH, generating strains ACT1GN and DUTRinACT1GN, which both carry the *ACT1p-CaCBGluc* fusion. *CaCBGluc* transcript levels driven by the *ACT1* promoter were similar in strains ACT1GN and DUTRinACT1GN, as expected (Fig. 7A); correspondingly, luciferase activities were nearly identical (Fig. 7B). Under the control of the *EFG1* promoter that was joined to the intact 5′ UTR (*R-UTR*), the *CaCBGluc* transcript level was about 5-fold higher than its junction to the deleted 5′ UTR sequence (allele Δ*Hpa-UTR*), suggesting that truncation of the 5′ UTR lowers transcript stability. It should be considered here that negative autoregulation known for the *EFG1* gene (Fig. 5) (6, 7) cannot occur for the described *CaCBGluc* fusions. Remarkably, however, in spite of considerable *CaCBGluc* transcript levels, luciferase activity was essentially lost in strain DUTRinEFG1GN. The complete loss of luciferase activity was surprising, considering that the *CaCBGluc* transcript level in this strain was even higher than in control strain DUTRinACT1GN (*CaCBGluc* transcribed by the *ACT1* promoter), which generated abundant luciferase activity. The results support the importance of the 5′ UTR *EFG1* sequence for the functional expression of the downstream ORF, which need not be the native *EFG1* ORF.

DISCUSSION

The dual activity of Efg1 as an activator and repressor of transcription requires proper timing and targeting of its activity. Although Efg1 is required to initiate hypha formation under normoxia (1, 2), its prolonged activity interferes with orderly filamentation (6, 7). Under some hypoxic conditions, Efg1 is not an activator but an efficient repressor of hypha formation (3, 4). Efg1 induces genes specific for the yeast (white) growth form, but by repressing *WOR1*, it prevents the rod (opaque) growth form (9). In metabolism, Efg1 induces genes involved in glycolysis, but it also represses genes in oxidative metabolism (3). Furthermore, Efg1 induces and represses hypoxia-specific genes, and it prevents inappropriate hypoxic regulation of genes not normally regulated by oxygen (4). Efg1 activity has hitherto been known to be regulated on posttranslational and transcriptional levels. Posttranslational modes of regulation include Efg1 phosphorylation by PKA isoforms (10, 11), which may occur directly at target genes (48), or physical association with regulatory factors like Flo8 and Czf1 (46). Transcriptional repression of *EFG1* expression is mediated by Sin3 (6) and Wor1 (9) and also by Efg1 itself (6, 7), causing negative autoregulation that prevents an overshoot of Efg1 activity. *EFG1* activation is mediated in an environment-dependent manner by Brg1, Bcr1, or Ace2 (8). Here, we report a novel mechanism regulating Efg1 biosynthesis on the translational level.

We present evidence that a 218-nt sequence of the 5′ UTR of its major transcript is required for Efg1 protein production. Because of negative autoregulation of *EFG1* (6, 7), transcript levels of the 218-nt deletion variant were even increased but still did not yield significant amounts of Efg1 protein. In wild-type cells, the major *EFG1* transcript was distributed mostly to polysomes, while the deleted transcript was distributed equally to monosomes and polysomes, suggesting that the 218-nt sequence activates Efg1

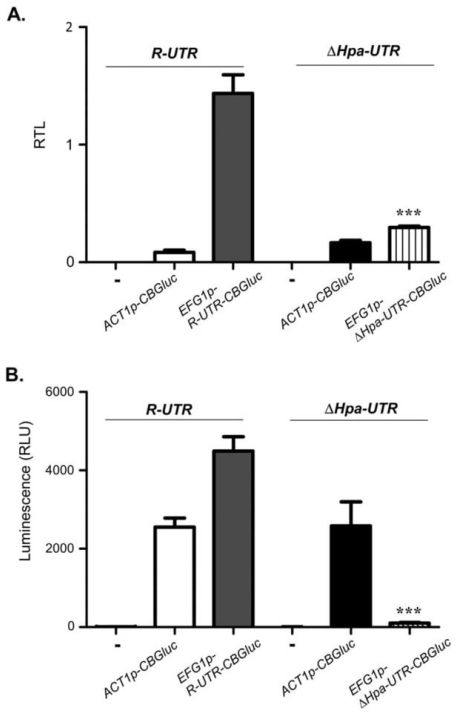

FIG 7 Deletions in 5′ UTR affect the translation of *CaCBGluc*. Strains containing either the intact *R-UTR* allele (strain PDUWT) or the Δ*Hpa-UTR* allele (strain PDUHH) of *EFG1* were modified further by replacing either the *ACT1* or *EFG1* ORF with the *CaCBGluc* ORF. Resulting strains include ACT1GN (*efg1/EFG1p-R-UTR-EFG1*, *ACT1/ACT1p-CaCBGluc*), EFG1N (*efg1/EFG1p-R-UTR-CaCBluc*), DUTRinACT1GN (*efg1/EFG1p-ΔHpa-UTR-EFG1*, *ACT1/ACT1p-CaCBGluc*), and DUTRinEFG1GN (*efg1/EFG1p-ΔHpa-UTR-CaCBGluc*). Strain PDUWT (*efg1/EFG1p-R-UTR-EFG1*) was used as a control (−). Strains were grown in YPD medium at 30°C to the exponential phase (OD_{600} of 0.5) and used for determining transcript and luciferase activity levels. (A) *CBGluc* transcript level. Relative transcript levels (RTL) of *CaCBGluc* were determined by qPCR, using the *ACT1* transcript for normalization. Error bars display standard errors of the means derived from three biological and three technical replicates. (B) Luciferase activity. Luminescence originating from 100 μl of cells was assayed after addition of 100 μl of Beetleglow reagent. Statistical significance was determined by comparing the EFG1GN and UTRinACT1GN strains, with a two-tailed, unpaired *t* test based on two biological and three technical replicates. *, $P < 0.05$; **, $P < 0.01$; ***, $P < 0.001$.

translation. This positive effect was observed even if the *EFG1* ORF was replaced by the ORF of a heterologous reporter gene, indicating that the activating function of the 5′ ORF does not depend on its native 3′ context. As expected from these results, the absence of this regulatory sequence in the short 2.2-kb transcript of the opaque form (or in the minor 2.2-kb transcript of the white yeast form) (6, 43, 45) is expected to reduce the production of Efg1 protein. This mechanism contributes to lowering Efg1 activity in opaque cells, which is already reduced on the transcriptional level (9, 43, 45), to prevent backward switching to the white (yeast) form. Clearly, low translation of the *EFG1* transcript in opaque cells (41) is not caused by an inhibitory effect of the 5′ UTR, as has been suggested elsewhere (41), but is due to the lack of the 218-nt sequence in the short opaque transcript (2.2 kb). The positive translational function of the 5′ UTR in the *EFG1* major transcript differs from other recently reported 5′ UTRs in transcripts of two different *C. albicans* genes. In contrast to *EFG1*, 5′ UTR sequences of both *UME6* and *WOR1* transcripts were found to negatively influence translation of the respective proteins (40, 41). Furthermore, both *UME6* and *WOR1* are positively autoregulated (40,

41, 49), while *EFG1* is negatively autoregulated. The different modes of autoregulation nevertheless lead to increased promoter activities and transcript levels of all three genes lacking the 5′ UTR (or relevant parts thereof); in the case of *UME6/WOR1*, this result is caused by relief of translational inhibition (increased protein levels stimulate promoter activity), while for *EFG1* this occurs because Efg1 production is reduced, which derepresses *EFG1* promoter activity.

The molecular mechanism by which the 5′ UTR sequences of *EFG1* or *UME6/WOR1* transcripts regulate translation is not known and needs experimental verification. The 218-nt sequence of the *EFG1* 5′ UTR is predicted to form a hairpin (Fig. 8), which possibly could help to generate an mRNA structure that is favorable for translational initiation. This potential structure could also be the target of RNA binding proteins that stimulate translation. For example, unwinding of RNA structures by binding of helicase eIF4A to the 5′ UTR has been reported elsewhere (50). In *C. albicans*, the Dom34 protein, a predicted component of the no-go transcript degradation pathway, was found to bind to the 5′ UTR of transcripts encoding protein O-mannosyltransferases and to promote their translation (36). Binding proteins could also have an inhibitory function, such as the Rim4 protein in the yeast *S. cerevisiae* that binds to the 5′ UTR of the *CLB3* transcript to inhibit its translation (51). Likewise, the Ssd1 protein represses translation of genes involved in cell growth and morphogenesis by binding to the 5′ UTR of target transcripts (38). In mammalian cells, glucose-induced translation of insulin requires proteins binding to the 5′ UTR of the encoding transcript (52). On the other hand, the 5′ UTR structures of several human gene transcripts are known to mediate translational control that is essential to prevent several serious diseases (51, 62). The function of 5′ UTR binding proteins is possibly related to the regulation of ribosomal assembly at the AUG initiation codon. Interestingly, the recruitment of regulatory factors to transcripts may depend not only on 5′ UTR or other transcript sequences, since promoters also can provide regulatory proteins that control the degradation, localization, and translation of transcripts (26, 27). It has been suggested that such proteins may be loaded onto the mRNA near its 5′ end early in transcription (28). Such a mechanism could also be operative for the *EFG1* 5′ UTR, because its positive effect was detected only in the context with its native upstream promoter sequences but not with heterologous *PCK1* and *ACT1* promoters, which were able to drive functional expression of the *EFG1* ORF lacking the 5′ UTR (1, 3, 43, 44). Although the functional interplay of promoter and 5′ UTR sequences remains to be established, it is possible that *EFG1* promoter sequences support the action of the 5′ UTR in translation, e.g., by transcript loading with positively acting translation factors. Several other mechanisms explaining the regulatory function of the 5′ UTR sequence in the major *EFG1* transcript are possible (50). Internal ribosome entry sites (IRESs) have been described not only for viral transcripts or genomes but also for translation of yeast genes involved in responses to stress or starvation, which require IRESs within transcripts (34, 53, 54). uORF sequences can occupy 5′ UTRs and contribute to regulation of eukaryotic translation (31, 32). In *C. albicans*, for example, a uORF regulates translation of the *GCN4* transcript (33). We identified a short uORF with an AUG start codon in the 5′ UTR of *EFG1* in the *C. albicans* strain ATCC 2013. However, this uORF does not appear to be relevant, since it does not occur in the *EFG1* 5′ UTR of strain SC5314 and its deletion did not influence functional expression of *EFG1* in strain ATCC 2013. However, it should be considered that in the yeast *S. cerevisiae* translational initiation has been observed also at non-AUG codons, especially at UUG and GUG (55), and the use of GUG for translational initiation in *C. albicans* has already been reported (56). Interestingly, assuming that UUG can be used for translational initiation in *C. albicans*, two uORFs placed side by side are predicted within the 218-nt regulatory sequence of the *EFG1* transcript (see Fig. S1 in the supplemental material). These uORFs could potentially encode peptides of 53 and 29 amino acids, respectively. In general, however, uORFs are known to negatively influence the translation of ORF sequences that are situated immediately downstream (31), rather than acting positively as in the case of the *EFG1* ORF. Since all

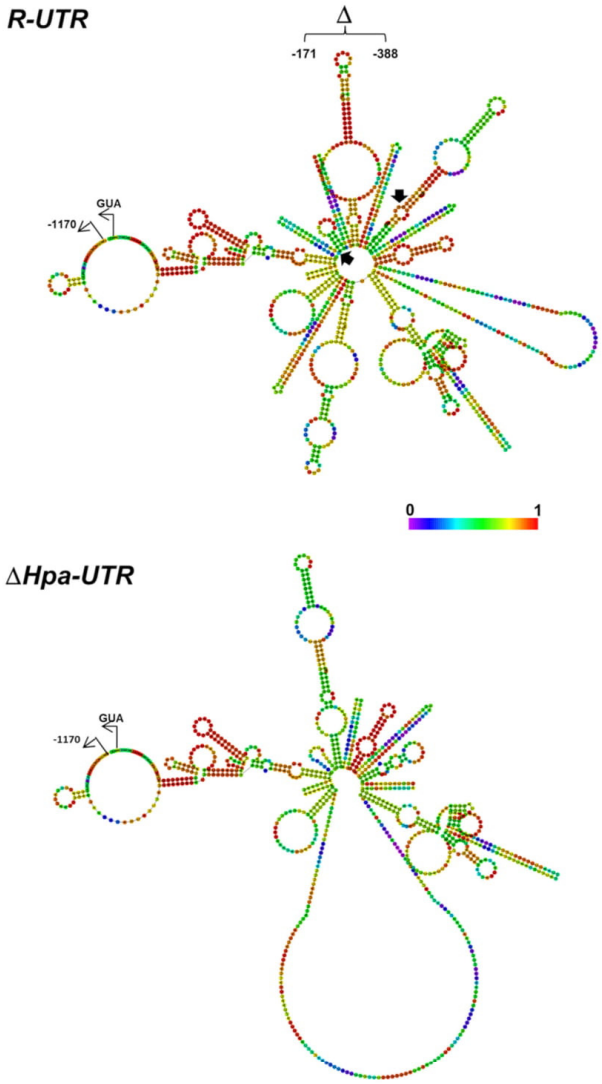

FIG 8 Secondary structure of *EFG1* 5′ UTR. Predicted folding structure of full-length 5′ UTR (*R-UTR*) and deleted 5′ UTR (Δ*Hpa-UTR*) of *EFG1*. The RNAfold program (http://rna.tbi.univie.ac.at/cgi-bin/RNAWebSuite/RNAfold.cgi) was used for prediction, and results were depicted as a centroid structure showing base pair probabilities. The color code indicates probabilities of base-pairing or single-strandedness in predicted paired and unpaired regions, respectively. Black arrows frame the region deleted in the Δ*Hpa-UTR* structure (Fig. S1), which lacks a strong hairpin between positions −327 and −229. Note that strong pairing is predicted between the 5′ end of the UTR (−1118 to −1100) and sequences preceding the AUG translational initiation codon (−112 to −25). This structure is still present in the deleted UTR.

identified uORFs also terminate in the 5′ UTR of *EFG1*, a potential translational read-through generating an extended Efg1 protein, as has been observed for Myc (57), can be excluded. Whatever the underlying mechanism of regulation by 5′ UTR sequences may be, it may be relevant for a significant number of virulence-related

C. albicans genes that carry extensive 5′ UTRs. It can also be speculated that such processes may become new targets for antifungal compounds.

MATERIALS AND METHODS

Strains and media. Strains used in this study are listed in Table S1 in the supplemental material. Strains were grown in liquid YP (1% yeast extract, 1% peptone) with either 2% glucose (YPD) or 10% horse serum, to induce filamentation. To induce filamentation on agar, strains were grown on Spider medium (0.3% beef extract, 0.5% peptone, 0.2% K_2HPO_4, 1% mannitol, and 2% agar, pH 7.2). An Invivo 200 hypoxia chamber (Ruskinn) was used for hypoxic growth (0.2% O_2).

Construction of strains containing deletions in the 5′ UTR of *EFG1*. Expression vector pTD38-HA (46) was modified to remove sequences encoding the N-terminal hemagglutinin (HA) tag, which has been shown to block filamentation phenotypes of Efg1 (8). For this purpose, an AflII restriction site was introduced by site-specific mutagenesis (QuikChange kit; Agilent) using primers MAflIIFor/rev (Table S2) downstream of the HA tag sequence, between positions −7 and −2 bp upstream of the *EFG1* ORF (sequence 5′-ACCCCTTAAGA ATG). The resulting plasmid pPD21HA-AB was cut with PacI and AflII to remove all upstream sequences, which were replaced by a fragment lacking HA sequences generated by PCR using primers 5UTREfgSphIFor/5UTREfgAflIIrev using pTD38-HA as the template. The resulting plasmid pPD21-AB contains 3.2 kb of upstream sequences (comprising 2 kb of promoter and 1.2 kb of 5′ UTR sequences) upstream of the *EFG1* ORF. To delete sequences within the 5′ UTR, novel restriction sites were inserted singly or in combination by site-specific mutagenesis at positions −1167 (SnaBI), −1112 (StuI), −787 (NruI), and −167 (HpaI), using primers listed in Table S2 (Fig. S1). Plasmids were digested pairwise using SnaBI/HpaI, StuI/NruI, NruI/HpaI (native HpaI site at −391), NruI/HpaI (−167), and HpaI (−391)/HpaI (−167) enzymes and religated, to generate plasmids pΔL-UTR, pΔSN-UTR, pΔNH-UTR, pΔNH2-UTR, and pΔHpa-UTR, respectively. Furthermore, the sequence between HpaI (−167) and position −6 was deleted using primer mutagenesis, to construct plasmid pΔsUTR. Plasmids were linearized with PacI (1.9 kb upstream of *EFG1* ORF) and transformed into strain HLC67 (*efg1* mutant lacking the *EFG1* ORF). The correct integration of the plasmid in the *EFG1* locus was confirmed by colony PCR using primers ColoEfg1For/ColoEfg1Rev.

Construction of strains producing click beetle luciferase. To construct a plasmid carrying a green click beetle luciferase gene with a *sat1* nourseothricin selection marker gene, the plasmid pGEM-HIS1-CBG (47) was restricted with BamHI and MscI (New England BioLabs [NEB]) to cut out and replace the *HIS1* gene sequence. The sequence for the *sat1* marker was obtained from the donor plasmid PFA-SAT1 (58) using the two restriction enzymes PvuII and BamHI. The obtained *sat1* sequence was then integrated into the pGEM plasmid directly downstream of the *CBG* gene via ligation to obtain the plasmid pGEM-SAT1-CBG, which was used as the *CBGluc-sat1* reporter cassette template. Reporter cassettes were amplified via PCR with the primer pairs inACT1-CBG-Fw/inACT1-SAT1-Bw and inEFG1-CBG-Fw/inEFG1-SAT1-Bw (Table S2). These primers carry 60-bp homology to the gene of interest, *ACT1* and *EFG1*, respectively. The DNA fragments were transformed into the parental strains PDUWT (*efg1/R-UTR-EFG1*) and PDUHH (*efg1/ΔHpa-UTR-EFG1*). Homologous integration of the luciferase-*sat1*-reporter cassette sequence occurred downstream of the respective start codon of *ACT1* or *EFG1* genes, resulting in 2 reporter strains each for PDUWT (ATC1GN and EFG1GN) and PDUHH (DUTRinACT1GN and DUTRinEFG1GN). Mutants were selected for positive luminescence signals, and correct integration was checked via colony PCR using the primer pairs ACT1 col Fw/CBG col Bw (*ACT1*) and EFG1 col Fw/CBG col Bw (*EFG1*). Mutants positive for both colony PCR and luminescence were used for further experiments.

Blotting procedures. For Northern blotting assays, the strains were grown at 30°C to the logarithmic phase, total RNA was isolated, and 8 μg of RNA was separated on agarose gels containing 1.2% formaldehyde. Following transfer to nylon membranes (Roche), blots were hybridized with ^{32}P-labeled probes for *EFG1* using primers ProFor and ProRev. For signal detection, the washed membranes were exposed to phosphor screen (Fujifilm) for 30 to 60 min and scanned by the FLA 5000 phosphorimager (Fujifilm).

For immunoblotting assays, YPD precultures grown overnight at 30°C in YPD medium were used to inoculate 30 ml of YPD medium. Strains were grown to an optical density at 600 nm (OD_{600}) of 0.1, harvested by centrifugation, frozen at −70°C for 1 h, and then thawed by addition of 500 ml of CAPSO buffer (20 mM *N*-cyclohexyl-2-hydroxyl-3-aminopropanesulfonic acid [CAPSO], pH 9.5, 1 M NaCl, 1 mM EDTA, 20 mM imidazole, 0.1% Triton X-100) containing protease inhibitor (cOmplete cocktail, Mini, EDTA-free; Roche). Cell extracts were prepared as described previously (8). Eighty micrograms of the crude cell extract was separated by SDS-PAGE (10% polyacrylamide) and analyzed by immunoblotting using anti-Efg1 antiserum (1:5,000) (8) or anti-histone H4 (Abcam; 1:5,000) to detect histone H4 as a loading control. Anti-rabbit-IgG-horseradish peroxidase (HRP) conjugate (1:10,000) was used as secondary antibody in all blotting assays. Signals generated by the chemiluminescent substrate (SuperSignal West Dura; Pierce) were detected by a LAS-4000 mini-imager (Fujifilm) and evaluated by Multi Gauge software (Fujifilm).

Polysome profiling. *C. albicans* strains PDUWT and PDUHH were grown exponentially in YPD medium to an OD_{600} of 0.4 to 0.6. For preparation of samples derived from cells following hyphal induction, exponentially growing cells were washed with 1× phosphate-buffered saline (PBS), resuspended in YP medium containing 10% horse serum (prewarmed at 37°C), and incubated at 37°C for 15 min. Preparation of cells for polysome gradients was performed as described previously (36, 59), with some modifications. A portion of the culture (80 ml) was recovered and chilled for 5 min on ice in the presence of 0.1 mg/ml cycloheximide (CHX). Cells were harvested by centrifugation at 6,000 × *g* for 4 min at 4°C and resuspended in lysis buffer (20 mM Tris-HCl, pH 8, 140 mM KCl, 5 mM $MgCl_2$, 0.5 mM dithiothreitol, 1% Triton X-100, 0.1 mg/ml cycloheximide, and 0.5 mg/ml heparin). After washing, cells

were resuspended in 700 μl of lysis buffer, 300 μl glass beads was added, and cells were disrupted by shaking on a Vortex Genie 2 (setting 8) using 6 cycles for 40 s. Between cycles, cells were placed on ice for 5 min. Lysates were cleared by centrifuging twice for 5 min, first at 5,000 rpm and then at 8,000 rpm for the recovered supernatant. Finally, glycerol was added to the supernatant at a final concentration of 5% before storing extracts at −70°C. Samples of 10 to 20 A_{260} units were loaded onto 10 to 50% sucrose gradients and were separated by ultracentrifugation for 2 h 40 min at 35,000 rpm in a Beckman SW41 rotor at 4°C. Then, gradients were fractionated using isotonic pumping of 60% sucrose from the bottom, followed by recording of the polysomal profiles by online UV detection at 254 nm (density gradient fractionation system; Teledyne ISCO, Lincoln, NE). To analyze the RNA of the polysomal fractions, RNA from 200 μl of each fraction was extracted using the GeneJET RNA extraction kit (Strek; Biotools). To each sample, 500 ng of *in vitro*-transcribed RNA (HiScribe T7 high-yield RNA synthesis kit; NEB) was added and used as spiked-in mRNA for normalization of the transcripts. After reverse transcription of the purified RNA (Maxima first-strand cDNA synthesis kit; Thermo Scientific), quantitative PCR (qRT-PCR) was performed using gene-specific primer pairs to quantify mRNAs of *EFG1* and *ACT1*. For each fraction, two biological replicates with three technical replicates were assayed on an Mx3000P Light Cycler (Stratagene), with 10 μl of cDNA, 4 μl EvaGreen qPCR mix II (Bio-Budget), and 3 μl each of forward and reverse oligonucleotide primers (400 pmol/μl) in each reaction mixture. The polymerase was activated at 95°C for 10 min, annealing was performed at 60°C for 15 s, extension was performed at 72°C for 30 s, and the denaturation step was performed at 95°C for 30 s, using a total of 50 cycles.

qRT-PCR. cDNA for qRT-PCR analysis was prepared from 2 μg of total RNA treated with DNase I (Thermo Fisher) using the Maxima first-strand cDNA synthesis kit (Thermo Fisher). Real-time PCR was performed in triplicate in 96-well plates using the EvaGreen dye (Bio-Budget). Primers used for qRT-PCR analysis are described in Table S2. Real-time PCR was performed using the following cycling conditions: step 1, 95°C for 15 min; step 2, 95°C for 15 s; step 3, annealing temperature of 60°C for 20 s; step 4, elongation, 72°C for 20 s; step 5, repeat of steps 2 to 4 39 times; step 7, melting curve of 50°C to 95°C every 0.4°C, hold for 1 s, and reading of plate. Expression levels of each gene were normalized to levels of an internal *ACT1* control using the Pfaffl method (60).

Luciferase assay. To measure click beetle luciferase activity in yeast cells, overnight cultures of PDUWT, PDUHH, ACT1GN, EFG1N, UTRinACT1GN, and UTRinEFG1GN were diluted to an OD_{600} of 1.0 in PBS buffer (140 mM NaCl, 3 mM KCl, 8 mM Na_2HPO_4, 1.8 mM KH_2PO_4, pH 7.4) and incubated at 30°C for 60 min at 180 rpm. One milliliter was transferred into fresh YPD medium and grown for 6 h at 30°C. All samples were set to an OD_{600} of 0.3 in 1 ml YPD and quickly frozen in liquid nitrogen. After thawing, 100 μl of the samples was transferred into a 96-well microtiter plate, and 100 μl Beetleglow (47) was added to start the reaction. Measurements were made in an Infinite M200 Pro plate reader (Tecan) with the following settings. Plates were shaken for 10 s at 140 rpm, and relative luminescence units (RLU) were measured for 1 s per well at 30°C. Each plate was measured 3 times, and the maximal luminescence values (L_{max}) were reported.

Data availability. All data are included in the article and supplemental files.

SUPPLEMENTAL MATERIAL

Supplemental material for this article may be found at https://doi.org/10.1128/mSphere.00280-18.

FIG S1, TIF file, 0.3 MB.

TABLE S1, DOCX file, 0.02 MB.

TABLE S2, DOCX file, 0.02 MB.

ACKNOWLEDGMENTS

This work was supported by the Infect-ERA JTC2 project FunComPath (http://www.funcompath.eu/) to J.F.E. P.A. was funded from Mineco and FEDER funds (BFU2016-77728-C3-3-P).

The authors declare no conflicts of interest.

REFERENCES

1. Stoldt VR, Sonneborn A, Leuker CE, Ernst JF. 1997. Efg1p, an essential regulator of morphogenesis of the human pathogen *Candida albicans*, is a member of a conserved class of bHLH proteins regulating morphogenetic processes in fungi. EMBO J 16:1982–1991. https://doi.org/10.1093/emboj/16.8.1982.
2. Lo HJ, Köhler JR, DiDomenico B, Loebenberg D, Cacciapuoti A, Fink GR. 1997. Nonfilamentous *C. albicans* mutants are avirulent. Cell 90:939–949. https://doi.org/10.1016/S0092-8674(00)80358-X.
3. Doedt T, Krishnamurthy S, Bockmühl DP, Tebarth B, Stempel C, Russell CL, Brown AJ, Ernst JF. 2004. APSES proteins regulate morphogenesis and metabolism in *Candida albicans*. Mol Biol Cell 15:3167–3180. https://doi.org/10.1091/10.1091/mbc.E03-11-0782.
4. Setiadi ER, Doedt T, Cottier F, Noffz C, Ernst JF. 2006. Transcriptional response of *Candida albicans* to hypoxia: linkage of oxygen sensing and Efg1p-regulatory networks. J Mol Biol 361:399–411. https://doi.org/10.1016/j.jmb.2006.06.040.
5. Lu Y, Su C, Mao X, Raniga PP, Liu H, Chen J. 2008. Efg1-mediated recruitment of NuA4 to promoters is required for hypha-specific Swi/Snf binding and activation in *Candida albicans*. Mol Biol Cell 19:4260–4272. https://doi.org/10.1091/mbc.E08-02-0173.
6. Tebarth B, Doedt T, Krishnamurthy S, Weide M, Monterola F, Dominguez A, Ernst JF. 2003. Adaptation of the Efg1p morphogenetic pathway in *Candida albicans* by negative autoregulation and PKA-dependent repression of the *EFG1* gene. J Mol Biol 329:949–962. https://doi.org/10.1016/S0022-2836(03)00505-9.
7. Lassak T, Schneider E, Bussmann M, Kurtz D, Manak JR, Srikantha T, Soll

DR, Ernst JF. 2011. Target specificity of the *Candida albicans* Efg1 regulator. Mol Microbiol 82:602–618. https://doi.org/10.1111/j.1365-2958.2011.07837.x.
8. Desai PR, van Wijlick L, Kurtz D, Juchimiuk M, Ernst JF. 2015. Hypoxia and temperature regulated morphogenesis in *Candida albicans*. PLoS Genet 11:e1005447. https://doi.org/10.1371/journal.pgen.1005447.
9. Lohse MB, Johnson AD. 2009. White-opaque switching in *Candida albicans*. Curr Opin Microbiol 12:650–654. https://doi.org/10.1016/j.mib.2009.09.010.
10. Bockmühl DP, Krishnamurthy S, Gerads M, Sonneborn A, Ernst JF. 2001. Distinct and redundant roles of the two protein kinase A isoforms Tpk1p and Tpk2p in morphogenesis and growth of *Candida albicans*. Mol Microbiol 42:1243–1257. https://doi.org/10.1046/j.1365-2958.2001.02688.x.
11. Bockmühl DP, Ernst JF. 2001. A potential phosphorylation site for an A-type kinase in the Efg1 regulator protein contributes to hyphal morphogenesis of *Candida albicans*. Genetics 157:1523–1530.
12. Ramage G, VandeWalle K, López-Ribot JL, Wickes BL. 2002. The filamentation pathway controlled by the Efg1 regulator protein is required for normal biofilm formation and development in *Candida albicans*. FEMS Microbiol Lett 214:95–100. https://doi.org/10.1111/j.1574-6968.2002.tb11330.x.
13. Stichternoth C, Ernst JF. 2009. Hypoxic adaptation by Efg1 regulates biofilm formation by *Candida albicans*. Appl Environ Microbiol 75:3663–3672. https://doi.org/10.1128/AEM.00098-09.
14. Yano J, Yu A, Fidel PL, Jr, Noverr MC. 2016. Transcription factors Efg1 and Bcr1 regulate biofilm formation and virulence during *Candida albicans*-associated denture stomatitis. PLoS One 11:e0159692. https://doi.org/10.1371/journal.pone.0159692.
15. Kadosh D. 2016. Control of *Candida albicans* morphology and pathogenicity by post-transcriptional mechanisms. Cell Mol Life Sci 73:4265–4278. https://doi.org/10.1007/s00018-016-2294-y.
16. Verma-Gaur J, Traven A. 2016. Post-transcriptional gene regulation in the biology and virulence of *Candida albicans*. Cell Microbiol 18:800–806. https://doi.org/10.1111/cmi.12593.
17. Dagley MJ, Gentle IE, Beilharz TH, Pettolino FA, Djordjevic JT, Lo TL, Uwamahoro N, Rupasinghe T, Tull DL, McConville M, Beaurepaire C, Nantel A, Lithgow T, Mitchell AP, Traven A. 2011. Cell wall integrity is linked to mitochondria and phospholipid homeostasis in *Candida albicans* through the activity of the post-transcriptional regulator Ccr4-Pop2. Mol Microbiol 79:968–989. https://doi.org/10.1111/j.1365-2958.2010.07503.x.
18. Shively CA, Kweon HK, Norman KL, Mellacheruvu D, Xu T, Sheidy DT, Dobry CJ, Sabath I, Cosky EE, Tran EJ, Nesvizhskii A, Andrews PC, Kumar A. 2015. Large-scale analysis of kinase signaling in yeast pseudohyphal development identifies regulation of ribonucleoprotein granules. PLoS Genet 11:e1005564. https://doi.org/10.1371/journal.pgen.1005564.
19. An HS, Lee KH, Kim J. 2004. Identification of an exoribonuclease homolog, CaKEM1/CaXRN1, in Candida albicans and its characterization in filamentous growth. FEMS Microbiol Lett 235:297–303. https://doi.org/10.1016/j.femsle.2004.04.048.
20. Lee KH, Kim SY, Jung JH, Kim J. 2010. Proteomic analysis of hyphae-specific proteins that are expressed differentially in *cakem1*/*cakem1* mutant strains of *Candida albicans*. J Microbiol 48:365–371. https://doi.org/10.1007/s12275-010-9155-4.
21. Verma-Gaur J, Qu Y, Harrison PF, Lo TL, Quenault T, Dagley MJ, Bellousoff M, Powell DR, Beilharz TH, Traven A. 2015. Integration of posttranscriptional gene networks into metabolic adaptation and biofilm maturation in *Candida albicans*. PLoS Genet 11:e1005590. https://doi.org/10.1371/journal.pgen.1005590.
22. Wells ML, Washington OL, Hicks SN, Nobile CJ, Hartooni N, Wilson GM, Zucconi BE, Huang W, Li L, Fargo DC, Blackshear PJ. 2015. Post-transcriptional regulation of transcript abundance by a conserved member of the tristetraprolin family in *Candida albicans*. Mol Microbiol 95:1036–1053. https://doi.org/10.1111/mmi.12913.
23. Cleary IA, Lazzell AL, Monteagudo C, Thomas DP, Saville SP. 2012. BRG1 and NRG1 form a novel feedback circuit regulating *Candida albicans* hypha formation and virulence. Mol Microbiol 85:557–573. https://doi.org/10.1111/j.1365-2958.2012.08127.x.
24. Elson SL, Noble SM, Solis NV, Filler SG, Johnson AD. 2009. An RNA transport system in *Candida albicans* regulates hyphal morphology and invasive growth. PLoS Genet 5:e1000664. https://doi.org/10.1371/journal.pgen.1000664.
25. Caballero-Lima D, Hautbergue GM, Wilson SA, Sudbery PE. 2014. In *Candida albicans* hyphae, Sec2p is physically associated with SEC2 mRNA on secretory vesicles. Mol Microbiol 94:828–842. https://doi.org/10.1111/mmi.12799.
26. Zid BM, O'Shea EK. 2014. Promoter sequences direct cytoplasmic localization and translation of mRNAs during starvation in yeast. Nature 514:117–121. https://doi.org/10.1038/nature13578.
27. Trcek T, Larson DR, Moldón A, Query CC, Singer RH. 2011. Single-molecule mRNA decay measurements reveal promoter-regulated mRNA stability in yeast. Cell 147:1484–1497. https://doi.org/10.1016/j.cell.2011.11.051.
28. Bellofatto V, Wilusz J. 2011. Transcription and mRNA stability: parental guidance suggested. Cell 147:1438–1439. https://doi.org/10.1016/j.cell.2011.12.002.
29. Kozak M. 2005. Regulation of translation via mRNA structure in prokaryotes and eukaryotes. Gene 361:13–37. https://doi.org/10.1016/j.gene.2005.06.037.
30. Dvir S, Velten L, Sharon E, Zeevi D, Carey LB, Weinberger A, Segal E. 2013. Deciphering the rules by which 5′-UTR sequences affect protein expression in yeast. Proc Natl Acad Sci U S A 110:E2792–E2801. https://doi.org/10.1073/pnas.1222534110.
31. Morris DR, Geballe AP. 2000. Upstream open reading frames as regulators of mRNA translation. Mol Cell Biol 20:8635–8642. https://doi.org/10.1128/MCB.20.23.8635-8642.2000.
32. Barbosa C, Peixeiro I, Romão L. 2013. Gene expression regulation by upstream open reading frames and human disease. PLoS Genet 9:e1003529. https://doi.org/10.1371/journal.pgen.1003529.
33. Sundaram A, Grant CM. 2014. A single inhibitory upstream open reading frame (uORF) is sufficient to regulate *Candida albicans GCN4* translation in response to amino acid starvation conditions. RNA 20:559–567. https://doi.org/10.1261/rna.042267.113.
34. Gilbert WV, Zhou K, Butler TK, Doudna JA. 2007. Cap-independent translation is required for starvation-induced differentiation in yeast. Science 317:1224–1227. https://doi.org/10.1126/science.1144467.
35. Pickering BM, Willis AE. 2005. The implications of structured 5′ untranslated regions on translation and disease. Semin Cell Dev Biol 16:39–47. https://doi.org/10.1016/j.semcdb.2004.11.006.
36. van Wijlick L, Geissen R, Hilbig JS, Lagadec Q, Cantero PD, Pfeifer E, Juchimiuk M, Kluge S, Wickert S, Alepuz P, Ernst JF. 2016. Dom34 links translation to protein O-mannosylation. PLoS Genet 12:e1006395. https://doi.org/10.1371/journal.pgen.1006395.
37. Wanless AG, Lin Y, Weiss EL. 2014. Cell morphogenesis proteins are translationally controlled through UTRs by the Ndr/LATS target Ssd1. PLoS One 9:e85212. https://doi.org/10.1371/journal.pone.0085212.
38. Lee HJ, Kim JM, Kang WK, Yang H, Kim JY. 2015. The NDR kinase Cbk1 downregulates the transcriptional repressor Nrg1 through the mRNA-binding protein Ssd1 in *Candida albicans*. Eukaryot Cell 14:671–683. https://doi.org/10.1128/EC.00016-15.
39. Bruno VM, Wang Z, Marjani SL, Euskirchen GM, Martin J, Sherlock G, Snyder M. 2010. Comprehensive annotation of the transcriptome of the human fungal pathogen *Candida albicans* using RNA-seq. Genome Res 20:1451–1458. https://doi.org/10.1101/gr.109553.110.
40. Childers DS, Mundodi V, Banerjee M, Kadosh D. 2014. A 5′ UTR-mediated translational efficiency mechanism inhibits the *Candida albicans* morphological transition. Mol Microbiol 92:570–585. https://doi.org/10.1111/mmi.12576.
41. Guan Z, Liu H. 2015. The *WOR1* 5′ untranslated region regulates white-opaque switching in *Candida albicans* by reducing translational efficiency. Mol Microbiol 97:125–138. https://doi.org/10.1111/mmi.13014.
42. Childers DS, Kadosh D. 2015. Filament condition-specific response elements control the expression of *NRG1* and *UME6*, key transcriptional regulators of morphology and virulence in *Candida albicans*. PLoS One 10:e0122775. https://doi.org/10.1371/journal.pone.0122775.
43. Sonneborn A, Tebarth B, Ernst JF. 1999. Control of white-opaque phenotypic switching in *Candida albicans* by the Efg1p morphogenetic regulator. Infect Immun 67:4655–4660.
44. Pierce JV, Kumamoto CA. 2012. Variation in *Candida albicans EFG1* expression enables host-dependent changes in colonizing fungal populations. mBio 3:e00117-12. https://doi.org/10.1128/mBio.00117-12.
45. Srikantha T, Tsai LK, Daniels K, Soll DR. 2000. *EFG1* null mutants of *Candida albicans* switch but cannot express the complete phenotype of white-phase budding cells. J Bacteriol 182:1580–1591. https://doi.org/10.1128/JB.182.6.1580-1591.2000.
46. Noffz CS, Liedschulte V, Lengeler K, Ernst JF. 2008. Functional mapping of the *Candida albicans* Efg1 regulator. Eukaryot Cell 7:881–893. https://doi.org/10.1128/EC.00033-08.

47. Kapitan M, Eichhof I, Lagadec Q, Ernst JF. 2016. Click beetle luciferases as dual reporters of gene expression in *Candida albicans*. Microbiology 162:1310–1320. https://doi.org/10.1099/mic.0.000329.
48. Schaekel A, Desai PR, Ernst JF. 2013. Morphogenesis-regulated localization of protein kinase A to genomic sites in *Candida albicans*. BMC Genomics 14:842. https://doi.org/10.1186/1471-2164-14-842.
49. Zordan RE, Miller MG, Galgoczy DJ, Tuch BB, Johnson AD. 2007. Interlocking transcriptional feedback loops control white-opaque switching in *Candida albicans*. PLoS Biol 5:e256. https://doi.org/10.1371/journal.pbio.0050256.
50. Leppek K, Das R, Barna M. 2018. Functional 5′ UTR mRNA structures in eukaryotic translation regulation and how to find them. Nat Rev Mol Cell Biol 19:158–174. https://doi.org/10.1038/nrm.2017.103.
51. Berchowitz LE, Gajadhar AS, van Werven FJ, De Rosa AA, Samoylova ML, Brar GA, Xu Y, Xiao C, Futcher B, Weissman JS, White FM, Amon A. 2013. A developmentally regulated translational control pathway establishes the meiotic chromosome segregation pattern. Genes Dev 27:2147–2163. https://doi.org/10.1101/gad.224253.113.
52. Muralidharan B, Bakthavachalu B, Pathak A, Seshadri V. 2007. A minimal element in 5′UTR of insulin mRNA mediates its translational regulation by glucose. FEBS Lett 581:4103–4108. https://doi.org/10.1016/j.febslet.2007.07.050.
53. Zhou W, Edelman GM, Mauro VP. 2001. Transcript leader regions of two Saccharomyces cerevisiae mRNAs contain internal ribosome entry sites that function in living cells. Proc Natl Acad Sci U S A 98:1531–1536. https://doi.org/10.1073/pnas.98.4.1531.
54. Reineke LC, Cao Y, Baus D, Hossain NM, Merrick WC. 2011. Insights into the role of yeast eIF2A in IRES-mediated translation. PLoS One 6:e24492. https://doi.org/10.1371/journal.pone.0024492.
55. Ingolia NT, Ghaemmaghami S, Newman JR, Weissman JS. 2009. Genome-wide analysis in vivo of translation with nucleotide resolution using ribosome profiling. Science 324:218–223. https://doi.org/10.1126/science.1168978.
56. Abramczyk D, Tchórzewski M, Grankowski N. 2003. Non-AUG translation initiation of mRNA encoding acidic ribosomal P2A protein in *Candida albicans*. Yeast 20:1045–1052. https://doi.org/10.1002/yea.1020.
57. Hann SR, Dixit M, Sears RC, Sealy L. 1994. The alternatively initiated c-Myc proteins differentially regulate transcription through a noncanonical DNA-binding site. Genes Dev 8:2441–2452. https://doi.org/10.1101/gad.8.20.2441.
58. Schaub Y, Dünkler A, Walther A, Wendland J. 2006. New pFA-cassettes for PCR-based gene manipulation in *Candida albicans*. J Basic Microbiol 46:416–429. https://doi.org/10.1002/jobm.200510133.
59. Garre E, Romero-Santacreu L, De Clercq N, Blasco-Angulo N, Sunnerhagen P, Alepuz P. 2012. Yeast mRNA cap-binding protein Cbc1/Sto1 is necessary for the rapid reprogramming of translation after hyperosmotic shock. Mol Biol Cell 23:137–150. https://doi.org/10.1091/mbc.E11-05-0419.
60. Pfaffl MW. 2001. A new mathematical model for relative quantification in real-time RT-PCR. Nucleic Acids Res 29:e45. https://doi.org/10.1093/nar/29.9.e45.
61. Pendrak ML, Roberts DD. 2011. Ribosomal RNA processing in *Candida albicans*. RNA 17:2235–2248. https://doi.org/10.1261/rna.028050.111.
62. Chatterjee S, Pal JK. 2009. Role of 5′- and 3′-untranslated regions of mRNAs in human diseases. Biol Cell 101:251–262. https://doi.org/10.1042/BC20080104.

2.4 Manuscript III: Morphogenesis regulated localization of protein kinase A to genomic sites in *C. albicans*

Contribution to Manuscript: 40 **%**

Prashant R. Desai was majorly involved in designing and concluding all the in-silico analysis. He was also involved in preparing the final figures and in writing the main part of the manuscript.

Individual contributor: for figures 2, 3 and 6. Tables S1 to S6.

Published in : BMC Genomics

Impact Factor : 4.4 (2012)

Schaekel *et al. BMC Genomics* 2013, **14**:842
http://www.biomedcentral.com/1471-2164/14/842

BMC Genomics

RESEARCH ARTICLE Open Access

Morphogenesis-regulated localization of protein kinase A to genomic sites in *Candida albicans*

Alida Schaekel[1,2], Prashant R Desai[1] and Joachim F Ernst[1,2*]

Abstract

Background: The human fungal pathogen *Candida albicans* is able to undergo morphogenesis from a yeast to a hyphal growth form. Protein kinase A (PKA) isoforms Tpk1 and Tpk2 promote hyphal growth in a signalling pathway via the transcription factor Efg1.

Results: *C. albicans* strains producing epitope-tagged Tpk1 or Tpk2 were used in genome-wide chromatin immunoprecipitation on chip (ChIP chip) to reveal genomic binding sites. During yeast growth, both PKA isoforms were situated primarily within ORFs but moved to promoter regions shortly after hyphal induction. Binding sequences for Tpk2 greatly exceeded Tpk1 sites and did not coincide with binding of the PKA regulatory subunit Bcy1. Consensus binding sequences for Tpk2 within ORFs included ACCAC and CAGCA motifs that appeared to bias codon usage within the binding regions. Promoter residency of Tpk2 correlated with the transcript level of the corresponding gene during hyphal morphogenesis and occurred near Efg1 binding sites, mainly on genes encoding regulators of morphogenesis.

Conclusions: PKA isoforms change their genomic binding sites from ORF to promoter regions during yeast-hyphal morphogenesis. Tpk2 binds preferentially to promoters of genes encoding regulators of cellular morphogenesis.

Keywords: *Candida albicans*, Protein kinase A, Tpk1, Tpk2, Efg1, Morphogenesis

Background

The fungus *Candida albicans* is an important cause of human disease, causing tenacious superficial and life-threatening systemic infections. Its virulence depends to a large extent on its ability to switch between a yeast and a hyphal growth form [1]. Environmental conditions favouring hyphal development include molecules of the human host acting as inducers, as well as physical parameters such as body temperature. Protein kinase A (PKA) isoforms Tpk1 and Tpk2 have crucial roles as signalling kinases because they mediate several adaptation responses to host contact [2-4]. In inducing conditions, cAMP is generated by adenylate cyclase (Cyr1) and triggers PKA activity by binding and removal of the inhibitory subunit Bcy1, which associates with Tpk1 and Tpk2 [5-7]. The cAMP-PKA pathway subsequently activates the Efg1 transcription factor, which represents the central hub controlling downstream events including morphogenesis and metabolic adaptation [1,8-10]. Efg1 fulfills its morphogenetic functions by association with co-regulators Czf1, Flo8, Slf1 and Slf2 [11,12]. Interestingly, in spite of their association with the same regulator protein Bcy1, both PKA isoforms exert specific environment-dependent functions with regard to hyphal morphogenesis [3] and Tpk2 but not the Tpk1 isoform mediates downregulation of *EFG1* expression early in hyphal induction [13].

PKA localization differs among species: in budding yeast the PKA holoenzyme is localized in the nucleus [14], whereas in fission yeast it resides in the cytoplasm [15] and in mammalian cells PKA catalytic subunits bind to anchoring proteins in different intracellular localizations [16,17]. In spite of these differences, it appears that in all species important AGC kinase activities are needed in the nucleus. Increased cAMP levels lead to partial entry of PKA catalytic subunits into nuclei of fission yeast [15] and mammalian cells [16,17]. In *C. albicans*, phosphorylation of the Tpk2 target protein Efg1 is likely to occur in the

* Correspondence: joachim.ernst@uni-duesseldorf.de
[1]Department Biologie, Molekulare Mykologie, Heinrich-Heine-Universität, Düsseldorf, Germany
[2]Manchot Graduate School Molecules of Infection, Heinrich-Heine-Universität, Düsseldorf, Germany

Schaekel *et al. BMC Genomics* 2013, **14**:842
http://www.biomedcentral.com/1471-2164/14/842

nucleus since Efg1 has been detected exclusively in the nucleus [18]. In *Saccharomyces cerevisiae*, activated PKA and the mitogen-activated protein kinase (MAPK) Hog1 were found to associate with promoters and coding regions of genes regulated by these kinases [19-21]. Action of the Hog1 MAPK on the Sko1 trancriptional repressor required the activity of kinase Sch9, which is structurally related to PKA, on the promoters of target genes [22]. The latter findings suggested that also in *C. albicans*, Tpk isoforms and possibly other kinases reside on genes that represent downstream targets of PKA signalling during hyphal morphogenesis. In this study, we strengthen this concept by demonstrating that PKA isoforms reside on specific genomic locations that change dramatically during morphogenesis from ORF to promoter regions. During the yeast-hyphal transition, genomic Tpk2 binding sites identify genes with known functions in dimorphism and suggest the identity of new genes involved in this cellular differentiation process.

Results and discussion

C. albicans strains producing HA-tagged PKA kinases

The single remaining allele encoding the catalytic subunits of PKA kinase was modified in heterozygous *C. albicans* mutants to add sequences specifying a C-terminal triple hemagglutinin (HA) epitope tag. Immunoblotting revealed the presence of HA-fusions to Tpk1 and Tpk2 proteins in cellular extracts of these strains during yeast growth (Figure 1A). Immunofluorescence microscopy revealed that the majority of fusion proteins resided in the cytoplasm of cells, while a minor fraction of $Tpk2^{HA}$ was also detectable at the inside rim of the nucleus (Figure 1B, yellow dots). Similar Tpk cellular localization was observed in cells that were briefly (30 min) induced by 10% serum to form hyphae (data not shown).

To verify that HA fusion proteins were functional in the constructed strains we tested their filamentous growth, which is known to be regulated by the activity of Tpk1 and Tpk2 proteins [2,3]. Inactivation of a single *TPK1* allele abolishes hyphal growth [3] but the $TPK1^{HA}$/*TPK1* transformant formed hyphae as the wild-type strain (Figure 1C) indicating that the $Tpk1^{HA}$ fusion protein is functional. Both *TPK2* alleles need to be inactivated to prevent hyphal growth [2]; therefore, it was verified that the filamentation phenotype of the $TPK2^{HA}$/*tpk2* strain mimicked the *TPK2*/*tpk2* strain but not the *tpk2*/*tpk2* homozygous mutant (Figure 1C). This result shows that the $Tpk2^{HA}$ fusion protein is functional. In summary, use of HA-tagged Tpk proteins revealed that in *C. albicans* as in fission yeast [15] the majority of PKA is located in the cytoplasm. The exclusive localization of a possibly non-functional Tpk1-GFP fusion within the nucleus [5] was not confirmed by the HA-tagged Tpk1 protein.

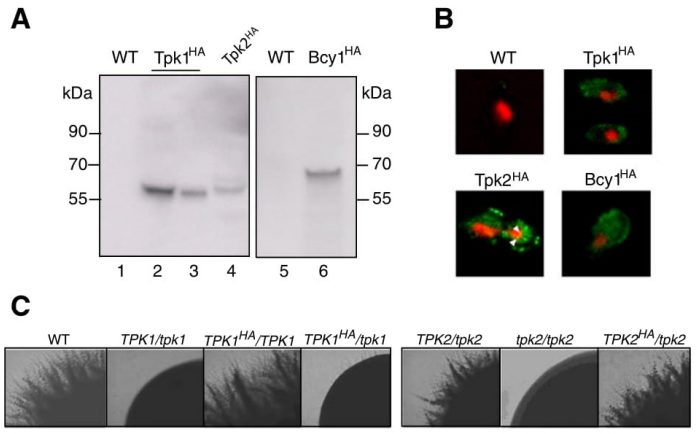

Figure 1 Epitope-tagged PKA in *C. albicans*. A. Immunoblotting to detect HA-tagged PKA subunits. Strains were grown in liquid YPD medium to OD_{600} = 0.6-0.8 and proteins in cell extracts (50 μg) were separated by SDS-PAGE (10% acrylamide), blotted onto PVDF membranes and probed using anti-HA antibody. Strains tested were CAF2-1 (WT: lanes 1, 5), AF1003 ($TPK1^{HA}$: lane 2), AF1004 ($TPK1^{HA}$: lane 3), AF1005 ($TPK2^{HA}$: lane 4) and AF1007 ($BCY1^{HA}$: lane 6). **B**. Fluorescence microscopy of transformant cells treated with rat anti-HA antibody, which was detected with FITC-labelled anti-rat antibody (green signal) and DAPI to detect nuclei (red signal); yellow overlay signals are indicated by white triangles. **C**. Filament formation of strains producing HA-tagged Tpk proteins. Strains CAF2-1 (wt), II (*TPK1/tpk1*), TPK7 (*TPK2/tpk2*), TPO7.4 (*tpk2/tpk2*), AF1003 ($TPK1^{HA}$/*TPK1*), AF1004 ($TPK1^{HA}$/*tpk1*) and AF1005 ($TPK2^{HA}$/*tpk2*) were grown for 3 d/37°C on Spider agar and single colonies were photographed.

Schaekel et al. BMC Genomics 2013, 14:842
http://www.biomedcentral.com/1471-2164/14/842

Genomic localization of Tpk proteins

The above results suggested that a minor fraction of cellular PKA catalytic subunits resides in the nucleus of *C. albicans* cells. Furthermore, the presence of PKA isoforms and other kinases at target genes had been demonstrated previously in *S. cerevisiae* [19-21]. To verify, if nuclear PKA isoforms bind specific genomic targets in *C. albicans* we performed ChIP chip experiments with strains containing HA-tagged PKA isoforms; strains producing authentic non-tagged Tpk proteins were used as reference strains. Tpk1 and Tpk2 localization was examined during yeast growth or alternatively, following a brief period (30 min) of hyphal induction by 10% serum. During this time period, early regulatory processes take place that reprogram cells to allow hyphal growth. This became evident in wild-type cells by the formation of germ tubes after 30–60 min of induction.

A significant number of Tpk genomic binding sites was identified in both yeast and hyphal cells in duplicate ChIP chip experiments (see Additional file 1: Tables S1-S4). About tenfold more Tpk2 than Tpk1 binding sites were detected during yeast growth but Tpk1 binding increased during hyphal induction. A particular importance of the Tpk2 isoform for *C. albicans* morphogenesis under liquid growth conditions was reported previously [3]. The most significant peaks, which were overlapping in both replicates, were defined as binding sites. These sites were associated with ORF and promoter sequences of target genes (promoter binding sites within two divergently transcribed genes were assigned to both genes). Analyses indicated that very rarely, both Tpk1 and Tpk2 bind to same gene (Figure 2A). An exception is *HGC1* encoding an important regulator of hypha formation [23], which bound both Tpk1 and Tpk2 during hyphal induction. This result indicates that both catalytic PKA isoforms have mostly different genomic targets.

Importantly, during yeast growth both Tpk1 and Tpk2 were bound mostly within ORFs of target genes, while hyphal induction reduced ORF binding and favoured promoter binding or joint promoter-ORF binding (Figure 2B). Under yeast and hyphal growth conditions, all Tpk1 target genes and the majority of Tpk2 target genes were different (Figure 2C). Thus, ORF-to-promoter switching rarely occurs on the same gene during yeast-hyphal morphogenesis.

Growth of *C. albicans* in rich medium does not trigger hyphal formation, because PKA activity is repressed by the regulatory PKA subunit Bcy1 [5]. To test if during yeast growth both Tpk isoforms and Bcy1 bind to ORFs a ChIP chip experiment was performed on a $BCY1^{HA}$/*BCY1* strain (AF1007). Immunoblotting showed the production of HA-tagged Bcy1 in transformants (Figure 1A) and immunofluorescence demonstrated that this protein resides mainly in the cytoplasm (Figure 1B). The $Bcy1^{HA}$ fusion produced by transformants is functional because the $BCY1^{HA}$/*BCY1* strain was insensitive to heat shock (2 h at 50°C) (data not shown), unlike a *BCY1*/*bcy1* strain [4]. Data analyses revealed a moderate number of genomic Bcy1 binding sites during yeast growth (see Additional file 1: Table S5). However, binding sites did not coincide to a great extent with Tpk1 or Tpk2 binding sites, either during yeast growth or during hyphal induction (Figure 2C). These results indicate that in general, Tpk1 or Tpk2 isoforms do not bind to target ORFs in the form of Tpk-Bcy1 holoenzyme complexes. Conceptually, ORF-bound Tpk proteins could either be active because of the absence of Bcy1 or their activities may be regulated by yet unknown mechanisms.

Gene ontology analysis of PKA binding sites

Gene ontology (GO) analyses [24] of genes close to or harbouring PKA binding sites revealed significant GO terms for Tpk2 kinase but not for the Tpk1 isoform in any growth condition. During yeast growth, Tpk2 bound preferentially to ORFs (or both ORF and promoters) of genes encoding components of the general transcription machinery (e. g. Asf1, Def1, Swi1, Spt6), in addition to ORFs encoding transcription factors involved in carbon source utilization (e. g. Rca1, Snf5, Tup1) or filamentous growth (e. g. Efg1, Tup1, Sfl1) (Figure 3A). Furthermore, ORFs of genes for components of signalling pathways leading to hyphal formation (e. g. Cek1, Msb2) were bound by Tpk2 during yeast growth (Figure 3A). During hyphal induction, Tpk2 bound mostly to promoter regions of genes involved in filamentous growth (40 genes including *HGC1*, *RAS1*) (Figure 3B). Tpk2 target sites included promoters of genes encoding 20 transcription factors directly binding DNA (mostly containing zinc finger motifs). In summary, Tpk2 genomic binding shows a distinctive pattern of binding to morphogenesis-related genes, specifically the binding to ORFs during yeast growth and to promoters during hyphal induction. Tpk2 target genes are often bound also by Efg1 [13,25,26] in promoter regions or by the Set3C histone deacetylase complex [27] within their ORFs (superscripts d, e, in Figure 3). Recently, direct binding of heat shock factor-type transcriptional regulators Sfl1 and Sfl2 to Efg1 has been demonstrated [12], a finding also associating the genomic localization of these regulators with Tpk2 binding sites. In summary, Tpk2 binding identifies genes with known functions in filamentous growth and predicts such functions for yet uncharacterized *C. albicans* genes (designated *ORF19.* in Figure 3).

ORF binding during yeast growth

ORF binding by PKA isoforms occurred mainly during yeast growth and included two relevant *C. albicans* genes, *EFG1* and *MSB2*. *EFG1* is required for the initial phase of yeast-hyphal transition but it is downregulated rapidly

Schaekel et al. BMC Genomics 2013, 14:842
http://www.biomedcentral.com/1471-2164/14/842

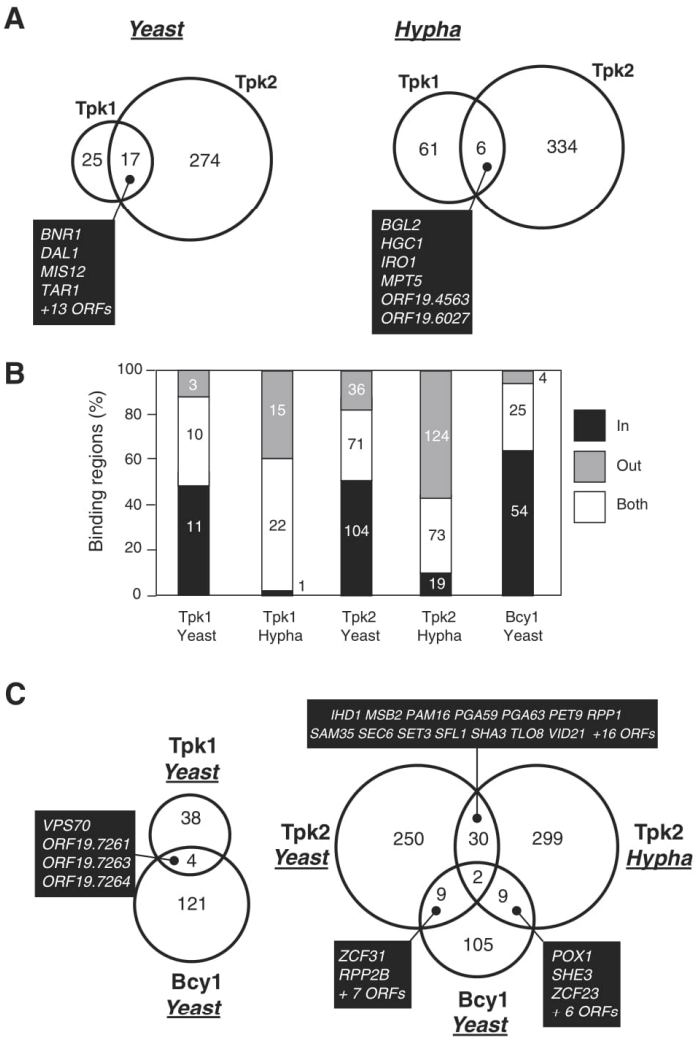

Figure 2 Genomic localization of PKA subunits. A. Genomic binding of PKA subunits. Venn diagrams number genes containing Tpk1 or Tpk2 binding sites in their promoter or ORF sequences; cells were grown in the yeast form or induced 30 min for hypha formation using 10% horse serum. Names of genes in the Tpk1/Tpk2 intersection are listed. **B**. Genomic PKA subunit localization. For each subunit, numbers of binding sites inside an ORF (black box), outside an ORF (promoter) (grey box) or at both sites (white box) are listed. **C**. Genomic binding of Tpk1, Tpk2 and Bcy1 subunits. The Venn diagram numbers indicate genes associated with the Tpk1 or Tpk2 catalytic subunit under yeast growth or hyphal induction, as well as the localization of the Bcy1 regulatory subunit during yeast growth. Gene names in the intersections are indicated.

by negative autoregulation to allow undisturbed morphogenesis [29]; downregulation requires the Tpk2 but not the Tpk1 PKA isoform [13]. *MSB2* encodes a membrane sensor for environmental cues leading to hypha formation via the Cek1 MAPK and its shed domain provides resistance to antimicrobial peptides [30,31].

During yeast growth, Tpk2 but not Tpk1 was bound to the *EFG1* ORF. Binding was also observed to the

GO term[1] (genome frequency)	Tpk2 binding genes annotated to the term[2] Name	Frequency[3]	*P* value[4]
A. Yeast growth			
Positive regulation of biological process (7.8%)	*ANB1 ASF1 CAT8* CEK1*[ce*] *CST20* CTA26*[de] *CTA3 DEF1*[acde*] *EFG1*[acde*] *ORF19.676 MSB2*[ce*] *NOT3* PDC2 RCA1* RIM8* SBA1*[de] *SFL1*[b*] *SHA3*[acde*] *SNF5* SPT5* SPT6* SWI1*[+] *YVH1* ZCF10 ZCF31 ORF19.2664 ORF19.3080 ORF19.3328 ORF19.4906 ORF19.5459*	15.3%	0.0322
Positive regulation of macromolecule metabolic process (3.49%)	*ANB1 ASF1 CAT8* CST20* CTA26*[de] *CTA3 EFG1*[acde*] *NOT3* PDC2 RCA1* SBA1*[de] *SFL1*[cb*] *SHA3*[acde] *SNF5* SPT5* SPT6* SWI1* ORF19.2664 ORF19.3328 ORF19.4906 ORF19.5459*	10.71%	0.0375
Carbon catabolite regulation of transcription from RNA polymerase II promoter (0.4%)	*CAT8* RCA1* SNF5* SPT6* SWI1* TUP1*[bde*]	3%	0.0788
B. Hyphal induction			
Growth (9.6%)	*AAF1*[ac*] *ACT1*[de*] *ADA2* AHR1*[a*] *BGL2 BNA4* BNI4* BRG1*[de*] *CLN3*[ac*] *DUR3* ERG5* HGC1*[c*] *HWP1*[ce*] *IRO1*[b*] *LPD1* MSB2*[c*] *MYO2* OSH3* PGA59*[de*] *PHR2* PMT1* PTP1* RAS1*[b*] *RFX2* RIM101*[cde*] *ROB1*[de*] *RPL6* SET3* SFL1*[c*] *SHA3*[acde*] *SHE3* SOG2* SPT3* SSN6*[cde*] *STP2*[cde*] *STP4*[de*] *TPS2*[de*] *VPS21* VPS41*[c*] *ZCF7* ORF19.4597 ORF19.6874*	19.3%	4.93e-06
Filamentous growth (9.3%)	*AAF1*[ac*] *ACT1*[de*] *ADA2* AHR1*[a*] *BNA4* BNI4* BRG1*[de*] *CLN3*[ac*] *DUR3* ERG5* HGC1*[c*] *IRO1*[b*] *LPD1* MSB2*[c*] *MYO2* OSH3* PGA59*[de*] *PHR2* PMT1* PTP1* RAS1*[b*] *RFX2* RIM101*[cde*] *ROB1*[de*] *RPL6* SET3* SFL1*[c*] *SHA3*[acde*] *SHE3* SOG2* SPT3* SSN6*[cde*] *STP2*[cde*] *STP4*[de*] *TPS2*[de*] *VPS21* VPS41*[c*] *ZCF7* ORF19.4597 ORF19.6874*	18.4%	1.63e-05
Cell communication (7.9%)	*AHR1*[a*] *ARF2 BNA4* BNI4* BRG1*[de*] *DHH1 DUR3* ERG5 GAL4*[de] *KIS2*[c] *MSB2*[c*] *PMT1* RAS1*[b*] *REG1 RIM101*[cde*] *RPL6 RTS1 SET3* SHA3*[acde*] *SHE3* SOG2* SOK1*[c] *TPS2*[de*] *VPS21* VPS41*[c*] *ZCF20 ORF19.1142 ORF19.177 ORF19.1994 ORF19.2726 ORF19.3936 ORF19.4488*	14.7%	0.0132
Regulation of filamentous growth (2.6%)	*AHR1*[a] *BRG1*[de*] *CLN3*[ac*] *HGC1*[c*] *MSB2*[c*] *MYO2* RAS1*[b*] *RFX2* RIM101*[cde*] *ROB1*[de*] *SET3* SFL1*[c*] *SPT3* SSN6*[cde*] *STP2*[cde*] *ZCF7**	7.3%	0.0119
Multi-organism process (6.5%)	*AAF1*[ac*] *ADA2* AHR1*[a*] *BGL2 BRG1*[de*] *CRZ2*[ac] *DHH1 ECE1*[ce*] *FCR3*[c] *GPM1 HGC1*[c*] *HWP1*[ce*] *HYR1*[c*] *IRO1* OSH3* PHR2* PMT1* RAS1*[b*] *RBT1 RBT4 RFX2* RIM101*[cde*] *ROB1*[de*] *SET3* SFL1*[c*] *SHE3* SPT3* SSN6*[cde*] *TPS2*[de*] *VPS21**	13.8%	0.0280
Nucleic acid binding transcription factor activity (3.4%)	*ADA2* AHR1*[a*] *BRG1*[de*] *CRZ2*[ac] *FCR3*[c] *GAL4*[de] *RFX2* RIM101*[cde*] *ROB1*[de*] *SFL1*[c*] *STP2*[cde*] *STP4*[de*] *ZCF20 ZCF21 ZCF23 ZCF7* ORF19.2743 ORF19.3328 ORF19.4125 ORF19.4972*	9.2%	0.0003
Sequence-specific DNA binding RNA polymerase II transcription factor activity (1.9%)	*AHR1*[a*] *GAL4*[de] *RIM101*[cde*] *ROB1*[+] *STP2*[cde*] *ZCF20 ZCF21 ZCF23 ZCF3* ZCF7* ORF19.2743 ORF19.3328*	5.5%	0.0089

Figure 3 GO terms of genes associated with Tpk2 binding sites. A. Tpk2 binding sites during yeast growth. **B**. Tpk2 binding sites during hyphal induction. GO terms for Tpk2 binding targets were identified in ChIP chip data using the CGD GO Term Finder tool (http://www.candidagenome.org/cgi-bin/GO/goTermFinder). [1]Genomic frequencies of genes corresponding to specific GO terms are expressed as percentages (gene number relative to 6,525 genes in the *C. albicans* genome [24]. Analysis conducted in April 2013. [2]Gene name or ORF19 nomenclature according to CGD [24]. Some genes were attributed to more than one GO term. Red lettering: Tpk2 binding in ORF; blue lettering: Tpk2 binding in promoter and ORF; black lettering: Tpk2 binding in promoter [a, b, c]Efg1 binds to promoter regions in [a]yeast growth, [b]hyphal induction or [c]biofilm induction [13,25,26]. [d, e]Set3 binding in [d]yeast or [e]hyphae inducing conditions [27]. [3]Percentages were calculated based on the number of genes in each GO category divided by the total number (196 genes for Tpk2 in yeast form and 218 genes for Tpk2 in hyphal inducing conditions). [4]*P* values for overrepresented categories were calculated using a hyper geometric distribution with multiple hypothesis correction according to the GO Term Finder tool website (http://www.candidagenome.org/help/goTermFinder.shtml). The *P* value cutoff used was 0.1. *Genes upregulated during hyphal induction [24,28].

upstream gene (*ORF19.612*) but not to the downstream gene (*ORF19.607*) of *EFG1* (Figure 4A). Similarly, Tpk2 but not Tpk1 bound the *MSB2* ORF in a distinct peak (Figure 4B, a). Comparisons of *MSB2* transcript levels in a wild-type strain and a homozygous *tpk2* mutant, grown in the yeast form, revealed no significant differences (Figure 4B, c). Similarly, *EFG1* promoter activity did not differ significantly between a wild-type and a *tpk2* mutant strain [13]. We conclude that Tpk2 residency at both target loci has no major influence on transcription/transcript levels, although subtle regulatory influences on gene expression cannot be excluded. A function of Tpk2 binding at ORFs is suggested by a distinct codon preference in the Tpk2 binding region (see below).

Promoter binding during hyphal induction

During hyphal induction PKA isoforms bound preferentially to promoter regions. At the *EFG1* promoter extensive binding of Tpk1 but not of Tpk2 was detected (Figure 4A). The broad Tpk1 binding area ranges from the *EFG1* transcriptional start site through 1169 bp untranslated upstream sequences and ends close to the 3′ end of the *EFG1* ORF. The Tpk1 binding area matches one of the major binding sites for Efg1 in the yeast form indicating that shortly after hyphal induction, Tpk1 binding occurs concomitant with the release of Efg1 [13]. *EFG1* promoter downregulation had been also observed in a *tpk1* mutant [13] suggesting that Tpk1 has no major role in negative autoregulation of *EFG1*.

Schaekel *et al. BMC Genomics* 2013, **14**:842
http://www.biomedcentral.com/1471-2164/14/842

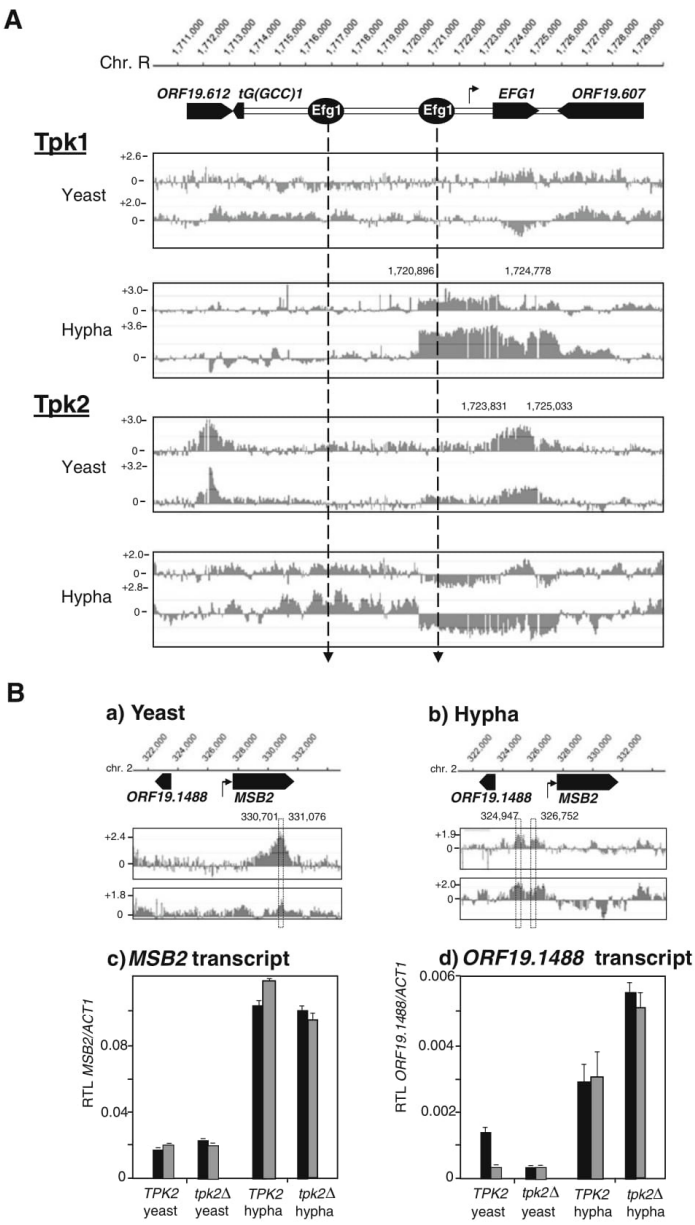

Figure 4 (See legend on next page.)

Schaekel *et al. BMC Genomics* 2013, **14**:842
http://www.biomedcentral.com/1471-2164/14/842

(See figure on previous page.)
Figure 4 Tpk binding to *EFG1* and *MSB2* loci. A. Binding to *EFG1*. Coordinates of *EFG1* and neighbouring genes on chromosome R are shown on top. Round circles (dotted lines) indicate the position of Efg1 binding during growth in the yeast form [13]; the kinked arrow indicates the transcript start site. The genomic localization of Tpk1 and Tpk2 was determined by ChIP chip assays on strains containing HA-tagged Tpk proteins relative to an unmarked control strain. For Tpk1 localization, the strain pair II (*TPK1/tpk1*)/AF1004 (*TPK1-3× HA/tpk1*) and for Tpk2 localization, the strain pair TPK7 (*TPK2/tpk2*)/AF1005 (*TPK2-3× HA/tpk2*) was used in ChIP chip. Graphs represent duplicates of Tpk^{HA} occupancy at the *EFG1* locus, ordinates represent scaled log_2 ratios. **B**. Binding to *MSB2*. Tpk2 enrichment in **(a)** the *MSB2* ORF of yeast cells or **(b)** in the *MSB2/ORF19.1488* upstream region of cells following hyphal induction; the most significant binding sequences are indicated by the dotted box. Transcript levels of *MSB2* **(c)** or *ORF19.1488* **(d)** in yeast or in induced cells were determined by qPCR in wild-type CAF2-1 (*TPK2*) or in *tpk2*Δ mutant cells (strain TPO7.4) growing in the yeast form or induced 30 min for hypha formation. Transcript levels relative to the *ACT1* transcript (RTL) are shown for two biological replicates (black and grey bars) indicating means and standard deviations for three technical replicates.

During hyphal morphogenesis, binding of Tpk2 within promoter regions of several genes was correlated with transcript levels of these genes (Figure 5A-C). The transcript of the *SOK1* gene (encoding a putative stress-regulated kinase [32]) was downregulated during hyphal induction in wild-type strains, which did not occur but was even upregulated in a *tpk2* mutant (Figure 5A). The Tpk2 binding peak (coordinates 1,271,612-1,272,002) lies directly upstream of the transcriptional start site of *SOK1* at position 1,272,810 (Figure 5A, kinked arrow) [33]. During hyphal induction, Tpk2 binding in the intergenic region between *ORF19.1488* and *MSB2* genes did not affect the *MSB2* transcript but correlated with an increased level of the *ORF19.1488* transcript in the *tpk2* mutant (Figure 4B). Furthermore, transcript upregulation of *HYR1* and *ECE1* genes, which are expressed specifically in the hyphal growth form [34,35], was completely abolished in the *tpk2*Δ strain (Figure 5B, C).

Promoter regions of *SOK1*, *HYR1* and *ECE1* genes are known to bind the Efg1 regulator relatively late during hyphal induction [26] or during biofilm formation [25], while no Efg1 binding was detected shortly (30 min) after hyphal induction [13]. Interestingly, Efg1 binding sequences are not identical but overlap partially with the

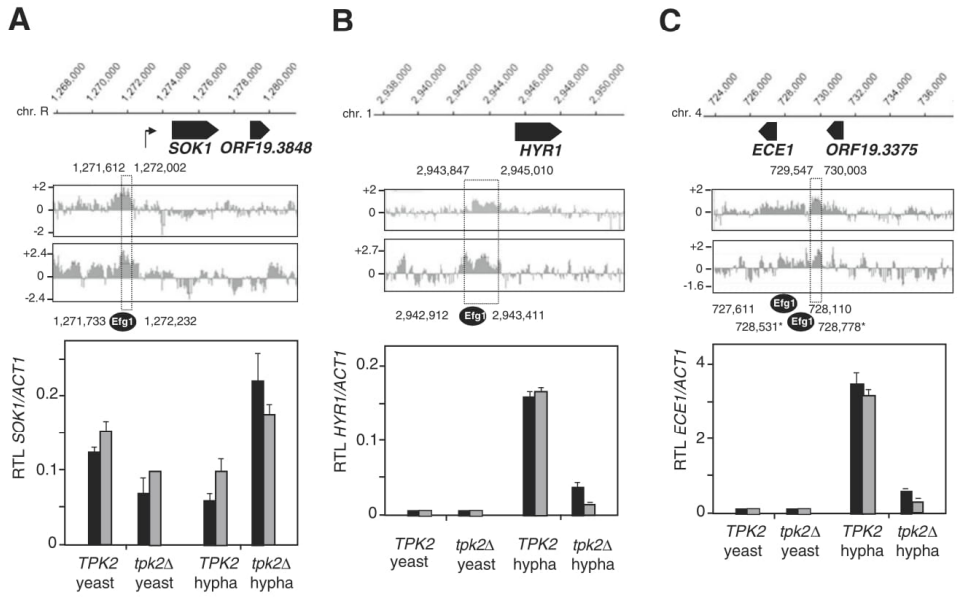

Figure 5 Tpk2 promoter binding during hyphal induction. Tpk2 localization was determined in cells induced for hypha formation at *SOK1* **(A)**, *HYR1* **(B)** and *ECE1* **(C)** genomic loci. ChIP chip occupancy values of $Tpk2^{HA}$ were determined in duplicates as in Figure 4; peak binding areas are marked by a dotted box. All three genes contain Efg1 binding sites within their promoters (circles) at the indicated coordinates; positions marked were reported by Nobile *et al.* [25] and by Lu *et al.* [26] (asterisks). The kinked arrow indicates the *SOK1* transcript start site [24]. Transcript levels for each gene during yeast growth or hyphal induction were determined by qPCR as in Figure 4B.

Schaekel et al. BMC Genomics 2013, 14:842
http://www.biomedcentral.com/1471-2164/14/842

sequences bound by Tpk2 (Figure 5A-C). Taken together, these results suggest that Tpk2 binding to promoters has the potential to regulate transcription of *C. albicans* genes both negatively and positively, possibly involving subsequent binding of Efg1 as a PKA phosphorylation target [9].

Sequence motifs in Tpk2 binding regions

Sequences representing the binding peaks of PKA were analysed for consensus sequences using the RSAT programs dyad-analysis and peak-motifs [36,37]; both algorithms generated identical results. While no significant consensus motifs were detected for Tpk1, Tpk2 showed clear sequence preferences. If cells were grown in the yeast form, Tpk2 binding occurred most frequently within ORFs (Figure 2B) at ACCAC, CCACC or CAGC motifs (Figure 6A). During hyphal induction, however, when Tpk2 binds predominantly within promoter regions (Figure 2B), a completely different set of binding preferences was found (Figure 6A). The identified A_5GA_5 and A_2GA_5 motifs match the A_2GA_5 motif for binding of the Azf1 transcriptional regulator in *S. cerevisiae*, which is required for glucose-induced gene transcription [38]. Consistent with this activity, effective hypha formation in *C. albicans* is known to require low levels of glucose [39]. The identified AAC, AAG and ACC repeats, which were identified in most Tpk2 binding sites, had been also detected previously for the Efg1 transcriptional regulator during hyphal induction [13]. The *HYR1* and *ECE1* genes, which are induced by hypha formation [34,35], contain these consensus sequence motifs, possibly to permit binding of kinase and its downstream target Efg1 to jointly trigger morphogenesis-dependent gene expression.

Binding of Tpk2 to many ORFs raised the question if such bound ORF sequences were as free as unbound regions to evolve sequence variants, e. g. with regard to the usage of synonymous codons. Therefore, we compared overall *C. albicans* codon usage with codon usage in ORF sequences bound by Tpk2. Specifically, we investigated if codons corresponding to the deduced Tpk2 binding consensus sequences would be preferred in the Tpk2 binding region. It was indeed found that usage of all six codons matching the Tpk2 consensus sequence during yeast growth was increased as compared to the average codon usage in *C. albicans* or to random set of 150 ORFs ("out group") that are not bound by Tpk2 (Figure 6B). In the case of histidine even a complete reversal of codon usage from the preferred CAT codon (15.62/1000 to 8.63/1000) to CAC (5.39/1000 to 11.4/1000) was observed in the Tpk2 binding region. This result suggests that ORF binding Tpk2 has a vital, yet unknown function, because it exerts selective pressure to restrict codon usage within ORFs. Codon usage has hitherto been related mainly to abundance of aminacyl-tRNAs [40].

PKA localization at the *EFG1* locus

The *EFG1* gene is a paradigm of both PKA and Efg1 binding to a genomic locus (scheme of main events in Figure 7). Early during hyphal induction the *EFG1* transcript level is lowered rapidly, presumably because the continued presence of Efg1 disturbs hyphal morphogenesis [29]. *EFG1* downregulation requires the Efg1 protein and the Tpk2 PKA isoform [13] within a short time window to initiate hyphal formation, because both proteins leave the *EFG1* locus rapidly thereafter. Possibly, genomic binding of both proteins prepares yeast cells to undergo hyphal morphogenesis rapidly in inducing environments. Binding of the Tpk1 isoform at promoter and coding region of *EFG1*, as well as binding of the Set3C histone deacetylase complex to the ORF [27] may also help to establish the repressed state of *EFG1* during hyphal formation. *EFG1* expression is probably regulated by additional proteins binding the *EFG1* promoter directly or indirectly by adapter proteins including Efg1. Candidate Efg1-binding proteins localized to the *EFG1* promoter include Czf1, Flo8, Sfl1, Sfl2 and Ndt80 proteins [11,12,25]. Tpk2 binding to the *SET3* and *SFL1* promoters, which we observed (Figure 3), may support this activity. Co-operation of Tpk2 and Efg1 may also occur at other genes regulated by hyphal induction including *HYR1*, *ECE1* and *SOK1* genes, as described above. Thus, the proposed Tpk2 phosphorylation of Efg1 [9,13] and other components of the transcriptional initiation machinery could occur directly at the promoters of genes regulating morphogenesis.

Conclusions

PKA isoforms Tpk1 and Tpk2 are crucial for the virulence of the human fungal pathogen *C. albicans* by regulating dimorphic growth. Tpk proteins mediate environmental cues and trigger hyphal morphogenesis by altering the transcriptional program. We show that Tpk2 and to a lesser extent Tpk1 bind to specific genomic sequences within ORFs and promoters of target genes. Growth in the yeast form triggers Tpk binding to CA-rich sequences within ORFs and appears to bias codon usage within the binding region. During hyphal induction Tpk2 associates with promoter regions of genes regulating or regulated by hyphal morphogenesis, often proximal to binding sites for the Efg1 transcription factor. These results suggest that genomic PKA proteins facilitate and/or prolong hyphal morphogenesis by acting on nearby transcription factors at genes regulating morphogenesis. Molecular mechanisms of PKA nuclear import, genomic recruitment and function remain to be established. In conclusion, we have demonstrated for the first time in a fungal

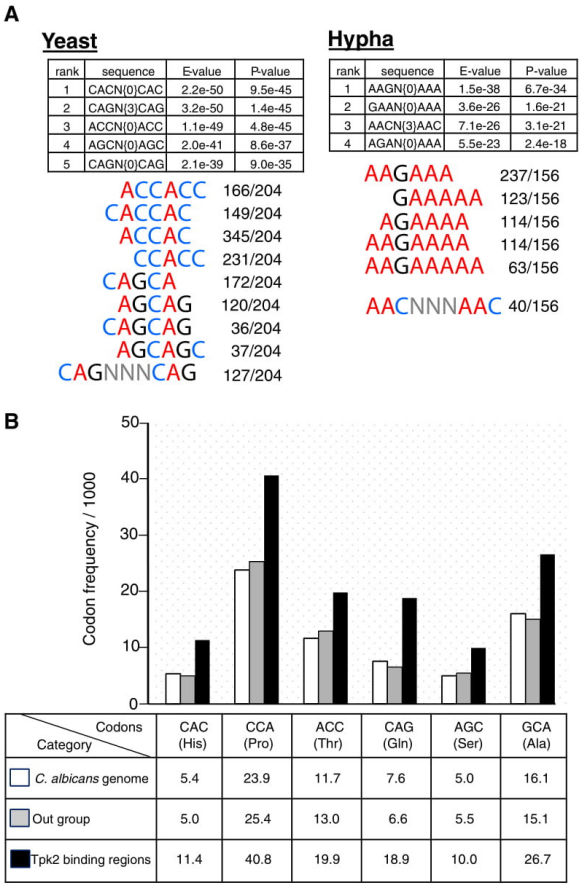

Figure 6 Tpk2 binding specificity. A. Consensus sequences for Tpk2 binding sites in yeast cells (left) or in cells induced for hypha formation (right). The program RSAT dyad-analysis [36] was used to predict consensus sequences. Predicted dyads (pairs of trinucleotides) common to Tpk2 binding sites were ranked and qualified by their *P-/E*-values; the frequencies of the deduced consensus sequences and of closely related sequences relative to all binding sites are listed below each table. **B**. Occurrence of trinucleotides/codons in ORF regions bound by Tpk2 during yeast growth. Codons corresponding to the Tpk2 binding consensus sequence are listed, along with codon frequencies in all *C. albicans* ORFs, in a randomly picked group of 150 genes not binding Tpk2 (out group) and in the 204 Tpk2 binding regions occurring mostly within ORFs.

pathogen that PKA isoforms, which are responsible for a relatively simple developmental program in a single cell, mark downstream target genes. Such binding analyses have predictive value because they link yet uncharacterized genes to signalling by PKA isoforms. This concept may hold true for other cellular differentiation processes involving other types of kinases and other species.

Methods

Strains and growth conditions

C. albicans strains are listed in Table 1 Strains were grown in liquid or on solid YPD, YPS and supplemented SD minimal medium, as described [13]. To induce hyphae the strains were grown at 37°C in YP medium containing 10% horse serum. *C. albicans* strains producing C-terminally HA-tagged PKA isoforms were constructed by

Schaekel *et al. BMC Genomics* 2013, **14**:842
http://www.biomedcentral.com/1471-2164/14/842

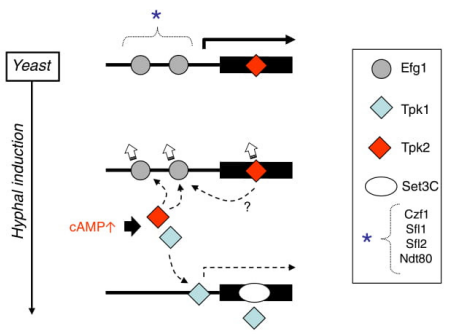

Figure 7 Residency of PKA isoforms at the *EFG1* locus during hyphal induction. During yeast growth, Efg1 [13] and Tpk2 proteins reside on promoter and ORF, respectively, and *EFG1* is transcribed at high levels (top). During initiation of hyphal formation, increased cAMP levels activate Tpk isoforms by removing Bcy1 repression and Tpk2 phosphorylates Efg1 [9]. This is followed by rapid removal of both Efg1 [13] and Tpk2 (indicated by open arrows). Subsequently the Tpk1 isoform enters the *EFG1* promoter at one of the previous Efg1 binding sequences and the Set3C histone deacetylase [27] occupies the ORF. Other proteins including Czf1, Sfl1, Sfl2 and Ndt80 are known to bind the *EFG1* promoter [12,25] and may contribute to Tpk-dependent regulation of *EFG1* expression.

transformation of heterozygous strains retaining a single allele of the respective gene. *HA-URA3* tagging cassettes were PCR amplified using oligonucleotide pairs on template plasmid p3HA-URA3, which generated PCR products ending in homologous sequences to target the respective genes [41]. Oligonucleotides Tpk1-HA (for)/(rev) and Tpk2-HA (for)/(rev) were used to generate tagged strains AF1003 ($TPK1^{HA}$/*TPK1*) from CAI4, AF1004 ($TPK1^{HA}$/*tpk1*) from FII4a and AF1005 ($TPK2^{HA}$/*TPK2*) from AF1001. Similarly, oligonucleotides Bcy1-HA (for)/(rev) were used to tag one of the *BCY1* alleles of strain CAI4 to generate strain AF1007 ($BCY1^{HA}$/*BCY1*). Correct chromosomal integration of tagging cassettes was verified by colony PCR using primers TPK1ver, TPK2ver, BCY1ver in combination with primer 3´Test HA-tag. Oligonucleotides are listed in Additional file 2: Table S6.

Immunodetection

Proteins containing a hemagglutinin (HA) antigenic tag were detected in cell extracts by immunoblotting using monoclonal rat anti-HA antibody (Roche; 1:1000), which was visualized on blots using peroxidase-coupled goat antibody (Pierce; 1:10000). Cells used for immunofluorescence microscopy were fixed by 4% formaldehyde and 1 ml of cell suspension were treated by zymolyase T100 (100 μg), glucuronidase (30 μl) and 10 mM DTT for 30 min at 30°C. Cells were pelleted and treated with 0.1% Triton X-100 for 5 min at room temperature. Cells (20 μl) were fixed to polylysine-coated glass slides and washed with PBS, followed by blocking of unspecific binding sites using 2% milk powder in PBS. The blocking solution was removed and 40 μl of rat anti-HA antibody (Roche; 1:100) were allowed to react 90 min at room temperature or overnight at 4°C in a wet chamber. Cells were washed and fluorescein isothiocyanate (FITC)-coupled goat anti-rat antibody (Jackson Immunologic Research Lab Inc.; 1:100) in 0.2% milk powder was added and allowed to react for 90 min at room temperature. For nuclear staining 20 μl diamidino-2-phenylindole (DAPI; 1 μg/ml) was added for 15 min at room temperature. Slides were washed by PBS and a drop of anti-fade (Pro-Long Anti-Fade, Sigma) was added before covering the specimen with a cover slip, which was sealed by nail polish. Microscopic inspection of FITC and DAPI fluorescence was done using a spinning disc confocal microscope (Cell Observer® SD; Yokogawa CSU-X1) and using the program Zen 2011 (Carl Zeiss) for evaluation of images.

Chromatin immunoprecipitation on microchips (ChIP chip)

The ChIP chip procedure was carried out essentially as described [13] except that magnetic beads with bound antibodies were eluted twice with elution buffer for 20 min at 65°C and that RNA was removed by adding 2.5 μl of RNase A (10 mg/ml; Qiagen). *C. albicans* genomic tiling microarrays were probed pairwise by immunoprecipitated chromatin of a strain producing an HA-tagged protein and a corresponding control strain. The following pairs of strains were used: II (*TPK1/tpk1*)/AF1004 (*TPK1-3× HA/tpk1*), TPK7 (*TPK2/tpk2*)/AF1005 (*TPK2-3× HA/tpk2*), CAF2-1 (*BCY1/BCY1*)/AF1007 (*BCY1-3× HA/BCY1*). Two independent cultures were assayed for each combination of strains. Significant binding peaks were defined as probes containing four or more signals above background in a 500 bp sliding window; the degree of significance depended on the FDR value. Results were visualized using the

Table 1 *C. albicans* strains

Strains		Reference
CAF2-1	*URA3/ura3::imm434*	[42]
CAI4	*ura3::imm434/ura3::imm434*	[42]
II	As CAI4 but *TPK1/tpk1::hisG-URA3-hisG*	[3]
FII4a	As CAI4 but *TPK1/tpk1::hisG*	[3]
AF1003	As CAI4 but *TPK1::(3xHA-URA3)/TPK1*	This work
AF1004	As FII4a but *TPK1::(3xHA-URA3)/tpk1::hisG*	This work
TPK7	As CAI4 but *TPK2/tpk2::hisG-URA3-hisG*	[2]
TPO7 (AF1001)	As TPK7 but *TPK2/tpk2::hisG*	[2]
TPO7.4	As CAI4 but *tpk2::hisG/tpk2::hisG-URA3-hisG*	[2]
AF1005	As AF1001 but *TPK2::(3xHA-URA3)/tpk2::hisG*	This work
AF1007	As CAI4 but *BCY1::(3xHA-URA3)/BCY1*	This work

program SignalMap (version 1.9). The most significant binding peaks (FDR ≤ 0.05), which coincided in both replicates, were analyzed by the program RSAT dyad-analysis to predict binding sequence from all peak genomic binding sites [36]. Codon usage of all *C. albicans* genes was derived from the Candida Genome Database [24] and codon usage in sequences of ORFs bound by Tpk2 were calculated using the Codon Usage Calculator [43].

Availability of supporting data

The data sets supporting the results of this article are available in the Candida Genome Database (CGD) repository: http://www.candidagenome.org/download/systematic_results/Schaekel_2013/.

Additional files

Additional file 1: Table S1. Lists Tpk1 binding sites during yeast growth. **Table S2.** Lists Tpk1 binding sites during hyphal induction. **Table S3.** Lists Tpk2 binding sites during yeast growth. **Table S4.** Lists Tpk2 binding sites during hyphal induction. **Table S5.** Lists Bcy1 binding sites during yeast growth.

Additional file 2: Table S6. List of oligonucleotides.

Competing interests

The authors declare that they have no competing interests.

Authors' contributions

AS did the experiments. AS and PD did the bioinformatics analysis. JFE did the experimental design and wrote the paper. All authors have read and approved the manuscript for publication.

Acknowledgements

We thank the members of the CAI center, Heinrich-Heine-Universität Düsseldorf, for assistance in microscopy. We thank K. Sanyal for helpful discussions. This project was supported by the Jürgen Manchot Stiftung Düsseldorf, by the Deutsche Forschungsgemeinschaft (ER47.13-1) and by ERA-NET PathoGenoMics project OXYstress.

Received: 3 June 2013 Accepted: 15 November 2013
Published: 1 December 2013

References

1. Sudbery PE: **Growth of *Candida albicans* hyphae.** *Nat Rev Microbiol* 2011, **9:**737–748.
2. Sonneborn A, Bockmühl DP, Gerads M, Kurpanek K, Sanglard D, Ernst JF: **Protein kinase A encoded by *TPK2* regulates dimorphism of the human pathogen *Candida albicans*.** *Mol Microbiol* 2000, **35:**386–396.
3. Bockmühl DP, Krishnamurthy S, Gerads M, Sonneborn A, Ernst JF: **Distinct and redundant roles of the two protein kinase A isoforms Tpk1p and Tpk2p in morphogenesis and growth of *Candida albicans*.** *Mol Microbiol* 2001, **42:**1243–1257.
4. Giacometti R, Kronberg F, Biondi RM, Passeron S: **Catalytic isoforms Tpk1 and Tpk2 of *Candida albicans* PKA have non-redundant roles in stress response and glycogen storage.** *Yeast* 2009, **26:**273–285.
5. Cassola A, Parrot M, Silberstein S, Magee BB, Passeron S, Giasson L, Cantore ML: ***Candida albicans* lacking the gene encoding the regulatory subunit of protein kinase A displays a defect in hyphal formation and an altered localization of the catalytic subunit.** *Eukaryot Cell* 2004, **3:**190–199.
6. Harcus D, Nantel A, Marcil A, Rigby T, Whiteway M: **Transcription profiling of cyclic AMP signaling in *Candida albicans*.** *Mol Biol Cell* 2004, **15:**4490–4499.
7. Hall RA, Mühlschlegel FA: **A multi-protein complex controls cAMP signalling and filamentation in the fungal pathogen *Candida albicans*.** *Mol Microbiol* 2010, **75:**534–537.
8. Stoldt VR, Sonneborn A, Leuker C, Ernst JF: **Efg1, an essential regulator of morphogenesis of the human pathogen *Candida albicans*, is a member of a conserved class of bHLH proteins regulating morphogenetic processes in fungi.** *EMBO J* 1997, **16:**1982–1991.
9. Bockmühl DP, Ernst JF: **A potential phosphorylation site for an A-type kinase in the Efg1 regulator protein contributes to hyphal morphogenesis of *Candida albicans*.** *Genetics* 2001, **157:**1523–1530.
10. Doedt T, Krishnamurthy S, Bockmühl DP, Tebarth B, Stempel C, Russell CL, Brown AJ, Ernst JF: **APSES proteins regulate morphogenesis and metabolism in *Candida albicans*.** *Mol Biol Cell* 2004, **15:**3167–3180.
11. Noffz CS, Liedschulte V, Lengeler K, Ernst JF: **Functional mapping of the *Candida albicans* Efg1 regulator.** *Eukaryot Cell* 2008, **7:**881–893.
12. Znaidi S, Nesseir A, Chauvel M, Rossignol T, D'Enfert C: **A Comprehensive functional portrait of two heat shock factor-type transcriptional regulators involved in *Candida albicans* morphogenesis and virulence.** *PLoS Pathog* 2013, **9:**e1003519.
13. Lassak T, Schneider E, Bussmann M, Kurtz D, Manak JR, Srikantha T, Soll DR, Ernst JF: **Target specificity of the *Candida albicans* Efg1 regulator.** *Mol Microbiol* 2011, **82:**602–618.
14. Griffioen G, Anghileri P, Imre E, Baroni MD, Ruis H: **Nutritional control of nucleocytoplasmic localization of cAMP-dependent protein kinase catalytic and regulatory subunits in *Saccharomyces cerevisiae*.** *J Biol Chem* 2000, **275:**1449–1456.
15. Matsuo Y, McInnis B, Marcus S: **Regulation of the subcellular localization of cyclic AMP-dependent protein kinase in response to physiological stresses and sexual differentiation in the fission yeast *Schizosaccharomyces pombe*.** *Eukaryot Cell* 2008, **7:**1450–1459.
16. Beene DL, Scott JD: **A-kinase anchoring proteins take shape.** *Curr Opin Cell Biol* 2007, **19:**192–198.
17. Sastri M, Barraclough DM, Carmichael PT, Taylor SS: **A-kinase-interacting protein localizes protein kinase A in the nucleus.** *Proc Natl Acad Sci USA* 2005, **102:**349–354.
18. Ernst JF, Bockmühl DP: **Gene expression and genetic techniques.** In *Candida and Candidiasis*. Edited by Calderone R. Washington: ASM Press; 2001:267–278.
19. Pokholok DK, Zeitlinger J, Hannett NM, Reynolds DB, Young RA: **Activated signal transduction kinases frequently occupy target genes.** *Science* 2006, **313:**533–536.
20. Cook KE, O´Shea EK: **Hog1 controls global reallocation of RNA PolII upon osmotic shock in *Saccharomyces cerevisiae*.** *G3 (Bethesda)* 2012, **2:**1129–1136.
21. Nadal-Ribelles M, Conde N, Flores O, González-Vallinas J, Eyras E, Orozco M, De Nadal E, Posas F: **Hog1 bypasses stress-mediated down-regulation of transcription by RNA polymerase II redistribution and chromatin remodeling.** *Genome Biol* 2012, **3:**R106.
22. Pascual-Ahuir A, Proft M: **The Sch9 kinase is a chromatin-associated transcriptional activator of osmostress-responsive genes.** *EMBO J* 2007, **26:**3098–3108.
23. Zheng X, Wang Y, Wang Y: **Hgc1, a novel hypha-specific G1 cyclin-related protein regulates *Candida albicans* hyphal morphogenesis.** *EMBO J* 2004, **23:**1845–1856.
24. Arnaud MB, Costanzo MC, Skrzypek MS, Binkley G, Lane C, Miyasato SR, Sherlock G: **The *Candida* Genome Database (CGD), a community resource for *Candida albicans* gene and protein information.** *Nucleic Acids Res* 2005, **33:**D358–D363. http://www.candidagenome.org/.
25. Nobile CJ, Fox EP, Nett JE, Sorrells TR, Mitrovich QM, Hernday AD, Tuch BB, Andes DR, Johnson AD: **A recently evolved transcriptional network controls biofilm development in *Candida albicans*.** *Cell* 2012, **148:**126–138.
26. Lu Y, Su C, Mao X, Raniga PP, Liu H, Chen J: **Efg1-mediated recruitment of NuA4 to promoters is required for hypha-specific Swi/Snf binding and activation in *Candida albicans*.** *Mol Biol Cell* 2008, **19:**4260–4272.
27. Hnisz D, Bardet AF, Nobile CJ, Petryshyn A, Glaser W, Schöck U, Stark A, Kuchler K: **A histone deacetylase adjusts transcription kinetics at coding sequences during *Candida albicans* morphogenesis.** *PLoS Genet* 2012, **8:**e1003118.
28. Nantel A, Dignard D, Bachewich C, Harcus D, Marcil A, Bouin AP, Sensen CW, Hogues H, Van het Hoog M, Gordon P, Rigby T, Benoit F, Tessier DC, Thomas DY, Whiteway M: **Transcription profiling of *Candida albicans* cells undergoing the yeast-to-hyphal transition.** *Mol Biol Cell* 2002, **13:**3452–65.

29. Tebarth B, Doedt T, Krishnamurthy S, Weide M, Monterola F, Dominguez A, Ernst JF: **Adaptation of the Efg1p morphogenetic pathway in *Candida albicans* by negative autoregulation and PKA-dependent repression of the *EFG1* gene.** *J Mol Biol* 2003, **329:**949–962.
30. Román E, Cottier F, Ernst JF, Pla J: **Msb2 signaling mucin controls activation of Cek1 mitogen-activated protein kinase in *Candida albicans*.** *Eukaryot Cell* 2009, **8:**1235–1249.
31. Szafranski-Schneider E, Swidergall M, Cottier F, Tielker D, Román E, Pla J, Ernst JF: **Msb2 shedding protects *Candida albicans* against antimicrobial peptides.** *PLoS Pathog* 2012, **8:**e1002501.
32. Bennett RJ, Johnson AD: **The role of nutrient regulation and the Gpa2 protein in the mating pheromone response of *C. albicans*.** *Mol Microbiol* 2006, **62:**100–119.
33. Tuch BB, Mitrovich QM, Homann OR, Hernday AD, Monighetti CK, De La Vega FM, Johnson AD: **The transcriptomes of two heritable cell types illuminate the circuit governing their differentiation.** *PLoS Genet* 2010, **6:**e1001070.
34. Birse CE, Irwin MY, Fonzi WA, Sypherd PS: **Cloning and characterization of *ECE1*, a gene expressed in association with cell elongation of the dimorphic pathogen *Candida albicans*.** *Infect Immun* 1993, **61:**3648–3655.
35. Bailey DA, Feldmann PJ, Bovey M, Gow NA, Brown AJ: **The *Candida albicans HYR1* gene, which is activated in response to hyphal development, belongs to a gene family encoding yeast cell wall proteins.** *J Bacteriol* 1996, **178:**5353–53560.
36. Van Helden J, Rios AF, Collado-Vides J: **Discovering regulatory elements in non-coding sequences by analysis of spaced dyads.** *Nucleic Acids Res* 2000, **28:**1808–1818.
37. Thomas-Chollier M, Herrmann C, Defrance M, Sand O, Thieffry D, Van Helden J: **RSAT peak-motifs: motif analysis in full-size ChIP-seq datasets.** *Nucleic Acids Res* 2012, **40:**e31.
38. Newcomb LL, Hall DD, Heideman W: ***AZF1* is a glucose-dependent positive regulator of *CLN3* transcription in *Saccharomyces cerevisiae*.** *Mol Cell Biol* 2002, **22:**1607–1614.
39. Hudson DA, Sciascia QL, Sanders RJ, Norris GE, Edwards PJ, Sullivan PA, Farley PC: **Identification of the dialysable serum inducer of germ-tube formation in *Candida albicans*.** *Microbiology* 2004, **150:**3041–3049.
40. Novoa EM, Ribas de Pouplana L: **Speeding with control: codon usage, tRNAs, and ribosomes.** *Trends Genet* 2012, **28:**574–581.
41. Prill SK, Klinkert B, Timpel C, Gale CA, Schröppel K, Ernst JF: ***PMT* family of *Candida albicans*: five protein mannosyltransferase isoforms affect growth, morphogenesis and antifungal resistance.** *Mol Microbiol* 2005, **55:**546–560.
42. Fonzi WA, Irwin MY: **Isogenic strain construction and gene mapping in *Candida albicans*.** *Genetics* 1993, **134:**717–728.
43. **Codon Usage Calculator.** http://geneinfinity.org/sms/sms_codonusage.html.

doi:10.1186/1471-2164-14-842
Cite this article as: Schaekel *et al.*: Morphogenesis-regulated localization of protein kinase A to genomic sites in *Candida albicans*. *BMC Genomics* 2013 **14**:842.

2.5 Manuscript IV: Genetic landscape of hypoxic filamentation in *Candida albicans*

Prashant R. Desai, Lasse van Wijlick, Mateusz Juchimiuk, Alida Schaekel, Yasemin Üstün, Christophe d´Enfert and Joachim F. Ernst

Contribution to Manuscript: 85 %

Prashant R. Desai was majorly involved in designing, performing and concluding the results. He prepared all the figures and wrote the initial draft and was also involved in editing the final draft of the manuscript.

Individual contributor: for Figures 3 to 11.

Partial contribution: for Figures 1 and 2.

Submitted to journal: Genetics (Under review)

submitted to *Genetics*

Genetic landscape of hypoxic filamentation in *Candida albicans*

Prashant R. Desai[1], Silas Mathias Janßen[1], Lasse van Wijlick[1], Mateusz Juchimiuk[1], Alida Schaekel[1], Yasemin Üstün[1], Christophe d´Enfert[2] and Joachim F. Ernst[1*]

[1]Department Biologie, Molekulare Mykologie, Heinrich-Heine-Universität, 40225 Düsseldorf, Germany

[2]Fungal Biology and Pathogenicity Unit, Department of Mycology, Institut Pasteur, INRA, Paris, France

Running Title: Hypoxic filamentation

Key words: *Candida albicans*, dimorphism, hypoxia, protein kinase A, Sch9, MAP kinase, Efg1, Ahr1, Crf1, Zcf14

*Corresponding author: Joachim F. Ernst, Molekulare Mykologie, c/o Institut fur Mikrobiologie, Universitätsstr. 1/26.12, 40225 Düsseldorf, Germany. E-mail: joachim.ernst@uni-duesseldorf.de

Abstract

Virulence of the human fungal pathogen *Candida albicans* depends on its ability to switch between a yeast and hyphal growth form. While signalling pathways mediating hypha formation under normoxia are known, little information exists on the regulation of filamentation under hypoxia. To identify hypoxic regulators, we first explored, if known normoxic regulators also are relevant for filamentation under hypoxia, in the presence or absence of elevated CO_2 levels. Phenotypic profiling of 28 mutants defective in normoxic filamentation revealed several regulator activities required for filamentation under both normoxia and hypoxia, but also positive regulators only needed under normoxia, of which several even acted as repressors of filamentation only under hypoxia. To identify additional regulators of hypoxic filamentation a set of 296 mutants lacking individual transcription factors or protein kinases was screened. Unexpectedly, hypoxic filamentation was abnormally upregulated in 21 mutants in the presence of 6 % CO_2, resembling the previously reported *sch9* mutant phenotype; furthermore, in 12 of such strains, normoxic formation of hyphae was completely blocked, thereby resembling the known phenotype of an *efg1* mutant. Transcript analyses of representative mutants identified the *UME6* gene as repression target of Zcf14 and Orf19.6874 under hypoxia; Orf19.6874 (renamed as Crf1) appears to act as CO_2-dependent repressor of filamentation not only under hypoxic but also normoxic conditions. The results reveal that *C. albicans* has the high potential to filament under hypoxia, but that this ability is suppressed normally by a surprisingly high number of specific regulators. While hypoxic niches in the human host may generally favour yeast proliferation, controlled relief of filamentation repression may be instrumental in specific hypoxic environments, e. g. during escape from immune cells or in the gastrointestinal tract.

Key words: *Candida albicans*, dimorphism, hypoxia, protein kinase A, Tor1, Sch9, MAP kinase, Efg1, Crf1, Zcf14

Author Summary

The fungal pathogen *Candida albicans* colonizes the human body at numerous sites that are depleted of oxygen and often enriched for CO_2. The fungus is able to adapt to these conditions by altering its metabolism and morphology, generally favouring the unicellular yeast over the multicellular hyphal growth form. We found that under hypoxia, yeast growth results from the combined action of several regulatory proteins that repress the filamentous growth form. Surprisingly, some of these repressors have a dual role, additionally serving as inducers of filamentation under normoxia. The function of such regulatory proteins is apparent by the hyperfilamentous phenotype of respective mutants in a hypoxic environment with high CO_2 levels. The results indicate the hidden potential of *C. albicans* to filament under hypoxia, which in the human host may become de-repressed to allow exit from immune cells or invasive growth.

Introduction

Candida albicans is a frequent commensal fungus in humans but in predisposed patients it thrives at multiple body sites to cause superficial and/or systemic disease [1-3]. Its alternating growth in either an unicellular yeast or a multicellular hyphal form is essential for its virulence [4]. *C. albicans* yeast cells rapidly increase numbers of infectious units and allow rapid dissemination in the host, while hyphal filaments allow entry into and exit from body cells or tissues by mediating adhesion and penetration of host cell membranes [5]. In addition, both growth forms serve as expression platforms for the production of various virulence factors including hydrolytic enzymes that damage the host [6].

The yeast-hyphal transition of *C. albicans* is the result of defined signalling pathways that are activated by environmental cues [4]. A major pathway includes adenylate cyclase Cyr1, which is activated by the Ras1 G-protein, bicarbonate (environmental CO_2) and serum components that triggers a peak of cAMP synthesis [7-9]. Elevated cAMP de-represses the function of protein kinase A (PKA) isoforms Tpk1 and Tpk2 [10,11], which in turn activate the central transcriptional regulator Efg1, which activates hypha-specific genes [12,13]. Activation of some hypha-specific genes may occur by PKA directly at their genomic sites [14]. Functioning downstream of Efg1, the Flo8, Ume6 and Eed1 transcriptional regulators are essential to drive polar growth [15-17]. In addition, during the initiation phase of hyphal development, negative regulators Nrg1 and Rpd3 are removed from some hypha-specific genes and allow an increase of histone H4 acetylation [13,18]. Requirements for maintenance of hyphal formation were reported recently and include recruitment of histone deacetylase Hda1 to prevent re-entry of repressor Nrg1, followed by recruitment of transcriptional activator Brg1 [19]. The latter events only occur, if the activity of Tor1 kinase is low, i. e. during nutrient-depletion or the inhibitory action of rapamycin or caffeine [20]. Low Tor1 activity was proposed to activate protein phosphatases Ptp2 and Ptp3, which

decrease the phosphorylation status of mitogen-activated protein kinase (MAPK) Hog1, which in its phosphorylated form blocks Brg1 promoter binding via repressor Sko1 [20].

Details of *C. albicans* morphogenetic signalling have hitherto been evaluated mainly under oxygen-replete conditions (normoxia), while in the infected human host many sites of fungal residency are hypoxic [21,22]. This refers especially to the gut, which is a frequent reservoir of *C. albicans* commensalism, but also to other internal organs including kidney and liver that may get colonized during disease progression. The degree of hypoxia varies between organs and within sites of the same organ and can reach anoxia. Insufficiently perfused tissues and the interior of cells, which *C. albicans* encounters during phagocytosis by immune and epithelial cells, also represent hypoxic environments. Typically, such body sites are not only oxygen-poor but also are enriched for CO_2. Human cells are known to cope with oxygen depletion by upregulation of transcription factor HIF1α, which re-directs activities from a normoxic to a hypoxic pattern of cellular physiology [23]. Some hypoxic responses are relevant to pathogen interaction, such as induction of phagocytosis, release of antimicrobial peptides and granular proteases, as well as increased production of VEGF and several cytokines including TNF, IL-1 and IL-12 by phagocytes [23]. Thus, the interaction of *C. albicans* with human cells that occurs under hypoxia and high CO_2 represents a scenario of interaction that awaits further study.

Hypoxic activities of *C. albicans* differ significantly from the normoxic patterns, because glycolysis, lipid biosynthesis, iron uptake and stress responses are upregulated, while oxidative metabolism is downregulated; in addition, some cell wall proteins are altered [24-28]. Hypoxia *per se* does not induce significant hyphal development in wild-type strains but surprisingly, it can elicit strong filamentation in some mutants. During surface-growth and temperatures <37 °C, mutants lacking the Efg1 regulator are hyperfilamentous under hypoxia, especially if its paralog Efh1 is deleted as well [24,29,30]. In this condition, Efg1 is

known to repress the Cek1-Cph1 signalling pathway in wild-type cells [31]. Flo8 and Czf1 transcription factors bind directly to Efg1 [32] and appear to regulate its activity under hypoxia or during embedded growth in agar [15,33]. Efg1 in turn downregulates the *ACE2* and *BRG1* genes, which stimulate filamentation under low oxygen; however, the activity of Ace2 and, in consequence of its entire regulatory hub, is strongly altered in the presence of high CO_2 levels [31]. The activity of these regulators is thought to control the commensal growth of *C. albicans* in the mouse gut in the yeast form [34-36]. Sch9, a kinase acting downstream of Tor1, has been described as another regulator of hypoxic filamentation, since *sch9* mutants are hyperfilamentous at low oxygen; interestingly, this occurs only under high CO_2 levels [37]. This phenotype is also detected during inhibition of Tor1 in wild-type cells, suggesting that a Tor1-Sch9 pathway limits hypoxic filamentation in a CO_2-dependent manner. At high CO_2 levels, Sch9 phosphorylates and thereby inactivates the Rca1 transcription factor responsible for expression of *NCE103* encoding carbonic anhydrase, which under low CO_2 levels is needed to generate bicarbonate [38,39]. Bicarbonate that is either generated spontaneously or by the action of Nce103, binds to and thereby activates the Cyr1 adenylate cyclase, leading to activation of the PKA pathway of filamentation [8]. A PKA-independent pathway of CO_2-dependent filamentation has also been reported [40]. The combination of high CO_2 and hypoxia stabilizes the Ume6 and Hgc1 proteins, key proteins upregulating hyphal morphogenesis [16,41], which under normoxia are degraded in consequence of Ofd1 prolyl hydroxylase activity; however, this effect was observed only, if hyphal formation had been initiated previously at 37 °C, in liquid media [42]. Molecular mechanisms of CO_2/bicarbonate sensing by Sch9, Flo8 or by other mechanisms are yet unknown.

Hypoxia, often in combination with hypercapnia (high CO_2), is a typical environment for *C. albicans* in the infected human host, which may control its transition from a

commensal to an invasive pathogen [43]. To gain a better understanding of the genetic requirements for hypoxic filamentation, we asked first, if any of the known regulators under normoxia are also required for filamentation under hypoxia. Second, we screened a genome-wide collection of mutants lacking in transcription factors or kinases for their hypoxia phenotypes. Remarkably, the results demonstrate differences with regard to the activities of regulatory proteins involved in normoxic and hypoxic filamention. Furthermore, an astounding number of regulators was identified that downregulate morphogenesis under hypoxia, while upregulating hypha formation under normoxia.

Results

Role of normoxic regulators of filamentation under hypoxia

To clarify the role of known normoxic regulators of filamentation under hypoxia, a series of respective mutants defective in hyphal initiation, maintenance or repression was tested. The mutant strains were grown on agar surfaces (YPS or Spider medium) at different temperatures (25 °C or 37 °C) under varying conditions of oxygen (21 % or 0.2 %), either in presence or absence of 6 % CO_2. In total, 8 different growth conditions were used for phenotypic testing of mutant strains (Fig. 1).

Under normoxia, a cAMP-dependent PKA pathway that is initiated by Cyr1 adenylyl cyclase and Ras1 is known to trigger filamentation [44,45]; in addition, a pathway including the MAP kinase Cek1 contributes to hypha formation in some conditions [31,46]. Hypoxic screening of mutants revealed components that are required for filamentation under both normoxia and hypoxia. Mutants lacking Ras1, Cyr1 [44,45], Flo8 [15], Ume6 [16] or Eed1 [17] were absolutely filamentation-negative; in addition, greatly reduced filamentation was observed in a mutant lacking Brg1 [47], under all conditions (Fig. 1). To note, colony diameters of *cyr1* and *ras1* mutants were greatly reduced under hypoxia, indicating that Cyr1 and Ras1 not only affect filamentation, but also growth in general in this condition. In contrast, mutants lacking Nrg1 or Tup1 were hyperfilamentous irrespective of oxygen (Fig. 1 C), indicating that the known repressor function of these proteins under normoxia [48,49] also extends to hypoxic conditions. Remarkably, in another major class of mutants, hypoxic filamentation was increased, while normoxic filamentation was absent or severely impaired. This regulatory pattern has previously been observed mainly in mutants lacking the transcription factor Efg1 [24,31]. The results obtained using known mutants (and supported by mutants identified by screening, as described below) indicate that components including the transcription factors Efg1 and Ahr1, cyclin Hgc1 or kinase Pbs2 act as normoxic

activators, but carry as second function as hypoxic repressors of filamentation. Remarkable deviations from the filamentation patterns of the described groups were also observed for individual mutants (e.g. lack of hypoxic filamentation at 25 °C but not at 37 °C by *cek1*, *hda1*, *sko1* or *ptp2* mutants) suggesting complex regulation not only by oxygen and CO_2 levels, but also by temperature. Importantly, besides indicating the complexity of environmental regulation, the results demonstrate that known regulators of filamentation under normoxia are not necessarily required or have contrasting functions under hypoxia.

Identification of novel hypoxic repressors of filamentation

The apparent differences between regulatory networks governing normoxic or hypoxic filamentation led us to search for novel regulators of hypoxic filamentation. For this purpose, libraries of mutants lacking 233 specific transcription factors and of 63 mutants lacking specific kinases [50-52] were screened by growing the strains on YPS agar (or on Spider agar) under hypoxic or normoxic conditions, either with or without 6 % CO_2 at 25 °C and 37 °C. Phenotypic profiling of identified mutants with abnormal hypoxic filamentation led to 3 classes of mutant phenotypes (Fig. 2). The first type of mutants was able to filament similar to the control strain at 37 °C under all normoxic conditions, but showed increased filamentation under hypoxia at elevated CO_2 levels (Fig. 2 A). Seven mutant strains (*zcf14*, *spp1*, *zcf21*, *gzf3*, *pho23*, *try4* and *cpp1* mutants) showed this phenotype, which corresponds to the previously described phenotype of the *sch9* mutant [37]. The second type of mutants comprising *efg1*, *zcf24*, *cap4*, *prr1*, *wor4*, *akl1*, *tye7*, *ace2* and *bcr1* mutants shared their hypoxic mutant phenotype with class 1 mutants (Fig. 2 B); however, these mutants were unable or severely deficient in their ability to form hyphae under all normoxic conditions. Phenotypes of *efg1*, *bcr1* and *ace2* mutants have been described previously and have led to the identification of a hypoxic regulatory hub comprising the Efg1, Bcr1 and Ace2

transcription factors [31]. As described previously, the *bcr1* mutant phenotypes mimicks the drastic hyperfilamentous phenotype of an *efg1* mutant, which occurs under hypoxia, even in the absence of CO_2 at low temperatures (25 °C); the deficiency of an *ace2* mutant to filament under hypoxia also has been reported [31,53]. Representative phenotypes of type 1 and 2 mutants are shown in Fig. 3, which indicate that the hyperfilamentous phenotype of most mutants is apparent at temperatures of up to 30 °C, while differences to the control strain become largely negligible at 33 °C. Thirdly, mutants including *pbs2* and *orf19.6874* mutants showed increased filamentation at 25 °C in the presence of 6 % CO_2 not only under hypoxia, but also under normoxia; both mutants differed, however, in their ability to filament under normoxia at 37 °C (Fig. 2 C). In conclusion, mutant screening led to the identification of a surprisingly large number of components downregulating filamentation under hypoxia. Surprisingly, mutants blocking solely hypoxic filamentation, while still allowing normoxic filamentation, were not found. All mutants with aberrant hypoxic phenotypes reflected defects in repressor activity for filamentation under hypoxia, which was in part associated with activator function under normoxia.

Orf19.6874 (Crf1) and Zcf14 are CO_2-dependent repressors of morphogenesis

Screening of mutants had revealed a strong CO_2-dependent phenotype in a mutant lacking *ORF19.6874*, which was hyperfilamentous at 25 °C under both hypoxia and normoxia, but only in the presence of CO_2 (Fig. 2 C). In the *C. albicans* genome sequence, *ORF19.6874* encodes a protein that is homologous to the *S. cerevisiae* Bas1 protein (38 % identity), which in this organism allows the basal and induced expression of genes involved in purine and histidine biosynthetic pathways [54]. *ORF19.6874* has been tentatively named as *BAS1* in the *Candida* genome database (http://www.candidagenome.org/), although a second gene, *ORF19.3809*, encodes a protein with even higher homology to ScBas1 (48 % identity). In *C.*

albicans, mutants defective in *ORF19.3809* and *ORF19.6874* affected filamentation differently, since the CO_2-dependent hyperfilamentation was only observed for the *orf19.6874* mutant, but not for the *orf19.3809* mutant (Fig. 4). Furthermore, growth tests revealed that under normoxia, the *orf19.3809* mutant, but not the *orf19.6874* mutant, showed slow growth in the absence of adenine (S1 Fig.). These results confirm that *ORF19.3809* represents the functional paralog of *ScBAS1* [47,55], while the function of *ORF19.6874* is different in *C. albicans*, because it regulates filamentation and partially, biofilm formation [56]. In the following, we have re-named *ORF19.6874* as *CRF1* (for CO_2-dependent repression of filamentation), but we have retained *BAS1* as the designation for *ORF19.3809*.

Mutant screening had also revealed genes encoding members of the $Zn(II)_2Cys_6$ (Zcf14, Zcf21, Zcf24) of zinc finger transcription factors, which act as repressors of filamentation during surface growth at 25 °C, but only under high CO_2 and hypoxia. The mutant filamentation phenotype in this condition is shown in Fig. 4, which demonstrates hyperfilamentation of the *zcf14* mutant, as compared to the control strain under hypoxia, but a wild-type filamentation phenotype under normoxia (Fig. 4). As expected, mutant phenotypes were restored by introducing intact *CRF1* or *ZCF14* ORFs in the respective mutants (see below).

Since the repressor function of both Crf1 and Zcf14 had been observed on agar, it was tested if these activities are also observed during growth in liquid medium. For this purpose, the control strain CAF2-1 and the *crf1* and *zcf14* mutants were grown in liquid YPS medium in normoxic or hypoxic conditions, in the presence of CO_2, and cellular morphologies were observed microscopically. In these conditions, the control strain grew mostly in a spherical yeast form, while the *crf1* mutant formed strong filaments in both normoxic and hypoxic cultures from 6 h up to 24 h of incubation. In contrast, the *zcf14*

mutant displayed a morphology similar to the control strain (Fig. 5). These results suggest that Crf1 acts as a CO_2-dependent repressor of filamentation during both surface and liquid growth, while the repressor function of Zcf14 appears confined to surface growth.

Hypoxic regulatory networks of Crf1 and Zcf14

To clarify the manner by which Crf1 or Zcf14 regulate filamentation in *C. albicans*, transcript levels of relevant regulators of filamentation were determined in a *crf1* and *zcf14* mutants and a control strain, grown on agar under hypoxia or normoxia. Both Ume6 and Brg1 have previously been described as key inducers of hypha formation under both conditions [16,47] and Nrg1, as well as Tup1, have been defined as strong general repressors of filamentation [48,49]. In the *crf1* mutant, the *UME6* transcript was strongly derepressed under all conditions and derepression was also observed for the *BRG1* transcript, but only under hypoxia (Fig. 6). In contrast, the transcripts of the Nrg1 and Tup1 repressor proteins were not significantly affected by mutation of *CRF1* (Fig. 6; S2 Fig.). Furthermore, transcripts for the filamentation-inducing transcription factors Efg1 [12,13] or Cph1 [46] were not consistently upregulated in a *crf1* mutation relative to the control strain (S2 Fig.).

In the *zcf14* mutant, derepression of *UME6* transcript levels was also detected, but only during hypoxic growth (Fig. 7). Other transcripts including *BRG1*, *CPH1*, *NRG1* or *TUP1* transcripts (Fig. 7; S3 Fig.) were not abnormally regulated in the *zcf14* strains relative to the control strain. In conclusion, the results involve the Ume6 transcriptional network as a key repression target of the Crf1 protein, if CO_2 levels are high, under all gaseous conditions, while Zcf14 appears to repress Ume6 only during growth under hypoxia.

To complement results obtained by surface growth of cells, RNA of strains grown in YPS liquid medium, under hypoxia and in the presence of CO_2, was also examined. Transcripts of relevant regulator genes demonstrated strong upregulation of the *UME6*

transcript in a *crf1* mutant at all time points (Fig. 8). Similarly to surface grown cells, consistent upregulation of the *UME6* and *BRG1* transcript was found and the transcript of the strong filamentation repressor Tup1 was largely unaffected in the *crf1* genetic background, while the transcript of the Nrg1 repressor was significantly reduced, as compared to the control strain. *UME6* and *BRG1* transcripts were also induced in the *zcf14* mutant (but less than in the *crf1* mutant), while *NRG1* and *TUP1* transcripts were unaffected. These results define Crf1 as a major negative regulator of the *UME6* gene under hypoxic conditions, irrespective of the mode of growth on an agar surface or in liquid medium, while the repressive action of Zcf14 appears more limited.

Furthermore, the transcriptional regulation of *CRF1* and *ZCF14* genes by oxygen conditions was determined. For this purpose, total RNA of control strain CAF2-1 grown on agar surface under hypoxic and normoxic conditions was isolated and transcript levels of both genes were determined by qPCR. In both conditions, no significant differences were observed for the *CRF1* transcript, while the *ZCF14* transcript was strongly induced under hypoxia (Fig. 9). Considering both transcript levels and mutant filamentation phenotypes, it appears that Zcf14 has its main function under hypoxia, while Crf1 has emerged as a major CO_2-dependent regulator of filamentation under all oxygen conditions.

CRF1 overexpression suppresses filamentation under hypoxic and normoxic conditions

The above results had indicated that Crf1 strongly downregulates morphogenetic pathways under high CO_2 conditions. To confirm this conclusion, it was tested if *CRF1* overexpression is able to suppress hyperfilamentation under hypoxic conditions in some of the above identified mutants. For this purpose, the *CRF1* or *ZCF14* ORFs were placed under transcriptional control of the repressible *tet* promoter (*tet*-off) [57] and the resulting plasmids were transformed into the control strain CAF2-1, as well as the *efg1*, *crf1*, *bcr1*,

zcf14, wor4 and *nrg1* mutants. As controls, transformants carrying a plasmid containing a fusion of the *tet*-promoter to the *RFP* reporter gene [57] were used. Filamentation phenotypes were examined during growth under hypoxia or normoxia in the absence of anhydrotetracycline (aTc) (*tet* promoter active) or in its presence (*tet* promoter inactive); results are summarized in Fig. 10.

Under hypoxic conditions at 25 °C with 6 % CO_2, i. e. a condition under which the hyperfilamentous phenotype of derepressed mutants is apparent, overexpression of *CRF1* was able to suppress the weak filamentous growth of the CAF2-1 control strain (S4 Fig.), but also hyperfilamentation of *efg1*, *crf1*, and *zcf14* mutants; suppression by *CRF1* overexpression did also occur at 37 °C under hypoxia in these strains (Fig. 10). Among the tested mutants, the *crf1* mutant is unique since it is able to filament under normoxia at 25 °C only in the presence of CO_2; this filamentation was restored by *CRF1* expression, as expected, while the suppressive activity of the *tet-CRF1* fusion was abolished in the presence of aTc. Interestingly, however, *CRF1* overexpression was unable to suppress hyperfilamentation of *bcr1* and *nrg1* mutant. These results have identified Crf1 as a potent repressor of hypha formation under normoxia and hypoxia, while Bcr1 and Nrg1 appear to function independently of Crf1. In contrast to *CRF1*, overexpression of *ZCF14* was able to suppress excessive filamentation of the *efg1* and *zcf14* mutants only at 25 °C (S4 Fig., Fig. 10).

Hyperfilamentation of *crf1* and *zcf14* mutants depends on *UME6* expression

To verify that the enhanced expression of *UME6* in *crf1* and *zcf14* mutants leads to hyperfilamentous growth, both alleles of *UME6* were deleted in *crf1* and *zcf14* mutants and filamentation phenotypes of the resulting strains were examined under hypoxia and under normoxia, in the presence of 6 % CO_2. We observed that the *crf1 ume6* and *zcf14 ume6*

double mutant strains were unable to filament, forming smooth colonies under normoxic and hypoxic conditions (Fig. 11 A). Furthermore, *UME6* overexpression using the inducible *tet*-promoter (*tet*-on) [58], in the presence of the aTc, was able to trigger hyperfilamentation of the control strain under all oxygen conditions (Fig. 11 B). The results strongly suggest that *UME6* represents a downstream, repressed target of Crf1 and Zcf14 proteins, which in mutants lacking these factors is activated to allow hyperfilamentous growth.

Discussion

Phenotypic profiling of existing and newly identified mutants has revealed an astounding complexity with regard to the requirements for filamentation in *C. albicans.* Several mutants were found to completely lose the ability to form hyphae, not only under normoxia, as had been described previously, but also under hypoxia. Such mutants are defective in elements of the PKA signalling pathway including Ras1, Cyr1 [44,45], Tpk2 [11] or Flo8 [15], but also in transcription factors Ume6 [16], Eed1 [17] or Brg1 [20]. In contrast, mutants lacking the Tup1 or Nrg1 repressors were hyperfilamentous not only under normoxia, as described previously [48,49], but also during hypoxia. Aside these extremes, several mutants were unable to filament under normoxia, but were still able to form hyphae under hypoxia at 37 °C. These mutants, which previously had been described to be completely defective in formation of filaments under normoxia, are lacking the normoxic hyphal activators Hda1, Sko1 or Ptp2 [20], or Hgc1 [41]. Under hypoxia, a surprisingly large group of mutants was filamenting normally at 37 °C and show even increased filamentation at 25 °C in the presence of CO_2, as compared to the wild-type control strain, while completely losing the ability to form hyphae under normoxia. This phenotype was identified in mutants lacking transcription factors, including Ace2 [31,53,59], Ahr1 [60], Cap4 (unknown function), Rim101 [61], Tye7 [62], Wor4 [63] and Zcf24 (unknown function), or in mutants lacking kinases Akl1 [64] and Prr1 (unknown function). The elements identified by this class of mutants have a dual function, acting as normoxic activators but as hypoxic repressors of hypha formation. The paradigm for this function is the Efg1 transcription factor, which represents the first discovered hypoxic regulator of filamentation in *C. albicans* [29,33]. Efg1 acts as repressor of filamentation, since *efg1* mutants grow in the form of hyperfilamentous colonies during growth on agar, at temperatures < 37 °C, even in the absence of CO_2 [24]. Recently, a transcriptional regulatory hub consisting of Efg1, Ace2, Brg1 and Bcr1 proteins

has been described to regulate hypoxic filamentation [31]. Lack of Efg1 or Bcr1 share repressor functions, while Brg1 and Ace2 act as inducer of hypoxic filamentation [31]. Interestingly, defects in proteins interacting physically with Efg1 such as Flo8 or Czf1 [32] show significant defects in filamentation [15,33].

The role of CO_2 in gene regulation of *C. albicans* has hitherto been studied largely under normoxic conditions. Bicarbonate generated spontaneously or by the action of carbonic anhydrase Nce103 activates the Cyr1 adenylate cyclase and an increase of cAMP triggers the PKA pathway of filamentation [8]; in addition, a PKA-independent pathway of CO_2-dependent filamentation is operative [40]. Recently, hypoxia in combination with high CO_2 was shown to trigger hypha formation in liquid cultures of the wild-type strain, but only after exposure to 37 °C to initiate hypha formation, while no filamentation was observed at lower temperatures [20]. We had previously reported a hyperfilamentous phenotype at 25 °C without a previous 37 °C step, as well as a different transcriptome in a *sch9* mutant in low oxygen and high CO_2, but not, if CO_2 was omitted; a similar phenotype was obtained by inhibition of Tor1 kinase in wild-type cells grown on an agar surface [37]. Tor1 functions upstream of Sch9 in a common pathway that was shown to affect the phosphorylation status of Hog1 and consequently the activity of Brg1 [20]. Here, we have identified 7 mutants that show a *sch9*-like mutant phenotype, if hypoxia and elevated CO_2 are combined (referred to as class C mutants). Mutants lacking transcription factors including Gzf3 [65], Try4 [66], Zcf14 or Zcf21 [52] were hypoxically hyperfilamentous in the presence of high CO_2, but filamented normally under normoxia. Thus, Sch9 and its phenotypic mimics act as repressors of filamentation under hypoxia in a CO_2-dependent manner. Another set of mutants defective in Pbs2, Hog1 or Crf1 (Orf19.6874) proteins showed a deregulated filamentation phenotype at high CO_2 levels, not only under hypoxia but also under normoxia; In the case of the *crf1* mutant, hyperfilamentation was also observed in liquid medium. To note, Pbs2 is the MAP

kinase kinase functioning upstream of the Hog1 MAP kinase, which signals adaptation to stress and downregulates filamentation [20,67]. Conceptually, based on similar mutant phenotypes, the Crf1 transcription factor may be part of or even a downstream target of Pbs2/Hog1 proteins, but this hypothesis needs to be verified experimentally. Expression of *CRF1* appears to be regulated by several regulators that were found to bind to its promoter region including Sfl1/Sfl2 [68], Cph2 [69] and Tpk2 kinase [14]. We conclude that a significant number of proteins downregulates filamentation under hypoxia. Remarkably, none of the numerous tested mutants, which were all constructed under normoxia, showed a complete growth defect under hypoxia and single mutations causing this phenotype either have not yet been described or do not exist. Conceivably, hypoxic growth *per se* may depend on two or more signalling pathways or does not require dedicated induction pathways. More speculatively, filamentation is the default growth mode under hypoxia, which is mostly repressed to direct yeast growth in this condition. A scheme summarizing components repressing filamentation under hypoxia is shown in Fig. 12.

Transcriptional analysis of *crf1* and *zcf14* mutants, defective in putative zinc finger proteins, indicated that the *UME6* transcript was strongly upregulated, which occurred in the presence of CO_2 under all conditions for the *crf1* mutant and only under hypoxia for the *zcf14* mutant; in addition, upregulation of the *BRG1* transcript was detected solely in the *crf1* strain. Under normoxia, Ume6 is known to be required for hyphal extension and to function downstream of other transcription factors that promote filamentation, including Efg1 [16,70]. Low oxygen and high CO_2 were shown to upregulate the *UME6* transcript and to stabilize the Ume6 protein to stimulate hypoxic filamentation in cells growing in liquid media [42]. Here we add that Ume6 has an essential role for hypha formation under hypoxia also during surface growth, a condition, in which several normoxic inducers functioning upstream of Ume6 are not required. Crf1 appears to assume a general role in CO_2-mediated

downregulation of *UME6*, independently of oxygen levels and independent of fungal growth on a surface or in liquid, while the repressive function of Zcf14 is restricted to hypoxia and surface growth. Accordingly, the hyperfilamentous phenotype of *crf1* or *zcf14* mutants was abolished in a genetic background lacking the *UME6* gene. Further evidence for the repressive function of Crf1 was obtained by overexpression of *CRF1*, which completely blocked the hypoxic hyperfilamentation of several upregulated mutants, with exception of the *nrg1* mutant. These results identify *UME6* as a key direct or indirect repression target of Crf1 and suggest that the repressor function of Crf1 requires the presence of Nrg1. The mode of action of Crf1 and other identified repressors may in fact be to activate general repressors of filamentation Nrg1 and/or Tup1 under hypoxia at specific genomic sites. Recently, regulation of the Tup1 general suppressor by the Wor1 transcription factor has been discovered [71]; in this case, Tup1 was inactivated rather than activated by this interaction, as suspected here for the function of hypoxic repressors of filamentation acting on Nrg1/Tup1. Furthermore, because *CRF1* overexpression was able to suppress hyperfilamentation of *zcf14* and *efg1* mutants, it is possible that Crf1 functions downstream of Zcf14 and Efg1, which may enhance the repressive action of Crf1.

C. albicans adapts to oxygen-poor environments that occur frequently in the human host [21,22,27] by altering its metabolism [24-26], but also by regulating its cellular morphology [31]. Within the hypoxic environment of the gut, as well as under low-oxygen *in vitro* conditions [31], the fungus grows predominantly in an unicellular yeast form that favours its persistence as regular commensal [43,72]. Transcriptional regulators maintaining the yeast growth mode including Ahr1, Gzf3, Tye7, Try4 and Zcf21, as described here, also have a role in adherence to host cells and thereby favour commensal colonization [43,73,74]. In contrast, vigorous hypha formation of *C. albicans* wild-type cells has been observed in other low-oxygen settings, e.g. during escape from macrophages [75,76], transit

across epithelia [17,77] or within biofilms [74,78]. It thus appears that under hypoxia, *C. albicans* is able to break out of its habitual commensal yeast growth and to form hyphae, which are required for aspects of its survival, invasion or host cell interaction. The present discovery of a great number of fungal regulatory proteins, which repress filamentation under hypoxia suggests that hypha formation of *C. albicans* is generally suppressed (and occasionally relieved), rather than being specifically induced under low-oxygen conditions. Experimentally, this trait is especially visible at lower than body temperatures, but it reveals the hidden potential of *C. albicans* to regulate its morphology by environmental parameters, which may become apparent especially in hypoxic body niches of the human host.

Material and methods

Strains and media

C. albicans strains are listed in S1 Table. A collection of defined *C. albicans* mutants lacking known or putative transcription factors (307 mutants corresponding to 233 loci) or kinases (139 mutants corresponding to 63 loci) was provided by D. Sanglard and A. Mitchell [50-52]. These mutants are part of a collection of knockout mutants available at the Fungal Genetic Stock Center (http://www.fgsc.net/). Strains were grown in liquid YP medium (1 % yeast extract, 2% peptone) containing 2 % glucose (YPD) or 2 % sucrose (YPS). Solid YPS and Spider media [46] contained 2 % agar. Modified YPS medium contained 1 mM caffeine or 3 µg/ml anhydrotetracycline (aTC). An Invivo200 hypoxia chamber (Ruskinn) was used for hypoxic growth under 0.2 % O_2 in the presence or absence of 6 % CO_2. For growth under hypoxic conditions, liquid media were pre-equilibrated overnight under hypoxic conditions before inoculation.

***C. albicans* deletion strain construction**

For deletion of *UME6* in *cfr1* (TF63) and *zcf14* (DSY2892) mutant strains, two disruption cassettes were generated using plasmid pSFS5 [79]. All oligonucleotide primers used in the following are listed in S2 Table. The upstream region of the *UME6* ORF was amplified by genomic PCR using primers 5UTLFor/5UTLRev and cloned between *Sac*I and *Not*I sites of plasmid pSFS5 to generate pSFS-U5. The *UME6* downstream region was amplified using primers 3UTLFor/3UTLRev and cloned into *Not*I and *Kpn*I of pSFS-U5 to generate outer deletion cassette in plasmid pSFSL-U5U3. Similarly, primer pairs 5UTSFor/5UTSrev and 3UTSFor/3UTSRev were used for construction of an inner deletion cassette in plasmid pSFSS-U5U3. The *Sac*I-*Kpn*I fragment of pSFSL-U5U3 was used for disruption of the first *UME6* allele in *crf1* and *zcf14* strains. Chromosomal integration of the deletion cassette was confirmed by colony PCR of transformants using primers 5UTRcoloF and SAT1rev. Heterozygous transformants PDAU1 (*crf1/*crf1 *UME6/ume6*::*SAT1*) and PDZU1 (*zcf14/zcf14 UME6/ume6*::*SAT1*) were grown overnight in liquid YCB-BSA medium (20 g yeast carbon base, 4 g bovine serum albumin and 2 g yeast extract per litre) to induce the excision of the cassette by FLP mediated recombination [79]. The corresponding strains were identified by colony size on YPD plates containing 25 µg/ml nourseothricin. Subsequently, these nourseothricin-sensitive strains were again transformed with the *Sac*I-*Kpn*I fragment of pSFSS-U5U3 for disruption of the second allele of *UME6*, resulting into double mutant strains PDAU3 (*crf1/crf1 ume6*::*SAT1/ume6*::*FRT*) and PDZU3 (*zcf14/zcf ume6*::*SAT1/ume6*::*FRT*). Further PDAU3 and PDZU3 strains were grown in YCB-BSA medium to evict the *SAT1* marker as mentioned earlier resulting into homozygous strains PDAU4 (*crf1/crf1 ume6::FRT/ume6::FRT*) and PDZU4 (*zcf14/zcf14 ume6::FRT/ume6::FRT*).

Strain PDNRU (*nrg1/nrg1 ura3*::*imm434*/*URA3*) containing *URA3* at its native locus was constructed from strain MMC4 (*nrg1/nrg1 ura3*::*imm434*/ *ura3*::*imm434*), as described previously [80].

Overexpression plasmids

To generate overexpression plasmids for *CRF1* (*ORF19.6874*), oligonucleotide pair CRF1SalIFo/CRF1NotIrev was used for genomic amplification of the *CRF1* ORF, which was cloned into *Sal*I and *Not*I sites of plasmid pNIM1R-dTOM2 [57], replacing the *RFP* gene to generate pNIMRX-CRF1. Similarly, oligonucleotide pair ZCF14For/ZCF14Rev was used for cloning of the *ZCF14* (*ORF19.2647*) ORF, which was inserted into plasmid between *Sal*I and *Not*I sites of plasmid pNIMRX-RFP (pNIM1R-dTOM2), to generate pNIMRX-ZCF14. Overexpression by pNIMRX-CRF1 and pNIMRX-ZCF14 is activated by binding of tetracycline transactivator (tTA) protein to the tetO operator sequences upstream of the *OP4* operator of the *tet* promotor, thereby inducing transcription of *CRF1* or *ZCF14*. The tTA protein is encoded by the cartTA gene under control of the *TDH3* promotor on the same plasmid [57]; plasmids also contains a *sat1* cassette encoding nourseothricin resistance and a split *ADH1* gene, which can be used for genomic integration [57]. For genomic integration of plasmids pNIMRX-CRF1, pNIMRX-ZCF14 and pNIMRX-RFP into host strains, the plasmids were digested *Apa*I and *Sac*II, the digested products were purified and used for transformation. Positive transformants were selected on YPD medium containing 200 µg/ml nourseothricin and correct integration of overexpression plasmids into the *ADH1* locus was confirmed by colony PCR using primers ADH1-verif and NIM1verif.

The plasmid Clp10::P_{TET}-UME6 encoding the Ume6 protein was linearized with *Stu*I within the *RPS1* sequence and transformed into *C. albicans* CEC2907 [58] selecting for

uridine prototrophy; the resultant strain was named CLvW119. Correct plasmid integration at the *RPS1* locus was confirmed by colony PCR using primers ClpUL and ClpUR.

Acknowledgments

We thank A. Dominguez, B. Hube, D. Kadosh, H. Liu, A. Mitchell, S. Noble, D. Sanglard for providing strains. Supported by ERA-Net PathoGenoMics project OXYstress (http://www.pathogenomics-era.net/FundedProjects3rdJoint) and by the Infect-ERA JTC2 project FunComPath (http://www.funcompath.eu/).

References

1. Casadevall A, Pirofski LA. Accidental virulence, cryptic pathogenesis, martians, lost hosts, and the pathogenicity of environmental microbes. Eukaryot Cell. 2007;6: 2169-2174.
2. Ghannoum MA, Jurevic RJ, Mukherjee PK, Cui F, Sikaroodi M, Naqvi A, et al. Characterization of the oral fungal microbiome (mycobiome) in healthy individuals. PLoS Pathog. 2010;6: e1000713.
3. Brown GD, Denning DW, Gow NA, Levitz SM, Netea MG, White TC. Hidden killers: human fungal infections. Sci Transl Med. 2012;4: 165rv13.
4. Sudbery PE. Growth of *Candida albicans* hyphae. Nat Rev Microbiol. 2011;9: 737-748.
5. Koh AY. Murine models of *Candida* gastrointestinal colonization and dissemination. Eukaryot Cell. 2013;12: 1416-1422.
6. Gow NA, van de Veerdonk FL, Brown AJ, Netea MG. *Candida albicans* morphogenesis and host defence: discriminating invasion from colonization. Nat Rev Microbiol. 2011;10: 112-122.
7. Rocha CR, Schröppel K, Harcus D, Marcil A, Dignard D, Taylor BN, et al. Signaling through adenylyl cyclase is essential for hyphal growth and virulence in the pathogenic fungus *Candida albicans*. Mol Biol Cell. 2001;12: 3631-3643.
8. Klengel T, Liang WJ, Chaloupka J, Ruoff C, Schröppel K, Naglik JR, et al. Fungal adenylyl cyclase integrates CO2 sensing with cAMP signaling and virulence. Curr Biol. 2005;15: 2021-2026.
9. Xu XL, Lee RT, Fang HM, Wang YM, Li R, Zou H, Zhu Y, Wang Y. Bacterial peptidoglycan triggers *Candida albicans* hyphal growth by directly activating the adenylyl cyclase Cyr1p. Cell Host Microbe. 2008;4:28-39.
10. Sonneborn A, Bockmühl DP, Gerads M, Kurpanek K, Sanglard D, Ernst JF. Protein kinase A encoded by *TPK2* regulates dimorphism of *Candida albicans*. Mol Microbiol. 2000;35:386-396.
11. Bockmühl DP, Krishnamurthy S, Gerads M, Sonneborn A, Ernst JF. Distinct and redundant roles of the two protein kinase A isoforms Tpk1p and Tpk2p in morphogenesis and growth of *Candida albicans*. Mol Microbiol. 2001;42: 1243-1257.

12. Stoldt, VR, Sonneborn A, Leuker C, Ernst JF. Efg1, an essential regulator of morphogenesis of the human pathogen *Candida albicans*, is a member of a conserved class of bHLH proteins regulating morphogenetic processes in fungi. EMBO J. 1997;16: 1982-1991.
13. Lu Y, Su C, Mao X, Raniga PP, Liu H, Chen J. Efg1-mediated recruitment of NuA4 to promoters is required for hypha-specific Swi/Snf binding and activation in *Candida albicans*. Mol Biol Cell. 2008;19: 4260-4272.
14. Schaekel A, Desai PR, Ernst JF. Morphogenesis-regulated localization of protein kinase A to genomic sites in *Candida albicans*. BMC Genomics. 2013;14: 842.
15. Cao F, Lane S, Raniga PP, Lu Y, Zhou Z, Ramon K, Chen J, Liu H. The Flo8 transcription factor is essential for hyphal development and virulence in *Candida albicans*. Mol Biol Cell. 2006;17: 295-307.
16. Banerjee M, Thompson DS, Lazzell A, Carlisle PL, Pierce C, Monteagudo C, et al. *UME6*, a novel filament-specific regulator of *Candida albicans* hyphal extension and virulence. Mol Biol Cell. 2008;19:1354–1365.
17. Martin R, Moran GP, Jacobsen ID, Heyken A, Domey J, Sullivan DJ, et al. The *Candida albicans*-specific gene *EED1* encodes a key regulator of hyphal extension. PLoS One. 2011; 6: e18394.
18. Lu Y, Su C, Wang A, Liu H. Hyphal development in *Candida albicans* requires two temporally linked changes in promoter chromatin for initiation and maintenance. PLoS Biol. 2011 Jul;9(7):e1001105.
19. Lu Y, Su C, Liu H. A GATA transcription factor recruits Hda1 in response to reduced Tor1 signaling to establish a hyphal chromatin state in *Candida albicans*. PLoS Pathog. 2012;8: e1002663.
20. Su C, Lu Y, Liu H. Reduced TOR signaling sustains hyphal development in *Candida albicans* by lowering Hog1 basal activity. Mol Biol Cell. 2013;24: 385-397.
21. Ernst JF, Tielker D. Responses to hypoxia in fungal pathogens. Cell Microbiol. 2009;11: 183-190.
22. Grahl N, Cramer Jr, RA (2010). Regulation of hypoxia adaptation: an overlooked virulence attribute of pathogenic fungi? Med Mycol. 48: 1-15.

23. Nizet V, Johnson RS. Interdependence of hypoxic and innate immune responses. Nat Rev Immunol. 2009;9: 609-617.
24. Setiadi ER, Doedt T, Cottier F, Noffz C, Ernst JF. Transcriptional response of *Candida albicans* to hypoxia: linkage of oxygen sensing and Efg1p-regulatory networks. J Mol Biol. 2006;361: 399-411.
25. Sosinska GJ, de Groot PWJ, Teixeira de Mattos MJ, Dekker HL, de Koster CG, Hellingwerf KJ, et al. Hypoxic conditions and iron restriction affect the cell-wall proteome of *Candida albicans* grown under vagina-simulative conditions. Microbiology. 2008;154: 510-520.
26. Synnott JM, Guida A, Mulhern-Haughey S, Higgins DG, Butler G. Regulation of the hypoxic response in *Candida albicans*. Eukaryot Cell. 2010;9: 1734-1746.
27. Sellam A, van het Hoog M, Tebbji F, Beaurepaire C, Whiteway M, Nantel A. Modeling the transcriptional regulatory network that controls the early hypoxic response in *Candida albicans*. Eukaryot Cell. 2014;13: 675-690.
28. Znaidi S, van Wijlick L, Cervantes AH, Sertour N, Desseyn JL, Vincent F, et al. Systematic gene overexpression in *Candida albicans* identifies a regulator of early adaptation to the mammalian gut. Cell Microbiol. 2018;11: e12890.
29. Sonneborn A, Bockmühl DP, Ernst JF. Chlamydospore formation in *Candida albicans* requires the Efg1p morphogenetic regulator. Infect Immun. 1999;67: 5514-5517.
30. Doedt T, Krishnamurthy S, Bockmühl DP, Tebarth B, Stempel C, Russell CL, et al. APSES proteins regulate morphogenesis and metabolism in *Candida albicans*. Mol Biol Cell 2004;15: 3167-3180.
31. Desai PR, van Wijlick L, Kurtz D, Juchimiuk M, Ernst JF. Hypoxia and Temperature Regulated Morphogenesis in *Candida albicans*. PLoS Genet. 2015;11: e1005447.
32. Noffz CS, Liedschulte V, Lengeler K, Ernst JF. Functional mapping of the *Candida albicans* Efg1 regulator. Eukaryot Cell. 2008;7: 881-893.
33. Brown DH Jr, Giusani AD, Chen X, Kumamoto CA. Filamentous growth of *Candida albicans* in response to physical environmental cues and its regulation by the unique *CZF1* gene. Mol Microbiol. 1999;34: 651-662.

34. Pierce JV, Kumamoto CA. Variation in *Candida albicans EFG1* expression enables host-dependent changes in colonizing fungal populations. MBio. 2012;3: e00117-00112.
35. Pierce JV, Dignard D, Whiteway M, Kumamoto CA. Normal adaptation of *Candida albicans* to the murine gastrointestinal tract requires Efg1p-dependent regulation of metabolic and host defense genes. Eukaryot Cell. 2013;12: 37-49.
36. Pande K, Chen C, Noble SM. Passage through the mammalian gut triggers a phenotypic switch that promotes *Candida albicans* commensalism. Nat Genet. 2013;45: 1088-1091.
37. Stichternoth C, Fraund A, Setiadi E, Giasson L, Vecchiarelli A, Ernst JF. Sch9 kinase integrates hypoxia and CO2 sensing to suppress hyphal morphogenesis in *Candida albicans*. Eukaryot Cell. 2011;10: 502-511.
38. Cottier F, Raymond M, Kurzai O, Bolstad M, Leewattanapasuk W, Jiménez-López C, , et al. The bZIP transcription factor Rca1p is a central regulator of a novel CO_2 sensing pathway in yeast. PLoS Pathog. 2012;8: e1002485.
39. Martin R, Pohlers S, Mühlschlegel FA, Kurzai O. CO_2 sensing in fungi: at the heart of metabolic signaling. Curr Genet. 2017;63: 965-972.
40. Du H, Guan G, Xie J, Cottier F, Sun Y, Jia W, et al. The transcription factor Flo8 mediates CO_2 sensing in the human fungal pathogen *Candida albicans*. Mol Biol Cell. 2012;23: 2692-2701.
41. Wang A, Raniga PP, Lane S, Lu Y, Liu H. Hyphal chain formation in *Candida albicans*: Cdc28-Hgc1 phosphorylation of Efg1 represses cell separation genes. Mol Cell Biol. 2009;29: 4406-4416.
42. Lu Y, Su C, Solis NV, Filler SG, Liu H. Synergistic regulation of hyphal elongation by hypoxia, CO(2), and nutrient conditions controls the virulence of *Candida albicans*. Cell Host Microbe. 2013;14: 499-509.
43. Böhm L, Torsin S, Tint SH, Eckstein MT, Ludwig T, Pérez JC. The yeast form of the fungus *Candida albicans* promotes persistence in the gut of gnotobiotic mice. PLoS Pathog. 2017;13: e1006699.
44. Inglis DO, Sherlock G. Ras signaling gets fine-tuned: regulation of multiple pathogenic traits of *Candida albicans*. Eukaryot Cell. 2013;12: 1316-1325.

45. Hogan DA, Muhlschlegel FA. *Candida albicans* developmental regulation: adenylyl cyclase as a coincidence detector of parallel signals. Curr Opin Microbiol. 2011;14: 682-686.
46. Liu H, Köhler J, Fink GR. Suppression of hyphal formation *in Candida albicans* by mutation of a STE12 homolog. Science. 1994;266: 1723-1726. Erratum in Science. 1995;267:217.
47. Homann OR, Dea J, Noble SM, Johnson AD. A phenotypic profile of the *Candida albicans* regulatory network. PLoS Genet. 2009;5: e1000783.
48. Braun BR, Johnson AD. Control of filament formation in *Candida albicans* by the transcriptional repressor TUP1. Science. 1997;277: 105-109.
49. Murad AMA, Leng P, Straffon M, Wishart J, Macaskill S, MacCallum D, et al. NRG1 represses yeast–hypha morphogenesis and hypha-specific gene expression in *Candida albicans*. EMBO J. 2001;20: 4742–4752.
50. Nobile CJ, Mitchell AP. Regulation of cell-surface genes and biofilm formation by the *C. albicans* transcription factor Bcr1p. Curr Biol. 2005;15: 1150-1155.
51. Blankenship JR, Fanning S, Hamaker JJ, Mitchell AP. An Extensive Circuitry for Cell Wall Regulation in *Candida albicans*. PLoS Pathog. 2010;6: e1000752.
52. Vandeputte P, Ischer F, Sanglard D, Coste AT. In vivo systematic analysis of *Candida albicans* Zn2-Cys6 transcription factors mutants for mice organ colonization. PLoS One. 2011;6: e26962..
53. Mulhern SM, Logue ME, Butler G. *Candida albicans* transcription factor Ace2 regulates metabolism and is required for filamentation in hypoxic conditions. Eukaryot Cell. 2006;5: 2001-2013.
54. Zhang F, Kirouac M, Zhu N, Hinnebusch AG, Rolfes RJ. Evidence that complex formation by Bas1p and Bas2p (Pho2p) unmasks the activation function of Bas1p in an adenine-repressible step of ADE gene transcription. Mol Cell Biol. 1997;17:3272-3283.

55. Wangsanut T, Ghosh AK, Metzger PG, Fonzi WA, Rolfes RJ. Grf10 and Bas1 regulate transcription of adenylate and one-carbon biosynthesis genes and affect virulence in the human fungal pathogen *Candida albicans*. mSphere. 2017;2: e00161-17.
56. Fox EP, Bui CK, Nett JE, Hartooni N, Mui MC, Andes DR, et al. An expanded regulatory network temporally controls *Candida albicans* biofilm formation. Mol Microbiol. 2015;96: 1226-1239.
57. Prieto D, Román E, Correia I, Pla J. The HOG pathway is critical for the colonization of the mouse gastrointestinal tract by *Candida albicans*. PLoS One. 2014 Jan 27;9: e87128.
58. Chauvel M, Nesseir A, Cabral V, Znaidi S, Goyard S, Bachellier-Bassi S, et alF. A versatile overexpression strategy in the pathogenic yeast Candida albicans: identification of regulators of morphogenesis and fitness. PLoS One. 2012;7: e45912.
59. Saputo S, Kumar A, Krysan DJ. Efg1 directly regulates *ACE2* expression to mediate cross talk between the cAMP/PKA and RAM pathways during *Candida albicans* morphogenesis. Eukaryot Cell. 2014;13: 1169-1180.
60. Askew C, Sellam A, Epp E, Mallick J, Hogues H, Mullick A, et al. The zinc cluster transcription factor Ahr1p directs Mcm1p regulation of Candida albicans adhesion. Mol Microbiol. 2011;79: 940-953.
61. Davis D, Wilson RB, Mitchell AP. RIM101-dependent and-independent pathways govern pH responses in *Candida albicans*. Mol Cell Biol. 2000;20: 971-978.
62. Askew C, Sellam A, Epp E, Hogues H, Mullick A, Nantel A, Whiteway M. Transcriptional regulation of carbohydrate metabolism in the human pathogen *Candida albicans*. PLoS Pathog. 2009;5: e1000612.
63. Lohse MB, Johnson AD. Identification and characterization of Wor4, a new transcriptional regulator of white-opaque switching. G3 (Bethesda). 2016;6: 721-729.
64. Bar-Yosef H, Gildor T, Ramírez-Zavala B, Schmauch C, Weissman Z, Pinsky M, et al. A Global Analysis of Kinase Function in Candida albicans Hyphal Morphogenesis Reveals a Role for the Endocytosis Regulator Akl1. Front Cell Infect Microbiol. 2018;8: 17.
65. Wang Y, Cao YY, Jia XM, Cao YB, Gao PH, Fu XP, et al. Cap1p is involved in multiple pathways of oxidative stress response in *Candida albicans*. Free Radic Biol Med. 2006;40: 1201-1209.
66. Finkel JS, Xu W, Huang D, Hill EM, Desai JV, Woolford CA, et al. Portrait of Candida albicans adherence regulators. PLoS Pathog. 2012;8: e1002525.

67. Arana DM, Nombela C, Alonso-Monge R, Pla J. The Pbs2 MAP kinase kinase is essential for the oxidative-stress response in the fungal pathogen *Candida albicans*. Microbiology. 2005;151: 1033-1049.
68. Znaidi S, Nesseir A, Chauvel M, Rossignol T, d'Enfert C. A comprehensive functional portrait of two heat shock factor-type transcriptional regulators involved in *Candida albicans* morphogenesis and virulence. PLoS Pathog. 2013;9: e1003519.
69. Lane S, Di Lena P, Tormanen K, Baldi P, Liu H. Function and Regulation of Cph2 in Candida albicans. Eukaryot Cell. 2015;14: 1114-1126.
70. Zeidler U, Lettner T, Lassnig C, Müller M, Lajko R, Hintner H, et al. UME6 is a crucial downstream target of other transcriptional regulators of true hyphal development in *Candida albicans*. FEMS Yeast Res. 2009;9: 126-142.
71. Alkafeef SS, Yu C, Huang L, Liu H. Wor1 establishes opaque cell fate through inhibition of the general co-repressor Tup1 in *Candida albicans*. PLoS Genet. 2018;14: e1007176.
72. Vautier S, Drummond RA, Chen K, Murray GI, Kadosh D, Brown AJ, et al. *Candida albicans* colonization and dissemination from the murine gastrointestinal tract: the influence of morphology and Th17 immunity. Cell Microbiol. 2015;17: 445-450.
73. Pérez JC, Johnson AD. Regulatory circuits that enable proliferation of the fungus *Candida albicans* in a mammalian host. PLoS Pathog. 2013;9: e1003780.
74. Finkel JS, Mitchell AP. Genetic control of *Candida albicans* biofilm development. Nat Rev Microbiol. 2011;9: 109-118.
75. Bain JM, Lewis LE, Okai B, Quinn J, Gow NA, Erwig LP. Non-lytic expulsion/exocytosis of *Candida albicans* from macrophages.
76. Jiménez-López C, Lorenz MC. Fungal immune evasion in a model host-pathogen interaction: *Candida albicans* versus macrophages. PLoS Pathog. 2013;9(11): e1003741.
77. Zink S, Nass T, Rösen P, Ernst JF. Migration of the fungal pathogen *Candida albicans* across endothelial monolayers. Infect Immun. 1996;64: 5085-5091.
78. Stichternoth C, Ernst JF. Hypoxic adaptation by Efg1 regulates biofilm formation by *Candida albicans*. Appl Environ Microbiol. 2009;75: 3663-3672.
79. Sasse C, Schillig R, Dierolf F, Weyler M, Schneider S, Mogavero S, et al. The transcription factor Ndt80 does not contribute to Mrr1-, Tac1-, and Upc2-mediated fluconazole resistance in *Candida albicans*. PLoS One. 2011;6: e25623.

80. Prill SK, Klinkert B, Timpel C, Gale CA, Schröppel K, Ernst JF. *PMT* family of *Candida albicans*: five protein mannosyltransferase isoforms affect growth, morphogenesis and antifungal resistance. Mol Microbiol. 2005;55: 546-60.

Figure legends

Fig. 1. Filamentation phenotypes of *C. albicans* mutants lacking known regulators of normoxic filamentation. Homozygous mutants carrying the indicated mutant alleles were grown on YPS agar under hypoxia (0.2 % O_2) or under normoxia (at 37 °C on Spider agar); as indicated, cells were incubated without (-) or with (+) 6 % CO_2. Following growth for 2 d at 37 °C or 4 d at 25 °C, filamentation phenotypes of colonies were assessed. Strain CAF2-1 was used as wild-type reference to established mutants known to be defective in (A, B) initiation and signalling, (C) repression and (D) maintenance of filamentation (listed in S1 Table). Colonies were found to be defective in filamentation (white squares) or to form few or abundant filaments (grey and black squares); phenotypic heterogeneity among single colonies is indicated by black-white/grey bipartite squares.

Fig. 2. Filamentation phenotypes of mutants with aberrant hypoxic filamentation identified by screening. Homozygous mutants carrying the indicated mutant alleles were identified by screening of mutant libraries lacking transcription factors or kinases. Filamentation phenotypes of control strain CAF2-1 were compared to (A) mutants with phenotypes similar the *sch9* mutant [37], (B) mutants with reduced and enhanced filamentation under normoxia and hypoxia, respectively and (C) mutants with derepressed filamentation at 25 °C in the presence of 6 % CO_2. Phenotypes were recorded as in Fig. 1.

Fig. 3. Filamentation phenotypes at different temperatures. Homozygous mutants carrying the indicated mutant alleles (S1 Table) were grown on YPS agar surface under normoxia 25, 30 or 33 °C. After incubation for 4 d (25 °C), 3 d (30 °C) or 2 d (33 °C) photographs of representative single colonies were taken.

Fig. 4. Hypoxic and normoxic filamentation phenotypes of *crf1*, *bas1* and *zcf14* mutants. Photographs of representative single colonies of strains CAF2-1(wild-type control), TF63 (*crf1*), TF16 (*bas1*) and DSY2892 (*zcf14*), grown on YPS agar under normoxia or hypoxia (0.2 % O_2) with 6 % CO_2 for 4 d at 25 °C or 2 d at 37 °C.

Fig. 5. Cell morphology of *crf1* and *zcf14* mutants in liquid medium. Strains CAF2-1 (wild-type control), TF63 (*crf1)* and DSY2892 (*zcf14*) were grown in liquid YPS medium at 30 °C (A) under hypoxia (0.2 % O_2) with 6 % CO_2, or (B) under normoxia with 6 % CO_2. Cells were harvested at 0 h, 6 h, 12 h and 24 h and photographed at 63 fold magnification.

Fig. 6. Crf1-dependent regulation of key regulators of filamentation under surface growth. A preculture of strains CAF2-1 (wild-type control) and TF63 (*crf1*) strains was grown at 30 °C in YPS liquid medium to the logarithmic phase (t = 0 min) and then plated on YPS agar, followed by 12 and 24 h of incubation under normoxia or hypoxia (0.2% O_2) with 6 % CO_2 at 30˚C. Total RNA of preculture and surface-grown cells was isolated and analysed by qPCR using gene specific primers for *UME6*, *BRG1* and *NRG1*. At each time point three biological replicates and three technical replicates of transcript levels were determined and values were calculated relative to the *ACT1* transcript (RTL), as mean ± standard deviations.

Fig. 7. Zcf14-dependent regulation of key regulators of filamentation under surface growth. Transcript levels of genes *UME6*, *BRG1* and *NRG1* in strains CAF2-1 and DSY2892 (*zcf14*) were determined and evaluated as in Fig. 6.

Fig. 8. Crf1- and Zcf14-dependent regulation of key regulatory genes of filamentation during growth in liquid medium. Transcript levels of genes *UME6*, *BRG1*, *NRG1* and *TUP1* in strains CAF2-1, TF63 (*crf1*) and DSY63 (*zcf14*) were determined by generating a preculture of strains in YPS liquid medium (t = 0 min), which was used to inoculate liquid YPS medium, which was incubated for 12 and 24 h under normoxia or hypoxia (0.2 % O_2), in the presence of 6 % CO_2 conditions at 30 °C. Total RNA of triplicate cultures was isolated at each time point and used to determine specific transcript levels by qPCR. Values were evaluated as in Fig. 6.

Fig. 9. Regulation of *CRF1* and *ZCF14.* Strain CAF2-1 was pregrown in YPS liquid medium, followed by growth on YPS agar under normoxia (white bars) or hypoxia with 6 % CO_2 (black bars) for 12 and 24 h at 30 °C as in Fig. 6. Transcript levels of genes *CRF1* and *ZCF14* were determined and evaluated as in Fig. 6.

Fig. 10. Overexpression of *CRF1* suppresses filamentation. Plasmids pNIMRX-RFP (control), pNIMRX-CRF1 (*CRF* overexpression) and pNIMRX-ZCF14 (*ZCF14* overexpression) were transformed in strains CAF2-1 (wild-type), HLC52 (*efg1)*, CJN702 (*bcr1)*, TF63 (*crf1)*, DSY2892 (*zcf14)* and PDNRU (*nrg1*). Transformants were grown on YPS agar containing or not containing 3 µg/ml anhydrotetracycline (aTC) and incubated under hypoxia (A) or normoxia (B) with CO_2 at 25 °C or under hypoxia at 37 ˚C (C). Colonies were defective in filamentation (white squares) or containing few or abundant filaments (grey and black squares, respectively).

Fig. 11. Crf1- and Zcf14-mediated suppression of filamentation depends on *UME6* expression. (A) Deletion of *UME6* abolishes filamentation caused by deletion of *CRF1* or

ZCF14. Strains tested were CAF2-1 (control),TF63 (*crf1*), DK312 (*ume6*), PDAU3 (*crf1*/crf1 *UME6*/*ume6*), PDAU4 (*crf1*/*crf1 ume6/ume6*), DSY2892 (*zcf14/zcf14*), PDZU3 (*zcf14/zcf14 UME6/ume6*), and PDZU4(*zcf14/zcf14 ume6/ume6*) (B) Overexpression of *UME6* induces filamentation under hypoxia in wild-type cells**.** Strain CLvW119 carrying plasmid pClp10TETUME6 expressing *UME6* under control of the inducible *tet* promoter was grown either in the absence or presence of 3 µg/ml anhydrotetracycline (aTC); in the presence of aTC, *UME6* overexpression occurs. All phenotypes were determined following growth at 25 °C on YPS agar under normoxia or hypoxia (0.2 % O_2) with 6 % CO_2 .

Fig. 12. Summary scheme of proteins repressing filamentation under hypoxia. *C. albicans* uses the indicated proteins to downregulate hypha formation under hypoxia during growth on an agar surface at 25 °C.

S1 Fig. Growth of *crf1* mutant is independent of adenine. (A) Spot dilution assay of strains on SD agar with or without 0.2 mM adenine. Logarithmically grown cells were serially diluted 10fold and spotted (top-to-bottom). Plates were examined after incubation under normoxia or hypoxia (0.2 % O_2) with 6 % CO_2 at 30 °C for 3 d. (B) Growth of strains in liquid SD medium without and with 0.2 mM adenine at 30 °C was monitored by measuring OD_{600} nm values at the indicated times. Strains tested were CAF2-1 and SN250 (wild-type controls), TF63 (*crf1*) and TF16 (*bas1*).

S2 Fig. Crf1-dependent regulation of key regulators of filamentation under surface growth. Transcript levels of genes *EFG1*, *CPH1* and *TUP1* in strains CAF2-1 and TF63 (*crf1*) were determined and evaluated as in Fig. 6.

S3 Fig. Zcf14-dependent regulation of key regulators of filamentation under surface growth. Transcript levels of genes *EFG1*, *CPH1* and *TUP1* in strains CAF2-1 and DSY2892 (*zcf14*) were determined and evaluated as in Fig. 6.

S4 Fig. Complementation of *crf1* and *zcf14* mutant phenotypes. Plasmids pNIMRX-CRF1 and pNIMRX-ZCF14 were transformed in CAF2-1 (control strain) and homozygous mutants TF63 (*crf1*) and DSY2892 (*zcf14*). Transformants were grown on YPS agar containing or not containing 3 µg/ml anhydrotetracycline (aTC); in the absence of aTC, *CRF1* and *ZCF14* are overexpressed. Cells were incubated under hypoxia (A) or normoxia (B) with CO_2 at 25 °C.

S1 Table. *C. albicans* strains.

S2 Table. List of oligonucleotides.

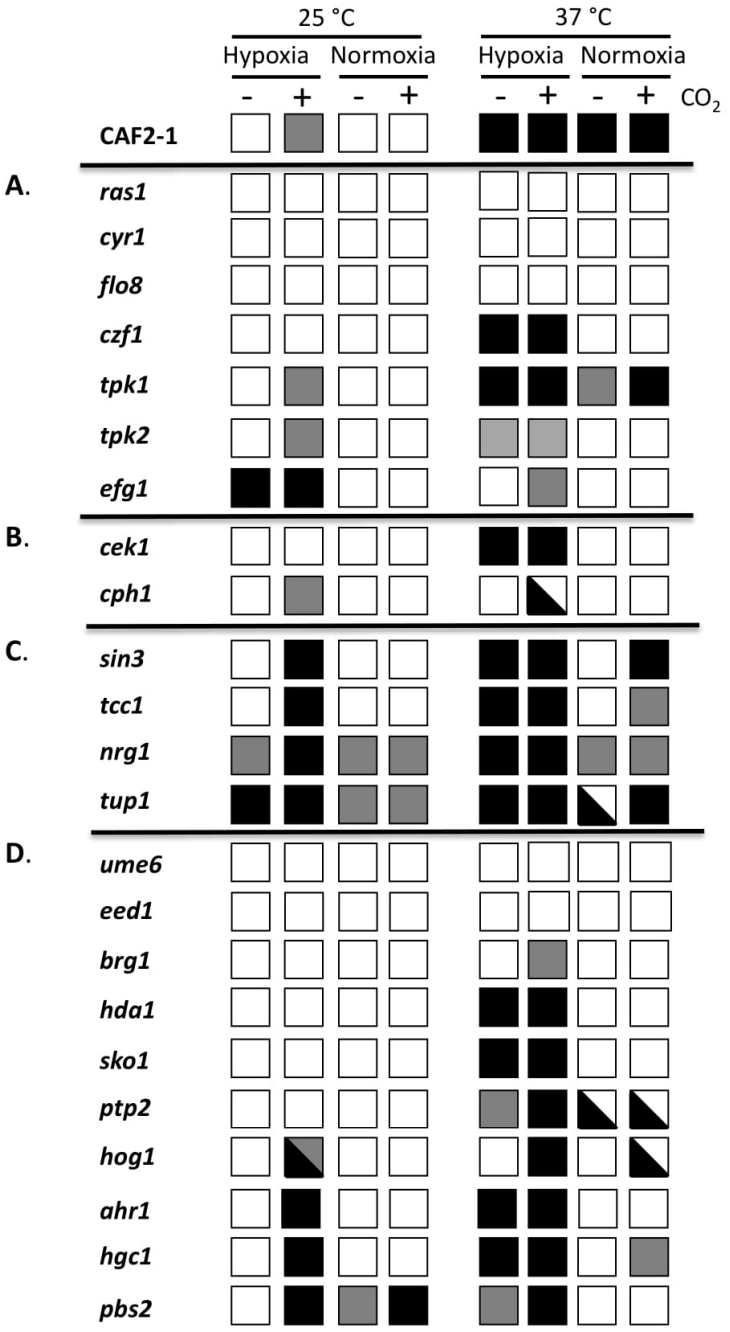
25 °C
37 °C
Hypoxia
Normoxia
Hypoxia
Normoxia
- + - + - + - + CO2
CAF2-1
A.
ras1
cyr1
flo8
czf1
tpk1
tpk2
efg1
B.
cek1
cph1
C.
sin3
tcc1
nrg1
tup1
D.
ume6
eed1
brg1
hda1
sko1
ptp2
hog1
ahr1
hgc1
pbs2

Figure 1

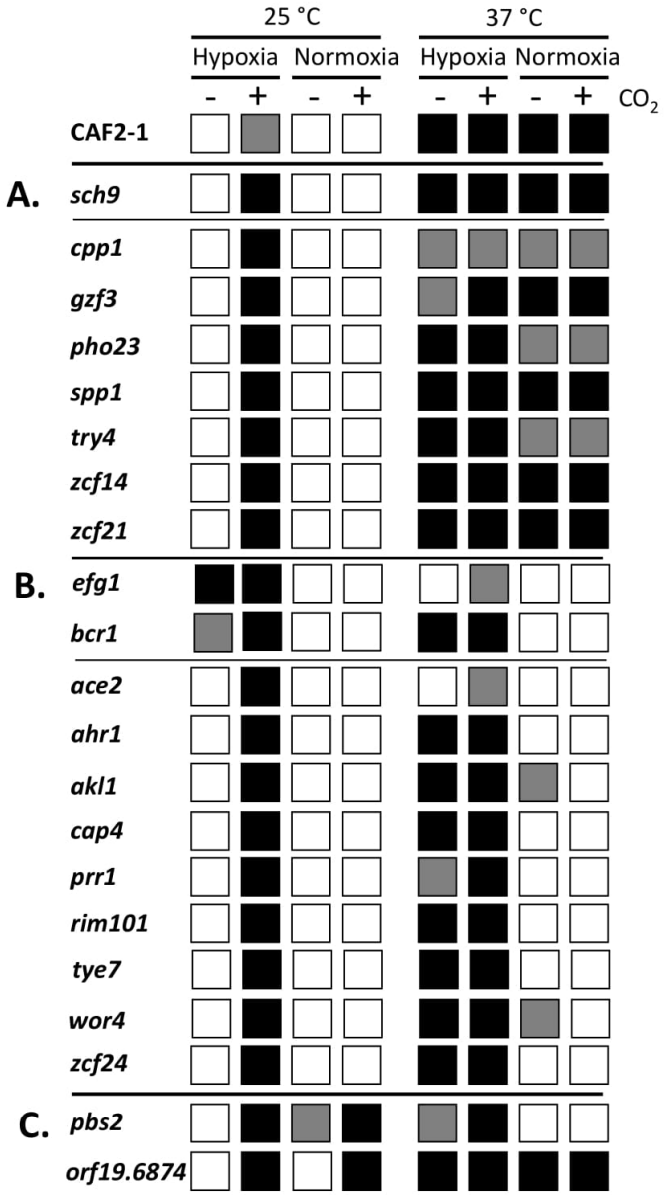
25 °C
37 °C
Hypoxia
Normoxia
Hypoxia
Normoxia
- + - + - + - + CO2
CAF2-1
A.
sch9
cpp1
gzf3
pho23
spp1
try4
zcf14
zcf21
B.
efg1
bcr1
ace2
ahr1
akl1
cap4
prr1
rim101
tye7
wor4
zcf24
C.
pbs2
orf19.6874

Figure 2

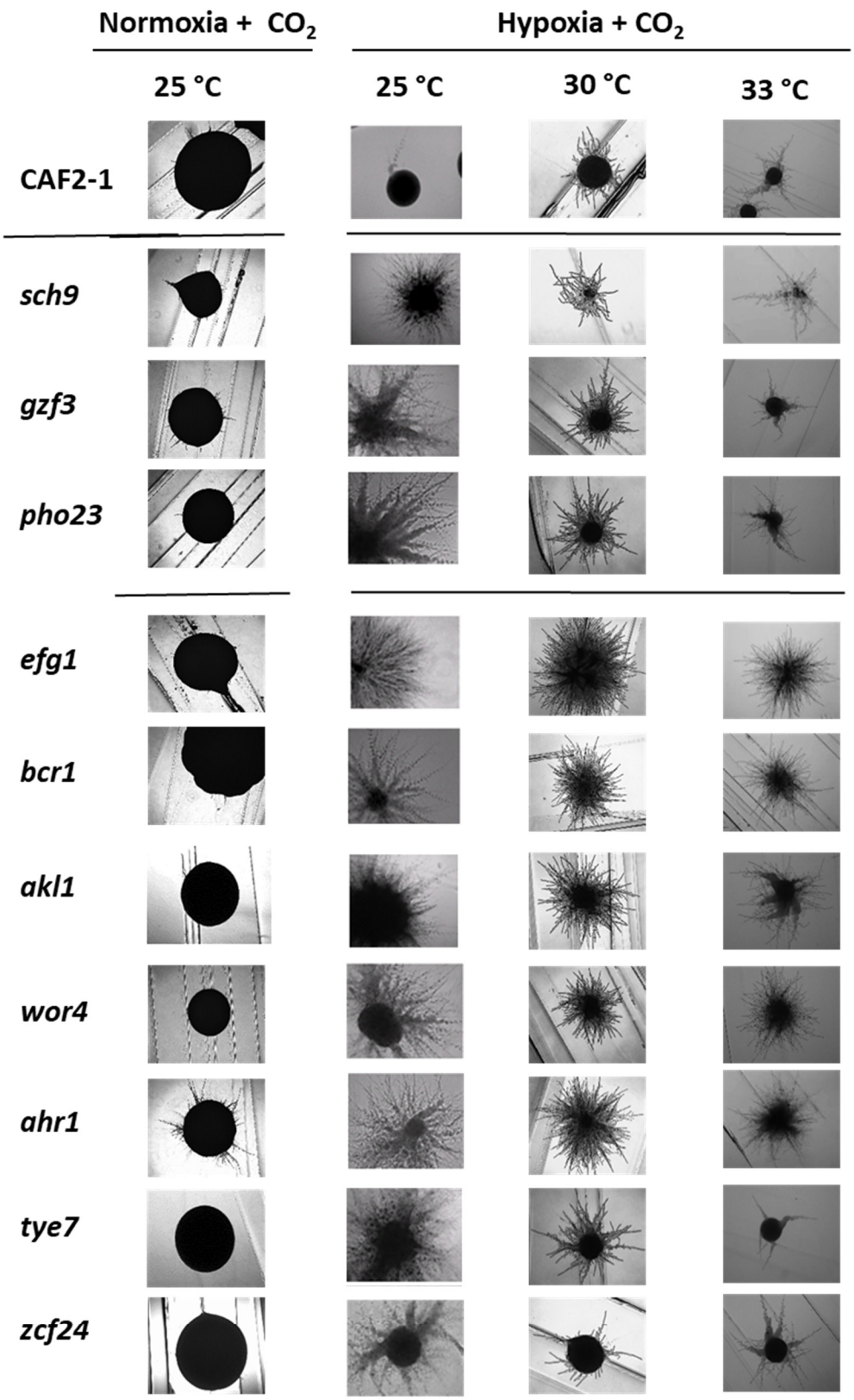
Normoxia + CO_2
Hypoxia + CO_2
25 °C
25 °C
30 °C
33 °C
CAF2-1
sch9
gzf3
pho23
efg1
bcr1
akl1
wor4
ahr1
tye7
zcf24

Figure 3

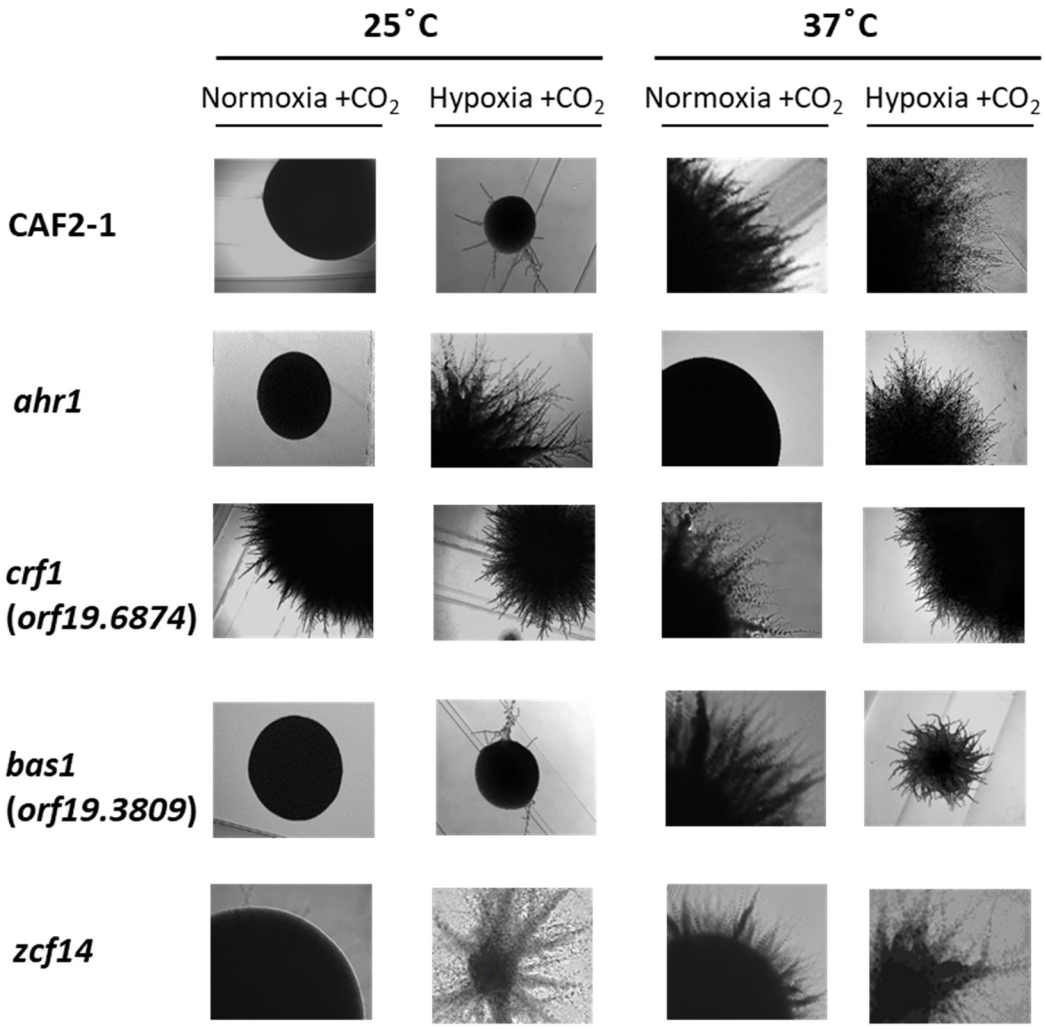
25˚C
37˚C
Normoxia +CO2
Hypoxia +CO2
Normoxia +CO2
Hypoxia +CO2
CAF2-1
ahr1
crf1
(orf19.6874)
bas1
(orf19.3809)
zcf14

Figure 4

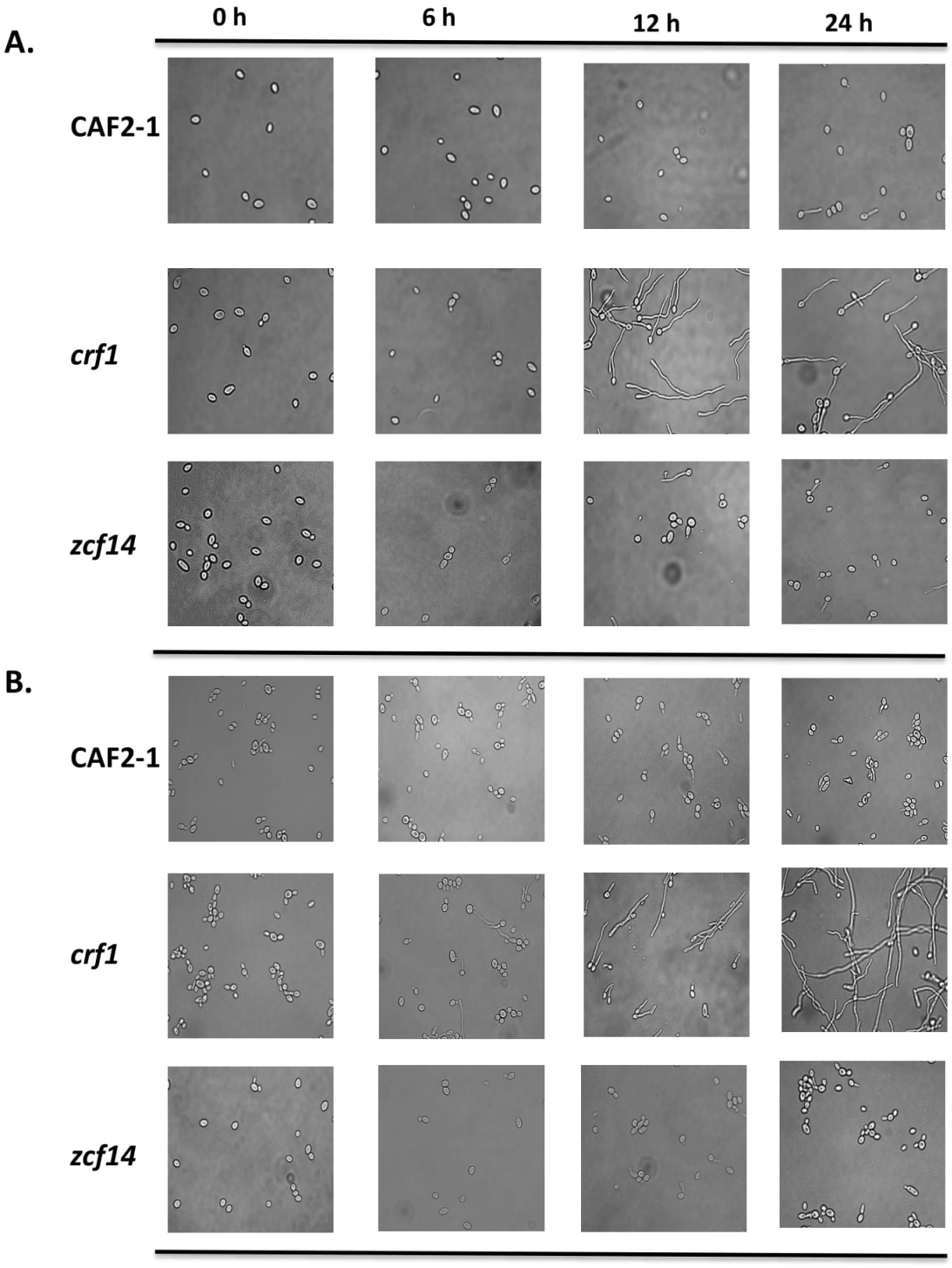

Figure 5

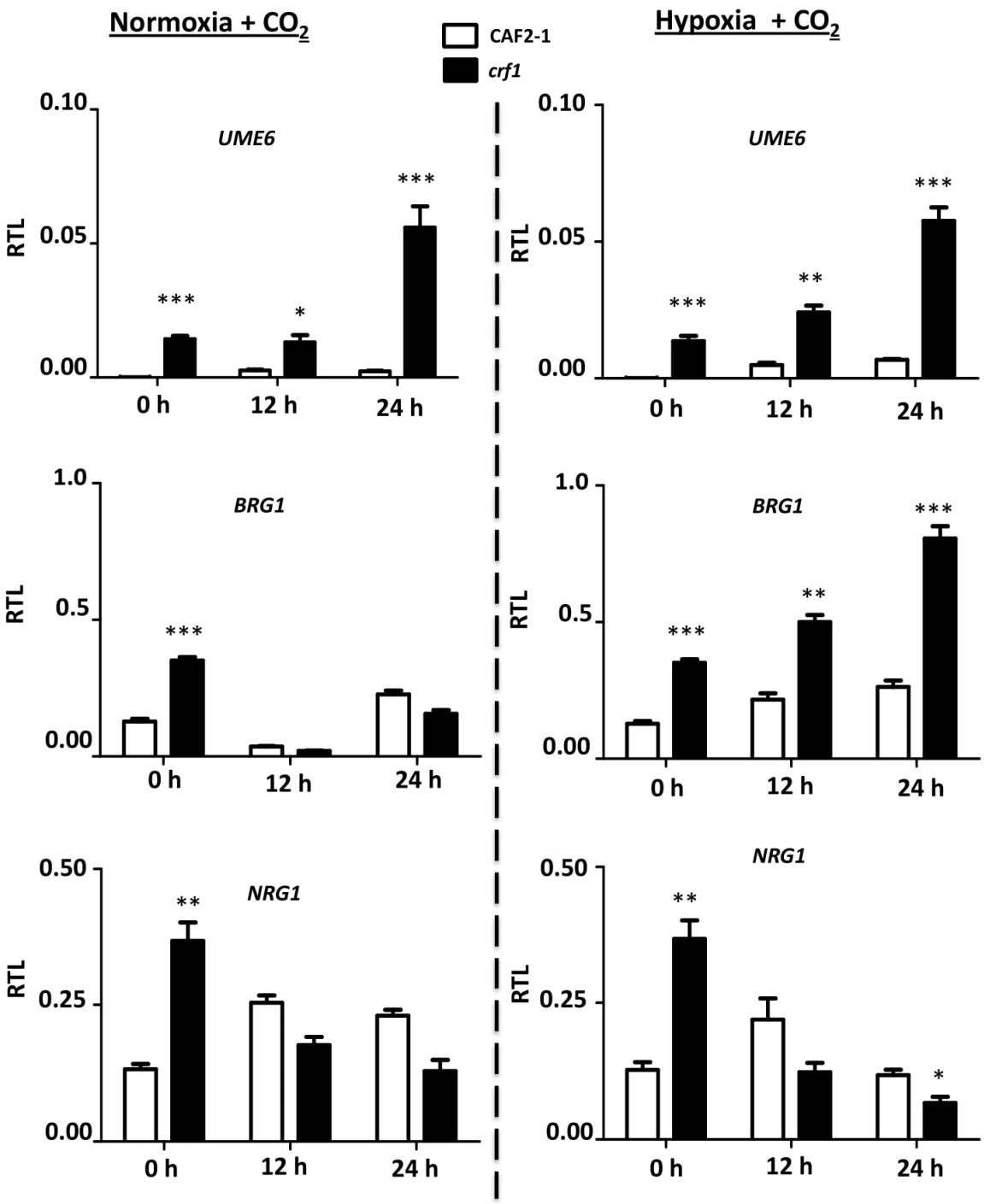
Normoxia + CO2
Hypoxia + CO2
CAF2-1
crf1
UME6
BRG1
NRG1
RTL
0 h
12 h
24 h

Figure 6

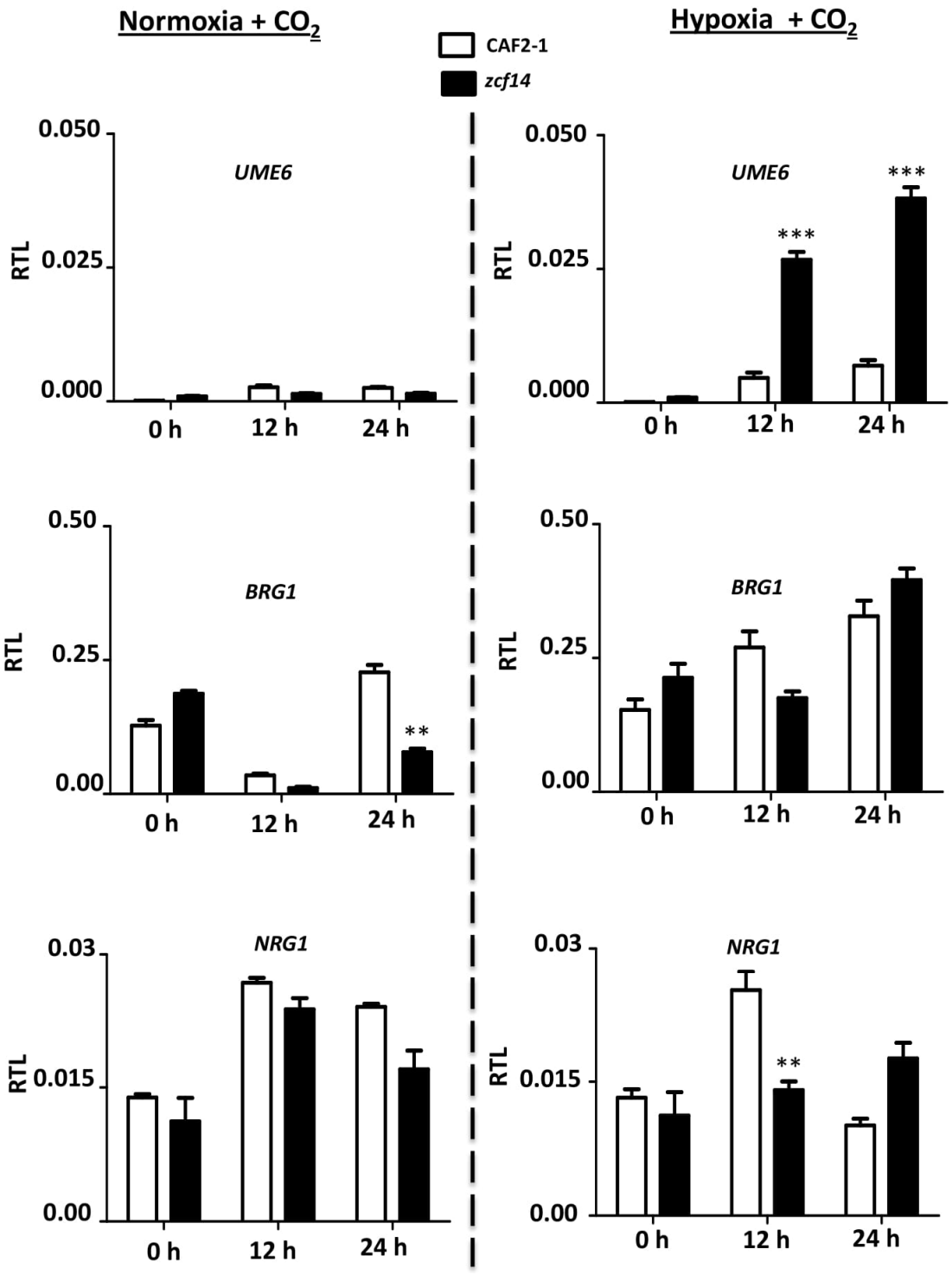
Normoxia + CO2
Hypoxia + CO2
CAF2-1
zcf14
UME6
BRG1
NRG1
RTL
0.050
0.025
0.000
0.50
0.25
0.00
0.03
0.015
0 h
12 h
24 h
***
**

Figure 7

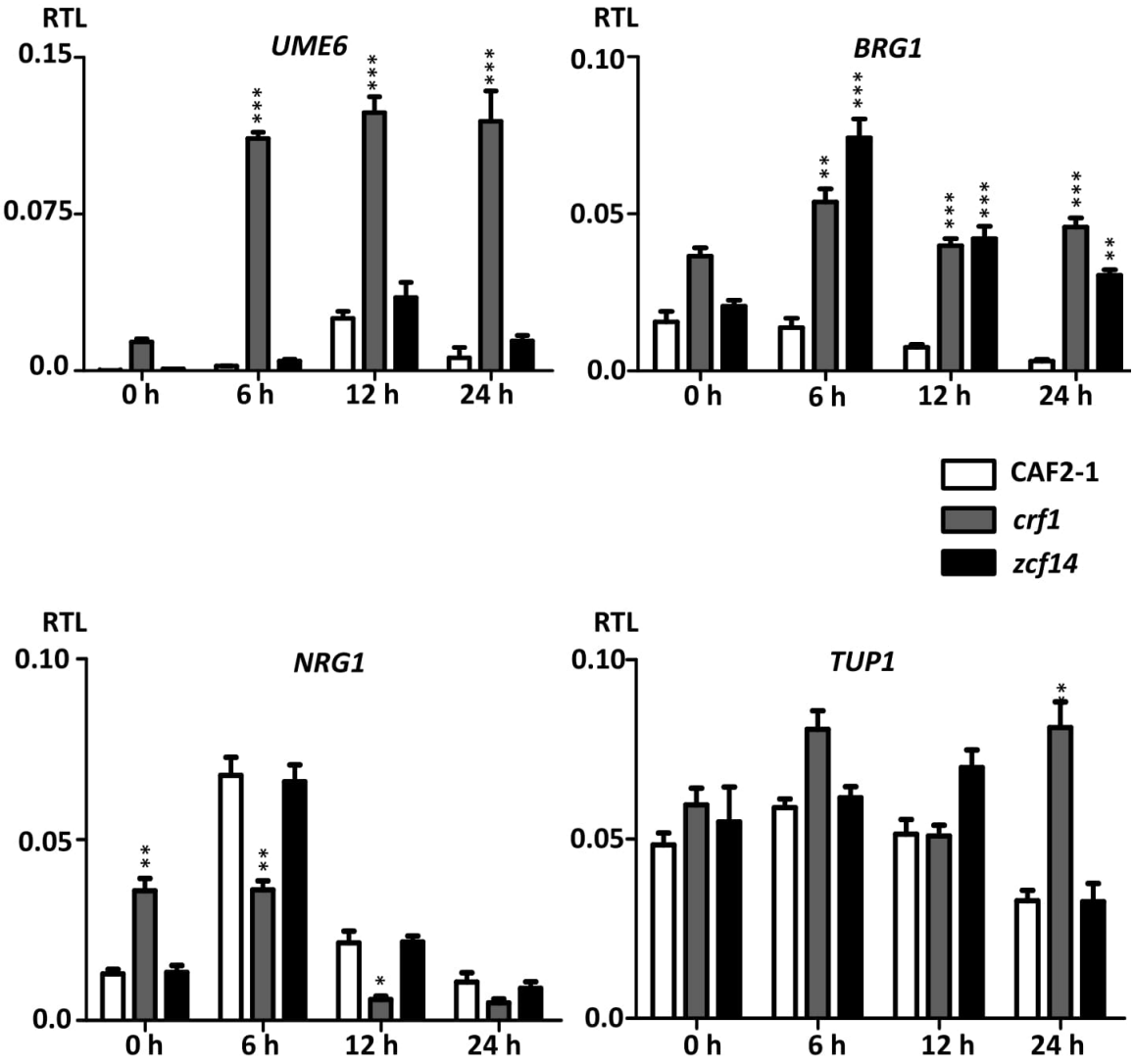
RTL
UME6
0.15
0.075
0.0
0 h
6 h
12 h
24 h
RTL
BRG1
0.10
0.05
0.0
CAF2-1
crf1
zcf14
RTL
NRG1
0.10
0.05
0.0
RTL
TUP1
0.10
0.05
0.0

Figure 8

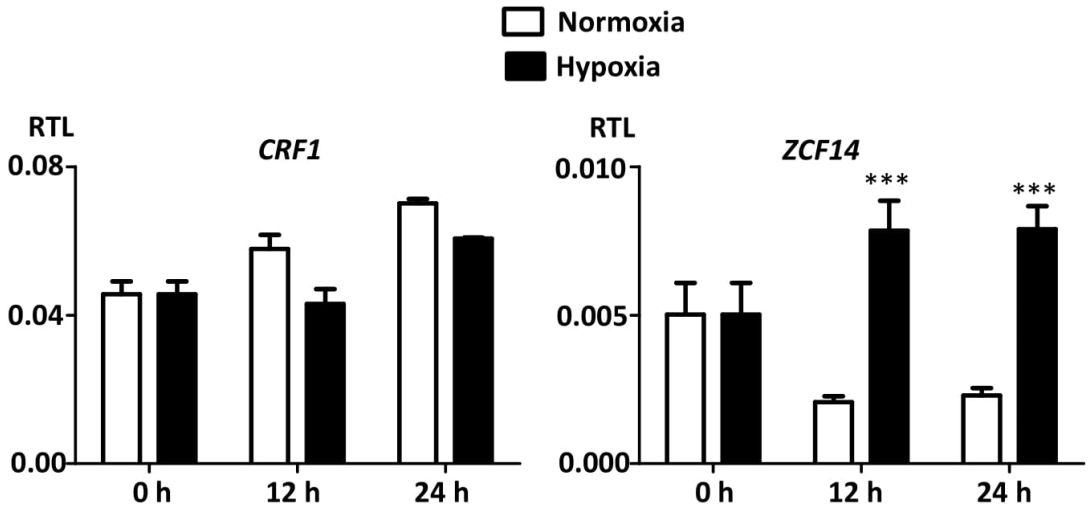
Normoxia
Hypoxia
RTL
CRF1
0.08
0.04
0.00
0 h
12 h
24 h
RTL
ZCF14
0.010
0.005
0.000
***
***
0 h
12 h
24 h

Figure 9

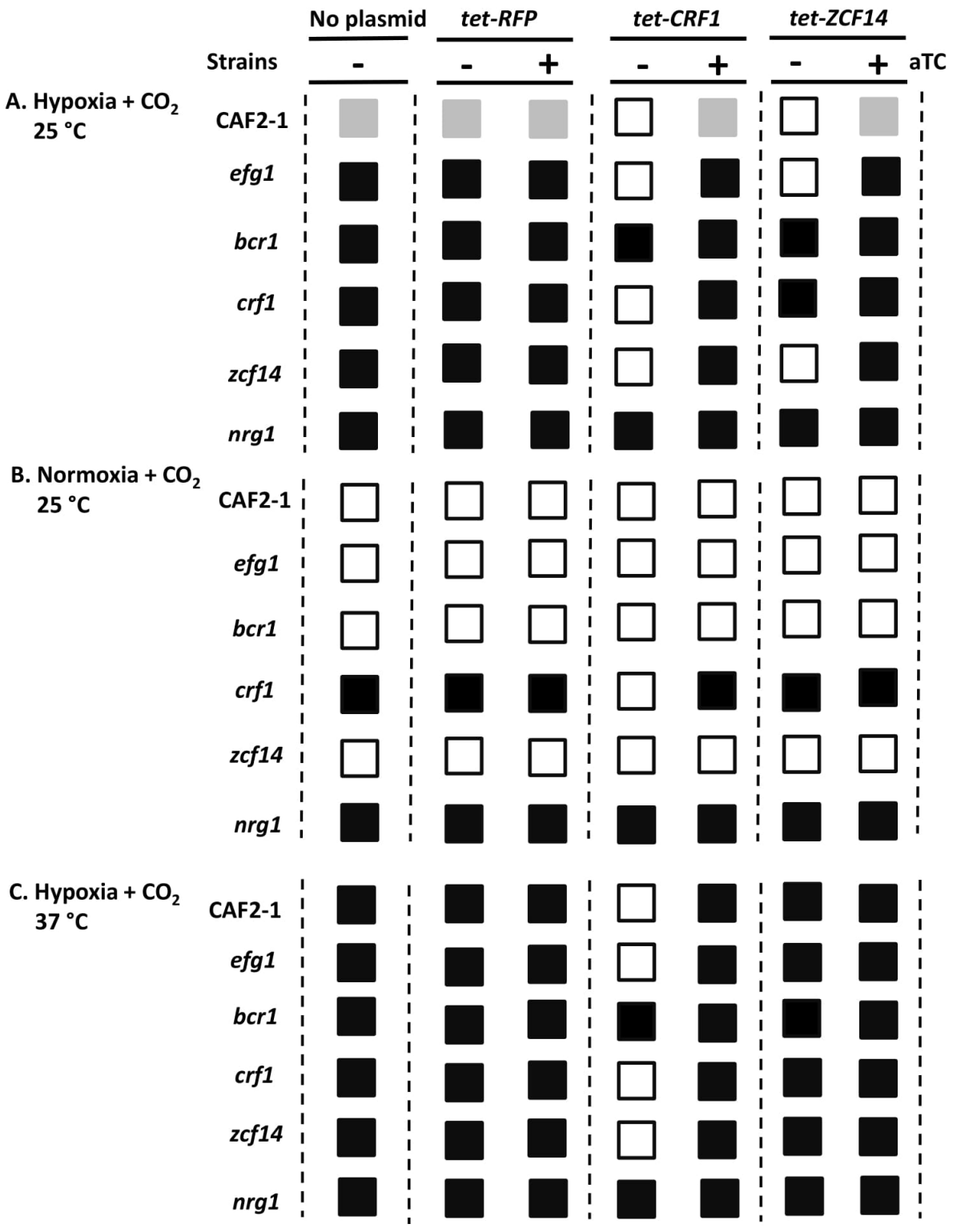
No plasmid
tet-RFP
tet-CRF1
tet-ZCF14
Strains
-
-
+
-
+
-
+
aTC
A. Hypoxia + CO2
25 °C
CAF2-1
efg1
bcr1
crf1
zcf14
nrg1
B. Normoxia + CO2
25 °C
CAF2-1
efg1
bcr1
crf1
zcf14
nrg1
C. Hypoxia + CO2
37 °C
CAF2-1
efg1
bcr1
crf1
zcf14
nrg1

Figure 10

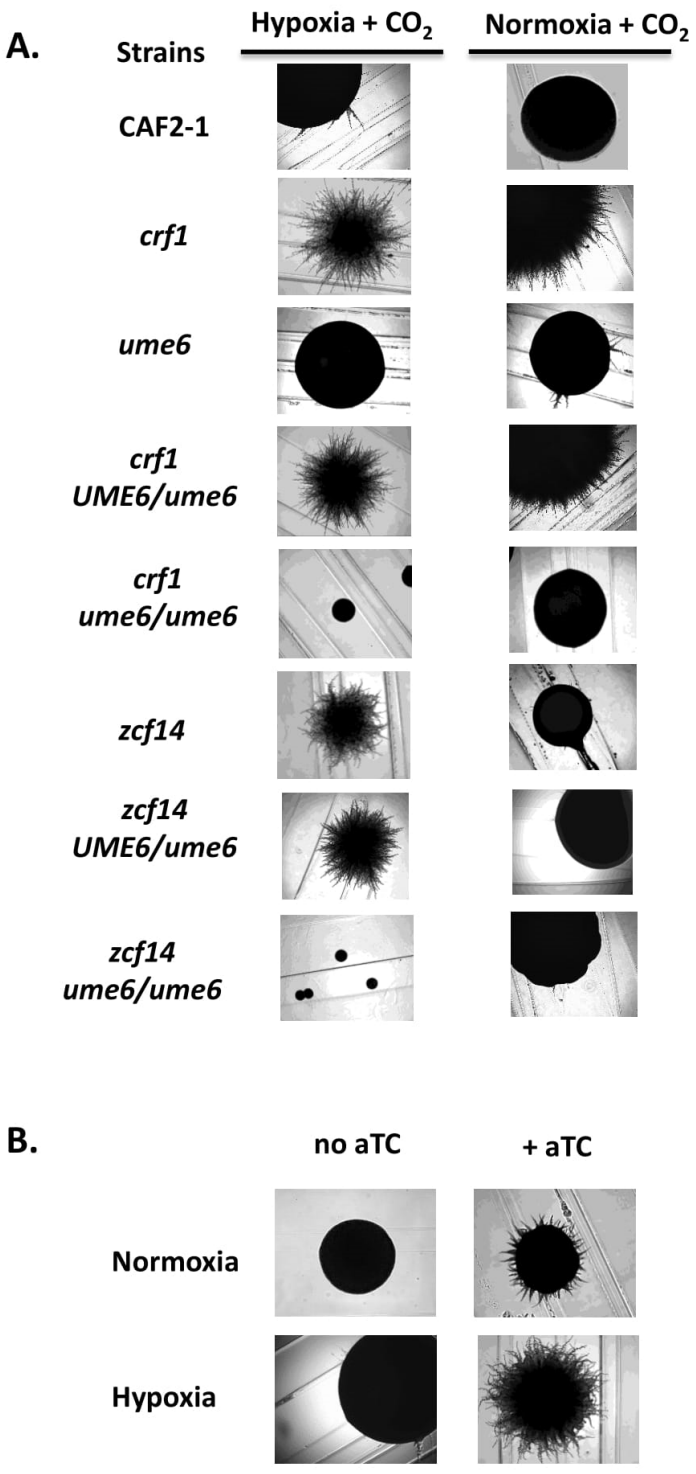
A.
Strains
Hypoxia + CO2
Normoxia + CO2
CAF2-1
crf1
ume6
crf1
UME6/ume6
crf1
ume6/ume6
zcf14
zcf14
UME6/ume6
zcf14
ume6/ume6
B.
no aTC
+ aTC
Normoxia
Hypoxia

Figure 11

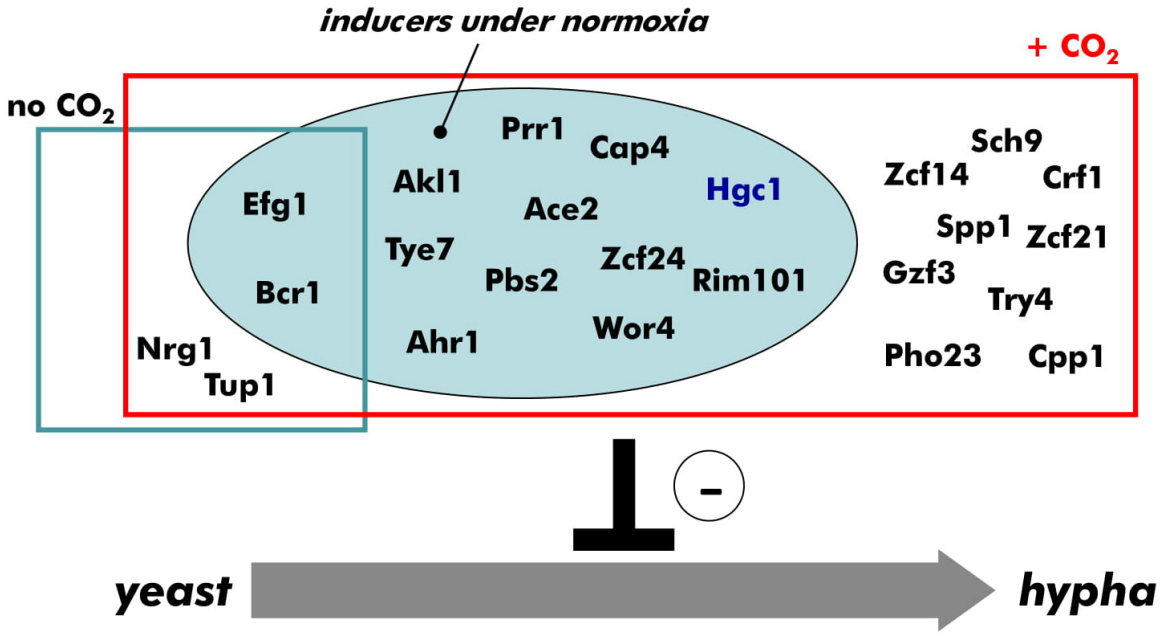
inducers under normoxia
+ CO2
no CO2
Prr1
Cap4
Akl1
Hgc1
Ace2
Efg1
Tye7
Zcf24
Pbs2
Rim101
Bcr1
Wor4
Ahr1
Nrg1
Tup1
Sch9
Zcf14
Crf1
Spp1
Zcf21
Gzf3
Try4
Pho23
Cpp1
yeast
hypha

Figure 12

3. Discussion

Fungi currently cause more that 2 million invasive infections each year and are a major health concern worldwide. The patients, who undergo solid organ transplantation, chemotherapy, abdominal surgery and individuals with neutropenia or immunocompromised conditions are at major risk of acquiring life-threatening fungal diseases like candidiasis, aspergillosis, cryptococcosis and pneumocytosis (Brown *et al*., 2012). In the last two to three decades, the prevalence of candidiasis has increased approximately 20 fold in western countries and 30-40 fold in South Asian countries (Chakrabarti 2013, Tan *et al*., 2015). Despite of a total estimate of 4-7 billion dollars spent for antifungal therapy each year, the mortality rate in patients of invasive candidiasis remains unexpectedly high, amounting to 50 % (Kullberg and Arendrup 2015, Benedict *et al*., 2018). Therefore, novel therapeutic interventions are currently required, for which an in depth understanding of fungal pathogenesis is needed with a special focus on fungal and host factors that play important roles during infection and disease.

C. albicans is the predominant fungal species, which causes superficial as well as invasive candidiasis in susceptible patients worldwide (Brown *et al*., 2012, Tan *et al*., 2015). In healthy individuals, *C. albicans* can asymptomatically colonise skin and mucosal surface as a commensal (Noble *et al*., 2016). However, several factors like poor hygiene, dysbiosis, antibacterial therapy, prolonged hospitalization and drop in host immune surveillance can trigger the virulent traits of *C. albicans*, which can lead to severe invasive candidiasis (Kullberg 2015). To grow invasively into tissues and internal organs, *C. albicans* can undergo morphological transition from yeast cells to hyphal cells. Several studies have highlighted that during infection, the reversible transition between yeast and hyphal morphotypes is critical for pathogenesis (Saville 2009 and Carsille *et al*., 2009). The commensal stage of *C. albicans* is predominantly in the yeast morphoform, and yeast cells can rapidly disseminate in the body via the blood stream, while hyphal cells express a variety of virulence factors including proteases, phospholipase, hydrolase and a so-called Candidalysin toxin, which can contribute to host invasion of *C. albicans* (Mayer *et al*., 2013, Dantes *et al*., 2016). Alteration in the host microenvironment, such as changes in body temperature, CO_2, pH, carbon source, micronutrients and exposure to immune cells, are known to influence the morphological

switching in *C. albicans*. The interplay of host niches with *C. albicans* that influences fungal morphogenesis has been intricately investigated since the last couple of decades. Certain fungal-specific signalling pathways (PKA pathway, MAPK pathway and RAM pathway) and transcription factors (Efg1, Cph1, Ace2, Ume6 and Brg1) have been identified, which play crucial roles in either sensing or generating cellular and transcriptional responses upon exposure to rapid changes in growth conditions (Biswas *et al*., 2007, Sudbery 2011). In addition, several studies have revealed that inactivation of these signalling pathways or transcriptional regulators can significantly affect the *in vivo* growth and virulence of *C. albicans* (Basso *et al*., 2018). Hence adaptation to the rapid changes in the host niches and regulating the yeast-to-hypha morphogenesis is crucial for the commensal and virulent lifestyle of *C. albicans.*

One of the overlooked aspects occurring in host niches, which can influence the growth and *in vivo* lifestyle of *C. albicans*, is the availability of oxygen (Ernst and Tielker 2009). It has been well established that oxygen levels vary significantly in host niches. Depending upon the tissue type, anatomical site, the presence or absence of inflammatory responses the oxygen levels can drastically vary from 14 % to less than 1 %, which is significantly less than atmospheric level of O_2 (21 %) (Ernst and Tielker 2009, Grahl *et al*. 2012). Importantly, *C. albicans* is highly adapted to survive in disparate host environments including oral, genital and gastrointestinal regions of healthy individuals, while it can colonise virtually any tissue or internal organ during systemic infection. It is evident that *C. albicans* is frequently exposed to hypoxic microenvironments and undergoes rapid adaptation to limiting amounts of oxygen during host colonisation (Grahl *et al*., 2012). However, fungal signalling pathways involved in sensing oxygen and molecular mechanism utilised for adaptation to hypoxic conditions are poorly understood.

Previously, a pioneering study investigated the influence of hypoxia on the growth of *C. albicans* under *in vitro* conditions (Setiadi *et al*., 2006). A genome-wide transcriptomal analysis of *C. albicans* grown under normal oxygen conditions (˜ 21 %) and hypoxia (0.2%) was performed and results revealed that specifically under hypoxia, *C. albicans* upregulates genes involved in sterol biosynthetic pathways and represses genes involved in respiration. In this same study, it was also discovered that Efg1, a transcription factor which is known for its role of inducing expression of genes required for filamentation under normoxic conditions,

prevents abnormal expression of genes (about 300 genes) under hypoxia. In addition, *efg1* mutants displayed hyperfilamentous growth under hypoxic conditions (0.2% O_2) at temperatures ≤ 35 ˚C, indicating that under oxygen-poor conditions, Efg1 functions as a repressor of filamentation, opposite to its function under normoxia. However, the mechanism, by which Efg1 represses filamentation under hypoxia remained unclear.

In this study we further investigated the regulatory network of Efg1 and have used different approaches to delineate novel transcriptional and post transcriptional regulatory mechanisms that are involved in hyphal morphogenesis and hypoxic adaptation of *C. albicans*.

3.1 Structural requirements for the hypoxic function of Efg1

A study in 1997 had primarily identified Efg1 as a major transcriptional regulator of morphogenesis in *C. albicans*, as deletion of *EFG1* blocked filamentation and overexpression of *EFG1* caused hyperfilamentation under normoxic conditions (Stoldt *et al*., 1997). Following this novel discovery, independent studies identified the two threonine residues T206 and T179 of Efg1, putatively phosphorylated by Tpk2 and Hgc1-Cdc28 kinases, respectively, to activate the hyphal inducer function of Efg1 (Bockmuhl and Ernst 2001, Wang *et al*., 2008). To identify the functional domains of Efg1 under normoxia, strains expressing truncated versions of *EFG1* gene were subjected to phenotypic profiling. Results revealed that the bHLH DNA domain of Efg1 (conserved in the APSES family of fungi), is important for maintaining normal yeast morphology and for hyphal induction (Noffz *et al*., 2008), while N- and C-terminal sequences are required for phenotypic switching (opaque-white switching). These studies highlighted the functional domains, which are important for hyphal induction function of Efg1 under normoxia. However, very little was known about the structural arrangements of Efg1 for its repressor function under hypoxia. Hence different *EFG1* alleles encoding variants mimicking phosphorylation (T206E or T179E) or non-phosphorylated variants (T206A or T179A) were integrated in an *efg1* mutant strain and phenotypes of transformants were examined under different normoxic and hypoxic conditions and at temperatures ranging from 25 ˚C to 37 ˚C. Interestingly, at temperatures below 35 ˚C, the strains producing Efg1 variants mimicking its phosphorylation (T206E and T179E) were unable to act as a repressors of filamentation whereas the non-phosphorylated (T206A and T179A) variants effectively repressed filamentation under hypoxia (Manuscript I, Figure 1). Also an N-terminally HA-tagged variant of Efg1, which was functional for its normoxic role as an inducer of

filamentation, was unable to complement for the hypoxic function of Efg1. The Efg1 function was restored upon removal of N- terminal HA-tag. Taken together, these results indicate that the normoxic and hypoxic functions of Efg1 require different structural requirements. While under normoxia, phosphorylated residues T206/T179 are essential for Efg1 to function as inducer of filamentation, lack of phosphorylation at T206/T179 sites and authentic N-terminus region of Efg1 are essential for repressive function under hypoxic conditions at temperature slightly below 37℃. Human skin and genital regions are known to be hypoxic in nature and the temperature of skin surface is below 35℃ (Evas *et al*., 2006 Sherwood and Huber 2010). Hence it is plausible under these oxygen poor niches, Efg1 might suppress filamentous growth of *C. albicans*, to colonise mammalian skin surface in the commensal yeast form.

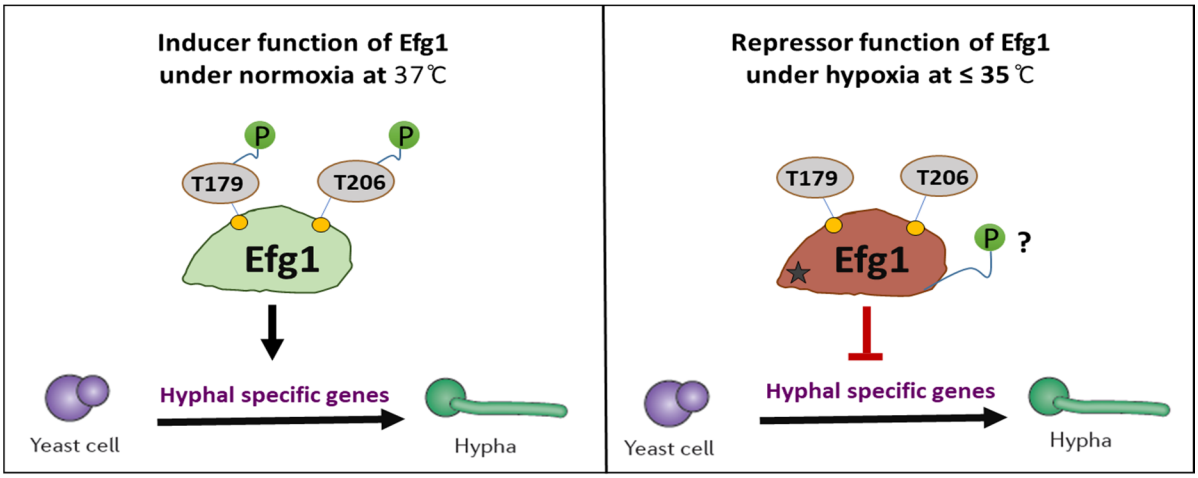

Figure 11. Efg1 requires different structural arrangements for its normoxic and hypoxic functions. Under normoxia at 37°C, Efg1 functions as an inducer of filamentation and phosphorylation at T179 and T206 residues is essential for induction of hyphal specific genes. But under hypoxia at temperature ≤ 35°C, Efg1 functions as repressor of filamantation. N-terminal region of Efg1 and non-phosphorylated status of T197 and T206 residues are important for hypoxic function of Efg1.

Considering the different structural requirement of Efg1 for its hypoxic function, it is possible that apart from T206/T179 sites, different threonine or serine sites of Efg1 might also be involved in structural modification of Efg1 to function as repressor of filamentation under hypoxia. There are potentially 50 threonine and serine sites in Efg1 that could be phosphorylated by a hypoxia specific kinase to active the hypoxic function of Efg1. Through further experimentation putative residues and posttranslational modification in Efg1 under hypoxia can be identified, based on the knowledge of residues and domains, which enable the hypoxic repressor function of Efg1. Strains can be generated, which retain only the

repressor function of Efg1, and tested for their ability to supress filamentation under in vivo conditions.

Interestingly, a recent study by the Pavelka group (Tso *et al*., 2018) showed that *C. albicans* strains, which were serially passaged through the GI tract of mice, developed increased competitive fitness to colonise the GI tract of mice; furthermore, this treatment caused mutations in transcription factors regulating filamentation. These gut evolved strains had several mutation in *FLO8* and *EFG1* genes and lost the ability to filament under in vitro inducing conditions. Subsequent experiments showed that the gut-evolved strains were avirulent and protected the gut colonised mice from systemic fungal infections. Taken together, these results indicate that harnessing the filamentation regulatory potential of Efg1 can lead to therapeutic interventions.

3.2 Genomic binding sites and transcriptional network of Efg1 under oxygen-poor conditions

Considering the contrasting function of Efg1 under hypoxia and the different structural conformation of Efg1 under hypoxic conditions, we speculated that the DNA binding motif, the genomic localisation and downstream genomic targets of Efg1 under hypoxia might be distinct compared to normoxic conditions. To identify the unique hypoxic target genes of Efg1, strains producing unmodified native Efg1 (test strain) or N-terminally HA-tagged Efg1, which is defective in hypoxic function (control strain), were grown under hypoxic conditions (0.2 % O_2) and using anti-EFG1 antibody, chromatin immunoprecipitation on chip was performed.

Interestingly, numbers for the genomic binding sites of native Efg1 (221 sites) were 2 fold higher compared to the HA-tagged Efg1 (100 sites) under hypoxia. Also, the number of genes bound by native Efg1 (297 ORFs) largely outnumbered the genes bound of HA-tagged Efg1 (111 ORFs), with an overlap of 23 ORFs (Manuscript I, figure 2). The DNA binding motif was predicted by analysing DNA sequences, which were bound by Efg1 under hypoxic conditions. Interestingly, the predicted hypoxic binding motif of Efg1 consisted of CA-specific repeats, which are distinct from the TATGCATA motif that is bound by Efg1 under normoxically grown yeast cells (Lassak *et al*., 2011). Further analysis of gene ontology of ORFs bound by native untagged Efg1 revealed enrichment of 41 genes involved in filamentation including *CYR1*,

TPK1, *STE11*, *CEK1*, *KIC1* and *CPH2* and 22 genes with transcription factor activity including *BCR1*, *TCC1*, *NRG1*, *TYE7* and *ZCF21*.

The binding of Efg1 in the promoter regions of genes involved in filamentation indicates the potential targets of hypoxic repressor function of Efg1. To verify this notion, wild-type strains and *efg1* mutants were grown under hypoxia or normoxic conditions and expression of target genes (*CYR1*, *TPK1*, *STE11*, *CEK1*, *CPH1* and *KIC1*) involved in filamentation process was examined in the presence and absence of Efg1. Interestingly, the transcript levels of *STE11*, *CEK1* and *CPH1* was highly augmented in *efg1* mutant strains (Manuscript I, figure 4). And conversely, the strains expressing functional *EFG1* displayed moderated expression of *STE11*, *CEK1* and *CPH1* transcripts. In addition to this, the hypoxia specific, CA-type consensus binding sequence of Efg1 was identified in the promoter region of *STE11* and *CEK1.* These results indicate that hypoxia can significantly influence the genomic binding sites and downstream target genes of Efg1. Although Efg1 binding was observed in promoter regions of genes involved in filamentation, the majority of these genes were exclusively observed only under hypoxic conditions indicating that Efg1 regulates distinct subsets of genes involved in the process of filamentation under normoxic and hypoxic conditions (Manuscript I, Supplemental figure 2) (Lassak *et al*., 2011). These results highlight the influence of oxygen poor conditions on the transcriptional networks of Efg1. Recently, we discovered that Tpk1 and Tpk2, which are the Efg1-regulating kinases, migrate to the nucleus and are bound in the promoter regions of target genes of Efg1 (Schaekel *et al.*, 2013). The close physical association of Tpk1/2 with genomic Efg1 targets might lead to rapid regulatory responses to changing microenvironments in host niches, e.g. during varyiations in oxygen and CO_2 concentrations.

3.3 Efg1 represses Cek1-mediated filamentation under hypoxia

The genomic binding of Efg1 was specifically observed in the promoter regions of *STE11* and *CEK1* genes under hypoxia (Manuscript I, figure 2) and, as experimental evidence suggested, Efg1 transcriptionally regulates the *STE11*, *CEK1* and *CPH1* genes (Manuscript I, figure 4). *STE11*, *CEK1* and *CPH1* are member of MAPK pathway, which senses cell wall stress and regulates filamentation, white-opaque switching and virulence in *C. albicans* (Roman *et al*., 2007). We hypothesised that Efg1 represses filamentation by regulating the Cek1-MAPK pathway during hypoxic surface growth. To test this hypothesis, wild type and *efg1* mutant strains were grown in normoxic or hypoxic conditions (0.2% O_2). Cell extracts of these strains

were used for immunoblotting, which revealed the accumulation of the phosphoform of the Cek1 kinase specifically in *efg1* mutant strains grown under hypoxia, while the phosphorylated Cek1 form was undetectable in hypoxically grown wild type strains, or in wild type strains and *efg1* mutants strains grown under normoxia (Manuscript I, figure 5).

In addition, the colony morphology of strains lacking *CPH1*, encoding a downstream transcription factor of the Cek1-MAPK pathway, and the double knockout mutant *cph1 efg1* were examined for its phenotype under normoxic and hypoxic conditions. Compared to the filamentous growth of the *efg1* mutant strain under hypoxia, both the mutant *cph1* and *cph1 efg1* strains formed non-filamentous colonies. This result indicates that the disruption of the *CPH1* gene abolishes the hypoxic phenotype (hyperfilamentous growth) of the *efg1* mutation. Hence in the absence of *EFG1*, excessive filamentation growth occurs via the Cek1-Cph1 MAPK pathway. These results were further verified by observing the hypoxic phenotype of strains overexpressing the *STE11*, *CEK1* and *CPH1* genes under hypoxia. Supporting the hypothesis, overexpression or enhanced production of components from Cek1-MAPK pathway leads to filamentous growth under hypoxia (Manuscript I, figure 5). These results indicate that under hypoxia, Efg1 prevents the abnormal expression of *STE11*, *CEK1* and *CPH1* and restricts the filamentation process under hypoxia to favour growth in the yeast morphology (Figure 12). Conceptually, during colonisation of specific host hypoxic niches, e. g. in the gut, *C. albicans* is dependent on the hypoxic function of Efg1 to suppress filamentation and to proliferate in the yeast morphoform.

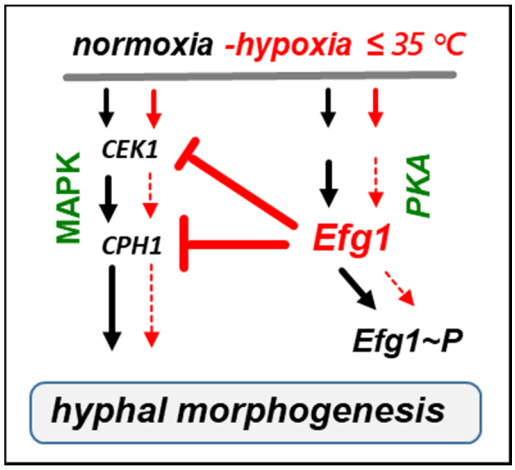

Figure 12. Presence of hypoxia alters the functioning of morphogenetic pathways. Under normoxia at 37℃, Cek1-MAPK and cAMP Pathways function independently and can induce filamentation. But under hypoxia at temperature ≤ 35℃, Efg1 supresses expression of *CEK1* and *CPH1* genes from Cek1-MAPK pathway and blocks filamentous growth.

3.4 Transcriptional circuits of inducers and repressors of filamentation form a regulatory hub to modulate morphogenesis under hypoxia

Ace2 is a transcription factor, which functions downstream of RAM pathway and mainly regulates cell separation genes under normal oxygen conditions (Saputo *et al*., 2014). Efg1 is known to repress the expression of *ACE2* and of cell separation genes under normoxic conditions (Wang *et al*., 2009), while under hypoxia, the roles of Efg1 and Ace2 are reversed, as Efg1 functions as a repressor of hypoxic filamentation and Ace2 is essential to support hypoxic filamentation (Setiadi *et al*., 2006, Mulhern *et al*., 2006). Independent studies have revealed that Efg1 and Ace2 regulate genes involved in glycolysis and oxidative metabolism (Deodt *et al*., 2004, Mulhern *et al*., 2006). These studies suggested that in spite of the antagonistic functions of Efg1 and Ace2, these two transcriptional regulators might co-regulate genes involved in filamentation under hypoxia. To identify the hypoxic regulatory circuit and an overlapping set of genes that are commonly regulated by Efg1 and Ace2, ChIP on chip assay was performed on strains that were grown under hypoxic conditions (0.2% O_2 and 6% CO_2) to decipher the of hypoxic target genes of Ace2; this study identified 296 genomic binding sites for Ace2. Interestingly, out of the 295 target genes that are bound by Ace2 under hypoxia, promoter regions of 53 ORFs were common targets for both Ace2 and Efg1 under hypoxia. Further sequence analysis revealed the potential consensus binding sequences of Ace2 under hypoxia as CAACAA and CACCAC. Interestingly, as discussed above, a similar motif had also been identified as potential genomic binding site for Efg1. These results suggest that Efg1 and Ace2 might compete for binding to an identical DNA binding motif in the promoter regions of the target genes, to transcriptionally regulate the expression of respective genes. Gene ontology analysis of shared targets of Efg1 and Ace2 revealed a subset of genes that are involved in of cell adhesion and biofilm formation in *C. albicans* (Manuscript I, figure 7). In addition, 12 transcription factors including *BCR1*, *BRG1*, *TYE7* and *ZCF21* were identified, which were bound by Efg1 and Ace2 specifically under hypoxia. As *BCR1* and *BRG1* are co-regulated by Efg1 and Ace2, the hypoxic functions of Bcr1 and Brg1 were studied. Under normoxia, Bcr1 is mainly involved in biofilm formation (Nobile *et al*., 2006). Interestingly, under hypoxia, the strains lacking *BCR1* displayed hyperfilamentous growth (Manuscript I, figure 9). Under normoxic conditions, Brg1 is required for regulation of hypha-specific genes (Du *et al*., 2012) and it was found to be also

required for filamentation under hypoxia (Manuscript I, figure 9). As hypoxic functions of Bcr1 and Brg1 were similar to the role of Efg1 and Ace2, respectively, we investigated whether Bcr1 and Brg1 could regulate *EFG1* and *ACE2* expression under hypoxia. Interestingly, the transcript levels of *ACE2* are positively influenced by Brg1, while Bcr1 represses the expression of *ACE2* under hypoxia. Taken together, these results indicate that hypoxic repressors Efg1 and Bcr1 and hypoxic activators Ace2 and Brg1 are mutually connected in a regulatory circuit to modulate hypoxic filamentation in *C. albicans.* These results have clarified that the function of morphogenetic pathways (PKA pathway and Cek1-MAPK pathway) and transcriptional regulators (Efg1, Bcr1, Ace2 and Brg1) are influenced by oxygen concentrations in the environment. Also presence of physiological temperature and elevated levels of CO_2 in combination with hypoxia can differentially influence the functioning of this newly identified regulatory circuit (Figure 13).

Earlier studies by Kumamoto group have shown that Efg1 and Efh1 (a paralouge of Efg1) are required for persistent colonisation of *C. albicans* in GI tract of mice (White *et al*., 2007). In a recently study (Witchley *et al*., 2019), the competitive fitness of 650 *C. albicans* mutant strains were quantified in a mouse model of GI commensalism. Interestingly, 5 transcriptional activators of filamentation; Efg1, Brg1, Tec1, Rob1 and Ume6 were identified as main regulators of population size of *C. albicans* during GI tract colonisation. Lack of any one of these transcriptional factors enhances the commensal fitness of *C. albicans* for GI tract colonisation. This study further established that enhanced commensal fitness or hypercolonisation in mutants strains (lacking either *EFG1*, *BRG1*, *TEC1*, *ROB1* or *UME6*) is due to downregulation of hyphal associated genes *HYR1* and *SAP6* (Witchley *et al*., 2019). Our results have shown that hypoxia and CO_2 in milieu alters signalling pathways and target genes of transcriptional factors in *C. albicans*. It remains to be investigated, whether hypoxia and CO_2 from the gut can influence the transcriptional factors besides Efg1, Brg1 and Ume6, which regulate expression of hyphal associated genes and modulate the population size of *C. albicans* for persistent colonisation in the GI tract.

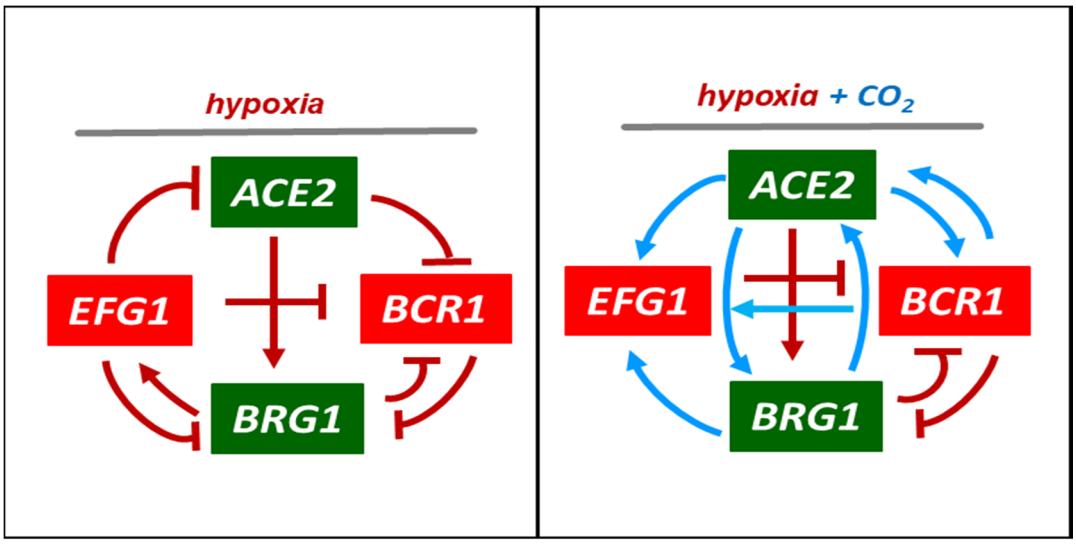

Figure 13. A hypoxic regulatory circuit consists of hypoxic repressors (Efg1, Bcr1) and hypoxic inducers (Brg1, Ace2) that are mutually connected to govern morphogenesis. The presence of CO_2 generates distinct responses from the hypoxic regulatory circuit.

3.5 The 5' UTR region of the *EFG1* transcript positively regulates its translation

In *white* (yeast) cell forms of *C. albicans*, the *EFG1* transcripts contain an 1170 nucleotide long 5' untranslated region (Tebarth *et. al*., 2003, Bruno *et al*., 2010). 5' UTR sequences can form considerable 3-dimensional structures based on Watson-Crick and non-canonial base paring that can potentially impact every step of translation (Leppek *et al*., 2018). The 5' UTR sequences are also known to contain a variety of cis regulatory elements, which can control protein levels by altering translation efficiency (Mignone et al., 2002, Kozak 2005, Childers *et al*., 2014). Hence, in order to investigate the role of the *EFG1* 5' UTR, we generated in total 7 strains, which either carry a full-length or truncated version of the *EFG1* 5' UTR (Manuscript II, figure I). The native *EFG1* 5' UTR was replaced with either full length or truncated version of *EFG1* 5' UTR, but the promoter and ORF of *EFG1* were kept intact. Integration of these constructs were done in an *efg1* homozygous mutant, in the remaining native promoter locus of *EFG1*. Since strains lacking *EFG1* have defect in repression of filamentation (Setiadi *et al*., 2006) we initially tested the strains harbouring different truncated version of *EFG1* for their ability to repress filamentation under hypoxic growth conditions. Firstly, we observed that the 3 strains carrying deletions in the *EFG1* 5' UTR region, ΔL-UTR (-1164 to -171 bp), ΔNH2-UTR (-784 to -171 bp) and ΔHpa-UTR (-388 to -171 bp) showed defects in repression of hypoxic filamentation (0.2% O_2 at 25˚C) and displayed a hyperfilamentous phenotype, which is similar

to the *efg1* null mutant strains (Manuscript II, figure 2). Interestingly, these three strains carrying specific deletions in the 5' UTR were also unable to induce filamentation under normoxic conditions (Manuscript II, figures 2 and 3). Further results revealed that deletions in the 5' UTR regions of *EFG1* do not lower the expression of *EFG1* transcript in tested strains, but surprisingly showed accumulation of the *EFG1* transcript *1*. Strains carrying deletions ΔL-UTR (-1164 to -171 bp) and ΔHpa-UTR (-388 to -171 bp) displayed of accumulation of *EFG1* transcripts and were completely devoid of Efg1 protein, while Efg1 protein could be detected in the wild-type and a reintegrant strain carrying the full length 5' UTR of *EFG1.* (Manuscript II, figure 5). The results indicated that the strains lacking a 218 nucleotide region in the 5' UTR of *EFG1* were unable to produce the Efg1 protein. This notion was verified by ribosome profiling (done in collaboration with Paula Alepuz), which revealed that strains expressing the ΔHpa-UTR version contain negligible amount of *EFG1* transcript in the polysomal fractions, as compared to the control strain. These results indicate that the 218 nucleotide region within the 5' UTR of the *EFG1* transcript is essential for its translation (Figure 14). Prior to this discovery, only two independent studies had identified a regulatory function of the 5' UTR region in *UME6* and *WOR1* transcripts; however, in both the cases, the respective 5' UTR sequences negatively influenced translation of these transcripts (Childers *et al*., 2015, Guan *et al*., 2015). Hence, this is the first study, which has identified a unique 5' UTR mediated regulation that positively influences the translation process and regulates morphogenesis in *C. albicans*. In dynamic host microenvironments, the 5' UTR of the *EFG1* may recruit ribosomes or other regulatory factors to fine tune the levels of Efg1, as it regulates genes involved in cellular metabolism, morphological switching, commensalism and modulates fungal population size of *C. albicans*.

The mechanism by which 5' UTR regulates the translation of *EFG1* remains to be investigated. 5' UTR can contain a zip code sequence that specifies alternative subcellular localization to a location, where mRNA transcripts are not translated (Pickering and Willis 2005). Certain 5' UTR also contain uORFs (short open reading frames upstream of the main ORF); uORFs can serve as alternative translation initiation sites and affect the translation of main ORF (Hinnebusch *et al*., 2016). Recently, it was shown that translation of *GCN4* is controlled by uORF-dependent mechanisms in *C. albcians* (Sundaram and Grant 2014). Interestingly, the 5' UTR of the *EFG1* also contains an uORF, potentially encoding for 4 amino acids. However, deletion of this uORF from the 5' UTR of the *EFG1* did not affect the translation of the *EFG1*

transcript. Possibly, the 5' UTR of the *EFG1* forms a hairpin structure (Manuscript II, figure 8) that interacts with translational regulatory proteins or might contain internal ribosome entry site that facilitates translation (Zhou *et al*., 2001). Recently, it was shown that the recruitment of regulatory proteins tothe 5' end of mRNA may occur early during transcription (Bellofatto and Wilusz 2011). Such mechanisms are also possible in case of Efg1, as the effect of 5' UTR on translation was observed only in case of its native promoter context, while heterologous *PCK1* and *ACT1* promoters were able to drive functional expression on *EFG1* ORF lacking the 5' UTR.

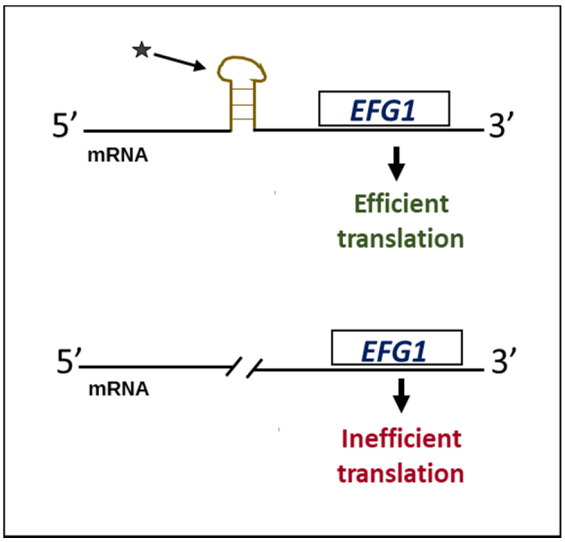

Figure 14. A 218 nucleotide region from the 5' UTR of *EFG1* is essential for the translation of *EFG1* transcript. *EFG1* transcripts contains an 1170 bp long 5' UTR. The status of secondary structure formed by a 218 nucleotide region of 5' UTR of *EFG1,* determines the cellular levels of Efg1 which governs the morphological transitions under normoxic and hypoxic conditions. *EFG1* transcripts lacking the 218 nucleotide region showed inefficient translation of *EFG1.*

In recent years, multiple studies have identified fungal-specific posttranscriptional mechanisms that are involved in yeast to hyphal transitions (Verma-Gaur and Traven 2016). In addition to 5' UTR mediated regulation, 3' UTR are involved in posttranscriptional mRNA regulation, including cellular localization and stability (Kadosh 2016, Mayr 2017). It remains to be investigated, whether the 3' UTR of *EFG1* is also involved in regulation of translation process. Strikingly, the regulatory proteins Dhh1 (helicase), Kem1 (exoribonuclease) and Ccr4-Pop4 (mRNA deadenylase) involved in mRNA decay pathway are also required for hyphal morphogenesis (An *et al*., 2004, Dagley *et al*., 2011). In *S. cerevisiae*, the Dom34 protein that is a member of no go-decay pathway of mRNA degradation, is involved in a translation quality control mechanism that recognises and degrades mRNAs stalled during translation (Passos *et*

al., 2009). Interestingly in *C. albicans*, Dom34 binds to the 5' UTR of transcripts encoding Pmt-type mannosyltransferases and favours their translation (van Wijlick *et al*., 2016). Similarly, the long 5' UTR in *EFG1* transcripts might facilitate binding of transitional regulatory proteins to initiate translation.

3.6 Genomic binding of PKA isoforms occurs near Efg1 binding sites

In *C. albicans,* the kinase A isoforms Tpk1 and Tpk2 are members of the cAMP-PKA pathway and regulate growth, filamentation, phenotypic switching and virulence (Sonneborn *et al*., 2000, Park *et al*., 2005, Coa *et al*., 2017). Studies in *S. cerevisiae* have shown that kinases Hog1 and Sch9 can be associated with the promoter regions of target genes to regulate the transcription of downstream ORFs (Pokholok *et al*., 2006, Pascual-Ahuir and Proft 2007, Nadal-Reibelles *et al*., 2012). As in *C. albicans* Tpk1 and Tpk2 are involved in various cellular functions and phosphorylate the transcription factor Efg1, we investigated whether these isoforms are also involved in regulating Efg1 target genes by localising to specific genomic sites. As Tpk1 and Tpk2 partly localise to the nucleus of *C. albicans*, the genomic binding of Tpk1 and Tpk2 was determined by ChIP on chip assay. The genomic binding targets bound by Tpk1 and Tpk2 largely were distinct during yeast and hyphal growth. Tpk1 and Tpk2 bound mostly within ORFs during yeast growth, while during hyphal induction, the binding was favoured in promoter regions. During hyphal induction, Tpk2 was bound mostly in the promoter regions of 40 different genes involved in filamentous growth (including *RAS1*, *SSN6* and *HGC1*) and 20 different binding sites were also observed in promoter regions of genes encoding transcription factors (including *AHR1*, *BRG1* and *SLF1*), mostly involved in regulation of filamentous growth. The genomic localisation of Tpk2 overlapped partially with sequences representing DNA binding targets of Efg1, since under hypha-inducing conditions, 13 target genes of Tpk2 were shared by Efg1 (Lu et al., 2008, Lassak et al., 2011, Nobile et al., 2012). Interestingly, we observed that the promoter region of the *HYR1* gene, which codes for a GPI-anchored hyphal cell wall protein that is required for hyphal growth and virulence, was bound by both Tpk2 and Efg1 (Bailey *et al*., 1996, Sohn *et al*., 2003). A similar binding of Tpk2 and Efg1 was observed in the promoter region of the *ECE1* gene, which produces the candidalysin toxin (Moyes *et al*., 2016). These results suggest that the Tpk1/Tpk2-mediated regulation of

Efg1 during hyphal-inducing conditions might occur in the promoter regions of Efg1 target genes, which could effectively influence the expression of genes regulated by Efg1.

The consensus sequence motif within the Tpk2 binding regions revealed that during yeast growth, the binding occurred within ORFs at ACCAC, CCACC or CAGC motifs. However, for binding during hyphal growth, Tpk2 was found to bind in promoter regions and the motif sequence was A_5GA_5 or A_2GA_5. This indicates that the binding motif and target genes drastically vary for Tpk2 during yeast and hyphal growth. As we observed Tpk2 binding within the ORF region, we found that the binding consensus sequence prefers 6 specific codons (CAC, CCA, ACC, CAG, AGC and GCA), which match the Tpk2 consensus sequence. Results revealed that occurrence of these 6 codons was significantly higher (2-3 fold) within the Tpk2 binding regions compared to the average occurrence of these codons in the genome of *C. albicans*. These results suggest that Tpk2 binding has contributed to the evolution of codon usage within ORFs of target genes. An independent study has identified recently the binding of a transcriptional activator Gcn4 within coding regions, demonstrating that Gcn4 binding within the coding region can activate cryptic internal promoters or canonical 5'-positioned promoters (Rawal *et al.,* 2018). Therefore, it is also possible that ORFs bound by Tpk2 could activate 5'-positioned promoters during yeast and hyphal growth of *C. albicans*.

3.7 Role of normoxic regulators in hypoxic filamentation

Most of the previous studies have investigated fungal biology by growing cells in planktonic growth conditions (liquid medium). However, the cellular and transcriptional responses of *C. albicans* can be distinct for growth on biotic and abiotic surfaces, compared to planktonic growth conditions (Kumamoto *et al*., 2005). *C. albicans* as a commensal and opportunistic pathogen grows on skin and tissue surface of mammalian host. The host niches often contain oxygen-poor environment with elevated levels of CO_2 (Ernst and Tielker 2009). Hence it is important to determine the factors, which regulate virulence traits such as hyphal morphogenesis during growth on tissue surface pertaining oxygen limiting conditions with high CO_2.

Over the years, 23 different factors have been characterised which are essential regulators of filamentation under normoxic conditions (Sudbery 2011, Noble 2017). We initially investigated whether the normoxic regulators of filamentation are also essential for

morphogenesis under hypoxia. Phenotypic profiling of mutant strains lacking each of the known normoxic regulators was carried out by testing growth on agar surfaces under normoxic or hypoxic conditions, either in presence or absence of CO_2 (Manuscript IV, figure 1).

In our study we observed the wild-type strain displayed hyperfilamentous growth at elevated temperatures (37 ℃) under hypoxia, while the strains lacking *CYR1* or *RAS1* genes formed nonfilamentous colonies that were reduced in colony size. Cyr1 and Ras1 are known to integrate environmental cues by elevating the intracellular levels of cAMP (Sudbery 2011) and it appears that activity of both of these genes is also required for hypoxic filamentation. In case of PKA kinase isoforms (*TPK1* and *TPK2*), we found that the *tpk2* mutant displayed considerable filamentation defects under hypoxia, while the *tpk1* strain was filamentous. Interestingly, the normoxic regulators of filamentation Efg1, Cph1, Flo8, Brg1, Ume6 and Eed1 were also required for hypoxic filamentation, while other regulators including Czf1, Cek1, Hda1, Sko1, Ahr1 and Hgc1 were dispensable for hypoxic filamentation.

Taken together, these results indicate major differences in the components required for the hyphal initiation and maintenance of filamentation under hypoxic and normoxic conditions.

3.8 Novel hypoxic regulators govern the process of filamentation under low oxygen and high CO_2 conditions

The remarkable differences in the factors involved in normoxic and hypoxic filamentation indicates a considerable rewiring in the transcriptional regulation of filamentation under hypoxia. We speculated that a greater number of transcriptional factors and kinases might be involved in regulation of hypoxic filamentation. Hence mutant libraries lacking transcription factors (233 mutant strains) and kinase mutant library (consisting of 63 mutant strains) (Blankenship *et al*., 2009, Vandeputte *et al*., 2012) were subjected to hypoxic phenotypic profiling.

In total 21 different mutant strains were newly identified in this study, which were unable to suppress hypoxic filamentation in the presence of CO_2 (Manuscript IV, figure 2). Based on the phenotype, the mutants were categorised in three different sets. Firstly, we identified a set of 7 mutants (*zcf14*, *zcf21*, *spp1*, *gzf3*, *pho23*, *try4* and *cpp1*) which displayed defects to repress filamentation under hypoxia with CO_2 at 25℃. These mutant phenotypes are identical

to the previously described hypoxic phenotype of the *sch9* mutant (Stichternoth *et al*., 2009). Secondly, we identified a set of 12 mutants including *zcf24*, *cap4*, *prr1*, *wor4*, *akl1*, *tye7*, *ace2* and *bcr1*, which were also defective in suppression of hypoxic filamentation at 25 ℃, but at 37 ℃ under normoxia (not hypoxia), these strains were unable to induce filamentation. Thirdly, a set of mutants consisting of *pbs2* and *bas1* (*Δorf19.6874*) mutants formed hyperfilamentous colonies upon exposure to CO_2 under both normoxic and hypoxic growth conditions at 25 ℃.

Although some mutants showed a reduction in growth rate, all mutants were able to grow under hypoxia. This finding suggests that *C. albicans* has a remarkable ability to strive under hypoxic conditions that is not dependent on the functioning of a single positive-acting transcription factor. However, to restrain filamentous growth under hypoxia with CO_2, *C. albicans* is dependent on 27 different repressors of filamentation, the majority of these were newly identified in this study. Numbers of regulators of filamentation required under normoxic and hypoxic conditions are depicted in Figure 15.

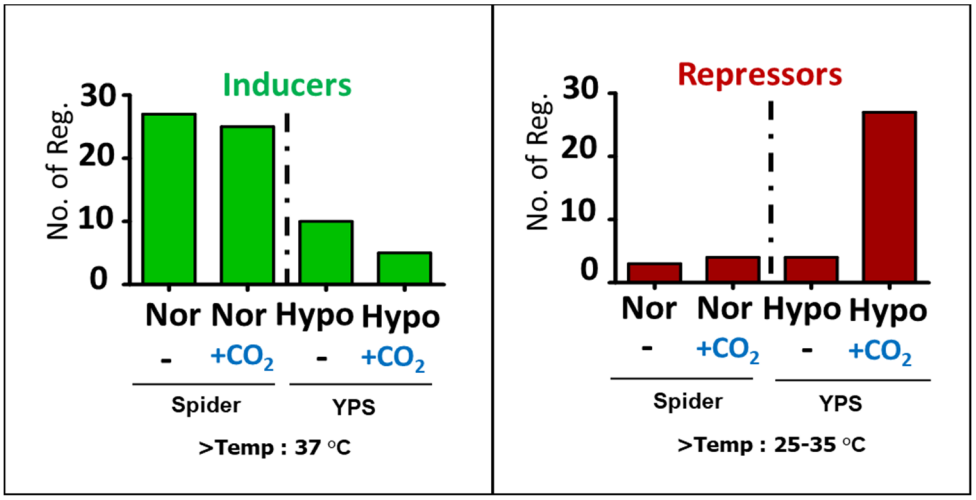

Figure 15. Numbers of regulators involved in filamentation under normoxia and hypoxia. Mutant libraries of transcription factors and kinases were screened for filamentation under normoxia (Nor) or hypoxia (Hypo). Colony morphologies of mutant strains were examined during growth on hypha-inducing agar (Spider or YPS medium) at temperatures ranging from 25 to 37 ℃. The first section of the figure (green colour) numbers inducers of filamentation required under normoxic and hypoxic conditions (with or without CO_2) at physiological temperature (37 ℃). The second section of the figure (red colour) reflects repressors of filamentation under normoxic and hypoxic conditions (with or without CO_2) at temperatures slightly below 37 ℃.

3.9 Crf1 and Zcf14 regulate expression of *UME6* and supress hypoxic filamentation

To further elucidate the molecular mechanism of newly identified hypoxic repressors of filamentation, two mutant strains lacking *ZCF14* and *ORF19.6874*, which displayed hyperfilamentous colonies under hypoxia (with CO_2), were selected for further investigation. Zcf14 belongs to the zinc cluster of proteins, which are known to be involved in regulation of growth, drug resistance and ergosterol biosynthesis (MacPerson *et al*., 2006).

Interestingly, in the case of *ORF19.6874*, we identified a homologue (*ORF19.3809*), which previously had been designated as *BAS1* in the genome database of *C. albicans*. An orthologue of these ORFs in *S. cerevisiae* is *ScBAS1,* which is involved in upregulation of genes involved in purine biosynthesis (Diagnan-Fornier *and* Fink 1992). Recently, a study found that *ORF19.3809* is also involved in regulation of purine biosynthesis and a *C. albicans* strain lacking *ORF19.3809* displayed adenine auxotrophy and attenuated virulence in a systemic mouse model of infection (Wangsanut *et al*., 2017). We determined that the paralog *ORF19.6874* is not involved in regulation of purine biosynthetic genes in *C. albicans*; therefore, we renamed *ORF19.6874* as *CRF1* (<u>C</u>O_2 dependent <u>R</u>epressor of <u>F</u>ilamentation), based on its hypoxic function.

In *C. albicans*, *UME6* and *BRG1* function as downstream targets of numerous filamentation regulating transcription factors including *EFG1* and *CPH1* and are required for induction of hypha-specific genes, while *NRG1* and *TUP1* function as a repressor of filamentation (Saville *et al*., 2003, Banerjee *et al*., 2008, Sudbery 2011). Hence to identify the hypoxic regulatory network of Crf1 and Zcf14, the transcript levels of major regulators of filamentation *EFG1*, *CPH1, BRG1, UME6*, *TUP1* and *NRG1* were analysed in homozygous mutants lacking *CRF1* or *ZCF14* genes under different normoxic and hypoxic conditions. Interestingly, mutant strains lacking the *CRF1* gene showed abnormally augmented levels of the *UME6* transcript compared to wild type strains (with CO_2) (Manuscript IV, figure 7). Conversely, the *NRG1* transcript level was reduced in *crf1* mutant strains (both under hypoxia and normoxia), but not in wild-type strains. Similarly, the increased levels of the *UME6* transcript and diminished level of *NRG1* were also observed in the *zcf14* homozygous mutant, but not under normoxia (with CO_2). Also the *NRG1* transcript levels were diminished in hypoxically grown *zcf14* mutant

(Manuscript IV, figure 7). These results indicate that Crf1 and Zcf14 are involved in the regulation of *UME6 and NRG1* to restrict the filamentous growth of *C. albicans* under oxygen poor and high CO_2 growth conditions. As expected, the hyperfilamentous phenotype of *crf1* and *zcf14* mutants was completely abolished in the double knockout mutant strains *crf1 ume6* and *zcf14 ume6* strains (Manuscript IV, figure 11). In contrast to the surface growth phenotype of *crf1* and *zcf14* mutants, only the *crf1* mutants displayed filamentous growth in liquid medium (under hypoxia and normoxia with CO_2), while the *zcf14* mutant and WT cells displayed the yeast phenotype (Manuscript IV, figure 5). These results indicate that the hypoxic repressor function of Crf1 is consistent during surface growth and planktonic growth conditions, while the Zcf14 function is restricted to surface growth conditions.

Further we observed that *CRF1* overexpression can supress the filamentous growth of wild-type strain under hypoxic and normoxic conditions in presence of CO_2. Overexpression of *CRF1* also supressed the hypoxic filamentous growth of *efg1, crf1 and zcf14* mutant strains. On other hand, the overexpression of *ZCF14* caused suppression of hypoxic filamentation only in case of *efg1* and *zcf14* mutants. However overexpression of *CRF1* or *ZCF14* could not supress the filamentous growth of *nrg1* mutants strains, this indicates that the repressor function of Nrg1 might be independent of Crf1 and Zcf14. Taken together these results indicate that Crf1 has strong potential to supress filamentation in presence of CO_2 (under both normoxic and hypoxic conditions), while the repressor function of Zcf14 appears specifically under hypoxia with CO_2 conditions.

In *C. albicans*, *UME6* upregulation induces filametation and promotes virulence-related activities (Banerjee *et al*., 2008, Carlisle *et al*., 2009) and two regulators Eed1 and Nrg1, which are known to regulate *UME6* expression, also influence the pathogenic potential of *C. albicans* (Saville *et al*., 2003, Martin *et al*., 2011). In a recent investigation several *C. albicans* genes were tested for their role in commensalism and it was observed that strains overexpressing *UME6* abolished commensal growth and strains were incompetent to colonise the GI tract of mice (Böhm *et al*., 2017). Another independent study showed that strains lacking *UME6* showed increased fitness compared to wild-type strains, indicating the role of *UME6* in regulation of fungal population during GI tract colonisation (Witchley *et al*., 2019). These studies suggest that strong modulation of Ume6 levels during host colonisation is critical as it regulates fungal population size during commensal growth and is also required for virulence.

Currently, there are two known post translational regulatory mechanisms which stabilizes Ume6 levels during filamentation under hypoxia and CO_2 conditions. Firstly under hypoxia at physiological temperature, the N-terminal region of Ofd1 (2-OG-Fe(II)-dependent dioxygenase) senses hypoxia and inhibits the activity of its C-terminal domain to stabilise the Ume6 protein, which can induce filamentation and maintain hyphal growth under low oxygen conditions (Lu *et al*., 2013). Secondly, under elevated CO_2 conditions, Ptc2 (a phosphatase) dephosphorylates Ssn3 kinase. The hypophosphorylated Ssn3 is unable to phosphorylate the S437 residue of Ume6, which prevents Ume6 from ubiquitination and degradation (Lu *et al*., 2019). Interestingly, in our study we identified the two novel hypoxic regulators Crf1 and Zcf14 which also control expression of *UME6* under hypoxia and CO_2 conditions. It remains to be investigated whether Crf1 and Zcf14 directly bind to the promoter regions of *UME6* and regulate the expression of *UME6*, or other hypoxic regulatory factors are involved to coordinate Crf1 and Zcf14 mediated regulation of *UME6*. In conclusion, the novel hypoxic repressor Crf1 and Zcf14 might tightly regulate and fine tune *UME6* expression, to generate niche-specific morphological adaptation of *C. albicans* in oxygen-poor and CO_2 -rich host microenvironment.

3.10 Role of hypoxic regulators in host colonisation and virulence of *C. albicans*

Fungal genes involved in hypoxic adaptation are also linked with fungal pathogenesis (Grahl *et al*., 2012). In our studies we identified the *RAS1* and *CYR1* genes, which are required for optimal growth and filamentation under hypoxic conditions and are also required for virulence (Leberer *et al*., 2001, Rocha *et al*., 2001, Mulhern *et al*., 2006, Bonhomme *et al*., 2011). Sch9 kinase, which integrates hypoxic and CO_2 and regulates filamentation under hypoxia and Ace2, which functions as inducer of filamentation under hypoxia, are both required for virulence of *C. albicans* (Kelly *et al*., 2004, Stichternoth *et al*., 2011, Liu *et al*., 2010). Efg1 is a master regulator of filamentation under normoxia, known to regulate expression of metabolic and cell surface genes, as well as to induce chlamydospore formation and phenotypic switching (Stoldt *et al*., 1997, Shrikantha *et al*., 2000, Setiadi *et al*., 2006, Noffz *et al*., 2008, Stichternoth *et al*., 2009). In contrast to its normoxic function, we discovered that under hypoxia Efg1 supresses filamentation at temperatures slightly below 37℃. Efg1 also regulates promotes commensal growth of *C. albicans* during GI tract colonisation (Pierce *et al*., 2012). Recently, it was discovered that for commensal lifestyle

and for prolonged colonisation in the GI tract, *C. albicans* requires the yeast morphofrom, because it is prevented by switching to the hyphal morphology (Bohum *et al*., 2017). As the GI tract of mice and humans is hypoxic and contains high levels of CO_2, it is likely that the hypoxic repressor function of Efg1 might be involved in suppression of filamentation to favour persistent commensal colonisation of the human host by *C. albicans*. Through mutant phenotype screening we have newly identified more than 20 hypoxic regulators including *CRF1*, *ZCF14*, *ZCF21*, *TYE7* and *TRY4*, which suppress filamentous growth under hypoxia in the presence of high CO_2 levels (Manuscript IV). Accordingly, recent studies have shown that *ZCF21*, *TYE7* and *TRY4* are necessary for the commensal lifestyle of *C. albicans* (Pérez *et al*., 2013, Böhm *et al*., 2017). Based on our result that strains lacking *ZCF21*, *TYE7* or *TRY4* have defects in suppression of hypoxic filamentation, it is possible that the *in vivo* fitness of these strains is compromised due to their inability to constrain filamentous growth in host hypoxic niches. A model depicting the role of hypoxic regulators in host colonisation is shown in figure 16.

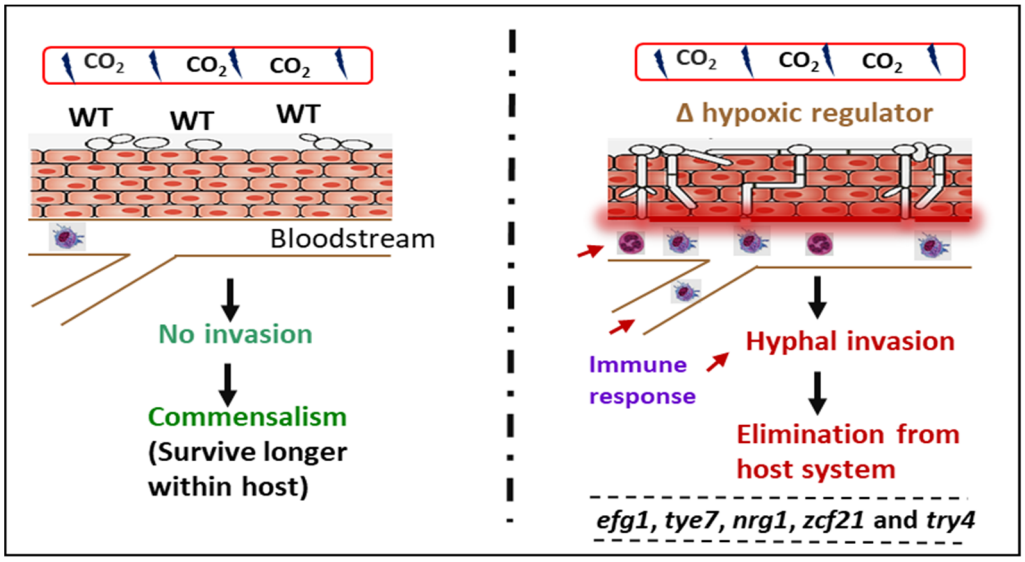

Figure 16. Influence of hypoxic regulators on filamentation and lifestyle of *C. albicans*. A model illustrating the role of hypoxic regulators for colonisation of *C. albicans* in oxygen-poor body niches. Restrained filamentous growth or non-incremental colonisation in yeast morphoform of *C. albicans* is tolerated by host immune system within certain body niches for e.g. in gastrointestinal tract. The GI tract is known to be hypoxic in nature and contain high CO_2 levels. Under these conditions blocking filamentous growth is critical, as filaments of *C. albicans* can grow invasively, damage the epithelial tissue and induce strong immunogenic response from host immune system. Therefore in order to adapt to oxygen poor GI tract during the commensal lifestyle, *C. albicans* might be dependent on the hypoxic repressors of filamentation to maintain population in yeast morphoform. We identified Efg1, Tye7, Zcf21, Nrg1 and Try4 function as repressor of filamentation under hypoxia (Manuscript IV, Bonhomme *et al*., 2011). And *C. albicans* strains lacking any of these regulators have severe defects in GI tract colonisation (Pierce *et. al.,* 2012, Pérez *et. al.,* 2013, Vautier *et al.,* 2015 *and* Böhm *et al.,* 2017). This indicates that adaptation to hypoxia and regulation of morphogenesis by hypoxic regulators is crucial for *C. albicans* especially during colonisation of GI tract.

It appears that to rapidly adapt to the changing oxygen and CO_2 conditions *in vivo*, *C. albicans* has evolved a large set of hypoxic regulators of filamentation. We observed that several transcriptional factors, which are not involved in regulation of filamentation under normoxia, are involved in repression of hypoxic filamentation. *C. albicans* appears to require such redundancy in repressors of hypoxic filamentation, while positive adaptation to hypoxia does not appears to be dependent on the function of single signalling pathway or morphogenetic regulator. In a recent study using a murine subdermal abscess model it was shown that at the site of infection, Polymorphonuclear Neutrophils (PMN) inflation caused hypoxic conditions, which triggered β-glucan masking in the cell wall of *C. albicans*, thereby leading to inefficient sensing of β-glucan by host dectin-1 on the surface of PMNs. This process caused reduced phagocytosis and killing of *C. albicans* by PMNs (Lopes *et al*., 2018). An independent study also established that hypoxically grown cultures of *C. albicans* display a higher tendency to mask the β-glucan levels at the cell surface (Pradhan *et al*., 2018). Masking of β-glucans impedes immune cell recognition and constitutes a prominent virulent trait of *C. albicans* (Erwing and Gow 2016). As we have identified multiple hypoxic regulators, which govern the filamentation process of *C. albicans*, it is possible that these hypoxic regulators are also involved in regulating hypha- associated cell surface genes and modulate exposure or masking of β-glucans under hypoxic conditions.

Although our results highlight that hypoxic regulators function in suppression of filamentous growth and might contribute to the commensal lifestyle of *C. albicans*, these factors might also be involved in the virulence of *C. albicans* under specific host niches. For instance, in case of *in vivo* murine model for disseminated candidiasis, it is observed that *C. albicans* colonises liver and spleen only in non-filamentous form, while during colonisation of kidneys, exorbitant filaments of *C. albicans* are observed (Lionakis *et al*., 2011). Internal organs and organ-specific tissues contain limiting amounts of oxygen, hence it is plausible that, for morphogenetic transitions during organ-specific adaptation, *C. albicans* is dependent on hypoxic regulators. However, additional experimental evidence needs to be gathered by studying the molecular functions of the multiple hypoxic regulators.

Investigating hypoxic regulatory networks and mechanisms, which control the growth and morphological transition of *C. albicans* under oxygen poor conditions, will potentially lead to new therapeutic strategies. In last decade, live attenuated strains of *C. albicans* were

developed harnessing the potential of repressors of filamentation. Firstly, the mice were treated with *C. albicans* strains overexpressing *NRG1* or *TUP1* (repressors of filamentation), the injected fungal cells were able to reach target organ and proliferate *in vivo* only in yeast morphoform but were unable to cause host damage (Saville *et al*., 2009). These same set of mice were further challenged with virulent wild-type *C. albicans* strains, these mice demonstrated strong immunity against systemic candidiasis and showed 100% survival rate (Saville *et al*., 2006, Saville *et al*., 2009). Similar to *NRG1* and *TUP1*, the newly identified *CRF1* gene might be a promising candidate, as overexpression of *CRF1* can effectively supress filamentous growth in *C. albicans*, under inducing conditions (Manuscript IV). Hence the filamentation regulatory network of *CRF1* needs further investigation. However currently the virulence attenuated fungal strains as a vaccine strategy for candidiasis remains less characterised, while the Als3-subunit vaccine is currently under the clinical trials (Cassone *et al*., 2013, Tso *et al*., 2018). Nevertheless, fungal transcription factors that can block the filamentous growth and supress the pathogenic potential of *C. albicans* under *in vivo* conditions, and also elicit the protective host immune response, can be considered as the potential candidates to develop vaccine against systemic candidiasis.

Since several decades, growth- and viability- inhibiting antifungal drugs are in commercial use, which have caused increase in corresponding drug-resistant strains. Recently, small compounds which are anti-virulence agents and specifically target functions essential for virulence, e.g. signalling pathways, transcription factors and mechanisms involved in hyphal morphogenesis in *C. albicans*, are being considered as potential drug targets (Fazly *et al*., 2013, Pierce and Lopez-Ribot 2013, Romo *et al*., 2017). A major advantage of anti-virulence agents is that these compounds directly inhibit the ability of pathogen to cause host tissue or organ damage and do not directly target the viability of pathogen. Hence these drugs may not generate high selective pressures, which often causes drug resistance. As we have identified several hypoxia specific regulators of filamentation, chemical libraries could be screened and small chemical compounds that interject the process of hypoxic adaptation and filamentation of *C. albicans* under *in vivo* conditions can be harnessed for development of novel anti-virulence compounds.

4. Summary

The fungus *Candida albicans* is an important human pathogen that causes tenacious superficial infections, but also life-threatening systemic diseases. On the other hand, *C. albicans* resides as a harmless commensal in the human gastrointestinal (GI) tract. Its virulence depends largely on morphological transition from a commensal yeast form to a multicellular hyphal growth form, which invades tissues. This morphogenesis is regulated by environmental factors that in the human body frequently include oxygen-poor niches (hypoxia) containing elevated CO_2 levels.

The transcription factor Efg1 of *C. albicans* has a dual function, because it induces hyphal formation under normoxic conditions, but represses filamentation under hypoxia. Threonine residues 179 and 206 of Efg1 are phosphorylated for its normoxic function, while the native N-terminal region and non-phosphorylated threonine residues of Efg1 were found to be required for its function as a repressor under hypoxia. The genomic localization of Efg1 under hypoxia identified 300 target genes, which overlap with targets of transcription factors Ace2, Bcr1 and Brg1 that together form a regulatory hub regulating filamentation. Transcriptional analysis revealed that members of the Cek1-MAPK pathway of filamentation are repression targets of the Efg1 network to favour yeast growth under hypoxia. Furthermore, it was established that the function of Efg1 as the key morphogenetic regulator of *C. albicans* is regulated by additional novel mechanisms. Firstly, it was found that a 218 nt region within the 5´ untranslated region of the *EFG1* transcript is important for its efficient translation. Also, it appears that phosphorylation of Efg1 already occurs at its target genes, because a part of the respective protein kinase A isoform Tpk2 co-localizes in the nucleus with Efg1.

Previous results had established that the Sch9 kinase prevents hyphal morphogenesis of *C. albicans* under hypoxia, but only in the presence of high CO_2 levels. To identify similarly acting regulators, a mutant library was screened that revealed 21 mutants growing in hyperfilamentous form under hypoxia and high CO_2 levels, while 12 mutants were also unable to filament under normoxia (as an *efg1* mutant). Transcript analysis of representative mutants lacking the Zcf14 or Crf1 proteins identified the *UME6* gene, which encodes an essential positive regulator of filamentation, as the repression target. Collectively, the results indicate that *C. albicans* has a high potential to filament under hypoxia, but this ability is suppressed normally by a surprisingly high number of specific regulators. While hypoxic niches in the human host may generally favour yeast proliferation, controlled relief of filamentation repression may be instrumental in specific hypoxic niches, e.g. during escape from immune cells or for exit from the GI tract.

5. References

Achterman RA and Theodore CW. Dermatophyte Virulence Factors: Identifying and Analyzing Genes That May Contribute to Chronic or Acute Skin Infections. International Journal of Microbiology 2012. Article ID 358305, 8 pages, 2012.

Andersen SB, Gerritsma S, Yusah KM, Mayntz D, Hywel-Jones NL, Billen J, … Hughes DP. The Life of a Dead Ant: The Expression of an Adaptive Extended Phenotype. The American Naturalist 2009. 174(3), 424–433.

Arsenault AB, Bliss JM. Neonatal Candidiasis: New Insights into an Old Problem at a Unique Host-Pathogen Interface. Curr Fungal Infect Rep. 2015 Dec 1;9(4):246-252.

Ashbee HR. Recent developments in the immunology and biology of *Malassezia* species. FEMS Immunol Med Microbiol 2006 47:14-23.

Askew C, Sellam A, Epp E, Hogues H, Mullick A, Nantel A, Whiteway M. Transcriptional regulation of carbohydrate metabolism in the human pathogen *Candida albicans*. *PLoS Pathog*. 5(10):e1000612. doi: 10.1371/journal.ppat.1000612. Epub 2009 Oct 9. PubMed PMID: 19816560; PubMed Central PMCID: PMC2749448.

Bailey DA, Feldmann PJ, Bovey M, Gow NA, Brown AJ. The *Candida albicans HYR1* gene, which is activated in response to hyphal development, belongs to a gene family encoding yeast cell wall proteins. J Bacteriol. 1996 Sep;178(18):5353-60.

Banerjee M, Thompson DS, Lazzell A, Carlisle PL, Pierce C, Monteagudo C, López-Ribot JL, Kadosh D. UME6, a novel filament-specific regulator of *Candida albicans* hyphal extension and virulence. *Mol Biol Cell*. 2008 Apr;19(4):1354-65.

Barbee ML and Taylor JW. Dating the molecular clock in fungi: How close are we? Fungal Biology 2010. v.24, p.1-16.

Basso V, d'Enfert C, Znaidi S, Bachellier-Bassi S. (2018) From Genes to Networks: The Regulatory Circuitry Controlling *Candida albicans* Morphogenesis. In: Current Topics in Microbiology and Immunology. 2018 Springer, Berlin, Heidelberg.

Bastidas RJ, Heitman J, Cardenas ME. The Protein Kinase Tor1 Regulates Adhesin Gene Expression in *Candida albicans*. PLOS Pathogens 2009. 5(2), e1000294.

Becerra, M. , Lombardía-Ferreira, L. J., Hauser, N. C., Hoheisel, J. D., Tizon, B. and Cerdán, M. E. (2002), The yeast transcriptome in aerobic and hypoxic conditions: effects of *hap1*, *rox1*, *rox3* and *srb10* deletions. Molecular Microbiology, 43: 545-555.

Bellofatto V, & Wilusz J. Transcription and mRNA Stability: Parental Guidance Suggested. Cell 2011 147(7), 1438–1439.

Ben-Ami R. Treatment of Invasive Candidiasis: A Narrative Review. *J Fungi (Basel)*. 2018 Aug 16;4(3):97.

Benedict K, Jackson BR, Chiller T, & Beer KD. Estimation of Direct Healthcare Costs of Fungal Diseases in the United States. Clinical Infectious Diseases 2018.

Benjamin DK Jr, Stoll BJ, Gantz MG,... Goldberg RN. Neonatal candidiasis: epidemiology, risk factors, and clinical judgment. Pediatrics. 2010 Oct;126(4):e865-73.

Berberi A, Noujeim Z, Aoun G. Epidemiology of Oropharyngeal Candidiasis in Human Immunodeficiency Virus/Acquired Immune Deficiency Syndrome Patients and CD4+ Counts. J Int Oral Health. 2015 Mar;7(3):20-3.

Biswas K and Morschhäuser J. The Mep2p ammonium permease controls nitrogen starvation-induced filamentous growth in *Candida albicans*. Molecular Microbiology, 2005 56: 649-669.

Biswas S, Van Dijck P, Datta A. Environmental sensing and signal transduction pathways regulating morphopathogenic determinants of *Candida albicans*. Microbiol Mol Biol Rev. 2007 Jun;71(2):348-76.

Blackwell, M. The fungi: 1, 2, 3 ... 5.1 million species? American Journal of Botany 2011. 98(3), 426–438.

Blankenship JR, Fanning S, Hamaker JJ, & Mitchell AP. An Extensive Circuitry for Cell Wall Regulation in *Candida albicans*. PLOS Pathogens 2010. 6(2), e1000752.

Blehert DS. Fungal Disease and the Developing Story of Bat White-nose Syndrome. PLOS Pathogens 2012. 8(7), e1002779.

Bockmühl DP, Krishnamurthy S , Gerads M , Sonneborn A, Ernst JF . Distinct and redundant roles of the two protein kinase A isoforms Tpk1p and Tpk2p in morphogenesis and growth of *Candida albicans*. Molecular Microbiology 2001. 42: 1243-1257.

Böhm L, Torsin S, Tint SH, Eckstein MT, Ludwig T, and Pérez JC. The yeast form of the fungus *Candida albicans* promotes persistence in the gut of gnotobiotic mice. PLOS Pathogens 2017. 13(10), e1006699.

Bongomin F, Gago S, Oladele RO, Denning DW. Global and Multi-National Prevalence of Fungal Diseases-Estimate Precision. J Fungi. 2017 18;3(4):57.

Bonhomme J , Chauvel M , Goyard S , RouxP , Rossignol T and d'Enfert, C. (2011), Contribution of the glycolytic flux and hypoxia adaptation to efficient biofilm formation by *Candida albicans*. Molecular Microbiology, 80: 995-1013.

Braun BR, & Johnson AD. Control of Filament Formation in *Candida albicans* by the Transcriptional Repressor *TUP1*. Science 1997. 277(5322), 105 LP-109.

Braun BR, Head WS, Wang MX, Johnson AD. Identification and characterization of TUP1-regulated genes in *Candida albicans*. Genetics. 2000 Sep;156(1):31-44.

Brown DH, Giusani AD, Chen X, Kumamoto CA. Filamentous growth of *Candida albicans* in response to physical environmental cues and its regulation by the unique *CZF1* gene. Molecular Microbiology 1999 34: 651-662.

Brown GD, Denning DW, Gow NAR, Levitz SM, Netea MG, White TC. Hidden Killers: Human Fungal Infections. Science Translational Medicine 2012 4(165), 165rv13 LP-165rv13.

Bruno VM, Wang Z, Marjani SL, Euskirchen GM, Martin J, Sherlock G, Snyder M. Comprehensive annotation of the transcriptome of the human fungal pathogen *Candida albicans* using RNA-seq. *Genome Res*. 2010 Oct;20(10):1451-8.

Butler, G., Rasmussen, M. D., Lin, M. F., Santos, M. A. S., Sakthikumar, S., Munro, C. A., … Cuomo, C. A. Evolution of pathogenicity and sexual reproduction in eight *Candida* genomes. Nature 2009 459, 657.

Calderón-Noreña DM, González-Novo A, Orellana-Muñoz S, Gutiérrez-Escribano P, Arnáiz-Pita Y, Dueñas-SanteroE, … de Aldana CRV. A Single Nucleotide Polymorphism Uncovers a Novel Function for the Transcription Factor Ace2 during *Candida albicans* Hyphal Development. PLOS Genetics 2015. 11(4), e1005152.

Cao C, Wu M, Bing J, Tao L, Ding X, Liu X, & Huang G. Global regulatory roles of the cAMP/PKA pathway revealed by phenotypic, transcriptomic and phosphoproteomic analyses in a null mutant of the PKA catalytic subunit in *Candida albicans*. Molecular Microbiology 2017. 105(1), 46–64.

Cao F, Lane S, Raniga PP, Lu Y, Zhou Z, Ramon K, Chen J, Liu H. The Flo8 transcription factor is essential for hyphal development and virulence in *Candida albicans*. *Mol Biol Cell*. 2006 Jan;17(1):295-307.

Carlisle PL, & Kadosh D. *Candida albicans* Ume6, a Filament-Specific Transcriptional Regulator, Directs Hyphal Growth via a Pathway Involving Hgc1 Cyclin-Related Protein. Eukaryotic Cell 2010. 9(9), 1320 LP-1328.

Carlisle PL, Banerjee M, Lazzell A, Monteagudo C, López-Ribot JL, Kadosh D. Expression levels of a filament-specific transcriptional regulator are sufficient to determine *Candida albicans* morphology and virulence. Proc Natl Acad Sci U S A. 2009 Jan 13;106(2):599-604.

Carreau A, El Hafny-Rahbi B, Matejuk A, Grillon C, Kieda C. Why is the partial oxygen pressure of human tissues a crucial parameter? Small molecules and hypoxia. J Cell Mol Med. 2011 Jun;15(6):1239-53.

Casadevall A. Fungal Diseases in the 21st Century: The Near and Far Horizons. Pathog Immun. 2018. 3(2):183-196.

Cassone A. Development of vaccines for *Candida albicans*: fighting a skilled transformer. Nature Reviews Microbiology 2013. 11, 884.

Chakrabarti A, Sood P, Rudramurthy, SM. Intensive Care Med. 2015 41: 285.

Challacombe SJ, and Naglik JR. The effects of HIV infection on oral mucosal immunity. Adv. Dent. Res. 2006. 19:29–35.

Chang YC, Bien CM, Lee H , Espenshade PJ and Kwon-Chung KJ (2007). Sre1p, a regulator of oxygen sensing and sterol homeostasis, is required for virulence in *Cryptococcus neoformans*. Molecular Microbiology, 64: 614-629.

Cheng G, Wozniak K, Wallig MA, Fidel PLJr, Trupin SR, Hoyer LL Comparison between *Candida albicans* agglutinin-like sequence gene expression patterns in human clinical specimens and models of vaginal candidiasis. Infection and immunity 2005. 73(3), 1656–1663.
Cheng SC, Quintin J, Cramer RA, ... Netea MG. mTOR- and HIF-1α-mediated aerobic glycolysis as metabolic basis for trained immunity. Science. 2014 Sep 26;345(6204):1250684.

Childers DS, Mundodi V, Banerjee M, Kadosh D. A 5' UTR-mediated translational efficiency mechanism inhibits the *Candida albicans* morphological transition. *Mol Microbiol*. 2014 May;92(3):570-85.

Childers DS, Raziunaite I, Mol Avelar G, Mackie J, Budge S, Stead D, … Brown AJP. The Rewiring of Ubiquitination Targets in a Pathogenic Yeast Promotes Metabolic Flexibility, Host Colonization and Virulence. PLOS Pathogens 2016. 12(4), e1005566.

Chowdhary A, Sharma C, Meis JF. *Candida auris*: A rapidly emerging cause of hospital-acquired multidrug-resistant fungal infections globally. PLOS Pathogens 2017 13(5), e1006290.

Chun CD, Liu OW, Madhani HD. A Link between Virulence and Homeostatic Responses to Hypoxia during Infection by the Human Fungal Pathogen *Cryptococcus neoformans*. PLOS Pathogens 2007 3(2): e22.

Clancy CJ and Hong NM. Systemic Candidiasis: Candidemia and Deep-Organ Infections. In Calderone, Richard A. and Clancy, Cornelius J.(ed), *Candida* and Candidiasis, 2012.Second Edition, p 429-441.

Conti HR, Bruno VM, Childs EE, Daugherty S, ... Kolls JK, Sinha S, Gaffen SL. IL-17 Receptor Signaling in Oral Epithelial Cells Is Critical for Protection against Oropharyngeal Candidiasis. Cell Host Microbe. 2016 Nov 9;20(5):606-617.

Conti HR, Gaffen SL. IL-17-Mediated Immunity to the Opportunistic Fungal Pathogen *Candida albicans*. J Immunol. 2015 Aug 1;195(3):780-8.

Conti HR, Shen F, Nayyar N, Stocum E, ... Gaffen SL. Th17 cells and IL-17 receptor signalling are essential for mucosal host defence against oral candidiasis. J Exp Med. 2009 Feb 16;206(2):299-311.

Crawford A, Wilson D. Essential metals at the host-pathogen interface: nutritional immunity and micronutrient assimilation by human fungal pathogens. *FEMS Yeast Res*. 2015 Nov;15(7):fov071.

Csank C, Schröppel K, Leberer E, Harcus D, Mohamed O, Meloche S, Thomas DY, Whiteway M. Roles of the *Candida albicans* mitogen-activated protein kinase homolog, Cek1p, in hyphal development and systemic candidiasis. Infect Immun. 1998 Jun;66(6):2713-21.
da Silva Dantas A, Lee KK, Raziunaite I, Schaefer K, Wagener J, Yadav B, & Gow NA. Cell biology of *Candida albicans*–host interactions. Current Opinion in Microbiology 2016 34, 111–118.

Dagley MJ, Gentle IE, Beilharz TH, Pettolino FA, Djordjevic JT, Lo TL, … Traven A. Cell wall integrity is linked to mitochondria and phospholipid homeostasis in *Candida albicans* through the activity of the post-transcriptional regulator Ccr4-Pop2. Molecular Microbiology 2011. 79(4), 968–989.

Daignan-Fornier B, Fink GR. Coregulation of purine and histidine biosynthesis by the transcriptional activators *BAS1* and *BAS2*. Proc Natl Acad Sci U S A. 1992 Aug 1;89(15):6746-50.
de Hoog S, Monod M, Dawson T, Boekhout T, Mayser P, Gräser Y. Skin fungi from colonization to infection. Microbiol Spectrum 2017. 5(4): FUNK-0049-2016.
Delaloye J, Calandra T.Invasive candidiasis as a cause of sepsis in the critically ill patient. Virulence. 2014 Jan 1; 5(1):161-9.

Dighton J. Fungi in Ecosystem Processes. 2016. Second ed. New York: Marcel Dekker.

Doedt T, Krishnamurthy S, Bockmühl DP, Tebarth B, Stempel C, Russell CL, Brown AJ, Ernst JF. APSES proteins regulate morphogenesis and metabolism in *Candida albicans*. Mol Biol Cell. 2004 Jul;15(7):3167-80.

Du H, Guan G, Xie J, Sun Y, Tong Y, Zhang L, Huang G. Roles of *Candida albicans* Gat2, a GATA-type zinc finger transcription factor, in biofilm formation, filamentous growth and virulence. PLoS One. 2012 7(1):e29707.

Ebersberger I, de Matos Simoes R, Kupczok A, Gube M, Kothe E, Voigt K, von Haeseler A. A Consistent Phylogenetic Backbone for the Fungi. Molecular Biology and Evolution 2011. 29(5), 1319–1334.

Eggimann P, Garbino J, Pittet D. Management of *Candida* species infections in critically ill patients.Lancet Infect Dis. 2003 Dec; 3(12):772-85.

Eltzschig HK, Carmeliet P. Hypoxia and inflammation. N Engl J Med. 2011 Feb 17;364(7):656-65.
Ernst JF and Tielker D. Responses to hypoxia in fungal pathogens. Cellular Microbiology 2009. 11: 183-190.

Erwig LP and Gow NAR. Interactions of fungal pathogens with phagocytes. Nature Reviews Microbiology 2016. 14, 163.

Evans, S. M., Schrlau, A. E., Chalian, A. A., Zhang, P., & Koch, C. J. Oxygen Levels in Normal and Previously Irradiated Human Skin as Assessed by EF5 Binding. Journal of Investigative Dermatology 2006. 126(12), 2596–2606.

Fang HM, Wang Y. RA domain-mediated interaction of Cdc35 with Ras1 is essential for increasing cellular cAMP level for *Candida albicans* hyphal development. Mol Microbiol 2006. 61: 484–496.

Fazly A, Jain C, Dehner AC, Issi L, Lilly EA, Ali A, Cao H, Fidel PL Jr, Rao RP, Kaufman PD. Chemical screening identifies filastatin, a small molecule inhibitor of *Candida albicans* adhesion, morphogenesis, and pathogenesis. Proc Natl Acad Sci U S A. 2013 Aug 13;110(33):13594-9.

Feng Q, Summers E, Guo B, Fink G. Ras signaling is required for serum-induced hyphal differentiation in *Candida albicans*. J Bacteriol. 1999 Oct;181(20):6339-46.

Ferwerda B, Ferwerda G, Plantinga TS, Willment JA, ... Netea MG. Human dectin-1 deficiency and mucocutaneous fungal infections. N Engl J Med. 2009 Oct 29;361(18):1760-7.

Filler SG, and Kullberg BJ. 2002. Candidemia, p.327–340. In R. Calderone (ed.), *Candida* and Candidiasis.ASM Press, Washington, DC.

Findley K, Oh J, Yang J, Conlan S, Deming C, Meyer JA, Schoenfeld D, Nomicos E, Park M; NIH Intramural Sequencing Center Comparative Sequencing Program, Kong HH, Segre JA. Topographic diversity of fungal and bacterial communities in human skin. Nature. 2013 Jun 20;498 (7454):367-70.
Finkel JS, & Mitchell AP. Genetic control of *Candida albicans* biofilm development. Nature Reviews Microbiology. 2011

Fisher MC, Henk DA, Briggs CJ, Brownstein JS, Madoff LC, McCraw SL, Gurr SJ. Emerging fungal threats to animal, plant and ecosystem health. Nature 2012. 11;484 (7393):186-94.

Foley K, Fazio G, Jensen AB, & Hughes WOH. The distribution of Aspergillus spp. opportunistic parasites in hives and their pathogenicity to honey bees. Veterinary Microbiology. 2014. Vol 169, 203-210.

Foxman B, Muraglia R, Dietz JP, Sobel JD, Wagner J. Prevalence of recurrent vulvovaginal candidiasis in 5 European countries and the United States: results from an internet panel survey. J Low Genit Tract Dis 2013;17:340–5.

François LM, Duncan W & Bernhard H. *Candida albicans* pathogenicity mechanisms. Virulence 2013 4(2), 119–128.

Fu Y, Ibrahim AS, Sheppard DC, Chen Y, French SW, Cutler JE, Filler SG and Edwards JE. *Candida albicans* Als1p: an adhesin that is a downstream effector of the *EFG1* filamentation pathway. Molecular Microbiology 2002 44: 61-72.

Gabaldón T, Miguel A. Naranjo-Ortíz, Marcet-Houben M. Evolutionary genomics of yeast pathogens in the Saccharomycotina, FEMS Yeast Research, Volume 16, Issue 6, September 2016.
Garcia-Solache MA, & Casadevall A. Global Warming Will Bring New Fungal Diseases for Mammals. MBio. 2010. 1(1), e00061-10.

Glocker E, Grimbacher B. Chronic mucocutaneous candidiasis and congenital susceptibility to Candida.Curr Opin Allergy Clin Immunol. 2010 Dec; 10(6):542-50.
Gow NA, van de Veerdonk FL, Brown AJ, & Netea MG. *Candida albicans* morphogenesis and host defence: discriminating invasion from colonization. Nature reviews. Microbiology 2011. 10(2), 112–122.

Gow NAR, Hube B. Importance of the *Candida albicans* cell wall during commensalism and infection. Current Opinion in Microbiology. 2012, Vol. 15, Issue 4, August, Pages 406-412.
Grahl N, Shepardson KM, Chung D, Cramer RA. Hypoxia and fungal pathogenesis: to air or not to air? Eukaryot Cell. 2012 May;11(5):560-70.

Guan Z, Liu H. The *WOR1* 5' untranslated region regulates white-opaque switching in *Candida albicans* by reducing translational efficiency. Mol Microbiol. 2015 Jul;97(1):125-38.
Guarner J, Brandt ME. Histopathologic Diagnosis of Fungal Infections in the 21st Century. Clinical Microbiology Reviews 2011. 24(2), 247 LP-280.
Guinea J. Global trends in the distribution of *Candida* species causing candidemia.Clin Microbiol Infect. 2014 Jun; 20 Suppl 6:5-10.

Gutiérrez-Escribano P, González-Novo A, Suárez MB, Li CR, Wang Y, de Aldana CR, Correa-Bordes J. CDK-dependent phosphorylation of Mob2 is essential for hyphal development in *Candida albicans*. Mol Biol Cell. 2011 Jul 15;22(14):2458-69.

Hall RA, Gow NA. Mannosylation in *Candida albicans*: role in cell wall function and immune recognition. Mol Microbiol. 2013 Dec; 90(6):1147-61.

Havlickova B, Czaika VA, Friedrich M. “Epidemiological trends in skin mycoses worldwide,” Mycoses 2008. vol. 51, no. 4, pp. 2–15.

Heckman DS, Geiser D M, Eidell BR, Stauffer RL, Kardos NL, & Hedges SB. Molecular Evidence for the Early Colonization of Land by Fungi and Plants. Science 2001. 293(5532), 1129 LP-1133.Mills BJW,

Batterman SA, Field KJ. Nutrient acquisition by symbiotic fungi governs Palaeozoic climate transition. Phil. Trans. R. Soc. B. 2017. 373.

Hernández-Santos N, Gaffen SL. Th17 cells in immunity to *Candida albicans*. Cell Host Microbe. 2012 May 17;11(5):425-35.

Herrero De Dios C, Roman E, Diez C, Alonso-Monge R, Pla J. The transmembrane protein Opy2 mediates activation of the Cek1 MAP kinase in *Candida albicans*. Fungal Genetics and Biology 2013. Volume 50, Pages 21-32.

Hickman MA, Zeng G, Forche A, Hirakawa MP, Abbey D, Harrison BD, Wang YM, Su CH, Bennett RJ, Wang Y, Berman J. The 'obligate diploid' *Candida albicans* forms mating-competent haploids. Nature. 2013 Feb 7;494(7435):55-9.

Hill JA, Hoot SJ, White TC, Cowen LE. Evolution of Drug Resistance in Fungi. In Evolution of Virulence in Eukaryotic Microbes 2013 (eds L. D. Sibley, B. J. Howlett and J. Heitman).

Hinnebusch AG, Ivanov IP, & Sonenberg N. Translational control by 5′-untranslated regions of eukaryotic mRNAs.Science 2016, 352(6292), 1413 LP-1416.

Homann OR, Dea J, Noble SM, Johnson AD. A Phenotypic Profile of the *Candida albicans* Regulatory Network. PLOS Genetics 2009 5(12): e1000783.

Horn DL, Neofytos D, Anaissie EJ, ... Webster KM Epidemiology and outcomes of candidemia in 2019 patients: data from the prospective antifungal therapy alliance registry. Clin Infect Dis. 2009. 48 2009 1695–1703.

Horn DL, Neofytos D, Anaissie EJ, Fishman JA, Steinbach WJ, Olyaei AJ, … Webster KM. Epidemiology and Outcomes of Candidemia in 2019 Patients: Data from the Prospective Antifungal Therapy Alliance Registry. Clinical Infectious Diseases 2009. 48(12), 1695–1703.

Hoyer LL, Green CB, Oh SH, Zhao X. Discovering the secrets of the *Candida albicans* agglutinin-like sequence (ALS) gene family--a sticky pursuit. Med Mycol. 2008 Feb;46(1):1-15.

Hughes AL, Todd BL, Espenshade PJ. SREBP Pathway Responds to Sterols and Functions as an Oxygen Sensor in Fission Yeast. Cell 2005 120(6), 831–842.

Hughes DP, Araújo J, Loreto R, Quevillon L, de Bekker, C. and Evans HC. From So Simple a Beginning: The Evolution of Behavioral Manipulation by Fungi. Advances in Genetics 2016. Vol 94,437-469.

Huppler AR, Bishu S, Gaffen SL. Mucocutaneous candidiasis: the IL-17 pathway and implications for targeted immunotherapy. Arthritis Res Ther. 2012 Jul 23; 14(4):217.
Imtiyaz HZ, Simon MC. Hypoxia-inducible factors as essential regulators of inflammation. Curr Top Microbiol Immunol. 2010;345:105-20.
Jackson AP, Gamble JA, Yeomans T, Moran GP, Saunders D, Harris D, Aslett M, Barrell JF, Butler G, … Berriman M. Comparative genomics of the fungal pathogens *Candida dubliniensis* and *Candida albicans*. Genome Res. 2009 Dec;19(12):2231-44.

Jacobsen ID, Wilson D, Wächtler B, Brunke S, Naglik JR, Hube B. *Candida albicans* dimorphism as a therapeutic target. Expert Review of Anti-Infective Therapy 2012. 10(1), 85–93.

James TY; et al. Reconstructing the early evolution of Fungi using a six-gene phylogeny. Nature 2006. 443 (7113): 818–22.

Jeanmonod R, Jeanmonod D. Vaginal Candidiasis (Vulvovaginal Candidiasis). In: StatPearls. Treasure Island (FL): StatPearls Publishing; 2019 Jan.

Jensen RH, Astvad KM, Silva LV, Sanglard D, ... Arendrup MC. Stepwise emergence of azole, echinocandin and amphotericin B multidrug resistance in vivo in *Candida albicans* orchestrated by multiple genetic alterations.J Antimicrob Chemother. 2015 Sep; 70(9):2551-5.

Jindal N, Gill P, Aggarwal A. An epidemiological study of vulvovaginal candidiasis in women of childbearing age. Indian J Med Microbiol 2007;25:175-6
Jones, T., Federspiel, N. A., Chibana, H., Dungan, J., Kalman, S., Magee, B. B., … Scherer, S. (2004). The diploid genome sequence of *Candida albicans*. Proceedings of the National Academy of Sciences of the United States of America 2004.101(19), 7329 LP-7334.

Kadosh D. Control of *Candida albicans* morphology and pathogenicity by post-transcriptional mechanisms. Cell Mol Life Sci. 2016 Nov;73(22):4265-4278.

Kanafani, Z. A., and J. R. Perfect. Antimicrobial resistance: resistance to antifungal agents: mechanisms and clinical impact. Clin. Infect. Dis. 2008 46:120–128.

Karhausen J, Furuta GT, Tomaszewski JE, Johnson RS, Colgan SP, Haase VH. Epithelial hypoxia-inducible factor-1 is protective in murine experimental colitis. J Clin Invest. 2004 Oct 15;114(8):1098-106.

Kashem SW, Kaplan DH. Skin Immunity to *Candida albicans*. *Trends Immunol*. 2016 Jul;37(7):440-450.

Kasper L, Seider K, Hube B. Intracellular survival of Candida glabrata in macrophages: immune evasion and persistence. FEMS Yeast Research 2015 Volume 15, Issue 5, fov042.

Kaur R, Ma B, Cormack BP. A family of glycosylphosphatidylinositol-linked aspartyl proteases is required for virulence of *Candida glabrata*. Proc Natl Acad Sci U S A. 2007 May 1;104(18):7628-33.

Kelly MT, MacCallum DM, Clancy S, Odds FC, Brown A. and Butler G. The *Candida albicans* CaACE2 gene affects morphogenesis, adherence and virulence. Molecular Microbiology 2004 53: 969-983.

Kett DH; Azoulay E, Echeverria PM, Vincent J-L. *Candida* bloodstream infections in intensive care units: Analysis of the extended prevalence of infection in intensive care unit study. Critical Care Medicine 2011. 39(4):665-670.

Kim YS, Ho SB. Intestinal goblet cells and mucins in health and disease: recent insights and progress. Curr Gastroenterol Rep. 2010 Oct;12(5):319-30.
Klunk C, Domingues E, Wiss K. (2014). An update on diaper dermatitis. Clinics in Dermatology 2014

Köhler JR, Casadevall A, Perfect J. The spectrum of fungi that infects humans. *Cold Spring Harb Perspect Med*. 2015. 5(1):a019273.

Kordalewska M, Lee A, Park S, Berrio I, Chowdhary A, Zhao Y, & Perlin DS. Understanding Echinocandin Resistance in the Emerging Pathogen *Candida auris* Antimicrobial Agents and Chemotherapy 2018. 62(6), e00238-18.

Kozak M. Regulation of translation via mRNA structure in prokaryotes and eukaryotes. Gene 2005, 21 Nov.Volume 361, Pages 13-37.

Lackey E, Vipulanandan G, Childers DS, Kadosh D. Comparative evolution of morphological regulatory functions in *Candida* species. Eukaryot Cell. 2013 Oct;12(10):1356-68.

Lane S, Birse C, Zhou S, Matson R, Liu H. DNA array studies demonstrate convergent regulation of virulence factors by Cph1, Cph2, and Efg1 in *Candida albicans*. J Biol Chem 2001.276: 48988–48996.

Lassak T, Schneider E, Bussmann M , Kurtz D , Manak JR, Srikantha T , Soll DR and Ernst JF. Target specificity of the *Candida albicans* Efg1 regulator. Molecular Microbiology 2011 82: 602-618.

Leaché AD. The Timetree of Life. S. Blair Hedges and Sudhir Kumar, editors. Integrative and Comparative Biology 2009. 50(1), 141–142.

Leberer E, Harcus D, Dignard D, Johnson L, Ushinsky S, Thomas D Y, Schröppel K. Ras links cellular morphogenesis to virulence by regulation of the MAP kinase and cAMP signalling pathways in the pathogenic fungus *Candida albicans*. Molecular Microbiology 2001 42(3), 673–687.

Leppek K, Das R, Barna M. Functional 5' UTR mRNA structures in eukaryotic translation regulation and how to find them. Nat Rev Mol Cell Biol. 2018 Mar;19(3):158-174.

Lewis LE, Bain JM, Lowes C, Gow NA, Erwig LP. *Candida albicans* infection inhibits macrophage cell division and proliferation. Fungal Genet Biol. 2012 Sep; 49(9):679-80.
Liang SC, Tan XY, Luxenberg DP, Karim R, Dunussi-Joannopoulos K, Collins M, Fouser LA. Interleukin (IL)-22 and IL-17 are coexpressed by Th17 cells and cooperatively enhance expression of antimicrobial peptides. J Exp Med. 2006 Oct 2;203(10):2271-9.

Lin CH, Kabrawala S, Fox EP, Nobile CJ, Johnson AD, & Bennett RJ. Genetic Control of Conventional and Pheromone-Stimulated Biofilm Formation in *Candida albicans*. PLOS Pathogens 2013 9(4), e1003305.

Lin L, Ibrahim AS, Baquir B, Avanesian V, Fu Y, Spellberg B. Immunological surrogate marker of rAls3p-N vaccine-induced protection against *Staphylococcus aureus*. FEMS Immunol Med Microbiol. 2009 Apr;55(3):293-5.

Lionakis MS, Lim JK, Lee CC, Murphy PM. Organ-specific innate immune responses in a mouse model of invasive candidiasis. J Innate Immun. 2011 Feb;3(2):180-99.

Liu H, Kohler J, Fink GR. Suppression of hyphal formation in *Candida albicans* by mutation of a STE12 homolog. Science 1994 266(5191), 1723 LP-1726.

Liu W, Zhao J, Li X, Li Y, Jiang L. The protein kinase CaSch9p is required for the cell growth, filamentation and virulence in the human fungal pathogen *Candida albicans*. FEMS Yeast Research 2010. 10: 462-470.

Lo H-J, Köhler JR, DiDomenico B, Loebenberg D, Cacciapuoti A, & Fink GR. Nonfilamentous *C. albicans* Mutants Are Avirulent. Cell 1997 90(5), 939–949.

Lohse MB, Gulati M, Johnson AD, Nobile CJ. Development and regulation of single- and multi-species *Candida albicans* biofilms. Nat Rev Microbiol. 2018 Jan;16(1):19-31.

Lohse MB, Johnson AD. White-opaque switching in *Candida albicans*. Curr Opin Microbiol. 2009 Dec;12(6):650-4.

Lopes JP, Stylianou M, Backman E, Holmberg S, Jass J, Claesson R, & Urban CF. Evasion of Immune Surveillance in Low Oxygen Environments Enhances *Candida albicans* Virulence. MBio 2018, 9(6), e02120-18.

Lorenz MC, Bender JA, Fink GR. Transcriptional response of *Candida albicans* upon internalization by macrophages. Eukaryot Cell. 2004 Oct;3(5):1076-87.

Lortholary O, Charlier C, Lebeaux D, Lecuit M, Consigny PH. Fungal infections in immunocompromised travelers. Clinical Infectious Diseases 2013 ;56:861-9.

Lowman DW, Greene RR, Bearden DW, Kruppa MD,... Netea MG, Williams DL. Novel structural features in *Candida albicans* hyphal glucan provide a basis for differential innate immune recognition of hyphae versus yeast. J Biol Chem. 2014 Feb 7;289(6):3432-43.

Lu Y, Su C, Liu H. *Candida albicans* hyphal initiation and elongation. *Trends Microbiol*. 2014 Dec;22(12):707-14.

Lu Y, Su C, Ray S, Yuan Y, & Liu H. CO_2 signaling through the Ptc2-Ssn3 axis governs sustained hyphal development of *Candida albicans* by reducing Ume6 phosphorylation and degradation. MBio 2019, 10(1), e02320-18.

Lu Y, Su C, Wang A, Liu H. Hyphal Development in *Candida albicans* Requires Two Temporally Linked Changes in Promoter Chromatin for Initiation and Maintenance. PLOS Biology 2011 9(7): e1001105.

Lücking R, Huhndorf S, Pfister DH, Plata ER, & Lumbsch HT. Fungi evolved right on track. Mycologia 2009. 101(6), 810–822.
Lutzoni F, Nowak MD, Alfaro ME, Reeb V, Miadlikowska J, Krug M, … Magallón S. Contemporaneous radiations of fungi and plants linked to symbiosis. Nature Communications 2018. 9(1), 5451.

MacCallum DM, Findon H, Kenny CC, Butler G, Haynes K, Odds FC. Different consequences of ACE2 and SWI5 gene disruptions for virulence of pathogenic and nonpathogenic yeasts. Infect Immun. 2006 Sep;74(9):5244-8.

MacCallum DM.Hosting Infection: Experimental Models to Assay *Candida* Virulence. International Journal of Microbiology, vol. 2012, Article ID 363764, 12 pages, 2012.

MacPherson S, Larochelle M, Turcotte B. A fungal family of transcriptional regulators: the zinc cluster proteins. Microbiol Mol Biol Rev. 2006 Sep;70(3):583-604.

Magee BB, Legrand M, Alarco A , Raymond M and Magee PT. Many of the genes required for mating in *Saccharomyces cerevisiae* are also required for mating in *Candida albicans*. Molecular Microbiology, 2002 46: 1345-1351.

Magee PT, Gale C, Berman J, Davis D. Molecular genetic and genomic approaches to the study of medically important fungi. Infect Immun. 2003 May;71(5):2299-309.

Malavia D, Lehtovirta-Morley LE, Alamir O, Weiß E, Gow NAR, Hube B, & Wilson, D. Zinc Limitation Induces a Hyper-Adherent Goliath Phenotype in *Candida albicans*. Frontiers in Microbiology 2017. Vol. 8, p. 2238.

Martchenko M, Levitin A, Hogues H, Nantel A, Whiteway M. Transcriptional rewiring of fungal galactose-metabolism circuitry. Curr Biol. 2007 Jun 19;17(12):1007-13.

Martin R, Moran GP, Jacobsen ID, Heyken A, Domey J, et al. (2011) The *Candida albicans*-Specific Gene *EED1* Encodes a Key Regulator of Hyphal Extension. PLOS ONE 6(4): e18394.

Massey SE, Moura G, Beltrão P, Almeida R, Garey JR, Tuite MF, Santos MAS. Comparative evolutionary genomics unveils the molecular mechanism of reassignment of the CTG codon in *Candida* spp. Genome Res 2003 13: 544–557.

Mayer FL, Wilson D, Hube B. *Candida albicans* pathogenicity mechanisms. Virulence. 2013 Feb 15; 4(2):119-28.

Mayr C. Regulation by 3'-Untranslated Regions. Annual Review of Genetics 2017, 51(1), 171–194.

McGirt LY, Martins CR. Dermatologic diagnoses in the perianal area. Clin Colon Rectal Surg. 2004 Nov;17(4):241-5.

Mengesha BG, Conti HR. The Role of IL-17 in Protection against Mucosal *Candida* Infections. *J Fungi (Basel)*. 2017 Sep 27;3(4):52.

Mennella TA, Klinkenberg LG, Zitomer RS. Recruitment of Tup1-Ssn6 by yeast hypoxic genes and chromatin-independent exclusion of TATA binding protein. *Eukaryot Cell*. 2003 Dec;2(6):1288-303.

Metin A, Dilek N, Bilgili SG. Recurrent candidal intertrigo: challenges and solutions. Clin Cosmet Investig Dermatol. 2018 Apr 17;11:175-185. doi: 10.2147/CCID.S127841.

Mignone F, Gissi C, Liuni S, Pesole G. Untranslated regions of mRNAs. Genome Biology 2002 3(3),reviews0004.1.

Miramón P, Lorenz MC. A feast for *Candida*: Metabolic plasticity confers an edge for virulence. PLOS Pathogens 2017 13(2), e1006144.
Miranda I, Silva-Dias A, Rocha R, Teixeira-Santos R, … Rodrigues AG. *Candida albicans* CUG Mistranslation Is a Mechanism To Create Cell Surface Variation. MBio 2013 4(4), e00285-13.

Miranda LN, van der Heijden IM, Costa SF, Sousa API, Sienra RA, Gobara S, … Levin AS. *Candida* colonisation as a source for candidaemia. Journal of Hospital Infection. 2009

Monge R, Román E, Nombela C, Pla J. Microbiology 2006 152(4):905-912.

Mourad A and Perfect JR. Tolerability profile of the current antifungal armoury. Journal of Antimicrobial Chemotherapy 2018.

Moyes DL, Wilson D, Richardson JP, Mogavero S, ...Hube B, Naglik JR. Candidalysin is a fungal peptide toxin critical for mucosal infection. Nature. 2016 Apr 7;532(7597):64-8.

Mueller U G, and Rabeling C. A breakthrough innovation in animal evolution. Proceedings of the National Academy of Sciences 2008. 105(14), 5287 LP-5288.

Mulhern SM, Logue ME, Butler G. *Candida albicans* transcription factor Ace2 regulates metabolism and is required for filamentation in hypoxic conditions. *Eukaryot Cell*. 2006 Dec;5(12):2001-13.

Muñoz JF, Gade L, Chow NA, Loparev VN, Juieng P, Berkow EL, Farrer RA, Litvintseva AP, Cuomo CA. Genomic insights into multidrug-resistance, mating and virulence in *Candida auris* and related emerging species. Nat Commun. 2018 Dec 17;9(1):5346.

Murciano C, Moyes DL, Runglall M, Tobouti P, Islam A, Hoyer LL, Naglik JR. Evaluation of the role of *Candida albicans* agglutinin-like sequence (Als) proteins in human oral epithelial cell interactions. *PLoS One*. 2012 7(3):e33362.

Nadal-Ribelles M, Conde N, Flores O, González-Vallinas J, Eyras E, Orozco M, de Nadal E, Posas F. Hog1 bypasses stress-mediated down-regulation of transcription by RNA polymerase II redistribution and chromatin remodeling. Genome Biol. 2012 Nov 18;13(11):R106.

Naglik JR, Moyes DL, Wächtler B, Hube B. *Candida albicans* interactions with epithelial cells and mucosal immunity. Microbes Infect. 2011 Nov;13(12-13):963-76.

Netea MG, Gow NA, Munro CA, Bates S, Collins C, Ferwerda G, … Kullberg BJ. Immune sensing of *Candida albicans* requires cooperative recognition of mannans and glucans by lectin and Toll-like receptors. The Journal of clinical investigation 2006. 116(6), 1642–1650.

Nett JE. Special Issue: *Candida* and Candidiasis. J Fungi (Basel). 2018 Jun 21;4(3):74.

Nobile CJ & Johnson AD *Candida albicans* Biofilms and Human Disease. Annual Review of Microbiology 2015.

Nobile CJ, Fox EP, Nett JE, Sorrells TR, Mitrovich QM, Hernday AD, Tuch BB, Andes DR, Johnson AD. A recently evolved transcriptional network controls biofilm development in *Candida albicans*. *Cell*. 2012 Jan 20;148(1-2):126-38.

Noble SM, French S, Kohn LA, Chen V, & Johnson AD. Systematic screens of a *Candida albicans* homozygous deletion library decouple morphogenetic switching and pathogenicity. Nature genetics 2010. 42(7), 590–598.
Noble SM, Gianetti BA, & Witchley JN. *Candida albicans* cell-type switching and functional plasticity in the mammalian host. Nature Reviews Microbiology 2017.

Noffz CS, Liedschulte V, Lengeler K, Ernst JF. Functional mapping of the *Candida albicans* Efg1 regulator. *Eukaryot Cell*. 2008 May;7(5):881-93.

Pagano L, Akova M, Dimopoulos G, Herbrecht R, Drgona L, Blijlevens N. Risk assessment and prognostic factors for mould-related diseases in immunocompromised patients. Journal of Antimicrobial Chemotherapy 2011;66:i5-i14

Pande K, Chen C, Noble SM. Passage through the mammalian gut triggers a phenotypic switch that promotes *Candida albicans* commensalism. Nat Genet. 2013 Sep;45(9):1088-91.

Pascual-Ahuir A, Proft M. The Sch9 kinase is a chromatin-associated transcriptional activator of osmostress-responsive genes. EMBO J. 2007 Jul 11;26(13):3098-108.

Passos DO, Doma MK, Shoemaker CJ, Muhlrad D, Green R, Weissman J, Hollien J, Parker R. Analysis of Dom34 and its function in no-go decay. Mol Biol Cell. 2009 Jul 1;20(13):3025-32.

Patel S, Majmundar SH. Physiology, Carbon Dioxide Retention. [Updated 2018 Oct 27]. In: StatPearls [Internet]. Treasure Island (FL): StatPearls Publishing; 2019

Patil S, Rao RS, Majumdar B, Anil S. Clinical Appearance of Oral *Candida* Infection and Therapeutic Strategies. Front Microbiol. 2015 Dec 17;6:1391.

Peay KG, Kennedy PG, and Talbot JM. Dimensions of biodiversity in the Earth mycobiome. Nature Reviews Microbiology 2016. 14, 434–447.

Pérez JC, Kumamoto CA, Johnson AD. *Candida albicans* Commensalism and Pathogenicity Are Intertwined Traits Directed by a Tightly Knit Transcriptional Regulatory Circuit. PLOS Biology 2013. 11(3): e1001510.

Perfect JR. The antifungal pipeline: A reality check. Nature Reviews Drug Discovery 2017.
Perlin DS. Echinocandin Resistance in Candida. Clin Infect Dis. 2015 Dec 1;61 Suppl 6(Suppl 6):S612-7.

Pfaller MA and Diekema DJ. Epidemiology of invasive candidiasis: a persistent public health problem. Clinical Microbiology Reviews 2007.

Pfaller MA, Pappas PG, Wingard JR. Invasive Fungal Pathogens: Current Epidemiological Trends. Clinical Infectious Diseases 2006. 43,S3–S14.

Phan QT, Myers CL, Fu Y, Sheppard DC, Yeaman MR… Filler SG. Als3 Is a *Candida albicans* Invasin That Binds to Cadherins and Induces Endocytosis by Host Cells. PLOS Biology 2007 5(3): e64.

Pickering BM, Willis AE.The implications of structured 5' untranslated regions on translation and disease. Seminars in Cell & Developmental Biology 2005.Volume 16, Issue 1, February, Pages 39-47.

Pierce CG, Lopez-Ribot JL. Candidiasis drug discovery and development: new approaches targeting virulence for discovering and identifying new drugs. Expert Opin Drug Discov. 2013 Sep;8(9):1117-26.

Pierce JV, Dignard D, Whiteway M, Kumamoto CA. Normal adaptation of *Candida albicans* to the murine gastrointestinal tract requires Efg1p-dependent regulation of metabolic and host defense genes. Eukaryot Cell. 2013 Jan;12(1):37-49.

Pierce JV, Kumamoto CA. Variation in *Candida albicans* EFG1 Expression Enables Host-Dependent Changes in Colonizing Fungal Populations. mBio 2012, 3 (4) e00117-12.

Pokholok DK, Zeitlinger J, Hannett NM, Reynolds DB, Young RA (2006) Activated signal transduction kinases frequently occupy target genes. Science 313: 533–536

Potrykus J, Ballou ER, Childers DS, Brown AJP. Conflicting Interests in the Pathogen–Host Tug of War: Fungal Micronutrient Scavenging Versus Mammalian Nutritional Immunity. PLOS Pathogens 2016 10(3): e1003910.

Pradhan A, Avelar GM, Bain JM, Childers DS, Larcombe DE, Netea MG, … Brown AJP. Hypoxia promotes immune evasion by triggering β-Glucan masking on *Candida albicans* cell surface via mitochondrial and cAMP-Protein Kinase A signaling. MBio 2018, 9(6), e01318-18.

Ramage G, Martínez JP, and López-Ribot JL. *Candida* biofilms on implanted biomaterials: a clinically significant problem. FEMS Yeast Research 2006. 6: 979-986.

Ramírez-Zavala B, Reuß O, Park YN, Ohlsen K, Morschhäuser J. Environmental Induction of White–Opaque Switching in *Candida albicans*. PLOS Pathogens 2008. 4(6): e1000089.

Rautemaa R, Ramage G Oral candidosis–clinical challenges of a biofilm disease. Crit. Rev. Microbiol.2011.37 328–336. 10.3109/1040841X.2011.585606

Rawal Y, Chereji RV, Valabhoju V, Qiu H, Ocampo J, Clark DJ, Hinnebusch AG. Gcn4 Binding in Coding Regions Can Activate Internal and Canonical 5' Promoters in Yeast. Mol Cell. 2018 Apr 19;70(2):297-311.e4.

Raymond J and Segrè D. The Effect of Oxygen on Biochemical Networks and the Evolution of Complex Life. Science 2006. 311(5768), 1764 LP-1767.

Remy W, Taylor TN, Hass H, Kerp H. Four hundred-million-year-old vesicular arbuscular mycorrhizae. Proc Natl Acad Sci U S A 1994. 91(25):11841-3.

Reuß O, Vik A, Kolter R Morschhäuser J.The SAT1 flipper, an optimized tool for gene disruption in *Candida albicans*. Gene 2004 Volume 341, 27 October 2004, Pages 119-127.

Richardson JP, Moyes DL. Adaptive immune responses to *Candida albicans* infection. Virulence. 2015. 6(4):327-37.

Richardson JP, Naglik JR. Special Issue: Mucosal Fungal Infections. J. Fungi 2018, 4, 43.

Rocha CR, Schröppel K, Harcus D, Marcil A, Dignard D, Taylor BN, Thomas DY, Whiteway M, Leberer E. Signaling through adenylyl cyclase is essential for hyphal growth and virulence in the pathogenic fungus *Candida albicans*. Mol Biol Cell. 2001 Nov;12(11):3631-43.

Rodrigues CF, Rodrigues ME, Henriques M. *Candida* sp. Infections in Patients with Diabetes Mellitus. J Clin Med. 2019 Jan 10;8(1):76.

Romo JA, Pierce CG, Esqueda M, Hung CY, Saville SP, Lopez-Ribot JL. In vitro characterization of a Biaryl Amide anti-virulence compound targeting *Candida albicans* filamentation and biofilm formation. Front Cell Infect Microbiol. 2018 Jul 10;8:227.

Rudkin FM, Bain JM, Walls C, Lewis LE, Gow NA, Erwig LP. Altered dynamics of *Candida albicans* phagocytosis by macrophages and PMNs when both phagocyte subsets are present. MBio. 2013 Oct 29;4(6):e00810-13.

Sanchez-Diaz A, Nkosi PJ, Murray S, Labib K. The Mitotic Exit Network and Cdc14 phosphatase initiate cytokinesis by counteracting CDK phosphorylations and blocking polarised growth. *EMBO J*. 2012 Aug 29;31(17):3620-34.

Sanglard D. Emerging Threats in Antifungal-Resistant Fungal Pathogens. Frontiers in Medicine 2016.

Sanglard D. Finding the needle in a haystack: Mapping antifungal drug resistance in fungal pathogen by genomic approaches. PLOS Pathogens 2019. 15(1), e1007478.

Sansonetti PJ and Medzhitov R. Learning Tolerance while Fighting Ignorance Cell. 2009 Volume 138, ISSUE 3, P416-420.

Santos MA, Tuite MF. The CUG codon is decoded in vivo as serine and not leucine in *Candida albicans*. Nucleic Acids Res. 1995 May 11;23(9):1481-6.

Saputo S, Chabrier-Rosello Y, Luca FC, Kumar A, Krysan DJ. The RAM Network in Pathogenic Fungi. Eukaryotic Cell 2012 11(6), 708 LP-717.

Saputo S, Kumar A, Krysan DJ. Efg1 directly regulates *ACE2* expression to mediate cross talk between the cAMP/PKA and RAM pathways during *Candida albicans* morphogenesis. Eukaryot Cell. 2014 Sep;13(9):1169-80.

Sarmiento-Ramírez JM, Abella-Pérez E, Phillott AD, Sim J, van West P, Martín MP, … Diéguez-Uribeondo J. Global Distribution of Two Fungal Pathogens Threatening Endangered Sea Turtles. PLOS ONE 2014. 9(1), e85853.

Sasse C, Hasenberg M, Weyler M, Gunzer M, Morschhäuser J. White-opaque switching of *Candida albicans* allows immune evasion in an environment-dependent fashion. Eukaryot Cell. 2013 Jan;12(1):50-8.

Saunte D, Mrowietz, U, Puig L, and Zachariae C *Candida* infections in patients with psoriasis and psoriatic arthritis treated with interleukin-17 inhibitors and their practical management. Br J Dermatol. 2017 177: 47-62.

Saville SP, Lazzell AL, Bryant AP, Fretzen A, Monreal A, Solberg EO, Monteagudo C, Lopez-Ribot JL, Milne GT. Inhibition of filamentation can be used to treat disseminated candidiasis. *Antimicrob Agents Chemother*. 2006 Oct;50(10):3312-6.

Saville SP, Lazzell AL, Chaturvedi AK, Monteagudo C, Lopez-Ribot JL. Efficacy of a genetically engineered *Candida albicans* tet-NRG1 strain as an experimental live attenuated vaccine against hematogenously disseminated candidiasis. Clin Vaccine Immunol. 2009 Mar;16(3):430-2.

Saville SP, Lazzell AL, Monteagudo C, Lopez-Ribot JL. Engineered control of cell morphology in vivo reveals distinct roles for yeast and filamentous forms of *Candida albicans* during infection. Eukaryot Cell. 2003 Oct;2(5):1053-60.

Schaller M, Mailhammer R, Grassl G, Sander CA, Hube B, Korting HC.Infection of human oral epithelia with *Candida* species induces cytokine expression correlated to the degree of virulence. J Invest Dermatol. 2002 118:652–657.

Scheele BC, Pasmans F, Skerratt LF, Berger L, Martel A, Beukema W, … Canessa S. Amphibian fungal panzootic causes catastrophic and ongoing loss of biodiversity. Science 2019. 363(6434), 1459 LP-1463.

Schweizer A, Rupp S, Taylor BN, Röllinghoff M, Schröppel. The TEA/ATTS transcription factor CaTec1p regulates hyphal development and virulence in *Candida albicans*. Molecular Microbiology 2000 38: 435-445.

Sellam A, Hogues H, Askew C, Tebbji F, van het Hoog M, Lavoie H, … Nantel A. Experimental annotation of the human pathogen *Candida albicans* coding and noncoding transcribed regions using high-resolution tiling arrays. Genome Biology 2010 11(7), R71.

Sellam A, van het Hoog M, Tebbji F, Beaurepaire C, Whiteway M, Nantel A. Modeling the transcriptional regulatory network that controls the early hypoxic response in *Candida albicans*. *Eukaryot Cell*. 2014 May;13(5):675-90.

Semenza GL. Oxygen-dependent regulation of mitochondrial respiration by hypoxia-inducible factor 1. Biochemical Journal 2007. 405(1), 1 LP-9.

Setiadi ER, Doedt T, Cottier F, Noffz C, Ernst JF. Transcriptional Response of *Candida albicans* to Hypoxia: Linkage of Oxygen Sensing and Efg1p-regulatory Networks. Journal home page for Journal of Molecular Biology 2006 Volume 361, Issue 3,Pages 399-411.
Sexton AC, Howlett BJ. Parallels in fungal pathogenesis on plant and animal hosts. *Eukaryot Cell*. 2006 5(12):1941-9.

Sharkey LL, McNemar MD, Saporito-Irwin SM, Sypherd PS, Fonzi WA. HWP1 functions in the morphological development of *Candida albicans* downstream of EFG1, TUP1, and RBF1. *J Bacteriol*. 1999 Sep;181(17):5273-9.

Sharma C, Kumar N, Pandey R, Meis JF, Chowdhary A. Whole genome sequencing of emerging multidrug resistant *Candida auris* isolates in India demonstrates low genetic variation. New Microbes New Infect. 2016 Jul 29;13:77-82.

Sherwood, S. C., & Huber, M. An adaptability limit to climate change due to heat stress. Proceedings of the National Academy of Sciences 2010. 107(21), 9552 LP-9555.
Si H, Hernday AD, Hirakawa MP, Johnson AD, Bennett RJ. *Candida albicans* white and opaque cells undergo distinct programs of filamentous growth. PLoS Pathog.2013 9(3):e1003210.

Simões J, Bezerra AR, Moura GR, Araújo H, Gut I, Bayes M, Santos MA. The Fungus *Candida albicans* Tolerates Ambiguity at Multiple Codons. Front Microbiol. 2016 Mar 31;7:401.

Simon MC, Keith B. The role of oxygen availability in embryonic development and stem cell function. Nat Rev Mol Cell Biol. 2008 Apr;9(4):285-96.

Singh A, Verma R, Murari A, Agrawal A. Oral candidiasis: An overview. J Oral Maxillofac Pathol. 2014 Sep;18(Suppl 1):S81-5.

Slutsky B, Staebell M, Anderson J, Risen L, Pfaller M, Soll DR. "White-opaque transition": a second high-frequency switching system in *Candida albicans*. J Bacteriol. 1987 Jan;169(1):189-97.

Sobel JD. Vulvovaginal candidosis.2007 Lancet 369:1961–1971.

Sohn K, Urban C, Brunner H, Rupp S. *EFG1* is a major regulator of cell wall dynamics in *Candida albicans* as revealed by DNA microarrays. Molecular Microbiology 2003 47: 89-102.

Soler-Hurtado MM, Sandoval-Sierra JV, Machordom A, Diéguez-Uribeondo J. *Aspergillus sydowii* and Other Potential Fungal Pathogens in Gorgonian Octocorals of the Ecuadorian Pacific. PloS One 2016 11(11), e0165992–e0165992.

Song Y, Cheon SA, Lee KE, Lee SY, Lee BK, Oh DB, Kang HA, Kim JY. Role of the RAM network in cell polarity and hyphal morphogenesis in *Candida albicans*. Mol Biol Cell. 2008 Dec;19(12):5456-77.

Sonneborn A, Bockmühl DP, Gerads M, , Kurpanek K, Sanglard D. and Ernst JF, Protein kinase A encoded by *TPK2* regulates dimorphism of *Candida albicans*. Molecular Microbiology 2000 35: 386-396.

Srikantha T., Tsai LK, Daniels K, Soll DR. EFG1 null mutants of *Candida albicans* switch but cannot express the complete phenotype of white-phase budding cells. J Bacteriol. 2000 182: 1580–1591.

Staab JF, Bradway SD, Fidel PL, Sundstrom, P. (1999). Adhesive and Mammalian Transglutaminase Substrate Properties of *Candida albicans* Hwp1. Science 1999 283(5407), 1535 LP-1538.

Staib, P. and Morschhäuser, J. Chlamydospore formation in *Candida albicans* and *Candida dubliniensis*– an enigmatic developmental programme. Mycoses 2007. 50: 1-12.

Stichternoth C, Ernst JF. Hypoxic adaptation by Efg1 regulates biofilm formation by *Candida albicans*. Appl Environ Microbiol. 2009 Jun;75(11):3663-72.

Stichternoth C, Fraund A, Setiadi E, Giasson L, Vecchiarelli A, Ernst JF. Sch9 kinase integrates hypoxia and CO2 sensing to suppress hyphal morphogenesis in *Candida albicans*. Eukaryot Cell. 2011 10(4):502-11.

Stoldt VR, Sonneborn A, Leuker CE, Ernst JF. Efg1p, an essential regulator of morphogenesis of the human pathogen *Candida albicans*, is a member of a conserved class of bHLH proteins regulating morphogenetic processes in fungi. EMBO J. 1997 15;16(8):1982-91.
Sudbery P, Gow NAR, & Berman J. The distinct morphogenic states of *Candida albicans*. Trends in Microbiology 2004 12(7), 317–324.

Sudbery PE. Growth of *Candida albicans* hyphae. Nature Reviews Microbiology 2011. 9, 737.
Sullivan DJ, Moran GP, and Coleman DC. *Candida dubliniensis*: ten years on," FEMS Microbiology Letters 2005. vol. 253, no. 1, pp. 9–17, 2005.

Summons RE, Bradley AS, Jahnke LL, Waldbauer JR. Steroids, triterpenoids and molecular oxygen. Philos Trans R Soc Lond B Biol Sci. 2006 Jun 29;361(1470):951-68.

Sun JN, Solis NV, Phan QT, Bajwa JS, Kashleva H, Thompson A, Liu Y, Dongari-Bagtzoglou A, Edgerton M, Filler SG. Host cell invasion and virulence mediated by *Candida albicans* Ssa1. PLoS Pathog. 2010 Nov 11;6(11):e1001181.

Sundaram A and Grant CM. A single inhibitory upstream open reading frame (uORF) is sufficient to regulate *Candida albicans GCN4* translation in response to amino acid starvation conditions.RNA 2014 April,20: 559-567.

Sundstrom P, Balish E, & Allen CM. Essential Role of the *Candida albicans* Transglutaminase Substrate, Hyphal Wall Protein 1, in Lethal Oroesophageal Candidiasis in Immunodeficient Mice. The Journal of Infectious Diseases 2002. 185(4), 521–530.

Sung GH, Poinar GO, Spatafora JW. The oldest fossil evidence of animal parasitism by fungi supports a Cretaceous diversification of fungal-arthropod symbioses. Molecular Phylogenetics and Evolution 2008. 49(2), 495–502.

Swidergall M, Solis NV, Lionakis MS, Filler SG. EphA2 is an epithelial cell pattern recognition receptor for fungal β-glucans. Nat Microbiol. 2018 Jan;3(1):53-61.

Synnott JM, Guida A, Mulhern-Haughey S, Higgins DG, Butler G. Regulation of the hypoxic response in *Candida albicans*. *Eukaryot Cell*. 2010 Nov;9(11):1734-46.
Szafranski-Schneider E, Swidergall M, Cottier F, … Ernst JF. Msb2 Shedding Protects *Candida albicans* against Antimicrobial Peptides. PLOS Pathogens 2012 8(2): e1002501.

Tan GSE, & Hsu LY. Overview of Fungal Infections. Modules in Biomedical sciences 2018.

Tan TY, Hsu LY, Alejandria MM, Chaiwarith R, Chinniah T, Chayakulkeeree M, … Van Pham H. Antifungal susceptibility of invasive *Candida* bloodstream isolates from the Asia-Pacific region . Medical Mycology 2016 54(5), 471–477.

Tao L, Du H, Guan G, Dai Y, Nobile CJ, ...Huang G. Discovery of a “White-Gray-Opaque” Tristable Phenotypic Switching System in *Candida albicans*: Roles of Non-genetic Diversity in Host Adaptation. PLOS Biology 2014 12(4): e1001830

Thompson DS, Carlisle PL, Kadosh D. Coevolution of morphology and virulence in *Candida species*. Eukaryot Cell. 2011 Sep;10(9):1173-82.

Tortorano AM, Kibbler C, Peman J, Bernhardt H, Klingspor L, Grillot R. Candidaemia in Europe: epidemiology and resistance.Int J Antimicrob Agents. 2006 May;27(5):359-66.

Treseder KK, & Lennon JT. Fungal Traits That Drive Ecosystem Dynamics on Land. Microbiology and Molecular Biology Reviews 2015. 79(2), 243 LP-262.

Tso GHW, Reales-Calderon JA, Pavelka N. The Elusive Anti-*Candida* Vaccine: Lessons From the Past and Opportunities for the Future. Frontiers in Immunology 2018, Vol. 9, p. 897.

Tso GHW, Reales-Calderon JA, Tan ASM, Sem X, Le GTT., Tan TG., … Pavelka, N. Experimental evolution of a fungal pathogen into a gut symbiont. Science 2018. 362(6414), 589 LP-595.

Ushinsky SC, Harcus D, Ash J, Dignard D, Marcil A, Morchhauser J, Thomas DY, Whiteway M, Leberer E. CDC42 is required for polarized growth in human pathogen *Candida albicans*. Eukaryot Cell. 2002 Feb;1(1):95-104.

Uwamahoro N, Verma-Gaur J, Shen HH, Qu Y, Lewis R, Lu J, … Traven, A. The Pathogen *Candida albicans* Hijacks Pyroptosis for Escape from Macrophages. MBio 2014 5(2), e00003-14
van der Velden A, Thomas AA.The role of the 5’ untranslated region of an mRNA in translation regulation during development.The International Journal of Biochemistry & Cell Biology.1999.Volume 31, Issue 1,Pages 87-106.

van Wijlick L, Geissen R, Hilbig JS, Lagadec Q, Cantero PD, Pfeifer E, … Ernst JF. Dom34 Links Translation to Protein O-mannosylation. PLOS Genetics 2016. 12(10), e1006395.

Vandeputte P, Pradervand S, Ischer F, Coste AT, Ferrari S, Harshman K, Sanglard D. Identification and functional characterization of Rca1, a transcription factor involved in both antifungal susceptibility and host response in *Candida albicans*. Eukaryot Cell. 2012 Jul;11(7):916-31.

Vautier S, Drummond RA, Chen K, Murray GI, Kadosh D, Brown AJ, Gow NA, MacCallum DM, Kolls JK, Brown GD. *Candida albicans* colonization and dissemination from the murine gastrointestinal tract: the influence of morphology and Th17 immunity. Cell Microbiol. 2015 Apr;17(4):445-50.

Vazquez JA, Sobel JD. Mucosal candidiasis. Infect. Dis. Clin. N. Am.2002 16:793–820.
Velegraki A, Cafarchia C, Gaitanis G, Iatta R, Boekhout T. Malassezia infections in humans and animals: pathophysiology, detection, and treatment. PLoS Pathog. 2015 Jan 8;11(1).

Verma A, Wüthrich M, Deepe G, Klein B. Adaptive immunity to fungi. Cold Spring Harb Perspect Med. 2015 5(3):a019612.

Verma-Gaur J, Traven A. Post-transcriptional gene regulation in the biology and virulence of *Candida albicans*. Cell Microbiol. 2016 Jun;18(6):800-6.

Vermout S, Tabart J, Baldo A,.... Mignon B. Pathogenesis of Dermatophytosis. Mycopathologia 2008 166: 267.

Vijaya D, Dhanalakshmi TA, Kulkarni S. Changing trends of vulvovaginal candidiasis. J Lab Physicians. 2014 Jan-Jun;6(1):28-30.

Vilela C, Ramirez CV, Linz B, Rodrigues-Pousada C, McCarthy JE. Post-termination ribosome interactions with the 5'UTR modulate yeast mRNA stability. EMBO J. 1999 Jun 1;18(11):3139-52.

Vyas VK, Barrasa MI, Fink GR.A *Candida albicans* CRISPR system permits genetic engineering of essential genes and gene families. Sci Adv 2015. 1:e1500248.
Wächtler B, Wilson D, Haedicke K, Dalle F, Hube B. From Attachment to Damage: Defined Genes of *Candida albicans* Mediate Adhesion, Invasion and Damage during Interaction with Oral Epithelial Cells. PLOS ONE 2011 6(2): e17046.

Wang X, Bing J, Zheng Q, Zhang F, Liu J, Yue H, Tao L, Du H, Wang Y, Wang H, Huang G. The first isolate of *Candida auris* in China: clinical and biological aspects. Emerg Microbes Infect. 2018 May 18;7(1):93.

Wang Y. Fungal Adenylyl Cyclase Acts As a Signal Sensor and Integrator and Plays a Central Role in Interaction with Bacteria. PLOS Pathogens 2013. 9(10): e1003612.

Wangsanut T, Ghosh AK, Metzger PG, Fonzi WA & Rolfes R J. Grf10 and Bas1 Regulate Transcription of Adenylate and One-Carbon Biosynthesis Genes and Affect Virulence in the Human Fungal Pathogen *Candida albicans*. MSphere, 2017(4), e00161-17.

Webb BJ, Ferraro JP, Rea S, Kaufusi S, Goodman BE, Spalding J. Epidemiology and Clinical Features of Invasive Fungal Infection in a US Health Care Network. Open Forum Infect Dis. 2018 Jul 31;5(8):ofy187.

Weerasuriya N, and Snape J. Oesophageal candidiasis in elderly patients: risk factors, prevention and management. Drugs Aging 2008 25, 119–130.

Weiss EL. Mitotic Exit and Separation of Mother and Daughter Cells. Genetics 2012. 192(4), 1165 LP-1202.

Wellington M, Koselny K, Sutterwala FS, Krysan DJ. *Candida albicans* triggers NLRP3-mediated pyroptosis in macrophages. Eukaryot Cell. 2014 Feb;13(2):329-40.

Wheeler RT, Kombe D, Agarwala SD, Fink GR. Dynamic, morphotype-specific *Candida albicans* beta-glucan exposure during infection and drug treatment. PLoS Pathog.2008 4(12):e1000227.

White SJ, Rosenbach A, Lephart P, Nguyen D, Benjamin A, Tzipori S, Whiteway M, Mecsas J, Kumamoto CA. Self-regulation of *Candida albicans* population size during GI colonization. PLoS Pathog. 2007 Dec;3(12):e184.

Whiteway M, Bachewich C. Morphogenesis in *Candida albicans*. Annu Rev Microbiol. 2007;61:529-53.

Willger SD, Puttikamonkul S, Kim KH, Burritt JB, Grahl N, Metzler LJ, Barbuch R, Bard M, Lawrence CB, Cramer RA Jr. A sterol-regulatory element binding protein is required for cell polarity, hypoxia adaptation, azole drug resistance, and virulence in *Aspergillus fumigatus*. PLoS Pathog. 2008 4(11):e1000200.

Williams D, Lewis M. Pathogenesis and treatment of oral candidosis. J Oral Microbiol. 2011 Jan 28;3:10.3402/jom.v3i0.5771.

Wisplinghoff H, Bischoff T, …,Edmond MB. Nosocomial Bloodstream Infections in US Hospitals: Analysis of 24,179 Cases from a Prospective Nationwide Surveillance Study, Clinical Infectious Diseases, Volume 39, Issue 3, 1 August 2004, Pages 309–317.
Witchley JN, Penumetcha P, Abon NV, Woolford CA, Mitchell AP, & Noble SM. *Candida albicans* morphogenesis programs control the balance between Gut commensalism and invasive infection. Cell Host & Microbe 2019 25(3), 432–443.e6.

Xie J, Tao L, Nobile CJ, Tong Y, Guan G,... Huang G. White-Opaque Switching in Natural MTLa/α Isolates of *Candida albicans*: Evolutionary Implications for Roles in Host Adaptation, Pathogenesis, and Sex. PLOS Biology 2014 11(3): e1001525.

Zavrel M, Majer O, Kuchler K, Rupp S. Transcription factor Efg1 shows a haploinsufficiency phenotype in modulating the cell wall architecture and immunogenicity of *Candida albicans*. Eukaryot Cell. 2012 Feb;11(2):129-40.

Zeilinger S, Gupta VK, Dahms TE, Silva RN, Singh HB, Upadhyay RS, Gomes EV, Tsui CK, Nayak S C. Friends or foes? Emerging insights from fungal interactions with plants. FEMS Microbiol Rev. 2016. 40(2):182-207.

Zheng X, Wang Y, Wang Y. Hgc1, a novel hypha-specific G1 cyclin-related protein regulates *Candida albicans* hyphal morphogenesis. EMBO J. 2004 Apr 21;23(8):1845-56.

Zhou W, Edelman GM, & Mauro VP. Transcript leader regions of two *Saccharomyces cerevisiae* mRNAs contain internal ribosome entry sites that function in living cells. Proceedings of the National Academy of Sciences 2001 98(4), 1531 LP-1536.

6. Curriculum Vitae

Name: Prashant Ramesh Desai

Date of birth: 29.09.1985

Birthplace: Belgaum, India

Nationality: Indian

Education and Research experience

04.2011 - 04.2017	Heinrich-Heine-Universitat Düsseldorf, Germany PhD student, Molecular Mycology
01.2008 - 03.2011	Institute of Microbial Technology, Chandigarh, India Research assistant
05.2005 - 08.2007	Master of Science (Microbiology), Bangalore University, India

Publications

Prashant R. Desai, Lasse van Wijlick, Mateusz Juchimiuk, Alida Schaekel, Christophe D'Enfert and Joachim F. Ernst. Genetic landscapes of hypoxic filamentation in *Candida albicans*. (Under review.).

Prashant R. Desai, Klaus Lengeler, Mario Kapitan, Silas Janßen, Paula Alepuz, Ilse D. Jacobsen and Joachim F. Ernst. The 5´ untranslated region of the *EFG1* transcript promotes its translation to regulate hyphal morphogenesis in *Candida albicans.* mSphere 5;3(4). July 2018

Prashant R. Desai*, Lasse van Wijlick*, Dagmar Kurtz, Mateusz Juchimiuk, Joachim F. Ernst. Hypoxia and temperature regulated morphogenesis in *Candida albicans*. PLoS Genetics 14;11(8). August 2015. (*Equal contribution)

Alida Schaekel, Prashant R. Desai and Joachim F. Ernst. Morphogenesis-regulated localization of protein kinase A to genomic sites in *Candida albicans.* BMC Genomics 14(1):842. December 2013.

Prashant R. Desai, Anil Thakur, Dwaipayan Ganguli, Sanjoy Paul, Joachim Morschhäuser and Anand K Bachhawat. Glutathione Utilization by *Candida albicans* requires a Functional Glutathione Degradation (DUG) Pathway and OPT7, an Unusual Member of the Oligopeptide Transporter Family. Journal of Biological Chemistry 286(48):41183-94. December 2011.

Amit K Yadav, Prashant R. Desai, Maruthi Nandan Rai, Rupinder Kaur, K Ganesan and Anand K Bachhawat. Gluathione biosynthesis in pathogenic yeasts *Candida albicans* and *Candida glabrata*: Essential in *C. glabrata* and essential for virulence of *C. albicans*. Microbiology 157(Pt 2):484-95. February 2011.

Presentations

Oral presentation titled ''Multiple repressors of hypoxic filamentation in *C. albicans* '' at "13th ASM meeting on *Candida* and Candidiasis" 2016 in Seattle, USA.

Oral presentation titled ''Hypoxia alters morphogenetic pathways in *C. albicans* '' at SMYTE conference "Small Meeting on Yeast Transporters and Energetics" 2015 in Lisbon, Portugal.

Oral presentation at Infect-ERA yearly meeting 2014 in Valencia, Spain.

Presented Poster at PathoGenomics Infect-ERA meeting 2014 in Vienna. Austria.

Presented Poster at ASM conference "11th ASM meeting on *Candida* and Candidiasis" 2012 in San Francisco, USA

Presented Poster at conference "Small Meeting on Yeast Transporters and Energetics" 2010 in New Delhi, India

Presented poster at conference on "Understanding and Managing Pathogenic Microorganisms" (UMPM) 2010 in Chandigarh, India

7. Acknowledgement

Foremost, I owe my highest gratitude to my PhD supervisor Prof. Joachim F. Ernst. During my course of PhD tenure he gave several interesting projects related to fungal biology, and introduced me to the realm of hypoxia. I am also thankful for his extraordinary guidance, patience, constructive criticism, valuable feedback and for great support till the end of my PhD work.

I am grateful to Prof. Georg Groth, as a mentor he was very supportive and encouraged my work.

I am thankful to Prof. Michael Feldbrügge for being my Co-supervisor. Prof. Feldbrügge gave valuable suggestions during Monday seminars, it helped me to reflect back upon the results and motivated me to pursue project in an effective manner. I am also grateful to him for providing me the lab facilities whenever it was required.

I would like to thank Marc, Lasse, Mario, Christoph, Mateusz and Quentin for maintaining collegial environment in lab. And for providing valuable feedback during seminars and generously sharing the reagents. It was also great fun to discuss on wide range of topics with Quentin and Mateusz during lunch sessions. I am also thankful to Agnes, Michaela, Uli, Ute and Elisabeth. They helped me with ordering materials and provided excellent assistance with administration stuff. It was good experience to have Evelyn and Silas as Master students. I wish them good luck with their career.

I am very grateful to Prof. Ilse Jacobsen (HKI-Jena), she was very supportive and generously provided lab facilities from HKI. It was fun to collaborate with Mario. Thank you for helping me during my stay in Jena. And for translating my thesis summary.

During my early days in Düsseldorf, Pilar and Teresa helped me to acclimatize in new working environment. And accompanied for several memorable tours to different parts of Germany.

I would like to thank Dr. Sigrun Feldbrügge, she was always there to help me with VISA and administration related work. I am very grateful to JUNO, they tirelessly work for student's welfare at HHU.

My Indian friends often kept my spirits high and encouraged me during 'not so happening days'. Ananda Ayyapan was always there with his kind support. It was great fun, random plans for trips and movie, watching TBBT and cooking on weekends. Get-together for tea and dinner sessions with Senthil, Bala and Sushma provided much needed break from daily routine. I also thank Senthil and Bala, they kept me motivated during final Dissertation period.

I owe a great debt of gratitude to Prof. Anand K. Bachhawat (IMTECH-India), he encouraged me to work on independent projects in his lab and gave proper direction during my early career stage. He was always open for scientific discussion and provided valuable career advice. He is an ideal mentor and vital source of inspiration for all the students.

My special thanks to Anil Thakur, he is more like a big brother and is always there with his constant support and guidance for personal and professional life. I am also thankful to Jaspreet, Anup, Shailesh, Zulfi, Aman and Sunil Shekar, they have remained friends since Imtech days.

I thank my friends Shridhar, Hari and Ram, they have backed me since Bachelor degree days, and often raised my spirits to get over gloomy phase of life.

Words will never be enough to describe the unconditional support my Papa and Amma have given for my career. Their unwavering faith, love and support are pillars of strength for me. Lastly, I like to express special appreciation to my wife Sarika, her encouragement and support keeps me motivated to pursue my career aspirations. Her presence has made my life blissful.

Declaration

I hereby declare that this thesis is an original work and has not been submitted in whole, or in part, for a degree at this or any other university. Nor does it contain, to the best of my knowledge and belief, any material published or written by any other person, except as acknowledged in the text. This thesis is in compliance with the "Principles for Ensuring Good Scientific Practice at the Heinrich-Heine-University Düsseldorf". I have not made any unsuccessful promotions.

Düsseldorf
Date: 05/07/2019

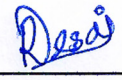

(Prashant Ramesh Desai)

Parts of this work have been published:

Prashant R. Desai, Lasse van Wijlick, Yasemin Üstün, Mateusz Juchimiuk, Alida Schaekel, Silas Janßen, Christophe D'Enfert and Joachim F. Ernst. Genetic landscapes of hypoxic filamentation in *Candida albicans*. (Under Review).

Prashant R. Desai, Klaus Lengeler, Mario Kapitan, Silas Janßen, Paula Alepuz, Ilse D. Jacobsen and Joachim F. Ernst. The 5´ untranslated region of the *EFG1* transcript promotes its translation to regulate hyphal morphogenesis in *Candida albicans*. mSphere 5;3(4). July 2018

Prashant R. Desai*, Lasse van Wijlick*, Dagmar Kurtz, Mateusz Juchimiuk, Joachim F. Ernst. Hypoxia and temperature regulated morphogenesis in *Candida albicans*. PLoS Genetics 14;11(8). August 2015. (* equal contribution)

Alida Schaekel, Prashant R. Desai and Joachim F. Ernst. Morphogenesis-regulated localization of protein kinase A to genomic sites in *Candida albicans* BMC Genomics 14(1):842. December 2013.